Signalling to intracellular Ca^{2+} channels

Abha Meena

Lucy Cavendish College
University of Cambridge

This dissertation is submitted for the degree of
Doctor of Philosophy

July 2015

Preface

This dissertation is the result of my own work performed in the Department of Pharmacology, University of Cambridge between October 20 IOand August 2014, and includes nothing which is the outcome of work done in collaboration except where specifically indicated in the text. This thesis is not substantially the same as any other that has been submitted for a degree, diploma or other qualification at this or any other establishment. The dissertation does not exceed the word limit approved the Biology Degree Committee.

Abha Meena

Acknowledgements

I owe my deepest gratitude to Professor Colin Taylor for his meticulous guidance from the preliminary to the concluding level, which enabled me to develop an understanding of the subject.

I would like to thank Prof. J. Mike Edwardson, my mentor Dr. Fiona Gribble, my pharmacology department tutor Dr. Robin Hiley, Dr. Lesley McVinish and my college tutor Dr. Orsola Rath Spivack for their constant support during my hard time in PhD and believing in my competence to pursue PhD.

I am also grateful to have worked in a lab with pleasant colleagues like Dr. Steve Tovey, Dr. Nadia Nisha Shah, Dr. Emily Taylor, Dr. Taufiq Ur Rahman, Dr. Dave Pole, Dr. Ana Rossi, Dr. Cristina Lopez Sanjurjo, Dr. Alap Chavda, Philippa Dale, Vera Konieczny, Mike Keebler and Nagendra Babu.

I thank Cambridge Commonwealth Overseas Trust, Department of Pharmacology, Laboratory of Professor Taylor, Lucy Cavendish College, Cambridge. U.K and Central Institute of Medicinal and Aromatic Plants (Council for Scientific and Industrial Research, India) for funding my studies.

I am also thankful to my friends in Cambridge and specially to Kanika Kankan for constantly encouraging me during my PhD and travelling with me around Cambridge.

Above all, I am deeply obliged to my Father (Mr. L.V. Meena), mother (Kamla Meena), Brother (Dr. Ashish Meena), Sister (Nidhi Meena) and the rest of my extended family for boosting my morale with encouraging words, blessings and prayers.

Last but not the least, I would also like to thank my colleague and dearest friend Dr. Suaib Luqman at CIMAP (CSIR) for helping me out in managing my job-related issues during my stay in Cambridge.

Summary

Ryanodine receptors (RyR), expressed within the ER or plasma membrane (PM), may contribute to regulated insulin secretion from pancreatic β-cells. Amplification by RyR of the Ca^{2+} signals evoked by voltage-gated Ca^{2+} channels may contribute to the second phase of insulin release, but the role of RyR in the plasma membrane is unresolved. My aim was to define the roles of RyR in pancreatic β-cells. I used INS-1E insulinoma cells, which have been reported to secrete insulin in response to glucose, to characterise the contribution of RyR to Ca^{2+} entry and release. KCl-evoked Ca^{2+} entry in INS-1E cells was mediated by L-type Ca^{2+} channels. Both caffeine and carbachol evoked Ca^{2+} entry and release. Caffeine-evoked Ca^{2+} entry was inhibited by ryanodine and nimodipine. This might be due to direct activation of RyR in the PM, or activation of other Ca^{2+}-permeable channels in the PM secondary to Ca^{2+} release via RyR. However, glucose did not evoke insulin secretion from INS-1E cells, and the Ca^{2+} signals evoked by caffeine and carbachol became very variable with increasing passage number. It was therefore impossible with INS-1E cells to establish the role of RyR in glucose-evoked insulin release, and preliminary results with primary β-cells suggested that the quantitative analyses required to identify modest contributions from RyR would be impracticable.

Previous work established that in HEK cells expressing type 1 parathyroid hormone receptors (PTH_1R), PTH(1-34) potentiated carbachol-evoked Ca^{2+} release via a mechanism that required local delivery of cAMP to IP_3 receptors (IP_3R) within signalling junctions. My aim was to establish whether the interaction between adenylyl cyclase (AC) and IP_3R persists during sustained stimulation with PTH, which has been reported to cause internalization of a functional PTH_1R signalling pathway. In HEK cells expressing type 1 PTH_1R, stimulation with PTH(1-34) for 1-60 min potentiated carbachol-evoked Ca^{2+} signals. The potentiation was greater after acute (1 min) relative to sustained (60 min) stimulation. However, intracellular concentrations of cAMP were greater after sustained stimulation. Inhibition of protein kinase A (PKA) or exchange proteins activated by cAMP (EPAC) had no effect on the Ca^{2+} signals evoked by carbachol after acute or sustained stimulation with PTH(1-34). Similar results were obtained with acute and sustained

stimulation with NKH477 to activate AC or with a membrane-permeant analogue of cAMP, 8-Br-cAMP. Paired combinations of the three stimuli – PTH(1-34), NKH477 and 8-Br-cAMP – had the same maximal effect as each alone during acute and sustained treatments. Neither acute nor sustained treatment with PTH(1-34) alone affected the Ca^{2+} content of the intracellular stores. These results indicate that sustained increases in cAMP reduce the extent to which cAMP potentiates carbachol-evoked Ca^{2+} release. Analyses of responses to PTH analogues that differ in their abilities to evoke internalization of signalling pathways and/or activate phospholipase C versus AC confirmed that the effects of acute and sustained stimulation with PTH on Ca^{2+} signalling were mediated by cAMP and unlikely to require internalization of PTH_1R.

Inhibition of AC with SQ22536 and 2′,5′-dideoxyadenosine reduced the amounts of cAMP produced by acute and sustained stimulation with PTH(1-34) by ~80%, but they had no effect on potentiation of carbachol-evoked Ca^{2+}signals. Inhibition of cyclic nucleotide phosphodiesterases with IBMX had no effect on the Ca^{2+} signals evoked by carbachol after acute stimulation with PTH(1-34). However, during sustained stimulation (60 min), when cAMP levels were increased ~15-fold by IBMX, carbachol-evoked Ca^{2+} signals were ~10-fold more sensitive to PTH(1-34), although the maximal potentiation remained smaller than observed during acute stimulation. Using an IP_3 biosensor to measure cytosolic IP_3 demonstrated that sustained stimulation with PTH(1-34) attenuated the carbachol-evoked increase in cytosolic IP_3 concentration. I conclude that acute and sustained responses to PTH(1-34) are mediated by local delivery of saturating concentrations of cAMP to IP_3R within signalling junctions. Sustained increases in cAMP, via mechanisms that do not involve internalization of PTH_1R or activation of PKA, diminish the effectiveness with which this local delivery of cAMP potentiates carbachol-evoked Ca^{2+} release, probably by diminishing carbachol-evoked IP_3 formation.

Abbreviations

ATP	Adenosine 5'-triphosphate
AC	Adenylyl cyclase
AA	Arachidonic acid
AKAP	A-kinase-anchoring proteins
8-Br-cAMP	8-Bromoadenosine 3′,5′-cyclic monophosphate
BAPTA	1,2-bis(o-aminophenoxy)ethane-N,N,N',N'-tetraacetic acid
BSA	Bovine serum albumin
CAX	Ca^{2+}/H^{+} exchanger
$CaCl_2$	Calcium chloride
CAD	C-terminal CRAC activation domain
CaM	Calmodulin
CCK	Cholecystokinin
CPA	Cyclopiazonic acid
cGMP	Cyclic guanosine 3',5'-monophosphate
CNGC	Cyclic nucleotide-gated channel
cADPR	Cyclic ADP ribose
cAMP	Cyclic adenosine 3',5'-monophosphate
CCh	Carbachol

CRAC	Ca^{2+} release-activated Ca^{2+} channel
CICR	Ca^{2+} -induced Ca^{2+} release
$[Ca^{2+}]_c$	Intracellular Ca^{2+} concentration
$[Ca^{2+}]_{ECF}$	Extracellular Ca^{2+} concentration
$[Ca^{2+}]$	Ca^{2+} concentration
DDA	2',5'-dideoxyadenosine
DMEM	Dulbecco's Modified Eagle's Medium
DM	Diabetes mellitus
DMSO	Dimethyl sulfoxide
DAG	Diacyl glycerol
Epac	Exchange protein activated by cAMP
ER	Endoplasmic reticulum
ERK	Extracellular signal-regulated kinases
ECM	Extracellular matirx
FRET	Fluorescence resonance energy transfer
FBS	Foetal bovine serum
FK	Forskolin
GPCR	G-protein-coupled receptor
GIP	Gastric inhibitory polypeptide

GLP-1	Glucagon-like peptide-1
GSIS	Glucose-stimulated insulin secretion
GEF	Guanine nucleotide exchange factor
GTP	Guanosine-5'-triphosphate
GRK	G-protein coupled receptor kinase
GFP	Green fluorescent protein
IBC	IP_3-binding core
IBMX	3-isobutyl-1-methylxanthine
IP_3	Inositol 1,4,5-trisphosphate
IP_3R	Inositol 1,4,5-trisphosphate receptor
I_{CRAC}	Ca^{2+} -release activated Ca^{2+} -current
IP_4	Inositol 1,3,4,5-tetrakisphosphate
IR	Insulin receptor
HEPES	4-(2-hydroxyethyl)-1-piperazineethanesulfonic acid
HBS	HEPES buffer saline
HCN	Hyperpolarization-activated cyclic nucleotide-gated channel
K_{ATP}	ATP-gated K^+ channel
KCl	Potassium chloride
K_D	Equilibrium dissociation constant

KRH	Krebs-Ringer bicarbonate HEPES buffer
MCU	Mitochondrial Ca^{2+} uniporter
NAD	Nicotinamide adenine dinucleotide
NADP	NAD phosphate
NAADP	Nicotinic acid adenine dinucleotide phosphate
NCX	Na^{+}/ Ca^{2+} exchanger
NO	Nitric oxide
NSCC	Non-selective cation channel
PTHrP	PTH-related peptide
PKA	Protein kinase A
PKC	Protein kinase C
PLC	Phospholipase C
PIP_2	Phosphatidylinositol 4,5-bisphosphate
PM	Plasma membrane
ROC	Receptor-operated Ca^{2+} channel
PMCA	Plasma membrane Ca^{2+} ATPase
PTH	Parathyroid hormone
PTH_1R	Parathyroid hormone receptor
PDE	Phosphodiesterase

RyR	Ryanodine receptor
SQ	SQ 22536
SR	Sarcoplasmic reticulum
SEM	Standard error of the mean
SMOC	Second messenger-operated Ca^{2+} channel
SOCE	Store-operated Ca^{2+} entry
STIM	Stromal interaction molecule
TPC	Two-pore channel
TRPC	Transient receptor potential channels
TNG	Trans-golgi network
VOC	Voltage operated Ca^{2+} channels
VRAC	Volume-regulated anion channels

Contents

Chapter 1. Introduction

Intracellular signalling is an intricate process. Cells continuously receive external stimuli, which often result in the formation of intracellular messengers. These messengers subsequently decode the external stimuli into a specific cellular response. The most important and extensively studied second messengers are Ca^{2+} and cyclic adenosine monophosphate (cAMP) (Sutherland, 1970; Zaccolo *et al.*, 2002). Exploring how changes in second messenger levels regulate various intracellular signalling pathways is an ongoing process. It could involve frequency, controlled amplitude and spatio-temporal modes of regulation (Berridge *et al.*, 2000). For example, periodic increases or decreases in the levels of second messengers can be observed when glucagon stimulates Ca^{2+} and cAMP oscillations in HEK-293 cells expressing type III adenylyl cyclase (Dyachok *et al.*, 2006; Wayman *et al.*, 1995). The cross-talk between Ca^{2+} and cAMP signalling pathways add a secondary level of complexity (Bruce *et al.*, 2003; Siso-Nadal *et al.*, 2009), enabling Ca^{2+} to regulate cAMP level and vice versa.

1.1 An overview of Ca^{2+} signalling

Ca^{2+} is an intracellular messenger that performs a diverse range of physiological and biochemical functions. Ca^{2+} signals are highly temporally and spatially organised (Berridge, 1997), and control a wide variety of complicated cellular process like embryonic pattern formation, exocytosis, fluid secretion, cell contraction, apoptosis and gene transcription, (Berridge, 2009). The cytosolic free Ca^{2+} concentration ($[Ca^{2+}]_c$) in resting cells is ~10-100nM. Activation of cells by depolarisation, mechanical deformation or by binding of ligands to receptors (e.g. hormones, neurotransmitters, etc) leads to increases in $[Ca^{2+}]_c$ up to ~1µM (Berridge *et al.*, 2003). Inside the cell, Ca^{2+} signals follow complex temporal and spatial arrangements. Prolonged increases in $[Ca^{2+}]_c$ are toxic. Cells have evolved mechanisms that allows tight regulation of $[Ca^{2+}]_c$ (Clapham, 1995). Increases in $[Ca^{2+}]_c$ occur either by Ca^{2+} entry across the plasma membrane (PM) or by Ca^{2+} release from intracellular stores. Both are mediated by opening of Ca^{2+}-permeable channels. Sequestration of Ca^{2+} occurs by various pumps and exchangers which continuously extrude Ca^{2+} into the extracellular space or intracellular stores. These processes together allow cells to rapidly and reversibly generate changes in $[Ca^{2+}]_c$ that effectively regulate cellular activity (Bootman *et al.*, 2001).

The endoplasmic reticulum (ER), or the sarcoplasmic reticulum (SR) in muscle, is the most important intracellular Ca^{2+} storage organelle. The free [Ca^{2+}] inside the ER/SR lumen is approximately~400µM (Miyawaki *et al.*, 1997). The continuous accumulation of Ca^{2+} from the cytosol into the ER is made possible by ER membrane-resident Ca^{2+} pumps and an ER resident Ca^{2+}-binding protein known as calreticulin (Michalak *et al.*, 1999). Other intracellular organelles that also contribute to the rise in $[Ca^{2+}]_i$ are the nucleoplasmic reticulum, mitochondria, Golgi apparatus, lysosomes, secretory vesicles and nuclear envelope. Each intracellular organelle has a specific signalling mechanism for the regulation of Ca^{2+} release through Ca^{2+} -permeable channels located in the membrane.

1.1.1. Ca^{2+} entry channels

The extracellular [Ca^{2+}] is ~2mM, compared to ~100nM in the cytosol. This gives an ~20,000-fold concentration gradient in [Ca^{2+}] across the PM (Clapham, 1995). In addition, the negative resting membrane potential adds a huge electrochemical difference, which favours Ca^{2+} influx across the PM (Parekh *et al.*, 2005). The Ca^{2+} channels that allow Ca^{2+} entry across the PM can be conveniently classified on the basis of their activation mechanisms. Voltage-operated Ca^{2+} channels (VOC) are activated by depolarisation of the PM. They are predominantly found in excitable cells, for example, pancreatic β-cells, muscle and neurons, and they typically contribute to large and rapid Ca^{2+} entry signals. VOCs are classified according to their voltage-sensitivity and pharmacological characteristics into three families: L-type (Ca_v1); P/Q, R and N-type (Ca_v2); and T-type (Ca_v3). Ca_v1 and Ca_v2 are activated by large membrane depolarisations, while Ca_v3 are low-voltage-activated channels (Braun *et al.*, 2008). Ca_v1 and Ca_v3 are expressed in pancreatic β-cells (Yang *et al.*, 2006).

Receptor-operated Ca^{2+} channels (ROC) are activated by binding of a ligand to an extracellular domain of the channel, which leads to conformational changes and opening of an intrinsic channel. ROCs are activated by a wide variety of agonists, for example ATP, 5-HT, glutamate and acetylcholine. ROCs include several structurally diverse families including Cys-loop receptors (e.g. nicotinic acetylcholine and 5-HT_3 receptors), glutamate receptors (e.g., AMPA and NMDA receptors) and P2X receptors (Heimes *et al.*, 2009; Inagaki *et al.*, 1995; Jacques-Silva *et al.*, 2010; Ruiz de Azua *et al.*, 2011)

Second messenger-operated Ca^{2+} channels (SMOCs) are a diverse category of channels that are activated by second messengers like diacylglycerol (DAG) and arachidonic acid. For example DAG activates some transient receptor potential channels (TRP), notably TRPC3, TRPC6 and TRPC7 (Hofmann *et al.*, 1999; Okada *et al.*, 1999). Some TRPCs are expressed in pancreatic β-cells (Islam, 2010). Arachidonic acid has been reported to activate channels (ARC) that appear to be specific oligomeric assemblies of Orai proteins (Mignen *et al.*, 2007).

Store-operated Ca^{2+} entry (SOCE) is mediated by Ca^{2+} release-activated Ca^{2+} channels (CRAC) (Parekh *et al.*, 2005). It is activated when the [Ca^{2+}] within the ER falls (Liou *et al.*, 2005; Luik *et al.*, 2006). SOCE requires both a stromal interaction molecule (STIM 1 or STIM 2), much of which is expressed in ER membranes, and Orai proteins, which are expressed in the PM (Lewis, 2007). With the decrease in ER luminal [Ca^{2+}], Ca^{2+} dissociates from the luminal EF-hand of STIM causing its oligomerization and translocation towards ER near the PM to form STIM puncta. The C-terminal CRAC activation domain (CAD) of STIM 1 can then interact with the C and N-termini of Orai1 to cause its pore to open. One suggestion is that tetrameric STIM CAD domains cause dimers of Orai to assemble into functional tetramers which then mediate Ca^{2+} entry (Cahalan, 2009; Luik *et al.*, 2006). STIM 2 can also stimulate SOCE, but STIM 2 responds to lesser reductions in luminal [Ca^{2+}] and may be involved in regulating basal rates of Ca^{2+} entry to replenish the ER Ca^{2+} stores (Brandman *et al.*, 2007; Parvez *et al.*, 2008). Recently the CAD domain of STIM was claimed to bind also to the C-terminal of the α-subunit of $Ca_v1.2$ to cause inhibition of the L-type Ca^{2+} channel (Park *et al*, 2010). This reciprocal regulation by STIM of SOCE (via Orai) and voltage-gated Ca^{2+} entry (via L-type Ca^{2+} channels) may account for the apparent absence or much diminished activity of SOCE in electrically excitable cells (Park *et al.*, 2010; Wang *et al.*, 2010). Whether reduced expression of STIM in pancreatic β-cells accounts for their active L-type Ca^{2+}channels and weak SOCE is not yet known (Rosker *et al.*, 2009).

1.1.2. Ca^{2+} release channels

Ca^{2+} release from intracellular stores mostly takes place via inositol trisphosphate receptors (IP_3R) and ryanodine receptors (RyR) (Foskett *et al.*, 2007; Lanner *et al.*, 2010). IP_3Rs are ligand-gated Ca^{2+} channels, mostly expressed in animal cells. IP_3Rs

are chiefly localised within the ER membrane, but they can also be present on other membranes, for example, the nuclear envelope (Rahman *et al.*, 2010), Golgi apparatus and plasma membrane. These channels have poor cation selectivity and a large conductance for Ca^{2+} (Rahman *et al.*, 2010).

There are three subtypes of IP_3Rs (IP_3R1, IP_3R2, IP_3R3) expressed in mammalian cells. Almost~70% of the amino acid sequences are similar in all the IP_3R subtypes, but they have distinct tissue distributions (Ross *et al.*, 1992; Taylor *et al.*, 1999) and some disparity in their regulation and sensitivity to IP_3 and its analogue adenophostin (Saleem *et al.*, 2012; Saleem *et al.*, 2013). Fully functional IP_3R channels are formed by their splice variants and homo-or hetero-tetramers of these subtypes (Taylor *et al.*, 1999). Each subunit of the tetramer consists of an IP_3-binding core (IBC), a large cytosolic regulatory domain, suppressor domain at its cytoplasmic N terminus, 6 transmembrane domains and a short cytoplasmic C-terminal tail (Foskett *et al.*, 2007). The last two transmembrane domains with the intervening luminal loop form the IP_3R channel pore.

For activation, IP_3R needs IP_3 and Ca^{2+} (Marchant *et al.*, 1997); however, other proteins and small intracellular molecules, for example, PKA (Nakade *et al.*, 1994), calmodulin (Taylor *et al.*, 2002) and ATP (Thrower *et al.*, 2000) can also modulate IP_3R activity. Small increases in $[Ca^{2+}]_c$ potentiate responses to IP_3, while larger increases (> 1µM) are inhibitory (Berridge *et al.*, 1989; Horne *et al.*, 1997; Marchant *et al.*, 1997). The mechanisms are not resolved, but IP_3 appears to control IP_3R gating by controlling whether Ca^{2+} binds to stimulatory or inhibitory binding sites (Adkins *et al.*, 1999; Foskett *et al.*, 2007; Taylor *et al.*, 2002; Taylor *et al.*, 2010). The lower level of $[Ca^{2+}]_c$ triggers Ca^{2+}-induced Ca^{2+} release (CICR) which is exhibited by both IP_3R and RyR. It allows the Ca^{2+} release from one IP_3R to stimulate neighbouring RyR or other IP_3Rs. CICR is important for generation of regenerative Ca^{2+} signals, since it allows the translation of local Ca^{2+} signals into a global increase in $[Ca^{2+}]_c$ (Berridge *et al.*, 2000). IP_3, a diffusible second messenger, is generated at the PM upon activation of a PM-localised GPCR that stimulates phospholipase C (PLC). Some of the links between GPCRs and ion channels are summarised in figure 1.1. Binding of IP_3 to the IBC of IP_3R evokes conformational changes (Seo *et al.*, 2012), which then lead to the opening of the pore located at the C-terminus of the tetramer. However, both Ca^{2+} and IP_3 are needed for the activation of IP_3R, yet the actual mechanism of how rearrangement of the N-terminus causes binding of Ca^{2+} and opening of the pore is not fully known.

Inactivation of IP_3 is regulated by its metabolism to inositol 1,3,4,5-tetrakisphosphate (IP_4) and inositol 1,4-bisphosphate (IP_2) by IP_3-kinase and IP_3 5-phosphatase, respectively. Studies in mouse neuroblastoma cells show that IP_3 has an estimated half-life of only~9 s (Wang *et al.*, 1995). IP_4 perhaps acts as a signalling molecule (Irvine, 2007). IP_4 has been reported to activate IP_3R in permeabilized cells, however, it is~100-fold less potent then IP_3 (Saleem *et al.*, 2013). IP_4 has also been proposed to regulate Ca^{2+} entry (Miller *et al.*, 2007), but the physiological role of IP_4 is not entirely clear.

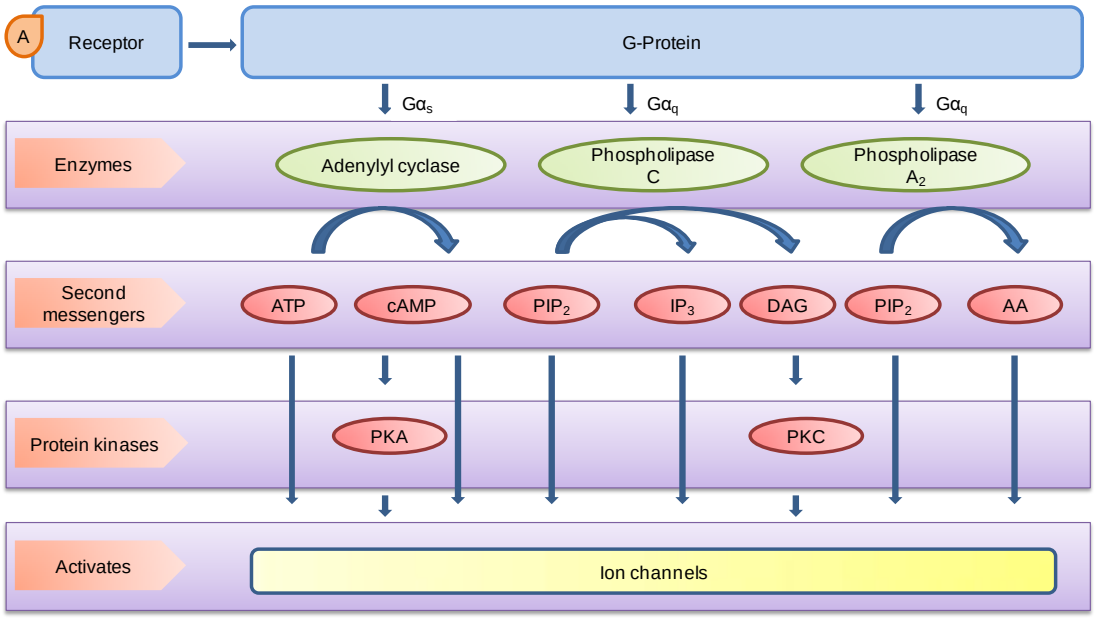

Figure 1.1. **Summary of key steps linking agonist activation of GPCR to ion channels**. GPCR catalyze, via exchange of GDP for GTP on the α-subunit of G proteins, activation of G proteins. Dissociated Gα-GTP and Gβγ subunits of the G-protein can then activate adenylyl cyclase, phospholipase C and phospholipase A_2, and directly regulate some ion channels. The enzymes catalyse formation of the second messengers, cAMP, IP_3, DAG, AA and PIP_2 which can directly activate ion channels. DAG and cAMP can also indirectly regulate ion channels via proteins kinases C and A, respectively.

RyR are another family of Ca^{2+} release channels found mainly in the membranes of ER/SR. These channels also have large-conductance and poor selectivity for Ca^{2+} (Fill *et al.*, 2002). Similar to IP_3R, RyR also follows a bell-shaped dependency for regulation by $[Ca^{2+}]_c$. These channels are activated by low $[Ca^{2+}]_c$ ranges between 1-10

μM and inactivated at higher $[Ca^{2+}]_c$ (1-10 mM) (Chen *et al.*, 1997; Hayek *et al.*, 2000; Meissner, 2004). According to Berridge *et al* (2000), RyR are also capable of propagating Ca^{2+} signals as regenerative waves across the cell. Apart from Ca^{2+}, ryanodine, a plant alkaloid, also activates RyR in a concentration-dependent manner. Stimulation with low ryanodine concentrations increases the open-probability of the channel (Buck *et al.*, 1992), whereas it inhibits channels at higher concentrations (Zimanyi *et al.*, 1992). A second messenger, cADPR, has been shown to activate RyR in numerous cell types (Lee, 1997; Ogunbayo *et al.*, 2011). However, the effect of cADPR on the RyR of muscle cells is still unclear (Copello *et al.*, 2001). Intracellular formation of cADPR occurs by the action of CD38 on nicotinamide adenine dinucleotide (NAD) (Howard *et al.*, 1993). The conversion of NAD phosphate (NADP) to nicotinic acid adenine dinucleotide phosphate (NAADP) is also catalysed by CD38. NAADP can also evoke release of Ca^{2+} (see below). The activation of CD38 is regulated by various factors like cyclic nucleotides, and specific cell-surface receptors. Depending on the activation mechanism, either cADPR or NAADP is formed (Lee, 2000).

Three subtypes of RyR are known viz. RyR1, RyR2 and RyR3; all the subtypes are expressed in mammalian cells. RyR1 is mostly expressed in skeletal muscle cells, RyR2 in cardiac cells and RyR3 in neurones and smooth muscle cells. However, the RyR3 expression level is generally much lower than that of RyR1 or RyR2. The most important role of RyR is in striated muscle cells. RyR mediates excitation-contraction coupling in these cells (Shoshan-Barmatz *et al.*, 1998). Depolarization of the PM activates VOCs, which are coupled to activation of RyR, but the activation mechanisms are different for each RyR subtype. RyR1 is directly activated by L-type Ca^{2+} channels, by a protein-protein interaction (Marx *et al.*, 1998). Whereas in cardiac myocytes, activation of L-type Ca^{2+} channels first mediates Ca^{2+} entry that consequently activates RyR2 by CICR. Activation of RyR, either indirectly by CICR or directly by coupling to L-type Ca^{2+} channels, triggers release of Ca^{2+} from the SR, which leads to contraction (Bers, 2002; Best *et al.*, 2012).

NAADP generation has also been shown to increase $[Ca^{2+}]_c$ upon stimulation with specific agonists (Guse *et al.*, 2008). It stimulates the release of Ca^{2+} from acidic organelles (Churchill *et al.*, 2002; Gambara *et al.*, 2008). The increases in $[Ca^{2+}]_c$ triggered by NAADP further stimulate release of Ca^{2+} form ER via IP_3R and RyR by CICR (Cancela *et al.*, 1999). Churchill *et al.* (2002) showed that NAADP stimulates a

lysosome-like structure present in sea urchin eggs. Indeed, this evidence suggested that NAADP mobilises Ca^{2+} from a lysosomal store. NAADP activates two pore channels (TPC) localised on the lysosomes, thereby releasing Ca^{2+} (Calcraft *et al.*, 2009; Galione *et al.*, 2010; Patel *et al.*, 2011). Mammalian TPCs have been classified as endolysosomal Ca^{2+} release channels. However, in a recent study, TPCs are described as Na^{+}-selective channels activated by $PI(3,5)P_2$ (Wang *et al.*, 2012). Hence, whether TPCs are Ca^{2+} release channels activated by NAADP or Na^{+}-selective channels activated by $PI(3,5)P_2$ is a matter of debate.

Sphingosine-1-phosphate and sphingosylphosphoryl choline can also induce release of Ca^{2+} within the cell. These are known to activate intracellular Ca^{2+} channels by acting on PM localised receptors, but they can also act directly to release Ca^{2+} from the ER. A channel responsible for this effect was initially suggested, but the original claim has been discredited (Rizzuto *et al.*, 2006; Schnurbus *et al.*, 2002).

1.1.3. Recovery from Ca^{2+} signals

Maintenance of the resting $[Ca^{2+}]_c$ and rapid recovery from increases in $[Ca^{2+}]_c$ are achieved by transport of Ca^{2+} out of the cytosol across the PM or membranes of intracellular organelles. Ca^{2+} extrusion across the PM takes place a) via high-affinity, low capacity ATP-dependent Ca^{2+} ATPases (PMCA) that hydrolyse ATP to transport Ca^{2+} towards the extracellular medium (Carafoli, 1991), b) via large capacity, low-affinity Na^{+}/Ca^{2+} exchangers (NCX) that use the electrochemical gradient of Na^{+} to extrude one Ca^{2+} in exchange for the influx of three Na^{+} ions (Brini *et al.*, 2009; Hilge, 2012).

Ca^{2+} uptake into SR/ER occurs through high-affinity, low capacity ATP-dependent SR/ER Ca^{2+}-ATPase pumps (SERCA) present on the SR/ER membrane (Strehler *et al.*, 2004). Inhibition of SERCA can be achieved using a variety of compounds (Michelangeli *et al.*, 2011), amongst which cyclopiazonic acid (CPA) and thapsigargin are the most frequently used. These compounds stabilize the Ca^{2+}-free conformation of SERCA. Thapsigargin binds irreversibly, whereas CPA is a reversible inhibitor.

Mitochondria also sequester Ca^{2+} via the mitochondrial Ca^{2+} uniporter (MCU) located in the inner mitochondrial membrane, using its electrochemical gradient (Colegrove *et al.*, 2000). The MCU is a Ca^{2+}-selective transporter; it uses the

mitochondrial membrane potential as the energy source for uptake of Ca^{2+} instead of coupling to ATP hydrolysis (Babcock *et al.*, 1997; Kirichok *et al.*, 2004). The MCU has low affinity for Ca^{2+} (10-20 μM), suggesting that the role of mitochondria in the regulation of $[Ca^{2+}]_c$ is marginal. Nevertheless, accumulation of Ca^{2+} by mitochondria during physiological cellular responses has been established (Glitsch *et al.*, 2002; Hajnoczky *et al.*, 1995; Olson *et al.*, 2010). This contradiction was explained by the distribution of mitochondria close to Ca^{2+}-permeable channels, where the local $[Ca^{2+}]_c$ was significantly higher in comparison to the global increase in $[Ca^{2+}]_c$ (Rizzuto *et al.*, 2009). The electrophysiological properties of the MCU and the importance of mitochondrial Ca^{2+} uptake were established long before the molecular identity of the MCU was known. A protein localised in the inner mitochondrial membrane, which forms multimeric complexes and is sensitive to ruthenium red (an inhibitor of mitochondrial Ca^{2+} uptake) has been recognised as the MCU. These results were further confirmed, when silencing the expression of this protein led to decreased mitochondrial Ca^{2+} uptake, and over-expression significantly increased mitochondrial Ca^{2+} uptake. In summary, these results suggest that the protein is MCU (Baughman *et al.*, 2011; De Stefani *et al.*, 2015; De Stefani *et al.*, 2011). Figure 1.2 illustrates the major routes for Ca^{2+} transport across membranes.

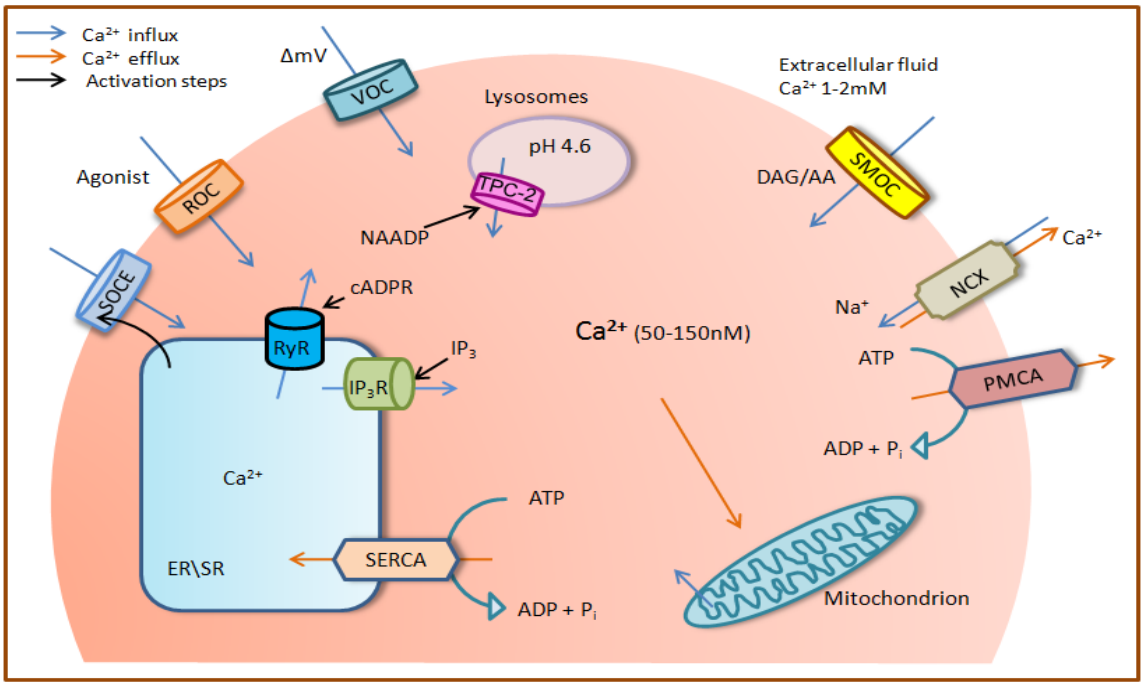

Figure 1. 2. **Ca^{2+} signalling pathways.** Routes for Ca^{2+} transport to and from the cytosol are shown. Ca^{2+} entry across the PM occurs via receptor-operated Ca^{2+} channels (ROCs), store-operated Ca^{2+} entry channels (SOCE), voltage-operated Ca^{2+} channels (VOCs), and second messenger-operated Ca^{2+} channels (SMOCs) activated by such intracellular signals as DAG and AA. Ca^{2+} release via ER Ca^{2+} channels occurs primarily via IP_3R and RyR activated by IP_3 and cADPR, respectively. NAADP, via TPC, mediates release of Ca^{2+} from lysosomes. Ca^{2+} sequestration takes place by the SERCA in the ER membrane, by an unidentified uptake mechanism in the lysosomal membrane, and by MCU in mitochondria. Extrusion of Ca^{2+} across the PM occurs via NCX and PMCA.

1.1.4. Spatio-temporal organization of Ca^{2+} signals

Interplay between the various Ca^{2+}-transporting proteins and the substantial buffering capacity of the cytosol allow spatially organised Ca^{2+} signals (Berridge, 1997), such that increases in $[Ca^{2+}]_c$ may either be restricted to the immediate vicinity of a single open channel or spread to include the entire cell. These local Ca^{2+} microdomains are the basic units of Ca^{2+} signalling. They allow each Ca^{2+} channel to direct Ca^{2+} distinctively to its targets (Fagan *et al.*, 1998; Jouaville *et al.*, 1999; Luzio *et al.*, 2007) or to a protein which removes Ca^{2+} from the cytosol. For both IP_3R and RyR, their stimulation by cytosolic Ca^{2+} allows CICR to propagate regenerative cytosolic Ca^{2+} signals (Lopez-Lopez *et al.*, 1995). Increasing concentrations of IP_3 cause Ca^{2+} release

events to grow from openings of individual IP_3R ('Ca^{2+} blips') to 'Ca^{2+} puffs', which arise from the coordinated opening of several clustered IP_3R, and eventually to Ca^{2+} waves that spread throughout the cell (Marchant *et al.*, 1999; Rahman *et al.*, 2009; Smith *et al.*, 2009). Such spatially organised Ca^{2+} signals have important physiological consequences. In smooth muscle, local Ca^{2+} release via RyR close to the PM causes relaxation by hyperpolarising the PM, while Ca^{2+} entry via depolarisation-evoked opening of L-type Ca^{2+} channels causes contraction (Nelson *et al.*, 1995). There are many other examples where a local increase in $[Ca^{2+}]_c$ is selectively directed to a specific target. These include the Ca^{2+} signals underlying exocytosis (Tse *et al.*, 1993), regulation of gene expression (Dolmetsch *et al.*, 1998), mitochondrial metabolism (Hajnoczky *et al.*, 1995), embryonic pattern formation, fertilisation and cell movement (Whitaker *et al.*, 2008), and apoptosis (Lordan *et al.*, 2009). Control of cellular process by Ca^{2+} microdomains therefore requires a close juxtaposition of different organelles associated with Ca^{2+} signalling. It is well recognised that local communications between different transporters and Ca^{2+}, Ca^{2+}-sensitive -Ca^{2+} channels and effectors support the versatility of Ca^{2+} signalling.

Sustained high $[Ca^{2+}]_c$ is cytotoxic for the cell, even so, Ca^{2+} controls comparatively long-lasting cellular process, for instance, insulin secretion (Gilon *et al.*, 2002), gene expression (Di Capite *et al.*, 2009) and fertilization (Miyazaki, 2007). This discrepancy between Ca^{2+}-dependent regulation of long-lasting intracellular processes without the cytotoxic effects of Ca^{2+} is overcome by cells showing cyclical increases in $[Ca^{2+}]_c$. Ca^{2+} oscillations have been observed in different cell types such as, pancreatic β-cells (Bertram *et al.*, 2010; Liu *et al.*, 1998), human embryonic kidney cells (Bird *et al.*, 2005; Thurley *et al.*, 2011), vascular endothelial cells (Zhu *et al.*, 2008), airway smooth muscle cells (Perez *et al.*, 2005) and hepatocytes (Rooney *et al.*, 1990). In non-excitable cells, Ca^{2+} oscillations are typically initiated by PLC-coupled receptors followed by cycles of reuptake and release from the ER. In these cases, Ca^{2+} entry is mediated by SOCE to sustain Ca^{2+} oscillations (Bird *et al.*, 2005; Wedel *et al.*, 2007). Whereas, in excitable cells, for example, pancreatic β-cells and cardiomyocytes, frequent increases in $[Ca^{2+}]_c$ are caused by cyclic depolarizations of PM localised VOC (Bers, 2002; Liu *et al.*, 1998).

PLC-evoked Ca^{2+} oscillations involve cyclical Ca^{2+} release and sequestration, to and from intracellular stores. The exact mechanism is not entirely understood, but two models have been proposed (Sneyd *et al.*, 2006). In the first model, $[Ca^{2+}]_c$ controls IP_3

formation by regulating PLC activity. Therefore, the Ca^{2+} oscillations are in synchrony to the changes in IP_3 concentration. In the second model, $[Ca^{2+}]_c$ controls its release from the ER by directly decreasing or increasing the IP_3R open probability at higher and low $[Ca^{2+}]_c$, respectively. Hence, Ca^{2+} oscillates in the presence of a continuously elevated IP_3 concentration. Furthermore, other studies have shown that Ca^{2+} oscillations occur both in the presence of oscillating and constant IP_3 concentration (Nash *et al.*, 2001), which suggests that the mechanism is most likely either receptor-specific or cell type-dependent.

Regardless of the fundamental feed-back mechanism, the temporal complexity of Ca^{2+} oscillations offers an encoding mechanism capable of controlling cellular processes, which not only depends on their frequency, but also on the duration and amplitude of the Ca^{2+} signals (Dolmetsch *et al.*, 1998; Thurley *et al.*, 2014). The complex temporal profile of Ca^{2+} signals, in combination with their delicate spatial control, further supports the versatility and specificity of Ca^{2+} as a second messenger.

1.2. cAMP as a second messenger

The 'second messenger' concept originated with the discovery of cAMP (Sutherland, 1970). Similar to Ca^{2+}, cAMP also regulates many cellular functions which include cell division, cell differentiation, gene transcription, and ion channel activity (Willoughby *et al.*, 2007). For cAMP, the mechanism of maintaining intracellular cAMP concentration is different from Ca^{2+}, synthesis of cAMP occurs mainly at the PM and its degradation occurs throughout the cytoplasm (Zaccolo *et al.*, 2002). Intracellular compartmentalization of cAMP is acquired by binding to different cAMP signalling components including phosphatases, protein kinase A (PKA), adenylyl cyclase (AC), phosphodiesterase (PDE) (Dessauer, 2009; Zaccolo, 2011).

So far there are ten AC isoforms are known, of which nine are membrane-bound and one is soluble. Each shows differential regulation and tissue distribution. All nine PM bound ACs have a similar structure, with two groups of six trans-membrane domains linked by a long cytosolic domain consisting of a highly conserved ATP-binding domain important for full AC activity (Willoughby *et al.*, 2007). Following activation of AC, cAMP is released locally and it is then recognised by various signalling pathways. The basal levels of cAMP are maintained by phosphodiesterases (PDE), which degrade cAMP to 5'-AMP.

There are three major cAMP signalling effectors (a) protein kinase A (PKA) (Walsh *et al.*, 1968), (b) exchange protein activated by cAMP (Epac) (de Rooij *et al.*, 1998), and (c) cyclic nucleotide-gated channels (CNGCs) (Nakamura *et al.*, 1987; Willoughby *et al.*, 2007). All three proteins contribute to the regulation of Ca^{2+}, but PKA and Epac play a significant role in release of Ca^{2+} from intracellular stores. PKA is the most common intracellular target for cAMP (Beavo *et al.*, 2002). Each PKA consists of two regulatory (R) subunits and two catalytic (C) subunits (Tasken *et al.*, 1997). Four R isoforms: RIα, RIβ, RIIα, RIIβ (Clegg *et al.*, 1988; Jahnsen *et al.*, 1986; Lee *et al.*, 1983; Scott *et al.*, 1987), and three C isoforms are known: Cα, Cβ, Cγ (Beebe *et al.*, 1990; Showers *et al.*, 1986; Uhler *et al.*, 1986). Each R subunit consists of two conserved cAMP-binding sites (Weber *et al.*, 1987) and a pseudo-substrate domain which inhibits the associated C subunit (Hofmann *et al.*, 1977; Poteet-Smith *et al.*, 1997). Near the N-terminal region of the RIIα subunit, there is a 44-residues long AKAP-binding domain (Carr *et al.*, 1991; Newlon *et al.*, 1997).

AKAPs belong to a family of scaffolding proteins of more than 20 members. Mostly they bind to RII isoforms, hence they target both type I and II PKA to specific sub-cellular organelles (Huang *et al.*, 1997). Binding of cAMP to PKA decreases the affinity of the R subunit for the C subunit. Consequently, the holoenzyme dissociates and the C subunits are released into the cytosol. AKAPs then regulate PKA-mediated phosphorylation of intracellular proteins and provide the way in which cAMP, via PKA, can regulate very specific cellular process.

Epac is also activated by increases in intracellular cAMP concentration (de Rooij *et al.*, 1998; Kawasaki *et al.*, 1998). Originally Epac was discovered while screening for cAMP-binding motifs and by homology to the Ras superfamily of guanine nucleotide exchange factors (GEFs) (de Rooij *et al.*, 1998; Kawasaki *et al.*, 1998). There are three types of Epac; Epac 1 (cAMP-GEFI) (de Rooij *et al.*, 1998; Kawasaki *et al.*, 1998), Epac 2 (cAMP-GEFII) (Kawasaki *et al.*, 1998) and Epac/cAMP-GEFI/II or Repac (related to Epac or guanine nucleotide exchange factor for RapI; GFR) (Ichiba *et al.*, 1999). Epac 1 comprises three domains; a cAMP domain (CBD), a guanine nucleotide-exchange domain and a dishevelled Eg1-10 pleckstrin (DEP) domain which supports Epac membrane localisation (de Rooij *et al.*, 2000; Kawasaki *et al.*, 1998; Rehmann *et al.*, 2003). Epac 2 has an extra CBD (de Rooij *et al.*, 2000; Ozaki *et al.*, 2000; Rehmann *et al.*, 2003), whereas, Repac does not have a CBD and is not therefore regulated by cAMP (Ichiba *et al.*, 1999). Binding of cAMP triggers the

guanine nucleotide exchange activity of the Epac, which subsequently activates Rap1 or Rap2, which are small ras-like GTPases (de Rooij *et al.*, 2000; de Rooij *et al.*, 1998; Kawasaki *et al.*, 1998; Mei *et al.*, 2002). It is anticipated that, in the absence of cAMP, Epac is in a conformation in which the CBD is folded upon the GEF domain. This inhibits the guanine nucleotide-exchange activity of the protein. Binding of cAMP then causes Epac to unfold and expose the GEF domain (de Rooij *et al.*, 2000; Rehmann *et al.*, 2003).

Regulation of Ca^{2+} release via Epac is independent of PKA. In the insulinoma cell lines INS-1E and clonal MIN-6 cells, glucagon-like-peptide 1 (GLP1) increased release of Ca^{2+} caused by Epac 2 linked activation of type 3 RyR (Kang *et al.*, 2001; Tsuboi *et al.*, 2003). In addition, agonists which stimulate cAMP-coupled receptors, such as the β_2-adrenoceptor, have also been shown to trigger release of Ca^{2+} (Schmidt *et al.*, 2001). cAMP, via Epac1, can activate Rap2B by enhancing its GTP loading. PLC_ε, which is stimulated by Rap2B, then catalyses formation of IP_3 and the subsequent release of Ca^{2+} from intracellular stores (Schmidt *et al.*, 2001)

CNGCs were first discovered in the PM of frog and toad rod outer segments. These channels are activated by both cGMP and cAMP with different potencies (Fesenko *et al.*, 1985; Haynes *et al.*, 1985; Nakamura *et al.*, 1987). While these channels allow the entry of Na^+ and Ca^{2+} into the cell, the ability of Ca^{2+} to block the entry of Na^+, indirectly supports the influx of divalent ions (Nakamura *et al.*, 1987). These channels play important roles in retinal photoreceptors, olfactory neurons and in heart by causing cAMP-mediated increases in $[Ca^{2+}]_c$ (Cukkemane *et al.*, 2011).

1.2.1. Cross talk between cAMP and Ca^{2+}

cAMP and Ca^{2+} pathways are not independent of each other. These two signalling pathways interact with each other at different levels and in a dynamic fashion (Bruce *et al.*, 2003; Siso-Nadal *et al.*, 2009). For example, oscillations in one messenger can instigate oscillation in the other (Gorbunova *et al.*, 2002; Willoughby *et al.*, 2006). In *Xenopus* spinal neurons, using mathematical modelling, it has been shown that cells are capable of generating their own characteristic patterns of Ca^{2+} and cAMP interaction, perhaps this allows cells to regulate uniquely their set of effector molecules such as transcription factors and kinases.

There are three main points where Ca^{2+} contributes to the modulation of cAMP levels: AC, PDE and GPCR. Through PKC, Ca^{2+} regulates phosphorylation and then desensitization of Gαs-coupled $\beta_{1/2}$-adrenoceptors (Guimond *et al.*, 2005), Ca^{2+} can alter AC activity (Cooper *et al.*, 1995) either by inhibiting (Dyer *et al.*, 2005) or by enhancing it (Wayman *et al.*, 1994). Ca^{2+} has also been reported to stimulate PDE activities (Sharma *et al.*, 1994). The family of ACs has been classified on the basis of their sensitivity to Ca^{2+}, where AC I, III, V, VI, VIII are Ca^{2+}- sensitive, and AC II, IV, VII are insensitive to Ca^{2+} (Willoughby *et al.*, 2007). In addition, different Ca^{2+}-sensitive ACs do not show similar sensitivity, AC VIII (Fagan *et al.*, 2000), AC I (Wayman *et al.*, 1994) and perhaps AC III (Dyer *et al.*, 2005) show increases in activity in the presence of Ca^{2+}, whereas AC V and VI activity are inhibited upon the entry of Ca^{2+} (Chiono *et al.*, 1995; Yu *et al.*, 1993).

PKA is the predominant means by which cAMP controls Ca^{2+} levels. PKA can phosphorylate all three subtypes of IP_3R (Nakade *et al.*, 1994; Tang *et al.*, 2003; Tertyshnikova *et al.*, 1998). But most efficiently it phosphorylates IP_3R1, while IP_3R2 and IP_3R are weakly phosphorylated (Wojcikiewicz *et al.*, 1998).
However, PKA-mediated phosphorylation of IP_3R1 is also debatable; PKA decreases the potency of IP_3 to IP_3R, hence affects IP_3R1 mediated release of Ca^{2+} from cerebellar microsomes (Supattapone *et al.*, 1988; Volpe *et al.*, 1990), but enhances the sensitivity of immuno-purified and reconstituted cerebellar IP_3R to IP_3 (Nakade *et al.*, 1994). In permeabilised cells, PKA-mediated phosphorylation of native IP_3R, increases the sensitivity to IP_3 (Wojcikiewicz *et al.*, 1998). The reason underlying these differences is not clear, but probably indicates the loss of an essential protein during isolation of IP_3R that is required for the effect of PKA. Nevertheless, it is generally accepted that PKA phosphorylates and sensitises the IP_3R.

PKA-mediated phosphorylation of IP_3R2 most likely occurs at Ser^{1687} (Sudhof *et al.*, 1991; Yamamoto-Hino *et al.*, 1994). Hormones or sulfhydryl reagents potentiate cAMP levels, which then enhance the release of Ca^{2+} from IP_3-sensitive intracellular stores (Bird *et al.*, 1993; Burgess *et al.*, 1991). In parotid acinar cells, stimulation of AC using forskolin showed phosphorylation of IP_3R2 and potentiation of Ca^{2+} release by carbachol. These responses were attenuated by the inhibition of PKA or mimetic mutations (Bruce *et al.*, 2002). Hence, it is confirmed that PKA phosphorylates IP_3R2 and thereby enhances its sensitivity to IP_3.

PKA phosphorylates rat IP_3R3 at three consensus sequences Ser^{934}, Ser^{1130} and Ser^{1457} (Blondel *et al.*, 1993) of which, Ser^{934} and Ser^{1130} are conserved within the human form of the IP_3R3 (Yamamoto-Hino *et al.*, 1994). However, the PKA effect on IP_3R3 is less clear in comparison to IP_3R1 and IP_3R2. In RINm5F cells an increase in IP_3R3 sensitivity to IP_3 is evoked by PKA-mediated phosphorylation (Wojcikiewicz *et al.*, 1998). Yet, others have indicated that PKA-mediated phosphorylation of the IP_3R blocks Ca^{2+} release (Giovannucci *et al.*, 2000; LeBeau *et al.*, 1999) by diminishing the open probability of intrinsic ion channels and by slowing the rate of IP_3-evoked Ca^{2+} release (Straub *et al.*, 2002).

PKA has also been shown to enhance the activity of RyR (Herrmann-Frank *et al.*, 1993). PKA-mediated phosphorylation and activation of RyR1 in skeletal and RyR2 in cardiac muscle is well established (Reiken *et al.*, 2003; Xiao *et al.*, 2006). In RyR1 channels, it is possibly via the dissociation of a FKBP12, which might also result in RyR channels gating stochastically rather than as an ensemble (Marx *et al.*, 1998). It is suggested that PKA and intracellular Ca^{2+} release channels form a signalling complex in combination with phosphatases that dephosphorylate the channels. For example, both peripheral and neuronal IP_3R1 and AKAP9 in combination are responsible for anchoring PKA to IP_3R1 (Tu *et al.*, 2004). The protein phosphatases, PP1 and PP2A, have been shown to from macro-molecular complexes with RyR1, RyR2 and IP_3R1 channels (DeSouza *et al.*, 2002; Marx *et al.*, 2001).

All three IP_3R subtypes are also directly regulated by high cAMP concentrations. cAMP increases the sensitivity of IP_3R to IP_3. It is suggested that cAMP either binds to a low-affinity binding site on IP_3R or to an IP_3R-associated protein (Tovey *et al.*, 2010; Tovey *et al.*, 2008). It was proposed that in HEK cells expressing parathyroid hormone receptor type 1(PTH_1R), adenylyl cyclase 6 (AC6) selectively communicated with IP_3R2 within AC6-IP_3R2 signalling junctions. These signalling junctions allow super-saturating concentrations of cAMP to directly sensitise IP_3R (Tovey *et al.*, 2008). These interactions are discussed further in chapter 3.

In some settings, cAMP affects release of Ca^{2+} by modulating the activity of PLC. In cardiac myocytes, stimulation of β-adrenoceptors evokes an increase in cAMP levels; the enhanced cAMP, through Epac-mediated activation of Rap1, increases PLC_ε activity and Ca^{2+} mobilisation (Oestreich *et al.*, 2007). In primary gastric smooth muscle cells, PKA by phosphorylating G-protein coupled receptor kinase-2 (GRK2) and RGS4 proteins enhances the capacity of these proteins to block Gαq resulting in

attenuation of PLCβ1 activity (Huang *et al.*, 2007). PKA-mediated phosphorylation of mouse prostacyclin receptors uncouples these receptors from Gq and thereby prevents PLC activation (Lawler *et al.*, 2001).

Increased cAMP levels indirectly regulate the activity of the Ca^{2+} pumps, SERCA and PMCA. The activity of SERCA proteins is inhibited by phospholamban in cardiac muscle cells. This inhibition is reversed by PKA-mediated phosphorylation of phospholamban (Brittsan *et al.*, 2000). In contrast, stimulation with G protein Rap1b constitutively activates SERCA proteins in platelets and megakaryocytes, PKA-mediated phosphorylation of Rap1b dissociates it and thereby decreases SERCA activity. PKA mediates phosphorylation of PMCA, thus enhancing its activity, by increasing its affinity for Ca^{2+}-calmodulin (Dean *et al.*, 1997; Gromadzinska *et al.*, 2001). In addition, increased cAMP concentrations also affect some Ca^{2+} entry channels. These channels are regulated by PKA-mediated phosphorylation. In cardiac myocytes, stimulation of β-adrenoceptors increases L-type Ca^{2+} channel activity and this is by AKAP79-tethered PKA-mediated phosphorylation (Gao *et al.*, 1997).

Further specific details of Ca^{2+} signalling in pancreatic β-cells (Chapter 2) and of the interplay between PTH, cAMP and Ca^{2+} signals (Chapters 3 and 4) are discussed in subsequent chapters.

1.3. Aims of the projects

Previous findings in this lab reported that, in RINm5F cells, a small number of RyR are localised in the PM and contribute to Ca^{2+} entry. In addition, several lines of evidence suggest that RyR may contribute to regulated insulin secretion (Johnson *et al.*, 2004; Takasawa *et al.*, 2010). All these observations encouraged me to define the presence and role of RyR in pancreatic-β cells. Since, RINm5F cells do not secret insulin, I have used INS-1E cells; these cells are reported to secrete insulin (Merglen *et al.*, 2004). Therefore, the primary aim of the work illustrated in Chapter 2, was to characterise Ca^{2+} entry and release pathways mediated by RyR in INS-1E cells.

Ca^{2+} signalling from IP_3R has been studied in HEK cells expressing PTH_1R. Previously, work from this lab proved that acute pretreatment with PTH stimulates AC via PTH_1R and potentiates IP_3-evoked Ca^{2+} signals, which were suggested to be mediated by AC-IP_3R signalling junctions (Tovey *et al.*, 2008). In addition, in a recent study, binding of PTH to PTH_1R at the plasma membrane was shown to stimulate internalisation of PTH_1R-AC signalling complexes, which then continue cAMP formation via AC for sustained durations (Ferrandon *et al.*, 2009). These results encouraged me to explore the effect of prolonged PTH(1-34) stimulation on carbachol - evoked Ca^{2+} responses.

DM, also known as gestational diabetes, occurs when pregnant women with no past history of diabetes develop a consistent increase in blood glucose levels. Patients with type 3 DM recover after the birth of the baby.

2.1.2. Biogenesis of insulin

Insulin was the first protein to have its amino acid sequence determined by Fred Sanger in 1958 (Sanger, 1988). It is produced and secreted into the plasma from β-cells in pancreatic islets of Langerhans (Seino *et al.*, 2010). In addition to β-cells, the islets of Langerhans also contain α-cells that produce glucagon, δ-cells that produce somatostatin, and γ-cells producing pancreatic polypeptide (Elayat *et al.*, 1995). Besides insulin secretion, β-cells also secrete C-peptides and amylin. The amount of C-peptide secreted from β-cells is similar to insulin levels. The basic role of C-peptides is to connect insulin chain A with chain B (described in next paragraph) (Munro *et al.*, 1987). Amylin also called islet amyloid polypeptide primarily slowdowns the rate of glucose entry into the bloodstream (Nishi *et al.*, 1990).

Insulin is composed of two polypeptide chains: chain A and chain B have 21 and 30 amino acid residues, respectively, in humans. The chains are linked by two disulphide bridges between residues A7 to B7 and A20 to B19 (Sanger, 1959; Sanger, 1950). However, in pancreatic β-cells primarily insulin is synthesized as a single polypeptide chain known as preproinsulin. It consists of a 24 amino acid signal peptide which orients the nascent polypeptide chain to the ER. Subsequently, after translocating into the lumen of the ER, preproinsulin is cleaved and forms proinsulin. In the lumen of ER, proinsulin folds into 3D conformation by forming three disulfide bonds (Huang *et al.*, 1995). After~5–10 min proinsulin assembles in the ER and moved to the trans-Golgi network (TGN) where immature insulin granules are formed. Transport of proinsulin to the TGN takes ~30 min. Maturation of proinsulin into active insulin occurs by the action of cellular endopeptidases called prohormone convertases and the exoprotease carboxypeptidase E (Fu *et al.*, 2013; Steiner *et al.*, 1967). The endopeptidases cleave proinsulin at 2 positions, one fragment is called C-peptide and another is active insulin consisting of chain A and B, linked by 2 disulfide bonds. Consequently, the mature insulin is enclosed inside mature granules waiting for metabolic signals to be exocytosed from the cell into plasma. Usually the increase in blood plasma glucose concentration stimulates insulin secretion. Once an insulin

molecule binds to insulin receptor (IR) and triggers protein activation cascade, predominantly it is released back into the extracellular fluid or degraded by the cell. The primary sites for insulin degradation are liver and kidney cells (Adrogue, 1992; Duckworth *et al.*, 1998; Mak *et al.*, 1992).

In humans, insulin instigates cellular responses by binding to the insulin receptor (IR). These receptors are transmembrane, multi-subunit glycoproteins which contain insulin-stimulated tyrosine kinase activity (Kaplan, 1984; Robinson *et al.*, 2000). The localisation of insulin receptors is variable, with the highest levels of expression in cells that are most responsive to insulin for glucose, lipid, and proteins especially adipose, skeletal muscle, and liver (Goren, 2005; Henquin *et al.*, 2003; Kang *et al.*, 2008). The insulin receptor was first identified over 25 years ago, its cDNA was cloned in 1985. The crystal structure of its extracellular domain and protein tyrosine were determined in 2006 (Lou *et al.*, 2006) and 1994 (Hubbard *et al.*, 1994) respectively. In mammals, the functional IR exists in two isoforms insulin receptor-A (IR-A) and insulin receptor B (IR-B), which results from alternative splicing of the initial transcript. The most significant functional difference among these two IR isoforms is the high affinity of IR-A for insulin like growth factor II (IGF-II). Largely IR-A is expressed during prenatal stages, it amplifies the effect of IGF-II during foetal development and embryogenesis. In addition to this, IR-A is also significantly expressed in adult tissue particularly in brain tissue. Conversely, IR-B is primarily expressed in adults, well-differentiated tissues, including liver, where it increases the metabolic effects of insulin (Belfiore *et al.*, 2009). Alteration in IR isoform expression in insulin target cells is one of the primary reasons of developing insulin resistance in DM-2. In few studies it is reported that expression of IR-A is increased in insulin target tissues from DM-2 patients, therefore suggesting that alteration in expression levels of IR isoforms may contribute to insulin resistance (Sesti *et al.*, 2001).

2.1.3. How does insulin secretion take place in pancreatic β-cells?

Glucose-stimulated insulin secretion (GSIS) from β-cells is biphasic. The first phase of insulin secretion peaks about 5-6 min after a rise in the plasma concentration of glucose. It is thought to be due to rapid release of a primed pool of readily releasable insulin-containing granules situated at the plasma membrane (Caumo *et al.*, 2004). The local sub-plasma membrane increase in $[Ca^{2+}]_c$ caused by opening of L-type Ca^{2+}

channels triggers exocytosis of these vesicles. The second phase of insulin release is slower and persists for as long as the plasma glucose concentration remains elevated. It requires refilling of insulin vesicles, translocation of granules from reserve pools to the PM, and Ca^{2+} signals to evoke exocytosis (Bratanova-Tochkova *et al.*, 2002; Islam, 2010; Schulla *et al.*, 2003).

Glucose enters β-cells via the GLUT transporter (GLUT-2 in kidney and bone cells or GLUT-1 in brain cells) in humans (Bertram *et al.*, 1998) and its oxidative metabolism increases the cytoplasmic ATP/ADP ratio (Spacek *et al.*, 2008). This causes closure of ATP-gated K^+ channels (K_{ATP}) in the PM, increasing membrane resistance and preventing K^+ from leaving the cell (Braun *et al.*, 2008). These changes, along with an unknown leak current, cause the PM to depolarise and activate $Ca_v1.2$ and $Ca_v1.3$, which then mediate Ca^{2+} influx. The rapid rise in $[Ca^{2+}]_c$ beneath the PM stimulates exocytosis of the large dense-core vesicles that contain insulin. This 'triggering pathway' is responsible for the first phase of insulin release (Islam, 2010; Schulla *et al.*, 2003). Its importance is clear from the clinical utility of the sulphonylurea drugs used to treat type 2 DM. These bind to K_{ATP} channels causing them to close and so mimic the effects of glucose on insulin secretion (Ashcroft, 2007). Figure 2.1. illustrates the triggering and amplifying pathways for insulin secretion in pancreatic β-cells.

Glucose can also stimulate insulin secretion independently of K_{ATP} channels. Glucose can, for example, stimulate some insulin release when subunits of the K_{ATP} channel are mutated or knocked out, or when they are locked open by diazoxide (with high-KCl to activate L-type channels) (Henquin, 2009; Reimann *et al.*, 1999; Seghers *et al.*, 2000; Tucker *et al.*, 1997). These K_{ATP} channel-independent pathways contribute most to the second phase of insulin secretion (Aizawa *et al.*, 1998; Henquin, 2009; Jacobson *et al.*, 2007). The mechanisms underlying these pathways are not clearly resolved. Evidence has been presented to implicate a volume-regulated anion channel (VRAC) (Best *et al.*, 2007), transient receptor potential channels (TRPM2) (Togashi *et al.*, 2006) and a variety of intracellular signalling molecules. These include cyclic AMP, which increases after glucose stimulation, and may activate protein kinase A (PKA) or exchange protein activated by cAMP (epac-2) to increase insulin secretion (Holz, 2004; Landa *et al.*, 2005; Leech *et al.*, 2010; MacDonald *et al.*, 2005; Straub *et al.*, 2001; Szaszak *et al.*, 2008).

Many additional signals modulate the responses of β-cells to glucose. Somatostatin and galanin suppress exocytosis of insulin granules by re-polarising the PM and so reducing $[Ca^{2+}]_c$ (Daunt *et al.*, 2006; Dufer *et al.*, 2004). Incretins, like glucagon-like peptide-1 (GLP-1) or gastric inhibitory polypeptide (GIP) potentiate the responses of β-cells to glucose via their ability to stimulate AC (Holst *et al.*, 2009). Exenatide (a synthetic exendin-4) is a stable analogue of GLP-1 that is now used to treat type 2 DM (Drucker, 2006a). GLP-1 also activates CD38 to catalyse synthesis of nicotinic acid adenine dinucleotide phosphate (NAADP) and cyclic ADP ribose (cADPR), NAADP stimulates Ca^{2+} release from acidic stores, and cADPR along with $[Ca^{2+}]_c$ acts as co-agonist to stimulate RyR to release Ca^{2+} . A global rise in $[Ca^{2+}]_c$ due to NAADP and cADPR triggers insulin secretion (Drucker, 2006; Holst *et al.*, 2008; Kim *et al.*, 2008; Ohta *et al.*, 2011). Ca^{2+} release from internal stores via RyR and IP_3R also contributes to a rise in $[Ca^{2+}]_c$ and stimulates insulin secretion from β-cells. (Islam, 2010; Islam, 2002).

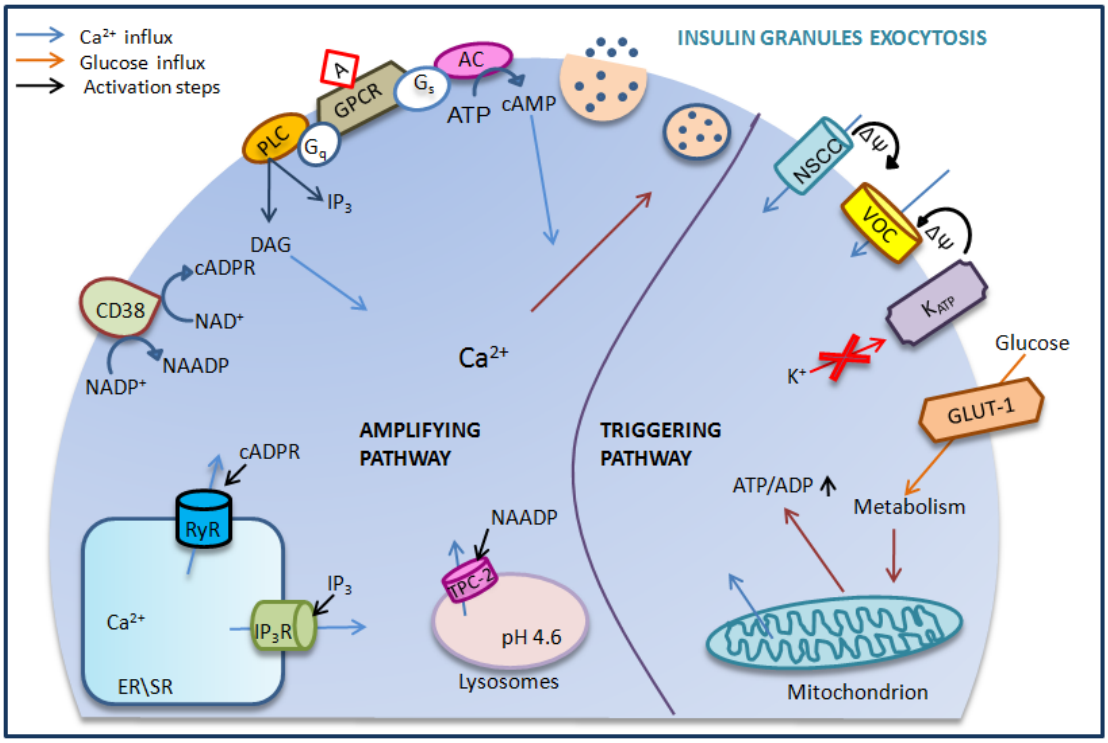

Figure 2.1. **Triggering and amplifying pathways for insulin secretion**
During the triggering pathway, glucose enters pancreatic β-cells via a transporter protein (GLUT-1). Glucose metabolism increases the ATP/ADP ratio, which causes the closure of K_{ATP} channels and opening of unknown non-selective cation channels (NSCC). This results in plasma membrane depolarisation (ΔΨ), opening of voltage-operated Ca^{2+} channels (VOC) and Ca^{2+} influx, which triggers exocytosis of insulin granules. During the amplifying pathway, agonist-induced G-protein-coupled receptor (GPCR) activation of Gs and Gq activate adenylyl cyclase (AC) and phospholipase C (PLC), respectively. AC catalyses the formation of cAMP, PLC leads to formation of IP_3 and DAG, which can stimulate release of Ca^{2+} from intracellular stores. CD38 catalyses formation of cADPR and NAADP, which also stimulate Ca^{2+} release from intracellular stores thus contributing to insulin exocytosis.

2.1.4. The role of ryanodine receptors in pancreatic β-cells

RyR are large proteins (four subunits of almost 5000 residues) that form Ca^{2+}-permeable non-selective cation channels (Giannini *et al.*, 1995; Islam, 2002; Otsu *et al.*, 1990). There are three subtypes (RyR1-3) that share ~60-70 % sequence similarity. Most studies suggest that β-cells express predominantly RyR2 and very few RyR1. RyR are expressed on ER and work from this laboratory suggests that RyR2 is also

expressed at the PM (Coronado *et al.*, 1994; Johnson *et al.*, 2004; Mitchell *et al.*, 2003; Rosker *et al.*, 2009). β-cells also express IP_3R (largely IP_3R3) (Johnson *et al.*, 2004), although the relative densities of IP_3R and RyR may differ between species. Mouse islets, for example, have very few IP_3R relative to RyR (Takasawa *et al.*, 1998).

Several lines of evidence suggest that RyR may contribute to regulated insulin secretion (Johnson *et al.*, 2004; Takasawa *et al.*, 2010). The ability of RyR to amplify, by Ca^{2+}-induced Ca^{2+} release, the Ca^{2+} signals evoked by L-type Ca^{2+} channels may allow them to contribute to the second phase of insulin release (Johnson *et al.*, 2004). RyR are regulated by many signals associated with glucose-and/or hormone stimulation of β-cells. Glucose increases both ATP and cADPR concentrations in β-cells, and both stimulate RyR (Kato *et al.*, 1999; Okamoto, 1999). Glucose and incretins stimulate increases in cAMP concentration in β-cells. Both PKA and Epac are implicated in the subsequent actions of cAMP (Kelley *et al.*, 2009; Leech *et al.*, 2010), and both regulate RyR (Holz, 2004; Holz *et al.*, 1999). In human islets, type 2 DM is associated with diminished expression of RyR2 and reduced levels of cADPR, whereas activation of RyR can trigger insulin secretion (Johnson *et al.*, 2004; Squires *et al.*, 2004; Takasawa *et al.*, 1998).

Most analyses of RyR in β-cells have assumed that their contributions come from mediating Ca^{2+} release from intracellular Ca^{2+} stores, but recent work from this laboratory provided evidence that small numbers of functional RyR2 are also expressed in the PM of RINm5F insulinoma cells and perhaps also in primary β-cells (Rosker *et al.*, 2009). The contribution of these RyR in the PM to insulin secretion or glucose-evoked Ca^{2+} signals is unknown, but they may contribute to regulation of both membrane potential and Ca^{2+} entry.

2.1.4. Aims

The aim of my project was to define the presence and role of RyR in pancreatic β-cells. The most convincing evidence for functional expression of RyR in the PM is provided by analyses of rat insulinoma cells (RINm5F cells) (Rosker *et al.*, 2009), but these are a poor model for β-cells because they do not secrete insulin in response to glucose.

For my work, I have used INS-1E cells, which have been reported to show important characteristics of pancreatic β-cells, like glucose responsiveness and insulin secretion between passages 40-100 (Merglen *et al.*, 2004). Originally, the parental cell line INS-1 was isolated from a rat insulinoma induced by X-ray irradiation (Asfari *et al.*, 1992). During expansion however, it was noted that INS-1 cells lacked a stable β-cell phenotype, owing to their non-clonal nature. Merglen and co-workers overcame these problems in 2004, by isolating a clonal INS-1E cell line, which showed stable and robust secretory responses to physiological changes in glucose concentrations (Merglen *et al.*, 2004). Furthermore, INS-1E cells respond to GLP-1 resulting in an increase in cAMP (Henquin *et al*, 2003) and they can be reliably transfected and loaded with fluorescent Ca^{2+} indicators (Woolcott *et al*, 2006).

The aim of the work described in chapter 2 was to characterise different Ca^{2+} entry and Ca^{2+} release pathways mediated by RyR in INS-1E cells. In addition to this, basic glucose-evoked Ca^{2+} oscillations were characterised in primary mouse pancreatic islets of Langerhans to determine their potential for use as a model to study RyR.

2.2. Materials and Methods

2.2.1 Materials

Table 2. 1. Lists the sources of the materials used. Table 2. 2 shows the list of solvents used to prepare different drugs.

Material	**Provider**
Caffeine	Sigma-Aldrich (Poole)
Pluronic acid	Sigma-Aldrich (Poole)
DMSO	Sigma-Aldrich (Poole)
Carbachol	Sigma-Aldrich (Poole)
Nimodipine	Sigma-Aldrich (Poole)
Foetal bovine serum (FBS)	Sigma-Aldrich (Poole)
Poly-L-lysine	Sigma-Aldrich (Poole)
Penicillin (100 U/ml) & streptomycin (100 μg/ml) solution	Sigma-Aldrich (Poole)
Amphotericin B	Sigma-Aldrich (Poole)
Ionomycin	Merck Euro Lab Ltd (Dorset).
Ryanodine	Ascent Scientific (Bristol)
Fura-2AM	Invitrogen (Paisley)
TryplExpress	Invitrogen (Paisley)
Advanced RPMI 1640 medium	Invitrogen (Paisley)
L-glutamine	Invitrogen (Paisley)
HEPES	Invitrogen (Paisley)
β mercaptoethanol	Invitrogen (Paisley)
Soybean trypsin inhibitor	Invitrogen (Paisley)
Collagenase P	Roche Applied Science (Welwyn Garden City)
DNase	Roche Applied Science (Welwyn Garden City)
RPM1 1640 medium	Invitrogen Ltd (Renfrew, Renfrewshire)
Collagen	Sigma-Aldrich (Poole)
poly-D-lysine	Sigma-Aldrich (Poole)
Gelatin	Sigma-Aldrich (Poole)
Fibronectin	Sigma-Aldrich (Poole)
BD Cell Tak	BD biosciences (Oxford)

Table 2.1. **Materials used**

Drugs	Solvent	Storage (°C)
Caffeine	Water (50 mM stock)	4
Carbachol (CCh)	Water (100 mM stock)	4
Ionomycin	DMSO (5 mM stock)	-20
Pluronic acid	Water (20 % stock)	20
Nimodipine	DMSO (10 mM stock)	4
Nimodipine	Methanol (10 mM stock)	4
Verapamil	Water ((10 mM stock)	4
Ryanodine	DMSO (100 mM stock)	-20

Table 2.2 **Solvents used to prepare drugs**

2.2.2. INS-1E cell culture

The rat insulinoma INS-1E cell line (passage 53) was kindly provided by Professor Pierre Maechler (Geneva, Switzerland) (Merglen *et al.*, 2004). INS-1E cells were maintained at 37 °C in humidified air containing 5% CO_2 and cultured in advanced RPMI 1640 medium containing 11 mM D-glucose supplemented with heat-inactivated foetal bovine serum (5%), L-glutamine (2 mM), sodium pyruvate (1 mM) HEPES (10 mM), and β-mercaptoethanol (50 μM). INS-1E cells were passaged at 80% confluence, and medium was replaced every third day. For single-cell analyses, cells were seeded (8 x 10^5 cells/well), and allowed to attach onto 22-mm round glass coverslips, each pre-coated with 0.01% poly-L-lysine for 48 h before performing experiments. For population-based assays, cells were seeded (50 x 10^6 cells/well) and allowed to grow for 48 h before experiments.

2.2.3. Mouse pancreatic islet isolation and primary culture

Pancreatic islets of Langerhans were isolated from male C57BL6 mice (12-weeks old) that were humanely sacrificed using Schedule 1 methods according to Home Office-approved procedures. Mice were killed by exposure to a rising concentration of CO_2 followed by dislocation of the neck. The pancreas and spleen were surgically removed *en bloc* and washed in ice-cold HEPES-buffered Krebs-Ringer phosphate buffer

containing 0.4% bovine serum albumin (KRH 0.4% BSA) composed of (mM): 129 NaCl, 5 $NaHCO_3$, 4.8 KCl, 1.2 KH_2PO_4, 1.2 $MgSO_4$, 2.5 $CaCl_2$, 5.6 glucose, 10 HEPES and 0.4% BSA (pH 7.4, NaOH). The spleen and any fat were excised from the pancreas, and the pancreas was further washed in fresh KRH 0.4% BSA. Each pancreas was partially digested by inflating it with 5 ml of ice-cold digest cocktail comprising KRH 0.4% BSA supplemented with collagenase P (0.85 mg/ml) and DNase I (0.1 mg/ml), soybean trypsin inhibitor (2.5 mg/ml) using a syringe and 30-gauge needle. Both the inflated pancreas and remaining digest cocktail were transferred into a 50-ml centrifuge tube and incubated in a water bath at 37°C for 14 min. This was followed by a vigorous shake for 1 min. The pancreas suspension was assessed by eye to ensure islets were disassociated from the exocrine tissue. If the tissue dissociation procedure was incomplete, the pancreas suspension was returned to the 37°C water bath for repeated cycles of 1 min in the water bath followed by a vigorous manual shake for 1 min until the pancreas digestion was complete (cloudy suspension free of large pieces of pancreatic tissue). The pancreatic tissue was then washed 3 times in 50 ml ice-cold KRH with 0.4% BSA by centrifuging the pancreas suspension at 4°C for 2 min at 150 x *g*. The supernatant was discarded between washes, and the remaining pellet (after completed wash steps) was re-suspended in 10 ml of ice-cold KRH with 0.4% BSA. Islets were easily distinguished as small dense oval structures, and separated manually from any exocrine tissue using a Leica MS5 stereomicroscope and a P200 Gilson pipette. Isolated islets were allowed to recover overnight by culturing in RPMI 1640 medium containing 11 mM D-glucose supplemented with heat-inactivated FBS (10%), penicillin (100 U/ml), streptomycin (100 µg/ml), and amphotericin B (0.25 µg/ml) at 37°C in a 5% CO_2 humidified atmosphere in suspension culture dishes. For measurements of $[Ca^{2+}]_c$, islets were allowed to attach to the central part of poly-L-lysine (0.01%)-coated 25-mm round glass coverslips for 24 h under the culture conditions mentioned above (Carter *et al.*, 2009)

2.2.4. Measurement of $[Ca^{2+}]_c$ in single INS-1E cells

Fura-2, a ratiometric Ca^{2+} indicator (Grynkiewicz *et al.*, 1985), was used to measure $[Ca^{2+}]_c$ in INS-1E cells as described in Rosker *et al.* (2009). Almost confluent cultures of INS-1E on 22-mm round, poly-L-lysine-coated coverslips were loaded with fura-2/AM (final concentration 2 µM, from a stock solution of 2 mM in DMSO, 45 min,

20°C) by incubation in KRH supplemented with Pluronic F127 (0.02%), washed and incubated for a further 45 min in KRH to allow de-esterification of the indicator. All experiments were performed in Krebs-Ringer bicarbonate HEPES buffer KRH, or Ca^{2+}-free KRH. KRH had the following composition: 137 mM NaCl, 5.36 mM KCl, 0.81 mM $MgSO_4$, 0.34 mM Na_2HPO_4, 0.44 mM KH_2PO_4, 1.26 mM $CaCl_2$, 4.17 mM $NaHCO_3$, 10 mM HEPES, 3 mM glucose, pH 7.4. $CaCl_2$ was omitted from Ca^{2+}-free KRH and 1 mM EGTA was added.

Single-cell measurements of $[Ca^{2+}]_c$ were performed in KRH at 20°C using an Olympus IX71 inverted fluorescence microscope. The cells were alternately excited at 5-s intervals with light (340 nm and 380 nm) provided by a Xe-arc lamp and monochromator, while collecting emitted light at 510 nm using a Luca EMCCD camera (Andor Technology, Belfast, UK). At the end of each experiment, the autofluorescence of cells was determined by quenching the fura-2 fluorescence by addition of ionomycin (1 µM) and $MnCl_2$ (10 mM). These autofluorescence values were subtracted from each fluorescence measurement at 340 nm and 380 nm before computing fluorescence ratios (F_{340}/F_{380}). MetaFluor software was used for the collection and analysis of fluorescence data. Each cell within a field was defined by a circular region of interest (ROI). Fluorescence from each ROI was analysed separately. Fluorescence ratios were calibrated to $[Ca^{2+}]_c$ using equation 2.1 (Grynkiewicz *et al.*, 1985):

$$[Ca^{2+}]_c = K_D \times \frac{(R-R_f)}{(R_b-R)} \times \frac{F_f}{F_b} \qquad \text{equation (2.1)}$$

Where K_D is the equilibrium dissociation constant of fura-2 for Ca^{2+} (220 nM), R the F_{340}/F_{380} determined in the cells, R_f is the F_{340}/F_{380} ratio in Ca^{2+}-free conditions; R_b is the ratio in saturating Ca^{2+}; F_f and F_b are the fluorescence intensities at 380 nm for Ca^{2+}-free and Ca^{2+}-saturated indicator, respectively. Calibrated results are presented as either $[Ca^{2+}]_c$ or $\Delta[Ca^{2+}]_c$ (i.e. the difference between $[Ca^{2+}]_c$ before and after stimulation). Results are expressed as means ± SEM.

2.2.5. Three sequential stimulations protocol

To determine the effects of one treatment (e.g., removal of extracellular Ca^{2+}) on the response to another treatment (e.g., addition of caffeine), the same cells were sequentially treated three times with the same stimulus, which was combined with the additional treatment during the second stimulation. The protocol allowed the control

response, the affect of the second treatment, and its reversibility to be conveniently measured.

Fura-2-loaded INS-1E cells were prepared for imaging (Section 2.2.4) and bathed in KRH (500 µl). The medium was removed and replaced with KRH containing the stimulus. After 5 min, the medium was removed, the cells were washed 3 times with KRH and incubated in the alternative medium (e.g., KRH, Ca^{2+}-free KRH) for 10 min. This medium was then removed and replaced with the same modified medium, but with the stimulus present. After 5 min, this medium was removed, the cells were washed in KRH, and they were again treated in KRH containing the first stimulus (conditions that exactly match the first stimulation). The methods used to record and calibrate fluorescence signals are described in Section 2.2.4. Figure legends describe the exact treatments.

2.2.6 Statistical analyses

The statistical analyses was performed at two levels because each experiment result consists of data collected from 3 independent coverslips, in which each coverslip consisted of ≥ 30 cells. Subsequently, one-way ANOVA analysis was also applied at two stages firstly to compare data collected between individual cells on each day, then on individual coverslips. Further, a Tukey post hoc test was used to compare all possible pair of means i.e. difference between first, second and third stimulation responses. One-way ANOVA was used because it allows one to separate the contribution of within-treatment variability and between treatment variability to the overall variance, and so to resolve whether difference between-treatment account for more variability than expected from the within-treatment variability.

2.3. Results

2.3.1. Mechanism of Ca^{2+} release in INS-1E cells

In most cell types, Ca^{2+} release from intracellular stores occurs via IP_3R and RyR (Foskett *et al.*, 2007; Lanner *et al.*, 2010) (Section 1.1.2). Similarly, in INS-1E cells, Ca^{2+} release from intracellular stores has been shown to be mediated via both RyR and IP_3R (Gamberucci *et al.*, 1999; Woolcott *et al.*, 2006). The aim for this study was to further validate previous findings, in addition to characterising whether these Ca^{2+}

release channels were functional in INS-1E cells. If so, this glucose-responsive insulinoma INS-1E cell line could then be used to investigate the roles of both RyR and IP_3R in insulin secretion. Caffeine was used to stimulate Ca^{2+} release through RyR as it has been reported that the ER of INS-1 cells expresses caffeine-sensitive RyR2 (Gamberucci *et al.*, 1999; Woolcott *et al.*, 2006). Carbachol (CCh, an agonist of muscarinic acetylcholine receptors) was utilised to stimulate Ca^{2+} release via IP_3R. CCh activates PLC, production of IP_3 and hence Ca^{2+} release from intracellular stores via IP_3R (Blondel *et al.*, 1993; Woolcott *et al.*, 2006).

A stimulation protocol was designed where INS-1E cells were sequentially challenged 3 times for durations of 5 min each with either caffeine or CCh in medium containing a basal non-stimulatory glucose concentration (3 mM), allowing a recovery period of 10 min between each challenge (Section 2.2.5). Caffeine reproducibly evoked an increase in $[Ca^{2+}]_c$ (Fig. 2.2A, D), in response to 3 successive challenges which were not significantly different. The peak rise in $[Ca^{2+}]_c$ ($\Delta[Ca^{2+}]_c$) evoked by caffeine was: 150 ± 19 nM, 120 ± 27 nM and 136 ± 17 nM, for the first, second and third challenges, respectively. CCh evoked a rise in $[Ca^{2+}]_c$ of 177 ± 31 nM, 147 ± 25 nM and 130 ± 14 nM for challenges one, two and three, respectively (Fig. 2.3A, C). These results suggested that both caffeine and CCh evoked robust increases in $[Ca^{2+}]_c$, thus making this three sequential stimulation protocol (Section 2.2.5) suitable for determining the effects of other manipulations (including antagonists, other stimuli, and the requirement for extracellular Ca^{2+}).

To examine the effects of extracellular Ca^{2+} on responses to caffeine or CCh, cells were first stimulated with caffeine or CCh, then normal KRH was exchanged for Ca^{2+}-free KRH containing EGTA (Fig. 2.2B, 2.3B) 30-s before the second challenge with CCh or caffeine in Ca^{2+}-free conditions; the extracellular Ca^{2+} was then restored prior to the third challenge. The data suggest that removal of extracellular Ca^{2+} reversibly attenuates the response to caffeine (Fig. 2.2B, E). The response to caffeine ($\Delta[Ca^{2+}]_c$) was 60 ± 10 nM in the absence of extracellular Ca^{2+}, but in its presence the responses were 163 ± 19 nM (first challenge) and 139 ± 20 nM (third challenge). Similarly, the response to CCh was 73 ± 22 nM in the absence of extracellular Ca^{2+}, but in its presence the responses were 183 ± 7 nM (first challenge) and 123 ± 26 nM (third challenge) (Fig. 2.3B, D). The two responses in the presence of extracellular Ca^{2+} were not statistically different. These results suggests that both caffeine and CCh can

stimulate release of Ca^{2+} from intracellular stores, but a significant component of the response requires extracellular Ca^{2+}.

When responses to caffeine in Ca^{2+}-free medium containing EGTA were studied (Fig. 2.2B, second peak), there was a sustained decrease in basal $[Ca^{2+}]_c$. Perhaps, the presence of EGTA in the Ca^{2+}-free KRH caused excessive loss of Ca^{2+} from the cells during the relatively prolonged incubation. This was potentially masking the profile of caffeine-evoked responses in Ca^{2+}-free conditions. Therefore, a further experiment was designed to overcome this potential problem. The experiment was repeated, but 2 min prior to the second challenge with caffeine, cells were bathed in Ca^{2+}-free KRH without EGTA (Fig 2.2C, second peak). After studying data from 89 cells, it was confirmed that the absence of EGTA in the Ca^{2+}-free KRH abolished the sustained decrease in basal $[Ca^{2+}]_c$ during caffeine responses in Ca^{2+}-free conditions (Fig. 2.2C, F, second peak). However a further complication was noted in that the third challenge to caffeine was now significantly lower than the first caffeine challenge. The problem with variability in the Ca^{2+} responses of INS-1E cells will be addressed later (Section. 2.3.3)

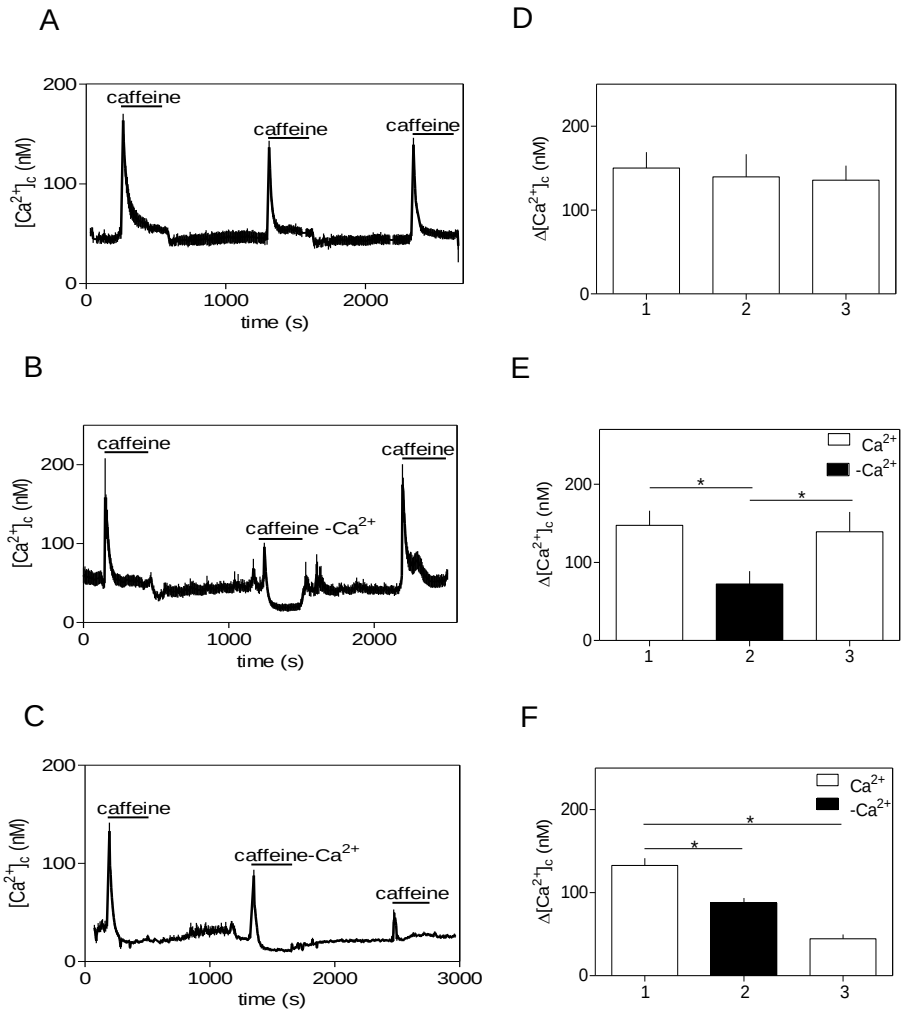

Figure 2.2. **Caffeine-evoked Ca^{2+} signals in INS-1E cells**

(**A, B, C**), Representative traces, from 37, 15 and 37 cells in 1 experiment respectively, show three successive stimulations with caffeine (10 mM, 5 min, with 10 min intervals between stimuli) in normal KRH (**A**) or in Ca^{2+}-free KRH with EGTA for the second challenge (**B**), or in Ca^{2+}-free KRH for the second challenge (**C**). (**D**, **E**, **F**) Summary results show the peak (after ~30-35s) increase in $[Ca^{2+}]_c$ ($\Delta[Ca^{2+}]_c$) evoked by caffeine (first, second and third challenge) (**D**), caffeine in Ca^{2+}-free KRH with EGTA (second challenge) (**E**) and caffeine in Ca^{2+}-free KRH (second challenge) (**F**) for each of the three challenges in each set of experiments. Results in D, E and F include only cells that responded to the first addition of caffeine (71%, 78% and 60% in D, E and F, respectively), and show means ± SEM from 3 independent experiments, with ~85, ~108 and ~60 cells analysed, respectively. $^{*}P < 0.05$ with one-way analysis of variance and Tukey multiple comparisons test.

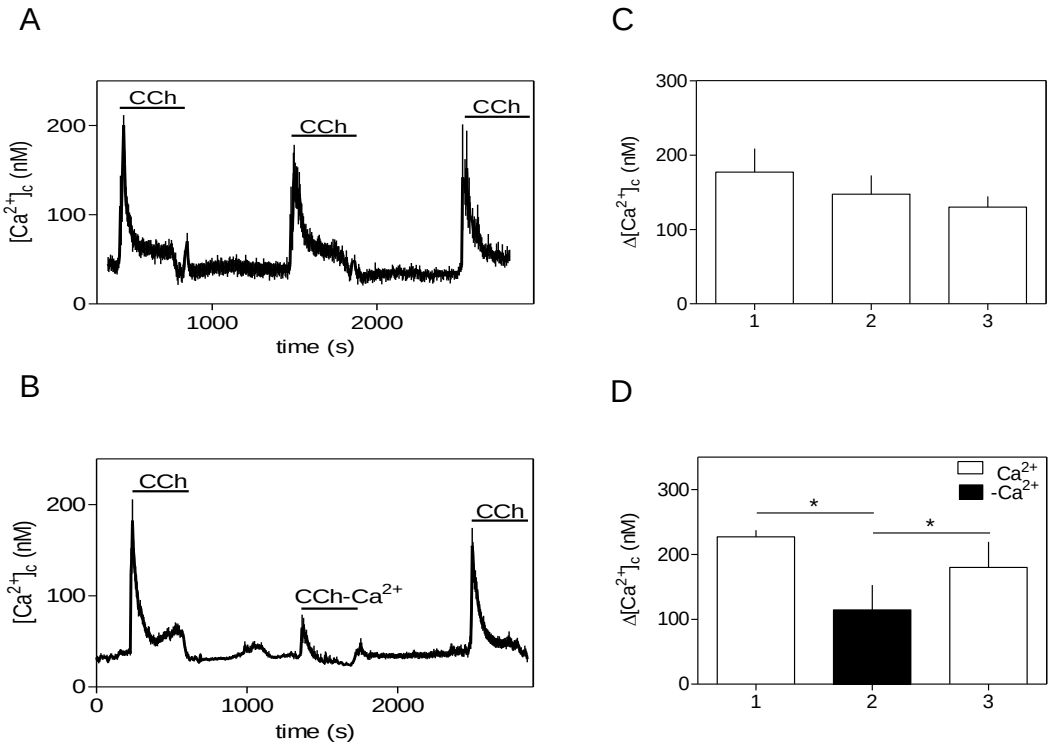

Figure 2.3. **CCh-evoked Ca^{2+} signals in INS-1E cells.** (**A, B**) Representative traces, from 10 and 21 cells from 1 experiment respectively, show three successive stimulations with CCh (100 µM, 5 min, with 10-min intervals between stimuli) in normal KRH (**A**) or in Ca^{2+}-free KRH for the second CCh challenge. (**C**, **D**) Summary results show the peak (after ~30-35s) increase in $[Ca^{2+}]_c$ evoked ($\Delta[Ca^{2+}]_c$) by CCh (first, second and third challenge) (**C**), or CCh in Ca^{2+}-free KRH (second challenge) (**D**), for each of the three challenges in each set of experiments. Results in C and D include only cells that responded to the first addition of CCh (70% and 69% in C and D, respectively), and show means ± SEM from 3 independent experiments, with ~79 and ~72 cells analysed, respectively. $^{*}P < 0.05$ with one-way analysis of variance and Tukey multiple comparisons test.

Subsequent experiments assessed the Ca^{2+}-dependence of the caffeine and CCh responses, and whether RyR had a role. In order to elucidate a role for RyR, the plant alkaloid, ryanodine, was used. Ryanodine inhibits RyR at micromolar concentrations in a use-dependent manner (Rousseau *et al.*, 1987; Smith *et al.*, 1988). The three sequential stimulus protocol was used with slight changes. Following the initial caffeine stimulus, cells were incubated alternatively with ryanodine (Fig. 2.4A, D) or

its solvent control, DMSO (Fig. 2.4C). The caffeine-evoked Ca^{2+} responses to the second and third challenges were therefore carried out in the presence of ryanodine to allow for its use-dependence. The response to caffeine added with ryanodine ($\Delta[Ca^{2+}]_c$) was 48 ± 20 nM (second challenge) and -12 ± 3 nM (third challenge). These responses were significantly lower than those to caffeine alone 161 ± 20 nM (first challenge). The two response in the presence (second challenge) and absence (first challenge) of ryanodine were significantly different (Fig. 2.4D), whereas, with DMSO there was no attenuation in the caffeine-evoked Ca^{2+} response (Fig. 2.4C, B).

The effects of ryanodine were then tested on CCh-evoked Ca^{2+} responses in INS-1E cells (Fig. 2.5). Following the first stimulation with CCh, ryanodine was added in the presence of CCh for the second challenge, and removed before the third CCh challenge. The response to CCh with ryanodine ($\Delta[Ca^{2+}]_c$) was 82 ± 25 nM (second challenge), but CCh alone caused a rise in $[Ca^{2+}]_c$ of 108 ± 16 nM (first challenge) and 60 ± 33 nM (third challenge). Thus, the presence of ryanodine (Fig. 2.5A; second challenge) did not cause a significant change in the CCh-evoked Ca^{2+} response (Fig. 2.5A). However, a significant attenuation in the CCh-evoked Ca^{2+} response was noted in the third challenge with CCh alone (Fig. 2.5A).

These results show that ryanodine inhibits caffeine-evoked Ca^{2+} entry and release in a use-dependent manner. However, CCh-evoked Ca^{2+} responses remain unchanged in the presence of ryanodine specifically during the second challenge.

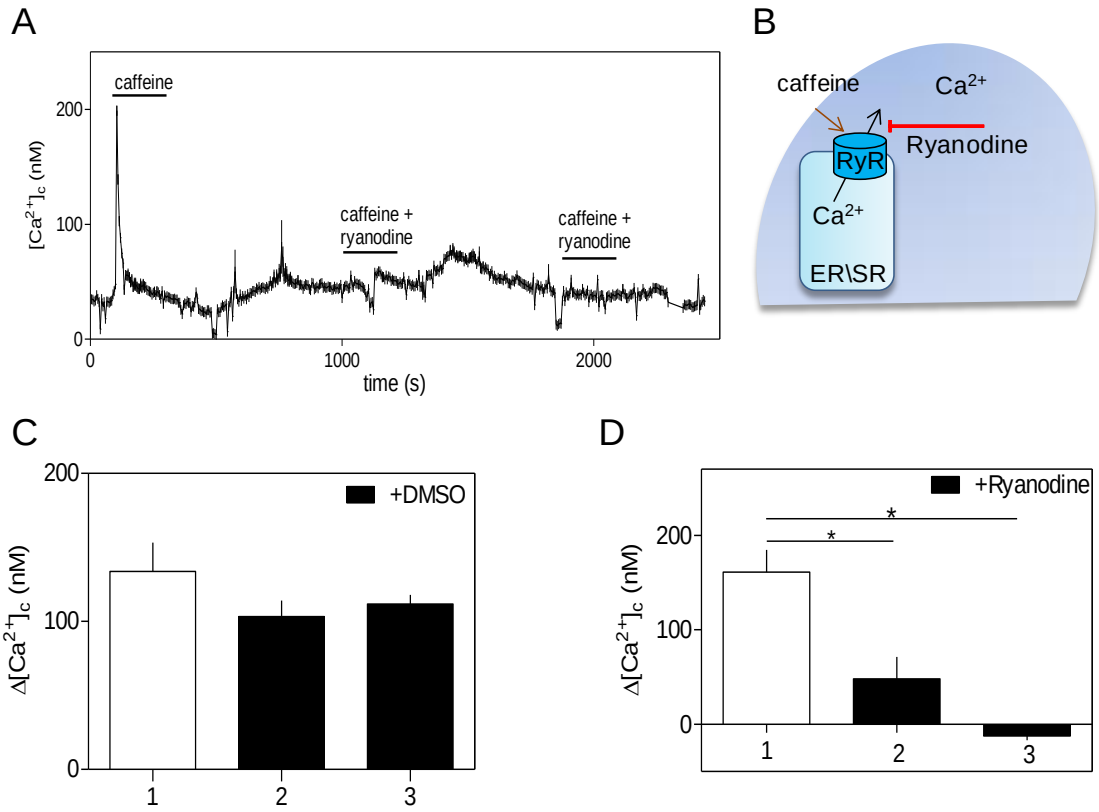

Figure 2.4. **Effect of ryanodine on caffeine-evoked Ca^{2+} signals**

(**A**) Representative trace, from 31 cells in 1 experiment, show three successive stimulations with caffeine (10 mM, 5 min, with 10-min interval between stimuli, first challenge), caffeine in the presence of ryanodine (100 µM) (second and third challenge) in normal KRH. (**B**) Inhibition of caffeine-evoked Ca^{2+} release using ryanodine. (**C, D**) Summary results show the peak (after ~30-35s) increase in $[Ca^{2+}]_c$ ($\Delta[Ca^{2+}]_c$) evoked by caffeine (10 mM) (first challenge) or caffeine with ryanodine (**D**) or DMSO (**C**) (second and third challenge) for each of the three challenges in each set of experiments. Result in C and D include only cells that responded to the first addition of caffeine (90% and 91%, in C and D respectively), and show means ± SEM from 3 independent experiments, with ~110 and ~113 cells analysed in C and D, respectively. $^{*}P < 0.05$ with one-way analysis of variance and Tukey multiple comparisons test.

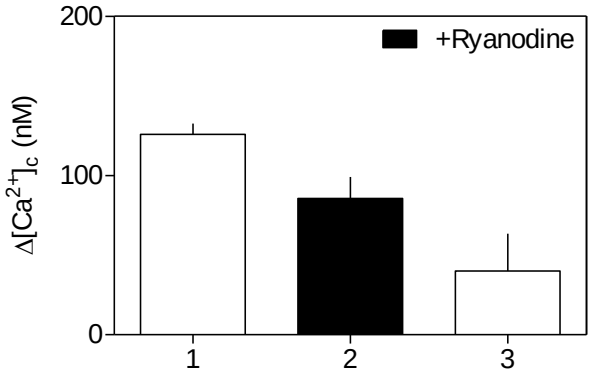

Figure 2.5. **Effect of ryanodine on CCh-evoked Ca^{2+} responses**
(**A**) Summary results show the peak (after ~30-35s) increase in $[Ca^{2+}]_c$ evoked by CCh (100 μM) with and without ryanodine (100 μM) ($\Delta[Ca^{2+}]_c$) for each of the three challenges in each set of experiments. Results include only cells that responded to the first addition of CCh (83%), and show means ± SEM from 3 independent experiments, with ~125 cells analysed.

2.3.2. Mechanism of Ca^{2+} entry in INS-1E cells

Ca^{2+} entry across the PM can be mediated by VOC in primary β-cells and INS-1E cells (Gustafsson *et al.*, 2005; Islam, 2010). To study Ca^{2+} entry pathways in pancreatic β-cells, a high-KCl concentration was used to trigger depolarisation of the PM, thereby activating VOC to allow Ca^{2+} entry from the extracellular medium (Gustafsson *et al.*, 2005; Lemmens *et al.*, 2001). To confirm previous findings, I characterised the KCl-evoked Ca^{2+} signalling pathways in INS-1E cells, and whether they were mediated by VOC.

The effects of KCl on $[Ca^{2+}]_c$ in INS-1E cells were assessed by the three sequential stimulus protocol as described in section 2.2.5. As expected, KCl caused robust increases in $[Ca^{2+}]_c$. The 3 successive challenges were not significantly different (Fig. 2.6A, C). The peak rises in $[Ca^{2+}]_c$ ($\Delta[Ca^{2+}]_c$) were: 1085 ± 133, 740 ± 138 and 798 ± 30 nM, for the first, second and third challenges, respectively. These results confirm that KCl-evokes an increase in $[Ca^{2+}]_c$ in INS-1E cells, as others have previously shown (Szollosi *et al.*, 2010; Woolcott *et al.*, 2006). To examine whether these KCl-evoked rises in $[Ca^{2+}]_c$ were mediated by Ca^{2+} entry or release pathways, the experiments were repeated in the absence of extracellular Ca^{2+}. Briefly, INS-1E cells were first stimulated with high-KCl in Ca^{2+}-containing KRH, and then bathed in Ca^{2+}-

free KRH prior to a second challenge with high-KCl in Ca^{2+}-free KRH, then Ca^{2+} was restored for the third high-KCl challenge. Changes in $[Ca^{2+}]_c$ ($\Delta[Ca^{2+}]_c$) were analysed for ~80 cells in each of 3 independent experiments. The results revealed that removal of extracellular Ca^{2+} reversibly inhibited the KCl-induced rises in $[Ca^{2+}]_c$ (Fig. 2.6B, D). The response to KCl ($\Delta[Ca^{2+}]_c$) was 7 ± 12 nM in the absence of extracellular Ca^{2+}, but in its presence the responses were 731 ± 113 nM (first challenge) and 662 ± 111 nM (third challenge). The two responses in the presence of extracellular Ca^{2+} were not statistically different. Similar results have been observed previously (Gustafsson *et al.*, 2005).

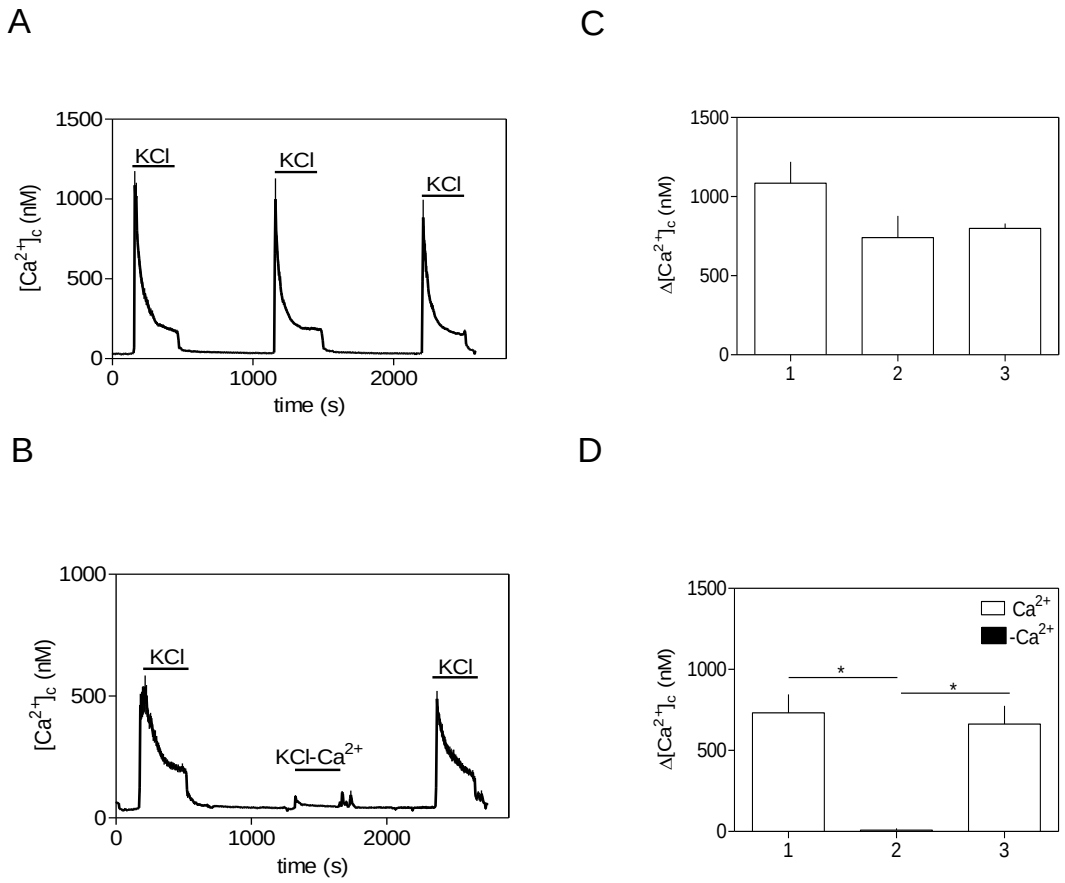

Figure 2.6. **KCl-evoked Ca^{2+} signals in INS-1E cells**. **(A, B)** Representative traces, from 39 and 35 cells in 1 experiment, respectively, show three successive stimulations with KCl (40 mM, 5 min, with 10-min intervals between stimuli) in normal KRH (**A**) or in Ca^{2+}-free KRH (**B**). (**C**, **D**) Summary results show the peak (after ~30-35s) increase in $[Ca^{2+}]_c$ ($\Delta[Ca^{2+}]_c$) evoked by KCl alone (first, second and third challenges) (**C**) and KCl-Ca^{2+} (second challenge) (**D**) for each of the three challenges in each set of experiments. Results in C and D include only cells that responded to the first addition of KCl (100% and 95% in C and D, respectively), and show means ± SEM from 3 independent experiments, with ~124 and ~80 cells respectively analysed in each. $^{*}P <$ 0.05 with one-way analysis of variance and Tukey multiple comparisons test.

An antagonist of L-type VOC, nimodipine, was used to examine whether the KCl-evoked Ca^{2+} entry in INS-1E cells was mediated by L-type VOC. Since, nimodipine is insoluble in water, methanol was used as a solvent. Controls were carried out to confirm the absence of methanol effects on the Ca^{2+} responses (Fig. 2.7A). INS-1E cells were first stimulated with KCl, then nimodipine or methanol (solvent control) was

added with KCl before the second challenge, and then removed prior to the third KCl challenge The % of methanol used to make final nimodipine concentration (10µM) in 5 ml KRH was 0.2%. A significant decrease in the KCl-evoked Ca^{2+} rises was observed in the presence of nimodipine. The increase in peak $[Ca^{2+}]_c$ was 330 ± 59 nM (second challenge) in the presence of nimodipine compared to the initial KCl-evoked Ca^{2+} response in the absence of nimodipine 1095 ±138 nM (first challenge) (Fig. 2.7B). When nimodipine was washed out before the third KCl challenge in the absence of nimodipine, there was no recovery in the KCl-evoked Ca^{2+} rises, ($\Delta[Ca^{2+}]_c$) was significantly lower (371 ± 60 nM, third challenge) compared to the first challenge (1095 ±138 nM) (Fig. 2.7B). Unfortunately, it became apparent from the solvent control experiments, that methanol may have contributed to some of the inhibition of the KCl responses observed (Fig. 2.7A). Since, the second challenge to KCl in the presence of methanol (solvent control) was significantly lower ($\Delta[Ca^{2+}]_c$ 627± 52 nM) than in its absence 1082 ± 49 nM (first challenge) (Fig. 2.7A). These results suggested that the inhibitory effect of methanol (solvent) could not be ruled out when interpreting the changes in KCl-evoked Ca^{2+} responses in the presence of the L-type VOC blocker nimodipine in these experiments.

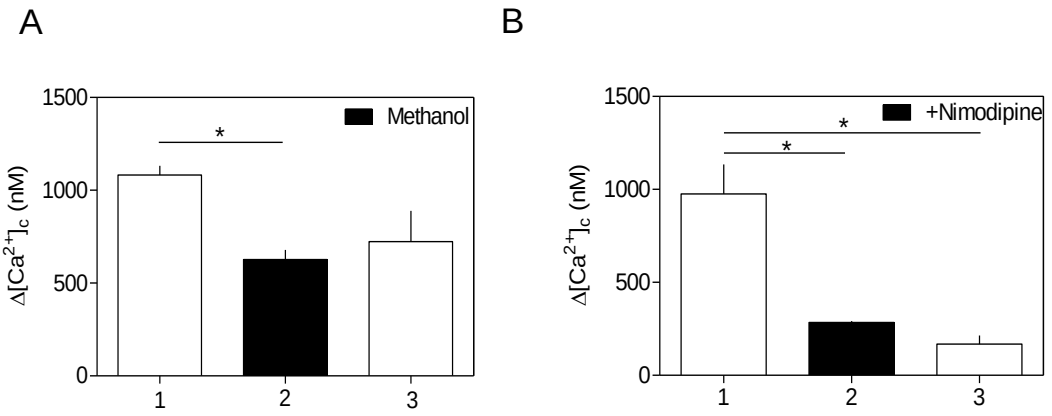

Figure 2.7. **Effect of nimodipine on KCl-evoked Ca^{2+} entry in INS-1E cells.** (**A**, **B**) Summary results show the peak (after ~30-35s) increase in $[Ca^{2+}]_c$ evoked by KCl (40 mM) ($\Delta[Ca^{2+}]_c$) for each of the three challenges in each set of experiment. Results include only cells that responded to the first addition of KCl (64% and 70% in A and B respectively), and show means ± SEM from 3 independent experiments, with ~79 and ~77 cells analysed in A and B, respectively. $^{*}P< 0.05$ with one-way analysis of variance and Tukey multiple comparisons test.

The effects of nimodipine on KCl-evoked Ca^{2+} responses were next examined using DMSO as a solvent. The % of DMSO used to make final nimodipine concentration (10μM) in 5 ml KRH was 0.2%. Figure 2.8A shows that nimodipine significantly inhibited KCl-evoked Ca^{2+} entry in comparison to the matched control experiment. The peak increase in $[Ca^{2+}]_c$ in the absence of nimodipine was 952 ± 101 nM (first challenge) and it was 347 ± 142 nM (second challenge) in its presence (Fig. 2.8A). However, recovery of the KCl-evoked response was not observed following removal of nimodipine: the peak increase in $[Ca^{2+}]_c$ was 220 ± 117 nM for the third challenge (Fig. 2.8A). The KCl-evoked increase in peak $[Ca^{2+}]_c$ in the presence of DMSO was 984 ± 27 nM (second peak), which was similar to the effect of KCl alone during the first challenge (1052 ± 38 nM (Fig. 2.8C). These results show that nimodipine inhibits KCl-evoked Ca^{2+} responses.

As nimodipine showed only 69% inhibition compared to the first peak response in INS-1E (Fig. 2.8A) and β-cells (Woolcott *et al.*, 2006). These results were confirmed using another L-type VOC inhibitor, verapamil (Fig. 2.8B) (Wollheim *et al.*, 1984). Verapamil almost completely inhibited KCl-evoked Ca^{2+} responses, the peak increase in $[Ca^{2+}]_c$ was 29 ± 9 nM (second challenge) in the presence of verapamil in comparison to 890 ± 165 nM in its absence (first challenge) and 440 ± 170 nM (third challenge) (Fig. 2.8B). The first and third KCl-evoked Ca^{2+} responses were not significantly different (Fig. 2.10B).

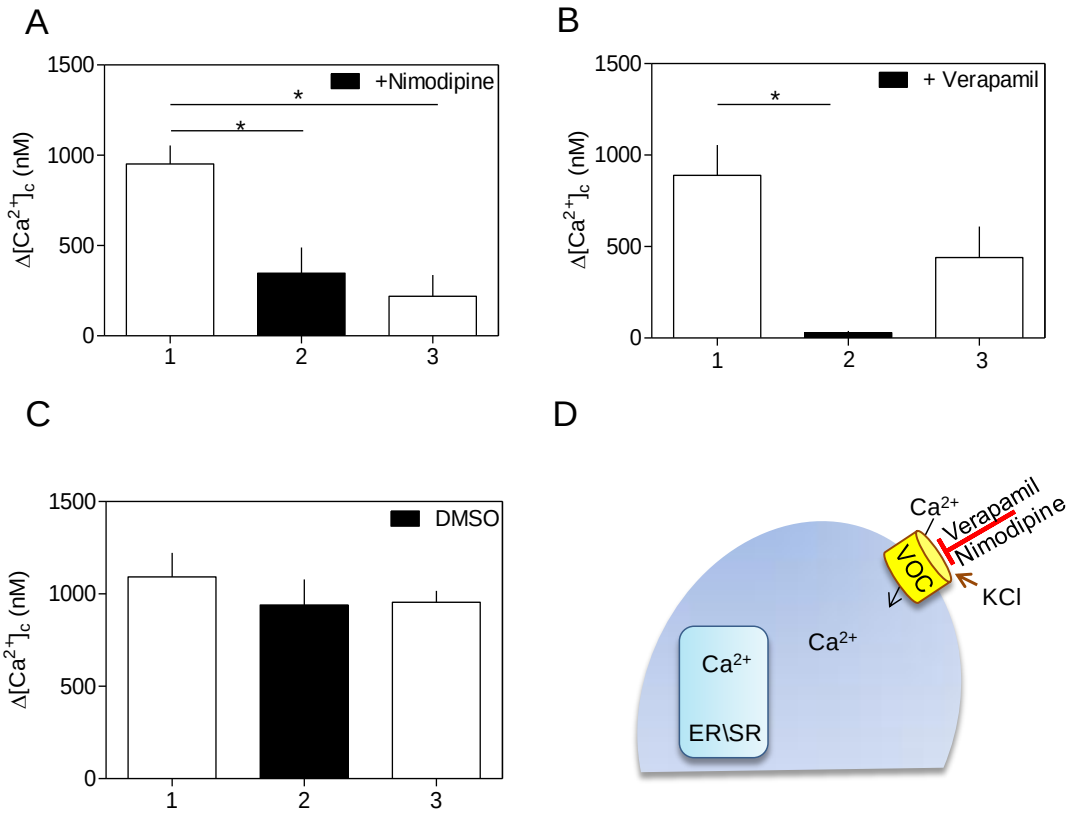

Figure 2.8. **Effect of nimodipine and verapamil on KCl-evoked Ca^{2+} entry in INS-1E cells.** (**A, B**, **C**) Summary results show the peak (after ~30-35s) increase in $[Ca^{2+}]_c$ evoked by KCl (40 mM) ($\Delta[Ca^{2+}]_c$) for each of the three challenges in each set of experiments. Results in A, B and C include only cells that responded to the first addition of KCl (94%, 96%, 95% respectively), and show means ± SEM from 3 independent experiments, with ~104, ~135 and ~111cells analysed in A, B and C respectively. $^{*}P < 0.05$ with one-way analysis of variance and Tukey multiple comparisons test. (**D**) Inhibition of KCl-evoked Ca^{2+} entry either using nimodipine or verapamil.

The effect of ryanodine on KCl-evoked Ca^{2+} responses was investigated by initially challenging INS-1E cells with KCl, then adding ryanodine with KCl for the second challenge, and subsequently removing ryanodine before the third KCl-challenge. The response to KCl with ryanodine ($\Delta[Ca^{2+}]_c$) was 894 ± 24 nM (second challenge), but the KCl alone response was 1202 ± 86 (first challenge) and 817 ± 76 nM (third challenge) (Fig. 2.9A). These results suggest that most likely ryanodine has no effect on KCl-evoked Ca^{2+} entry.

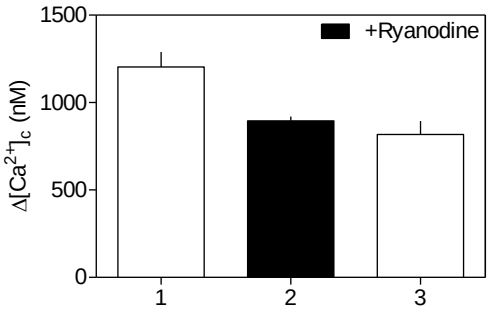

Figure 2.9. **Effect of ryanodine on KCl-evoked Ca^{2+} entry in INS-1E cells**
(**A**) Summary results show the peak (after ~30-35s) increase in $[Ca^{2+}]_c$ evoked by KCl (40 mM) with and without ryanodine (100 µM) ($\Delta[Ca^{2+}]_c$) for each of the three challenges in each set of experiments. Results include only cells that responded to the first addition of KCl (60%), and show means ± SEM from 3 independent experiments, with ~75 cells analysed in each. No significant differences were observed.

Nimodipine was used to examine whether VOC contribute to the caffeine-evoked Ca^{2+} responses. While performing this experiment DMSO was used as solvent and the % of DMSO used to make final nimodipine concentration (10µM) in 5 ml KRH was 0.2%. INS-1E cells were first stimulated with caffeine alone, nimodipine was then added with caffeine during the second challenge, and nimodipine was then removed before the third caffeine-challenge. The response to caffeine with nimodipine ($\Delta[Ca^{2+}]_c$) was 94 ±19 nM (second challenge), but the response to caffeine alone was 196 ± 31 nM (first challenge) and 65 ± 21 nM (third challenge). The two responses to caffeine after exposure to nimodipine (second and third challenges) were significantly different from the response to the first stimulation with caffeine (Fig. 2.10). These results show that caffeine-evoked Ca^{2+} signals are inhibited by the inhibition of L-type VOC.

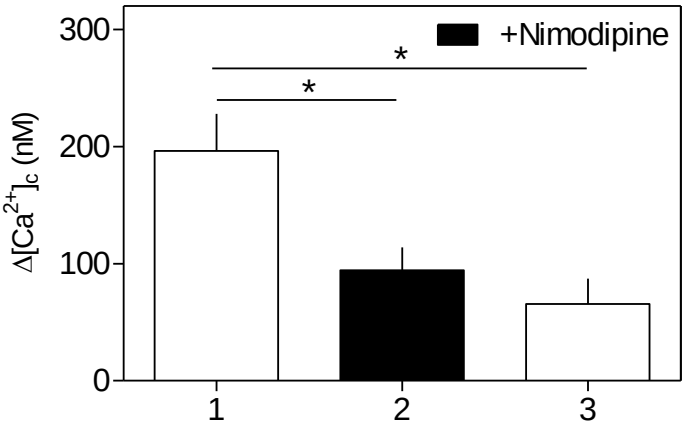

Figure 2.10. **Effect of nimodipine on caffeine-evoked Ca^{2+} signals.** Summary results show the peak (after ~30-35s) increase in $[Ca^{2+}]_c$ evoked by caffeine (10 mM) with and without nimodipine (10 μM) ($\Delta[Ca^{2+}]_c$) for each of the three challenges in each set of experiments. Results include only cells that responded to the first addition of caffeine (60%), and show means ± SEM from 3 independent experiments, with ~125 cells analysed in each. $^{*}P < 0.05$ with one-way analysis of variance and Tukey multiple comparisons test.

2.3.3. INS-1E cells do not show consistent caffeine, CCh or KCl-evoked Ca^{2+} signals

INS-1E cells respond to caffeine, CCh and KCl with an increase in $[Ca^{2+}]_c$ (Fig. 2.2, 2.3, 2.8), but there was variability in the responses of INS-1E cells to caffeine (Fig. 2.11), CCh (Fig. 2.12) and KCl (Fig.2.6C, D) between cell batches. The Ca^{2+} responses for caffeine-evoked signals were~2-fold higher from the initial set of experiments (Fig. 2.11A) compared to those performed later (Fig. 2.11B). For CCh-evoked Ca^{2+} responses, the Ca^{2+} release was~2-fold lower in later experiments, and the three successive challenges were different (Fig. 2.12B). For KCl-evoked responses, the Ca^{2+} signals decreased by~0.3-fold (Fig. 2.6D) in comparison to the initial set of experiments (Fig. 2.6C). This variability was observed between successive passages making replicate experiments difficult.

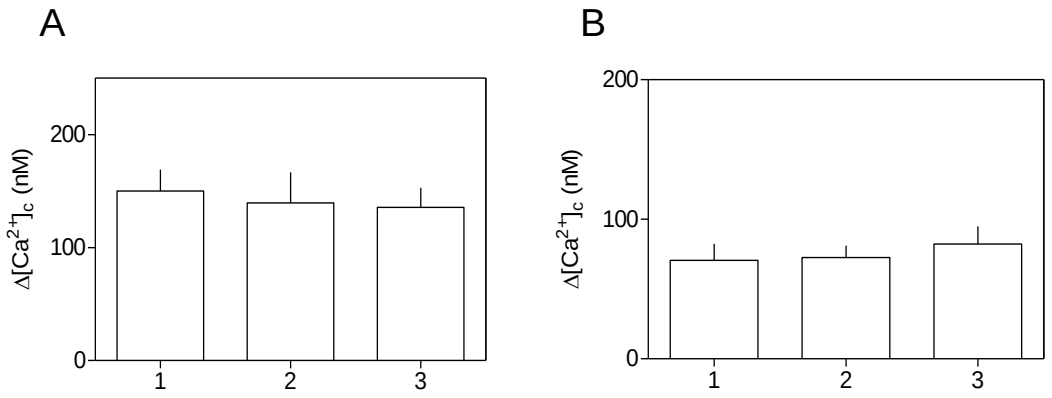

Figure 2.11. **Variable caffeine-evoked Ca^{2+} signals from different passages of INS-1E cells.** (**A**, **B**) Summary results show the peak (after ~30-35s) increase in $[Ca^{2+}]_c$ evoked by caffeine (10 mM, 5 min) ($\Delta[Ca^{2+}]_c$) for each of the three challenges in each set of experiments. Results in A and B include only cells that responded to the first addition of caffeine (78% and 80% in A and B, respectively), and show means ± SEM from 3 independent experiments, with ~108 (passage 52) and ~112 cells (passages 57 and 58) analysed in A and B respectively.

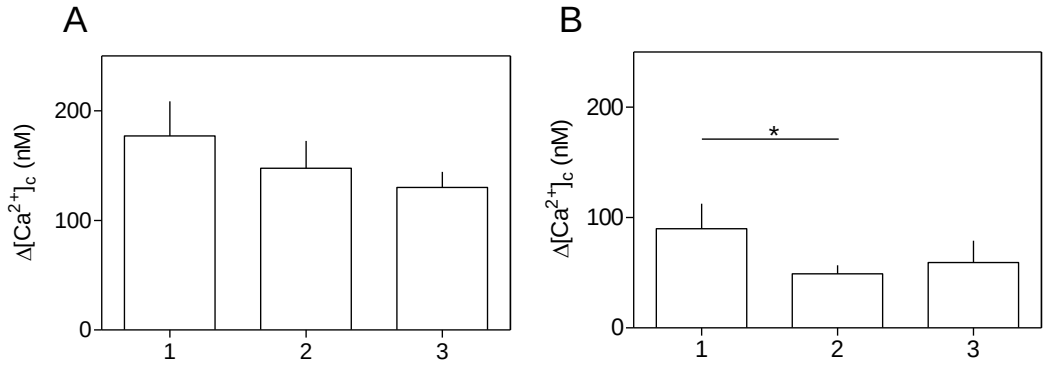

Figure 2.12. **Variability of** CCh**-evoked Ca^{2+} signals from different passages of INS-1E cells.** (**A**, **B**) Summary results show the peak (after ~30-35s) increase in $[Ca^{2+}]_c$ evoked by CCh (100 μM, 5 min) ($\Delta[Ca^{2+}]_c$) for each of the three challenges in each set of experiments. Results in A and B include only cells that responded to the first addition of CCh (68% and 70% in A and B, respectively), and show means ± SEM from 3 independent experiments, with ~ 99 (passage 52) and ~109 cells (passages 57 and 58) analysed in A and B respectively. $^{*}P < 0.05$ with one-way analysis of variance and Tukey multiple comparisons test.

2.3.4. Glucose-evoked Ca^{2+} oscillations in mouse pancreatic islets of Langerhans

Given the variability of the Ca^{2+} signals in INS-1E cells, mouse islets of Langerhans were considered as an alternative model for assessing the contributions of RyR to Ca^{2+} signals in β-cells. Mouse islets of Langerhans showed robust Ca^{2+} oscillations in response to glucose (10 mM) for up to 60 min (Fig. 2.13). However, the success rate for completing experiments was very low because there were problems with adherence of islets (they often detached during sustained recordings) and the cell viability was often low.

For single-cell imaging experiments, islets were seeded onto poly-L-lysine (0.01%)-coated 22-mm round glass coverslips for 24 h under the culture conditions as described in section 2.2.3. However, most islets failed to adhere to the coverslips. Whilst troubleshooting the adherence problems, islets were plated onto different extracellular matrixes such as collagen (0.1%), poly-D-lysine (0.2%), gelatin (0.4%), fibronectin (50 μg/ml) and BD Cell Tak (12.5 μg/ml) and extracellular matrix (ECM), but none of these resolved the issue completely. These issues were addressed using different optimisation strategies a) performing experiments at 37°C, b) dye loading and de-esterification in serum-free RPMI 1640 medium rather than KRH, however the problems mainly persisted.

The biggest problem with islets after 24 h of culture was that because of their large size, the central core starts to appear necrotic. Probably, it was a consequence of inadequate oxygen supply (Kuhn *et al.*, 1985). Hence, even if an islet was attached adequately to the coverslip, due to β-cell death at the core of these islets, they did not respond to glucose. This issue was addressed by seeding islets immediately after isolation onto poly-L-lysine-coated coverslips and performing experiments within 24 h. However, the success rate remained very low because of low throughput: a maximum of only 2 islets could be viewed per coverslip. Most of the islets did not adhere to the coverslips and the islets which adhered did not consistently show glucose-evoked Ca^{2+} responses. In situations where responses were observed, islets often detached from the coverslip before completion of the experiment. Hence, calibration of $[Ca^{2+}]_c$ signals was impossible. These issues made it impossible to obtain sufficient recordings from of islets to measure and analyse $[Ca^{2+}]_c$ signals.

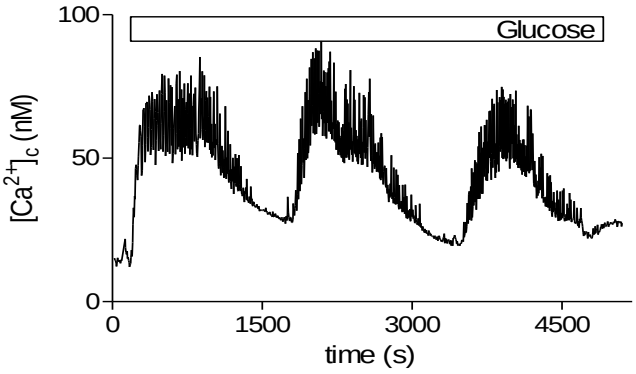

Figure 2.13. **Glucose-evoked Ca^{2+} oscillation in pancreatic β-cells**
After culturing mouse islets for 2 days, cells were loaded with Fura-2 on the third day. A typical trace shows glucose (10mM)-evoked increase in $[Ca^{2+}]_c$ in a single mouse islet. Slow waves showing regular rise and fall in $[Ca^{2+}]_c$ were associated with fast oscillations superimposed upon the plateau when $[Ca^{2+}]_c$ was elevated.

2.4. Discussion

Several studies propose that RyR might contribute to regulation of insulin secretion during the second phase of insulin release (Johnson *et al.*, 2004; Takasawa *et al.*, 2010). Also, in human islets, type 2 DM is associated with reduced expression of RyR2, whereas activation of RyR can trigger insulin secretion (Johnson *et al.*, 2004; Squires *et al.*, 2004; Takasawa *et al.*, 1998) (see section 2.1.4). Considering these published reports, with the long term aims a) to define the presence of RyR in β cells and b) to understand the role of RyR in insulin secretion specifically in type 2 DM condition following study was designed. Firstly, basic Ca^{2+} signalling pathways and insulin secretion assays were characterised in INS-1E cells. My results establish that in INS-1E cells, RyR and IP_3R mediate Ca^{2+} release from intracellular stores (Fig. 2.2B-F, 2.3B, D) and L-type VOCs have long been established as a Ca^{2+} entry pathway (Fig. 2.6A, C) (Gustafsson *et al.*, 2005). RyR- and IP_3R-mediated Ca^{2+} release has been shown in previous studies (Blondel *et al.*, 1993; Gustafsson *et al.*, 2005; Woolcott *et al.*, 2006). Also in addition to KCl (Fig. 2.6A, C), RyR (Fig. 2.2A, B) may also be involved in Ca^{2+} entry in INS-1E cells.

RyR-mediated Ca^{2+} entry and release were further confirmed using ryanodine (Fig. 2.4, 2.4). The presence of RyR in pancreatic β-cells cells has also been confirmed by others previously (Chen *et al.*, 1996; Gustafsson *et al.*, 2005; Lemmens *et al.*, 2001;

Mitchell *et al.*, 2003; Woolcott *et al.*, 2006). Ryanodine inhibits RyR in a use-dependent manner. It inhibits open RyR channels, hence causing inhibition of Ca^{2+} signals mediated by RyR. Partial inhibition of caffeine-evoked Ca^{2+} response in a second challenge (Fig. 2.4A, D) might be because of sub-population of open RyR channels, which were inhibited by ryanodine. Complete inhibition of the caffeine-evoked Ca^{2+} response in the third challenge (Fig. 2.4A, D) is possibly because, by the third caffeine stimulation, all remaining RyR may be open to be inhibited by ryanodine. The use-dependent effect of ryanodine is well established (Chen *et al*, 1996).

These results suggest that the caffeine-evoked Ca^{2+} entry and release are probably mediated via RyR located on PM (Moonga *et al.*, 2002; Rosker *et al.*, 2009) and in stores. RyR located on PM may cause Ca^{2+} entry via three mechanisms (Fig. 2.14). Firstly, indirectly by activation of Ca^{2+}-sensitive non-selective cation channels like transient receptor potential (TRP) channels, specifically TRPM4 or TRPM5 (Cheng *et al.*, 2007; Liman, 2010). These might cause further depolarization and so greater activation of L-type VOC (Fig. 2.14). Secondly, by causing PM depolarization by itself. A small number of RyRs in the PM may be sufficient as both RyR and IP_3R have large conductance, hence very few channels can mediate significant Ca^{2+} entry (Fig. 2.14) (Dellis *et al.*, 2006; Rosker *et al.*, 2009). A third mechanism for Ca^{2+} entry across the plasma membrane involves activation of SOCE, stimulated by Ca^{2+} release from intracellular stores RyR (Fig. 2.14) (Holz, 2004; Holz *et al.,* 1999). Apart from these an additional effect of caffeine observed by Islam *et al.* (1995) was that caffeine by inhibiting PDE probably increases intracellular cAMP accumulation, which may further stimulate Ca^{2+} entry via PKA phosphorylation of VOC (Islam *et al.*, 1995). My results have not thus far discriminated between the three alternatives. The caffeine-evoked Ca^{2+} entry observed could be due to Ca^{2+}entry via directly by RyR activation, increased activity of VOC, and activation of SOCE or possibly a combination of all three.

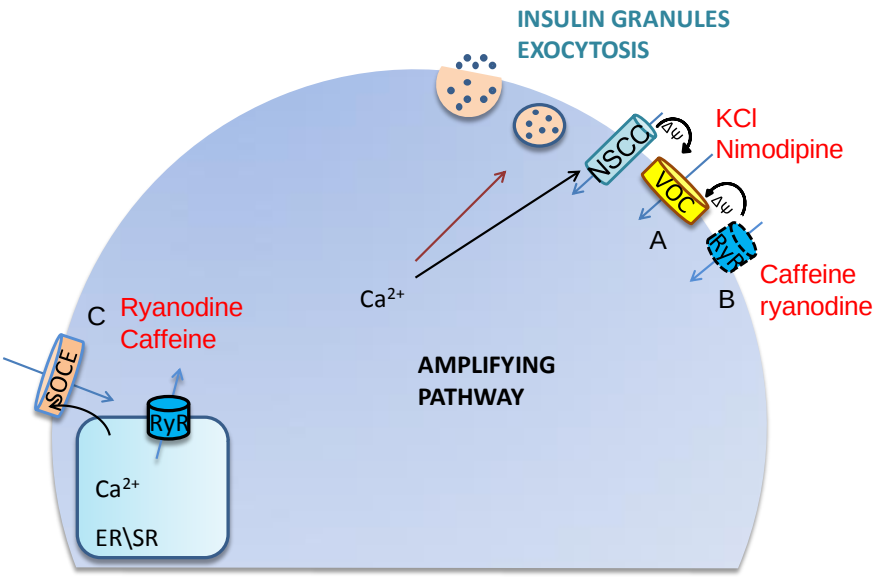

Figure 2.14. **Novel ryanodine receptor-mediated Ca^{2+} entry pathway in pancreatic β-cell.** (**A**) Ca^{2+} entry mediated by VOC. (**B**) Ca^{2+} entry mediated by plasma membrane localised ryanodine receptor (RyR) directly or indirectly by depolarising VOCs. (**C**). Ca^{2+} entry mediated by SOCE triggered upon stores depletion by RyR.

CCh-evoked Ca^{2+} signals were not affected by inhibition of RyR (Fig. 2.5A). Data obtained from this work corroborate what others have previously shown (Graves *et al.*, 2003; MacMillan *et al.*, 2005). This perhaps suggests that CCh-evoked Ca^{2+} release pathways are independent of caffeine-evoked Ca^{2+} release pathways. However, caffeine-evoked Ca^{2+} signals should be assessed in the presence of an IP_3R inhibitor to prove this argument. The decrease observed in CCh-evoked Ca^{2+} responses in the third challenge (Fig. 2.5A), might be a consequence of ryanodine treatment in the second challenge (Fig. 2.5A). Perhaps high ryanodine concentrations inhibited other PM non-selective ion channels like TRP channels or/and unknown receptors in internal stores or caused a change in membrane potential, which affect IP_3-mediated Ca^{2+} release (MacMillan *et al.*, 2005). In pancreatic β-cells (Renuka *et al.*, 2006; Tamarina *et al.*, 2005), glucose stimulates PLC, leading to the formation of IP_3 and DAG. In a few reports IP_3R-mediated Ca^{2+} release is associated with weak SOCE in pancreatic β-cells (Dyachok *et al.*, 2001; Dyachok *et al.*, 2004). Perhaps in my results Ca^{2+} release seen in Ca^{2+}-free conditions (Fig. 2.4B), could be responsible for triggering weak SOCE in the presence of extracellular Ca^{2+}.

KCl-evoked Ca^{2+} entry mediated by VOC is well characterized in pancreatic β-cells and INS-1E cells (Gustafsson *et al.*, 2005). My results (Fig. 2.6A, C) are in

agreement with these previous studies. Using two approaches these results were further confirmed a) by performing experiments under Ca^{2+}-free conditions (Fig. 2.6B, D) and b) by using L-type VOC blocker such as nimodipine (Szollosi *et al.*, 2010) and verapamil (Fig. 2.8).

When compared, the Ca^{2+} response observed via KCl-evoked Ca^{2+} entry (Fig. 2.8A, C) is considerably higher compared to Ca^{2+} signals evoked by caffeine (Fig. 2.2A, D) and CCh (Fig. 2.3A, C). It might indicate that in pancreatic β-cells, a major contribution of Ca^{2+} entry is via VOC. Previously, it was shown that Ca^{2+}entry via VOC can also stimulate Ca^{2+}-induced Ca^{2+} release (CICR) (Lemmens *et al.*, 2001). Possibly, in my data (Fig. 2.6A, C) the initial rise in KCl-evoked Ca^{2+} entry could be due to activation of VOC. The Ca^{2+}-entry from the VOC could then stimulate CICR, and the subsequent depletion of the ER stores could activate SOCE, which may explain the sustained components of the KCl-evoked Ca^{2+} responses (Dyachok *et al.*, 2001; Liu *et al.*, 1997). Inhibition of RyR did not affect KCl-evoked Ca^{2+} signals (Fig. 2.9) (Graves *et al.*, 2003; Gustafsson *et al.*, 2005; Holz *et al.*, 1999). Hence, KCl-evoked Ca^{2+} entry was found not to be associated with CICR. Alternatively, caffeine-evoked Ca^{2+} signals were significantly affected by inhibition of L-type VOC (Fig. 2.10). These results land support to the hypothesis that PM RyR may mediate Ca^{2+} entry.

A residual KCl-evoked Ca^{2+}entry in second challenge is observed after inhibition of L-type VOC (Fig. 2.8A) using nimodipine. It could be because a) due to activation of other VOC present in pancreatic β-cells like the P/Q type VOC and non-selective cation channels like TRP channels, which are found in pancreatic β-cells, b) due to lower sensitivity of β-cells to nimodipine. The latter has been previously reported, whereby human β-cells showed differential expression of L-type Ca^{2+} channel subtypes, containing more Cav 1.3 channels, which are less sensitive to nimodipine than Cav 1.2 channels (Pollo *et al.*, 1993). Hence, by using verapamil (Fig. 2.8B) I further confirmed that Ca^{2+} entry is also mediated by L-type VOC. Others have also observed inhibition of KCl-evoked Ca^{2+} signals using verapamil (Findlay *et al.*, 1985; Wollheim *et al.*, 1984).

Despite characterising Ca^{2+} entry and release pathway in INS-1E cells, these cells were found to be impracticable to examine the physiological role and location of RyR in pancreatic β-cells because INS-1E cells did not show reproducible Ca^{2+} signals when stimulated with caffeine, CCh and KCl, over different passages (Fig. 2.6C, D, 2.11, 2.12). These cells were found not to be suitable to perform 96-well plate population-

based assays (Tovey *et al.*, 2006) as that demands confluent, adherent cultures of cells in a monolayer and INS-1E cells do not grow in monolayers. Dr Nadia Shah from our research group has shown that the INS-1E cells used in this study failed to exhibit the characteristic GSIS. Work carried out by Dr Nadia Shah suggested the INS-1E cells had developed a hypersensitive response to sub-physiological glucose levels and additionally failed to show the characteristic dose-dependent GSIS. This is most likely due to following reasons

a) the de-differentiation of INS-1E cells back to an insulinoma type, which has been previously observed in other β-cell lines (Efrat, 1999). This occurs due to an increase in hexokinase activity required to overcome the metabolic demands of rapidly dividing cells (Efrat, 1999).

b) One of the major causes for type 2 DM is persistently increased glucose concentration in plasma. It results in decreased sensitivity to glucose, and accompanying insulin resistance. Previously, it is published that culturing of INS-1 cells at high glucose concentration (≥ 11mM) causes reduction in insulin gene transcription and decreases binding activity of β-cell specific transcription factors STF1 and C activators (Olson *et al.*, 1998). Although my experiments are unlikely to be prone to glucose-evoked insulin resistance (because that is a response at target tissue), but they may be prone to local accumulation of insulin in culture feeding back to affect GSIS. Yet, the possibilities of chronic exposure of INS-1E cells to the supraphysiological concentration of glucose (≥11mM) present in the growth medium affected the characteristic responses of INS-1E cell line reported by Merglen *et al* (2003) cannot be ruled out completely.

In addition to this it is also suggested that higher glucose concentrations (≥ 11mM) in growth medium causes toxicity of β-cells. The toxic effect arising due to higher glucose concentrations can be reversed, if cells were grown at lower glucose concentration (≥ 2.5mM) within few weeks of higher glucose concentration exposure. However; it is irreversible if cells were cultured at higher glucose concentrations for months (Eizirik *et al.*, 1992; Gleason *et al.*, 2000). Perhaps this glucose toxic effect is could also be responsible for changes in caffeine, CCh and KCl-evoked Ca^{2+} responses with the increasing passage numbers.. In contrast to these reports, others have observed GSIS in INS-1E cells even after growing in culture medium supplemented with ≥11 mM glucose (Gamberucci *et al.*, 1999; Kang *et al.*, 2003; Zuniga-Hertz *et al.*, 2015), yet the possibility of developing diabetic β-cell characteristic in INS-1E cells cannot be

ruled out. The only alternative is to grow INS-1E cells in culture medium supplemented with ≤2.5 mM glucose and then measure GSIS. It is shown that cells grown under these conditions show reproducible Ca^{2+} signals and GSIS. To measure GSIS cells were bathed in glucose free medium for~2 hr before assessing insulin secretion (Maechler *et al.*, 2000; Maechler *et al.*, 2000). Presumably it enhances GSIS upon stimulation with different glucose concentrations. In addition to these improvements in culturing INS-1E cells, the best alternative to replace INS-1E was to use primary mouse pancreatic islets of Langerhans. Glucose-evoked Ca^{2+} oscillations in mouse pancreatic islets of Langerhans have been observed previously (Fridlyand *et al.*, 2010). However this alternative was also found unworkable.

My primary results conclude that in INS-1E cells RyR and IP_3R mediates Ca^{2+} release and VOC mediates Ca^{2+} entry. Additionally, Ca^{2+} entry is also found to be sensitive to caffeine and ryanodine. However, due to inconsistent response of INS-1E cells and primary mouse islets this project was impossible to carry on for this thesis. Hence, the direction of this thesis was changed to study Ca^{2+} signalling mediated via PTH receptors (Chapter 2 and 3).

2.5. Conclusions

Results in chapter 2 show that in INS-1E cells, RyR and IP_3R are major Ca^{2+} release pathways and Ca^{2+} entry is largely mediated by L-type VOC. These observations are consistent with many published analysis of β-cells and INS-1E cells (Blondel *et al.*, 1993; Gustafsson *et al.*, 2005; Woolcott *et al.*, 2006). Ca^{2+} entry may be mediated directly by plasma membrane ryanodine receptors (Rosker *et al.*, 2009), it may result from release of Ca^{2+} via intracellular RyR causing activation of Ca^{2+}-sensitive non-selective cation channels or it may mediated by store-operated Ca^{2+} entry after release of Ca^{2+} via intracellular RyR. However, results also provided evidence for a Ca^{2+} entry pathway that is sensitive to caffeine and/or ryanodine. I consider these possible mechanisms to account for these observations.

Chapter 3. Potentiation of carbachol-evoked Ca^{2+} signals by acute and sustained stimulation by PTH is mediated by cAMP

3.1. Introduction

3.1.1. Parathyroid hormone

In the chief cells of the parathyroid glands, parathyroid hormone (PTH) is synthesised as a precursor protein, pre-pro PTH (115 residues) (Habener *et al.,* 1975; Kemper *et al.,* 1974). The 'pre' sequence (25 residues) directs the pre-proPTH mRNA-ribosome complex towards the ER, where the hydrophobic nature of the 'pre' sequence facilitates penetration of pre-pro PTH across the ER membrane (Habener *et al.,* 1978). Cleavage of the 'pre' sequence from proPTH occurs within the ER inter-cisternal space, before its entry into the ER (Habener *et al*., 1979; Habener *et al*., 1979). The 'pro' sequence is a short peptide, similar to other secretory proteins for example proalbumin (Patterson *et al.,* 1977) and targets PTH to the Golgi apparatus. Within the Golgi, the 'pro' sequence is cleaved from the N-terminal region of the pro-PTH and the mature 84-residue PTH peptide is then packaged into vesicles before regulated release (Habener *et al*., 1979) into the plasma.

Secretion of PTH from chief cells is controlled by the concentration of Ca^{2+} in the extracellular fluid ($[Ca^{2+}]_{ECF}$): higher $[Ca^{2+}]_{ECF}$ inhibits secretion, whereas lower $[Ca^{2+}]_{ECF}$ stimulates it (Care *et al.,* 1966). Ca^{2+}-sensing receptors sense the change in $[Ca^{2+}]_{ECF}$ and regulate secretion of PTH (Brown, 1993; Brown, 2013; Brown *et al.,* 2001; Racke *et al.,* 1993). In addition to an increase in $[Ca^{2+}]_{ECF}$, secretion of PTH *in vivo* also depends on the rate at which $[Ca^{2+}]_{ECF}$ changes. This contributes to a steep inverse sigmoidal relationship between $[Ca^{2+}]_{ECF}$ and secreted PTH (Brown *et al.,* 2001; Grant *et al.,* 1990). These characteristics ensure that chief cells secrete higher amounts of PTH into the blood plasma soon after a rapid decrease in plasma $[Ca^{2+}]$. PTH leads to an increase in the plasma $[Ca^{2+}]$ and a decrease in plasma phosphate levels (Brown *et al*., 2001). PTH either directly or indirectly affects the kidney (Gesek *et al*., 1992; Knox *et al*., 1975), bone (Hurwitz, 1996) and small intestine to regulate plasma $[Ca^{2+}]$ (Hurwitz, 1996; Nemere *et al*., 1986; Yoshimoto *et al*., 1986). In the kidney, PTH

stimulates phosphate secretion (Grose *et al.*, 1968; Mercado *et al.*, 1975) and Ca^{2+} reabsorption from the distal tubule (Houillier, 2013; Jeon, 2008). PTH also up regulates the activity of 1α-hydroxylase, the enzyme responsible for biosynthesis of 1,25-dihydroxy vitamin D_3 (Fraser *et al.*, 1973; Takeyama *et al.*, 1997). PTH, by increasing the formation of 1,25-dihydroxyvitamin D_3, increases the absorption of both Ca^{2+} and phosphate from the intestine. PTH also promotes release of Ca^{2+} and phosphate from the bone matrix (Boden *et al.*, 1990; Christakos *et al.*, 2014). The effects of PTH on the balance between the absorption of Ca^{2+} from the intestine, release of Ca^{2+} as from bone, and Ca^{2+} reabsorption by the kidney restore the normal [Ca^{2+}] in blood plasma (Fig. 3.1).

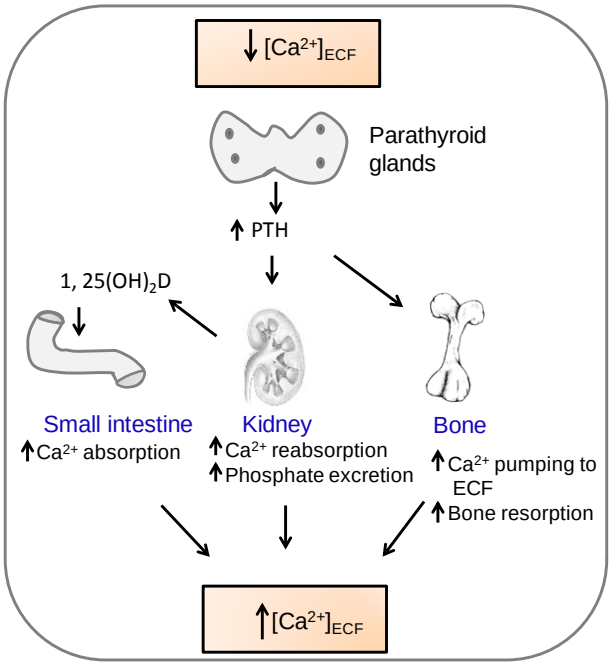

Figure 3.1. **Regulation of $[Ca^{2+}]_{ECF}$ by the endocrine system.** A decrease in $[Ca^{2+}]_{ECF}$ stimulates release of PTH from the parathyroid gland. Increased PTH levels in extracellular fluid stimulate processes that restore normal $[Ca^{2+}]_{ECF}$. These include increased Ca^{2+} resorption from bone, increased Ca^{2+} reabsorption from kidney cells, and reduced Ca^{2+} loss from small intestine mediated by the effects of PTH on vitamin D metabolism. Image was redrawn from (Brini *et al.*, 2013). 1,25-dihydroxyvitamin D_3 ($1,25(OH_2)D$)

3.1.2. Parathyroid hormone receptors

Three PTH receptor (PTHR) subtypes have been identified and cloned: parathyroid hormone receptor type 1 (PTH_1R) (Abou-Samra *et al.*, 1992; Juppner *et al.*, 1991), parathyroid hormone receptor type 2 (PTH_2R) (Usdin *et al.*, 1995) and parathyroid hormone receptor type 3 PTH_3R (Rubin *et al.*, 1999; Rubin *et al.*, 1999). Each PTHR type shows significant variation in its tissue distribution and ligand specificity. PTH_1R, is primarily expressed in kidney and bone cells (Tian *et al.*, 1993; Urena *et al.*, 1993). PTH and PTH-related peptide (PTHrP), a different gene product with significant N-terminal homology with PTH, show similar potency for activation of PTH_1R (Abou-Samra *et al.*, 1992; Juppner *et al.*, 1991). PTH_2R, which shares 30-60% amino acid identity with PTH_1R, is expressed mainly in brain and pancreatic tissues (Usdin *et al.*, 1995). In contrast with PTH_1R, PTH_2R is activated only by PTH, but not by PTHrP (Usdin *et al.*, 1995). In addition to PTH, PTH_2R can also be potently activated by an N-terminal 39-residue tuberoinfundibular peptide (TIP39), an endogenous peptide found in the hypothalamus (Dobolyi *et al.*, 2002; Usdin *et al.*, 2002; Usdin *et al.*, 1999). PTH_3R was first identified and cloned from zebrafish. The identification was based on its similarity to zebrafish PTH_2R (Rubin *et al.*, 1999; Rubin *et al.*, 1999). Zebrafish PTH_3R was potently activated by PTH in comparison to PTHrP. No known mammalian homologue of $zPTH_3R$ has been identified (Hoare *et al.*, 2000).

PTHRs belong to the GPCR class II family. Other receptors that belong to this family include the receptors for glucagon, calcitonin, secretin, and vasoactive intestinal peptide (Harmar, 2001; Mannstadt *et al.*, 1999; Pellegrini *et al.*, 1998). It is established that PTH_1R and PTH_2R couple to at least two intracellular signalling pathways: Gs which stimulates AC, and Gq which stimulates PLC (Abou-Samra *et al.*, 1992; Behar *et al.*, 1996; Huang *et al.*, 1996; Usdin *et al.*, 1995) . This coupling to dual signalling pathways is a characteristic feature of class II GPCR (Abou-Samra *et al.*, 1992; Behar *et al.*, 1996; Iida-Klein *et al.*, 1992; Jelinek *et al.*, 1993). In comparison to PTH_1R and PTH_2R, less is known about the signalling pathways activated by $zPTH_3R$. However, a few studies suggest that binding of PTH to these receptors stimulates cAMP formation (Rubin *et al.*, 1999).

3.1.3. The binding domain of PTH_1R

PTH is a polypeptide and consists of 84-residues (PTH(1-84)). However, it is well established that the first 34 residues at the N-terminal region are fully active and stimulate responses both *in vivo* and *in vitro* (Potts *et al.*, 1971; Tregear *et al.*, 1973). The C-terminal residues may protect the peptide from enzymatic degradation *in vivo* (O'Riordan *et al.*, 1973; Potts *et al.*, 1971; Tregear *et al.*, 1973).

Comparison of PTH(1-34) sequences from ten different animal species has revealed that the first six N-terminal residues are highly conserved among all these species. Hence, this region is important for either binding or activation of the PTH_1R. Using a synthesised peptide, Ala^4Tyr^{34}hPTH(1-34) NH_2, it was shown that Val^2 is crucial for activation, and Glu^4 for binding of PTH(1-34) to PTH_1R (Gardella *et al.*, 1991). The second important binding domain of PTH(1-34) peptide to PTH_1R exists in the C-terminus and is highly conserved among all animal forms of PTH (Toribio *et al.*, 2002). Sequential truncation of C-terminal residues show that residues between 15-34 of PTH(1-34) form a C-terminal domain that is involved in receptor binding (Caulfield *et al.*, 1990; Gardella *et al.*, 1993; Nussbaum *et al.*, 1980). In comparison to the first and second binding domains of PTH(1-34), the third domain consists of only 1 residue *i.e.* Lys at position 13. Deletions or mutations in any of these receptor-binding regions cause a substantial loss in the binding to and activation of PTH_1R by PTH (Adams *et al.*, 1998; Zhou *et al.*, 1997).

Similar to PTH(1-34), three important ligand-binding domains have been specified within the tertiary structure of PTH_1R. The N-terminal domain, the juxta-membrane region of the transmembrane domains, and the extracellular loops (Behar *et al.*, 2000; Bergwitz *et al.*, 1996; Hoare *et al.*, 2001; Juppner *et al.*, 1994). Almost all members of class II GPCR have six highly conserved extracellular cysteine residues within the N-terminal region (Lee *et al.*, 1994). These residues form disulphide bonds (Grauschopf *et al.*, 2000) that may allow the PTH_1R to attain a conformation needed for binding of the 25-32-residue C-terminus of PTH (Pellegrini *et al.*, 1998). Additionally, chimeric human/rat and rat/human PTH_1R hybrids confirmed the interaction of the N-terminus of PTH_1R with the C-terminal domain of PTH(1-34) (Juppner *et al.*, 1994). From other chimeric studies, it was confirmed that the fifth transmembrane domain of PTH_1R interacts with the N-terminal domain of PTH(1-34) (Gardella *et al.*, 1994). The PTH_1R second ligand-binding domain (the juxtamembrane region of PTH_1R) binds to

the 13th (a highly conserved lysine) and 19th residues of PTH(1-34) (Adams *et al.*, 1998; Pellegrini *et al.*, 1998; Shimizu *et al.*, 2002). The PTH_1R first extracellular loop is important for binding with the mid-region of PTH(1-34) (Greenberg *et al.*, 2000; Piserchio *et al.*, 2000) and the third extracellular loop binds exclusively with N-terminal residues (residues 1 and 2) of PTH(1-34) (Hoare *et al.*, 2001).

3.1.4. Coupling of PTH_1R to Gs

Stimulation with PTH activates cAMP formation in cells expressing endogenous (Chase *et al.*, 1967; Mine *et al.*, 1989; Smith *et al.*, 1975) or recombinant PTH_1R (Abou-Samra *et al.*, 1992; Pines *et al.*, 1994; Takasu *et al.*, 1999; Tovey *et al.*, 2008). These studies also confirmed that PTH activates cAMP formation at very low concentrations in comparison to those required for Ca^{2+} responses.

The plasma membrane-localised AC converts ATP to cAMP, after the activation of Gs-coupled receptors (Simonds, 1999). These results suggest that stimulation with PTH activates cAMP formation, via coupling of PTH_1R with Gs and thereby activation of AC. This hypothesis was proved in a study where in HEK-PR1 cells PTH(1-34) via PTH_1R enhanced the photo-labelling of Gs by a photoreactive GTP analogue (Schwindinger *et al.*, 1998).

Higaki *et al.* (1992) suggested that insertion of Zn^{2+} bridges between two histidine residues can block the mobilization of two regions of a protein relative to each other (Higaki *et al.*, 1992). A related investigation was done on PTH_1R receptors and revealed that formation of Zn^{2+} bridges between transmembrane domains 3 and 6 of PTH_1R inhibits the activation of Gs (Sheikh *et al.*, 1999). Binding of PTH might change the conformation of transmembrane domains 3 and 6, thereby allowing Gs to gain access to PTH_1R (Sheikh *et al.*, 1999). Further, studies performed using chimeras of the secretin receptor and PTH_1R also supported the contribution of transmembrane domains 3 and 6 in the activation of Gs (Vilardaga *et al.*, 2001). In a chimera consisting of cytoplasmic and transmembrane domains of the secretin receptor and the extracellular domains of PTH_1R, substitution of transmembrane domains 3 and 6 with that of PTH_1R showed an increase in cAMP levels when stimulated with PTH (Vilardaga *et al.*, 2001). In addition to this, in common with β-adrenoceptors, mutations in the N-terminal regions of the third intracellular loop of PTH_1R significantly affect Gs coupling (Huang *et al.*, 1996; Ostrowski *et al.*, 1992). In COS-7 cells substitution of

Lys^{382} with Ala within the N-terminal loop of the third transmembrane domain of PTH_1R decreased PTH-stimulated cAMP formation. However, in oocytes PTH_1R two residues Thr^{381} and Lys^{382} are critical for showing the similar effect. Hence, possibly Gαs-GDP binds to the third intracellular loop of PTH_1R and with PTH binding, transmembrane domains 3 and 6 separate and GDP is replaced with GTP on Gαs.

Besides, cAMP formation, coupling of PTH_1R with Gi causes inhibition of cAMP formation which has been proved in photoaffinity labelling (Schwindinger *et al*., 1998) and functional studies (Iida-Klein *et al*., 1995; Pines *et al*., 1994). Pertussis toxin, which inhibits coupling of Gi to associated GPCR enhanced PTH-stimulated cAMP formation in COS-7 cells (Iida-Klein *et al*., 1995; Pines *et al*., 1994). Deletion of the C-terminal tail of PTH_1R also increased PTH-stimulated cAMP formation and interestingly it was unaffected by pre-treatment with pertussis toxin. This shows that the PTH_1R C-terminal tail couples with Gi (Iida-Klein *et al*., 1995). These observations show that a single receptor can either activate or inhibit AC. Other receptors like β_2-adrenoceptors also share similar properties (Xiao *et al*., 1999; Xiao *et al*., 1995). The change of β_2-adrenoceptor coupling from Gs to Gi is regulated by the PKA-mediated phosphorylation of the receptor (Daaka *et al*., 1997). The importance for the present work is that binding of different PTH analogues to PTH_1R stimulates AC and thereby cAMP formation. Subsequently, the cAMP produced potentiates release of Ca^{2+} from intracellular stores (Fig. 3.2) (Tovey *et al.*, 2008).

3.1.5. Regulation of $[Ca^{2+}]_c$ by PTH

PTH stimulates both several Ca^{2+} entry pathways and release of Ca^{2+} from intracellular stores. In, for example, hepatocytes (Klin *et al.*, 1994), smooth muscle cells (Picotto *et al.*, 1997) and cardiac myocytes, (Rampe *et al.*, 1991), stimulation with PTH causes Ca^{2+} entry across the PM. Whole-cell recording confirms that stimulation with PTH increases the probability of Ca^{2+} channel opening and use of selective L-type Ca^{2+} blockers such as nimodipine and verapamil confirms that PTH modulates Ca^{2+} entry by L-type Ca^{2+} channels (Klin *et al.*, 1994; Picotto *et al.*, 1997; Rampe *et al.*, 1991). The PTH-potentiated Ca^{2+} entry is dependent on cAMP and PKA, and mimicked by cell-permeable cAMP analogues (Fritsch *et al.*, 1988; Klin *et al.*, 1994; Picotto *et al.*, 1997; Smogorzewski *et al.*, 1993) and agonists of AC like forskolin (Picotto *et al.*, 1997; Smogorzewski *et al.*, 1993). Inhibition of PKA, using H89, blocked PTH-mediated

Ca^{2+} entry consistent with PKA stimulating L-type Ca^{2+} channels (Klin *et al.*, 1994; Picotto *et al.*, 1997).

PTH hyperpolarises the plasma membrane of osteoblasts (Ferrier *et al.*, 1988; Fritsch *et al.*, 1988) and distal convoluted tubule cells (Barry *et al.*, 1998), perhaps due to Ca^{2+}-mediated activation of K^+ channels (Ferrier *et al.*, 1988). The exact identity of the Ca^{2+} channels responsible is unclear, but their pharmacology is consistent with them being VOC (Barry *et al.*, 1998; Friedman *et al.*, 1994; Gesek *et al.*, 1992; Matsunaga *et al.*, 1994).

In osteoblasts (Dunlay *et al.*, 1990; Kaplan *et al.*, 1995; Wiltink *et al.*, 1993) and kidney cells (Dunlay *et al.*, 1990; Schwindinger *et al.*, 1998), PTH potentiates release of Ca^{2+} from intracellular stores. In these cells expressing either recombinant (Abou-Samra *et al.*, 1992; Bringhurst *et al.*, 1993; Pines *et al.*, 1996; Takasu *et al.*, 1999) or endogenous (Dunlay *et al.*, 1990; Kaplan *et al.*, 1995; Wiltink *et al.*, 1993) PTH_1R, stimulation with PTH causes formation of IP_3. This suggests that PTH_1R might stimulate PLC via Gq proteins. This hypothesis was proved by Schwindinger *et al.* in 1998, using a photo-affinity label linking with GTP which showed that PTH_1R can activate Gs, Gq and Gi (Schwindinger *et al.*, 1998). In addition, inhibition of Na^{2+}-K^+-ATPase by PTH in renal proximal tubules, which is mediated by AA, was inhibited by anti-$G_{q/11}$ antibodies (Derrickson *et al.*, 1997).

Binding of PTH within the N-terminal tail region of PTH_1R stimulates coupling of PTH_1R similarly for both Gq and Gs proteins. The binding site for Gq proteins within the N-terminal tail region (third intracellular loop) of the PTH_1R is adjacent to the Gs-binding site (Huang *et al.*, 1996). The ability of PTH_1R to couple with Gq and Gs is dependent on the number of expressed PTH_1R (Guo *et al.*, 1995; Schwindinger *et al.*, 1998). In cells expressing PTH_1R (~400 000 receptors/cell), receptors couple to both Gq and Gs, whereas, with fewer receptors (~72 000 receptors/cell), PTH_1R preferentially couples to only Gs (Guo *et al.*, 1995; Schwindinger *et al.*, 1998). In kidney and bone cells, the characteristics of PTH to stimulate dual signalling pathways might be due to higher numbers of expressed PTH_1R receptors (Takasu *et al.*, 1999; Takasu *et al.*, 1999). There are a few other settings where stimulation with PTH potentiated release of Ca^{2+} from intracellular stores, which was not mediated via the Gq/PLC signalling pathway. In rat osteosarcoma cells, no IP_3 formation was observed when stimulated with PTH (Babich *et al.*, 1991; Seuwen *et al.*, 1995), also inhibition of IP_3R using heparin in HEK-293 cells also did not affect PTH-potentiated release of

Ca^{2+} (Seuwen *et al.*, 1995; Tong *et al.*, 1996). If IP_3 did not mediate the potentiation of Ca^{2+} release by PTH, then it was obvious to consider contributions from NAADP and cADPR. However, experimental data reported by Tong *et al.* (1996) indicates that neither NAADP nor cADPR were associated with PTH-evoked Ca^{2+} release. In addition, inhibition of RyR did not affect PTH-potentiated Ca^{2+} release (Seuwen *et al.*, 1995). The significance for the present work is that binding of different PTH analogues to PTH_1R stimulates either Gq or Gs, or both signalling pathways and thereby leads to the formation of IP_3 or cAMP respectively. These second messengers, either independently or in combination (Tovey *et al.*, 2008), regulate release of Ca^{2+} from intracellular stores (Fig. 3.2).

3.1.6. Selective activation of signalling pathways using PTH analogues

PTH analogues have been designed and used to show different signalling pathways triggered upon binding of PTH to PTH_1R (Table 3.1). Modifications in the PTH_1R expression density on the cell surface can also favour selective coupling to AC or PLC (Guo *et al.*, 2010; Mahon, 2012; Taylor *et al.*, 2012). Association of the C-terminal tail of PTH_1R with the scaffold proteins, Na^+/H^+ exchange regulatory factors-1/2 (NHERF-1/2), both of which are expressed in HEK cells (Wang *et al.*, 2010), favours coupling via Gq and/or Gi/o to PLCβ (Mahon, 2012; Wang *et al.*, 2007). cAMP can also indirectly stimulate IP_3 formation. As binding of cAMP to Epac1 has been reported to allow it to activate the small G protein, Rap 2B, and it then stimulates PLCε (Schmidt *et al.*, 2001). In the present work different PTH analogues have been used to scrutinize the different signalling pathways activated by PTH_1R.

	G protein coupling	β-arrestin coupling	PTH_1R/ agonist internalization	Cell types	References
PTH(1-34)	Gs and Gq	full agonist	Yes	HEK-PR1, COS-7-PR1, U2OS-PR1, mouse fibroblasts, CHO-K1-PR1	(Bisello *et al.*, 2002; Castro *et al.*, 2002; Cupp *et al.*, 2013; van der Lee *et al.*, 2013)
PTHrP(1-36) & PTHrP(1-34)	Gs and Gq	full agonist	Yes	HEK-PR1, CHO-K1-PR1	(Bisello *et al.*, 2002; Cupp *et al.*, 2013; Dean *et al.*, 2008)
PTH(2-38)	Gs only	weak partial agonist	No	CHO-K1-PR1	(Cupp *et al.*, 2013)
PTH(1-31)	Gs & Gq strong partial agonist	full agonist	Yes	HEK-PR1, COS-7-PR1, CHO-K1-PR1	(Cupp *et al.*, 2013; Takasu *et al.*, 1999)
PTH(3-34)	Gs weak partial agonist	Inactive	No	HEK-PR1, COS-7-PR1 CHO-K1-PR1	(Cupp *et al.*, 2013; van der Lee *et al.*, 2013)
Tyr^1PTH(1-34)	Gs	weak partial agonist	No	CHO-K1-PR1	(Cupp *et al.*, 2013)

Table 3.1. **Examples of PTH analogues that allow selective coupling of PTH_1R to Gs and Gq**

3.1.7. Sustained signalling from type 1 PTH receptor

Binding of PTH and PTHrP to PTH_1R follows a two-step process. The first step involves an interaction between the C-terminal residue, the binding domain of the ligand, and the large extracellular N-terminal domain of the PTH_1R. Second, a slow interaction between the N-terminal signalling domain of the ligand with the juxtamembrane (J) region of the PTH_1R, which consists of the extracellular loops and seven transmembrane helices. The resulting high-affinity complex between the ligand and PTH_1R acquires a conformation capable of interacting selectively with a G protein or other signalling proteins (Dean *et al.*, 2006; Ferrandon *et al.*, 2009).

PTH_1R has the capacity to form two pharmacologically distinct, high-affinity, conformational states. One conformation called 'RG', is sensitive to GTPγS and is therefore most probably associated with heterotrimeric G proteins. A second conformation, termed R^0, is insensitive to GTPγS and is therefore functionally uncoupled from G proteins (Dean *et al.*, 2008; Okazaki *et al.*, 2008). PTH or PTHrP residues that interact with the J-domain of the receptor are important in determining the signalling proteins with which active PTH_1R interacts (Cupp *et al.*, 2013; Ferrandon *et al.*, 2009; Pioszak *et al.*, 2009). Different analogues of PTH(1-34) favour PTH_1R coupling to G protein or to the other signalling protein, according to their specific mode of activation (Table 3.1).

The signalling pathways activated by different analogues of PTH(1-34) are GPCR kinases (GRK) and β-arrestin (Gesty-Palmer *et al.*, 2011). PTH_1R binding to β-arrestin triggers PTH_1R desensitization by uncoupling receptors from G-proteins (Feinstein *et al.*, 2011). However, β-arrestin can also recruit additional signalling pathways, like extracellular signal-regulated kinases (ERK 1/2) (Gesty-Palmer *et al.*, 2006). In addition to these interactions, recently it has been shown that binding of PTH(1-34) to PTH_1R initiates internalization of active PTH_1R/Gs/AC signalling complexes (Ferrandon *et al.*, 2009).

Modification in the N-terminus of PTH(1-34) showed even more selectivity than PTH(1-34) itself for the R^0 conformation (Okazaki *et al.*, 2008). In whole cells, acute incubation with analogues that bind most selectively to R^0, form longer-lasting complexes with PTH_1R, more sustained activation of PTH_1R and Gs, and more sustained stimulation of AC (Dean *et al.*, 2008; Ferrandon *et al.*, 2009; Okazaki *et al.*, 2008). Thus, AC activity measured 60 min after brief (10 min) exposure to PTH(1-34)

is greater than for PTHrP(1-36), even though the initial response to each is similar (Bisello *et al.*, 2002; Vilardaga *et al.*, 2002). Nevertheless, long-lasting active G-protein-coupled signalling via N-terminally modified PTHrP(1-36) has also been observed (Bisello *et al.*, 2002).

Most likely two factors are accountable for the sustained activation of AC by PTH(1-34). Firstly, the high-affinity R^0-PTH complex may provide a pool of PTH(1-34)-bound PTH_1R that can isomerize to the RG conformation, and so sustain activation of Gs at the plasma membrane after removal of free PTH(1-34). Secondly, and possibly more importantly, brief stimulation with PTH(1-34) causes fast internalization of functional PTH·PTH_1R·Gs/β-arrestin·AC signalling complexes via a β-arrestin- and dynamin-dependent endocytic pathway (van der Lee *et al.*, 2013). These complexes, in which β-arrestin facilitates rather than blocks Gs activation (Wehbi *et al.*, 2013), continue to generate cAMP from early endosomal compartments (Feinstein *et al.*, 2011; Ferrandon *et al.*, 2009).

Termination of signalling takes place when the retromer protein complex directs the signalling proteins towards the Golgi apparatus (Feinstein *et al.*, 2011). PTHrP(1-36) does not evoke this internalization (Ferrandon *et al.*, 2009). Similar agonist-evoked internalization of functional signalling pathways has been reported for other GPCRs (Calebiro *et al.*, 2009; Calebiro *et al.*, 2010; Irannejad *et al.*, 2013). The significance for the present work is that internalized PTH_1R signalling complexes and those at the plasma membrane may deliver cAMP to different intracellular compartments.

3.1.8. PTH triggers crosstalk between cAMP and Ca^{2+}

PTH potentiates the Ca^{2+} release evoked by IP_3-linked agonists (Buckley *et al.*, 2001; Short *et al.*, 2000; Tovey *et al.*, 2003). Low PTH concentrations did not stimulate IP_3 formation or Ca^{2+} release on their own, but they significantly potentiated the Ca^{2+} release evoked by CCh (Buckley *et al.*, 2001; Short *et al.*, 2000; Tovey *et al.*, 2003). Surprisingly, PTH potentiated the amount of Ca^{2+} release even by maximal CCh concentrations (Short *et al.*, 2000; Tovey *et al.*, 2003). Similar to PTH(1-34), forskolin (FK), which stimulates AC directly, 8-Br-cAMP, a membrane-permeant cAMP analogue and other agonists which activate AC through endogenous receptors (Tovey *et al.*, 2008), potentiated CCh-evoked Ca^{2+} responses. Although higher cAMP levels are

required to mimic PTH(1-34) effects as the level of cAMP formation using FK and prostaglandin E_1 was less in comparison to PTH.

Potentiation of CCh-evoked Ca^{2+} release by PTH(1-34), FK or 8-Br-cAMP was not mediated by PKA or Epac1/2 (Tovey *et al.*, 2010; Tovey *et al.*, 2008) since inhibition of PKA did not affect the CCh-evoked Ca^{2+} signal. By contrast PKA inhibition prevented FK-, PTH-, and 8-Br-cAMP-stimulated phosphorylation of various proteins in HEK-PR1 cells. Similarly, stimulation of HEK-PR1 cells with 8-Br-2′-O-methyladenosine-3′,5′-cAMP which selectively activates Epacs (Christensen *et al.*, 2003) had no effect on CCh-evoked Ca^{2+} signals, whereas 8-Br-cAMP potentiated them. Although, these results suggested that PKA and Epac1/2 are not involved but the possibility cannot be ruled out as the role of Epac1/2 should have been confirmed by using specific and non toxic inhibitor, which have not been available until now.

Increasing intracellular cAMP levels by inhibiting PDE using IBMX did not potentiate the CCh response. Furthermore reducing the cAMP formation (by almost ~ 80%) by inhibiting AC with SQ22536/2',5'-dideoxyadenosine (SQ/DDA) did not affect the ability of PTH(1-34) to potentiate responses to CCh (Tovey *et al.*, 2008). The calculated global intracellular cAMP was ~1000-fold too low to affect all the intracellular IP_3R. Therefore, it was entirely clear that the effects of IBMX are insufficient to allow cAMP to globally regulate IP_3Rs. These results can be explained if cAMP signalling occurs locally within a hyperactive signalling complex i.e. 'cAMP junctions', where IP_3R and AC are associated. Tovey *et al*. (2008) proposed that within this complex super-saturating cAMP concentrations pass directly from AC to IP_3R, and are inaccessible to PDE. Upon stimulation, AC generates more cAMP than needed to maximally sensitize IP_3R. Thus, it operates with a large safety margin which enables IP_3R sensitization even when cAMP production is substantially reduced by inhibiting AC. This hypothesis was further supported by complete inhibition of cAMP formation in a few cAMP junctions, achieved by inhibition of expression of Gαs by means of siRNA, which affected PTH potentiation more strongly than partial inhibition of all AC (Tovey *et al.*, 2008).

It was suggested that possibly the low affinity of IP_3R for cAMP ensures junctions are isolated from surrounding AC-IP_3R complexes, because the super-saturating cAMP concentration needed to effectively sensitize IP_3R is not achieved by diffusing cAMP. In this setting, the concentration-dependent effect of PTH or FK is

attained via recruitment of more hyper-active cAMP junctions instead of the graded global increase in cAMP concentration (Tovey *et al.*, 2008).

In permeabilized DT40 cells expressing single subtypes of each IP_3R, cAMP sensitized IP_3-evoked Ca^{2+} release from all three subtypes of IP_3R (Tovey *et al.*, 2010). Based on immunoprecipitation and siRNA studies, the specific subtypes of IP_3R and AC involved in the hyperactive cAMP junctions were identified. IP_3R type 2 (IP_3R2) and AC type 6 (AC6) were found to be specifically associated (Tovey *et al.*, 2008). These hyperactive cAMP junctions suggest a new interaction between Ca^{2+} and cAMP, and a novel signalling model based on recruitment of hyperactive IP_3R2-AC6 complexes in response to agonist stimulation. The significance for the present work is that when PTH_1R-AC signalling complexes are internalised (Ferrandon *et al.*, 2009) (see Section. 3.1.7), the interactions between AC and IP_3R might be reconfigured.

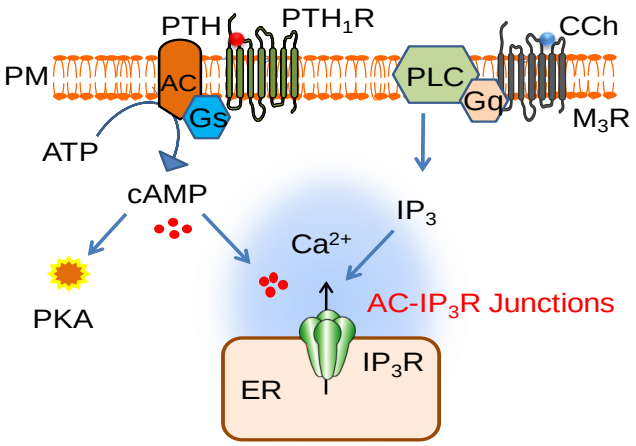

Figure 3.2. **Ca^{2+} signalling mediated via AC-IP_3R junctions**. In HEK-PR1 cells, binding of PTH to PTH_1R activates Gs and binding of CCh to muscarinic acetylcholine receptors (M_3R) activates Gq. Gs activates AC, and Gq stimulates PLC. These enzymes catalyze formation of the second messengers, cAMP and IP_3. IP_3 activates IP_3R to release Ca^{2+} from ER. cAMP activates PKA and can also directly sensitise IP_3R to IP_3 leading to enhanced Ca^{2+} release. AC-IP_3R junctions are defined as a hyperactive signalling complex, where supersaturating cAMP concentration directly sensitise IP_3R to IP_3.

3.1.9. Aims

In this chapter two questions associated with the effects of sustained stimulation with PTH(1-34) are addressed:

a. Does sustained stimulation with PTH(1-34) cause sustained potentiation of CCh-evoked Ca^{2+} signals?

b. Does cAMP mediate sustained stimulation of CCh-evoked Ca^{2+} signals by PTH(1-34)?

3.2. Materials and Methods

3.2.1. Materials

Table 3.2 lists the sources of materials used. Table 3.3 shows the PTH analogues used. All analogues were the human forms and were either supplied by Bachem (Bubendorf, Switzerland) or, for PTHrP(1-36), custom-synthesized by Selleckchem (Boston, MA). Table 3.3 lists of solvents used to prepare drugs.

Material	**Provider**
H89 dihydrochloride	R&D Systems (Minneapolis, MN)
8-Br-cAMP	R&D Systems (Minneapolis, MN)
2',5'-dideoxyadenosine (DDA)	Merck Biosciences (Middlesex, UK)
NKH477	Merck Biosciences (Middlesex, UK)
SQ22536	Merck Biosciences (Middlesex, UK)
[2, 8-^{3}H]-adenine	Perkin Elmer (Waltham, MA)
1, 2-bis(o-aminophenoxy)ethane-N, N, N, N'-tetraacetic acid (BAPTA)	Molekula (Gillingham, UK)
Carbamoylcholine chloride (CCh)	Sigma-Aldrich (Gillingham, UK)
3-isobutyl-1-methylxanthine (IBMX)	Sigma-Aldrich (Gillingham, UK)
Ionomycin	Scientific (Stockport, UK)
Cell culture media, G-418	Life Technologies (Paisley, UK)
Fluo 4AM, fura 2AM	Life Technologies (Paisley, UK)
ESI-09	Biolog Life Science Institute (Bremen, Germany)

Table 3.2. **Materials used**

PTH(1-34)	SVSEIQLMHNLGKHLNSMERVEWLRKKLQDVHNF
PTH(2-38)	VSEIQLMHNLGKHLNSMERVEWLRKKLQDVHNFVALG
Tyr^{1}PTH(1-34)	YVSEIQLMHNLGKHLNSMERVEWLRKKLQDVHNF
PTHrP(1-36)	AVSEHQLLHD KGKSIQDLRRRFFLHHLIAEIHTAQI
PTHrP(1-34)	AVSEHQLLHDKGKSIQDLRRRFFLHHLIAEIHTA
PTH(1-31)	SVSEIQLMHNLGKHLNSMERVEWLRKKLQDV

Table 3.3. **Sequences of the human PTH and PTHrP analogues used**

Drug	Solvent	Storage (^{o}C)
H89	Water (25 mM stock)	-20
8-Br-cAMP	Water (10 mM stock)	-20
DDA	HBS (200 µM, final concentration)	4
NKH477	Water (10 mM stock)	4
SQ22536	HBS (1 mM, final concentration)	4
BAPTA	HBS (2.5 mM, final concentration)	-20
IBMX	Water (100 mM stock)	-20
ESI-09	DMSO (50 mM stock)	-20
PTH analogs	Water (100 µM stock)	-20

Table 3.4. **List of solvents used to prepare drugs**

3.2.2. Culture of HEK-PR1 cells

Human embryonic kidney 293 (HEK293) cells stably-expressing human parathyroid hormone receptor type 1 (HEK-PR1cells) (Short *et al.*, 2000) were cultured in Dulbecco's modified Eagle's/Ham's F-12 medium supplemented with foetal calf serum (10 %) and G-418 (800 µg/ml), at 37° C in 5 % CO_2 and 95 % air. Cells were grown in 175-cm^2 flasks and used or passaged when confluent. The HEK-PR1 cells were established in this laboratory using methods fully described in (Short *et al.*, 2000).

3.2.3. Measurement of $[Ca^{2+}]_c$ in HEK-PR1 cell populations

Measurements of $[Ca^{2+}]_c$ in cell populations were performed as previously described (Tovey *et al.*, 2008). Fluo4-AM was dissolved in DMSO to produce a 2 mM stock concentration and then diluted in HBS to a final concentration of 2 µM. The non-ionic detergent Pluronic F127 (0.02 %) was added to avoid micelle formation. Confluent cultures of HEK-PR1 cells in 96-well plates were loaded with indicator for 1 h at 20

°C. Complete cytosolic de-esterification of the indicator was achieved by subsequent incubation in HBS with Pluronic F127 (0.02%) for 45 min (20 °C).

$[Ca^{2+}]_c$ was monitored using a fluorescence plate-reader (FlexStation III, MDS Analytical Devices) equipped to allow a maximum of 3 automated fluid additions (Tovey *et al.*, 2006). Simultaneous readings of 8 wells were recorded, with excitation at 485 nm and emission collected at >525 nm (the peak emission wavelength of Ca^{2+}-bound Fluo-4). Each well was monitored at intervals of 1.44s for a total of 120 s, unless otherwise stated.

Fluorescence values were analyzed with SoftMaxPro software, converted to $[Ca^{2+}]_c$ using equation 3.1, and fitted to the Hill equation using GraphPad Prism to obtain concentration-effect relationships. Results, $\Delta[Ca^{2+}]_c$, are expressed as means ± SEM.

$$[Ca^{2+}]_c = K_d \times \frac{(F - F_{min})}{(F_{max} - F)} \qquad \text{equation (3.1)}$$

where K_d is the dissociation constant of Fluo 4 for Ca^{2+} (345 nM) and F is the fluorescence value obtained. Calibration was done *in situ* in parallel wells. Values for F_{min} (fluorescence in the absence of Ca^{2+}) and F_{max} (fluorescence with saturating Ca^{2+}) were obtained by addition of BAPTA (10 mM) with 0.2 % Triton X-100 (F_{min}), or $CaCl_2$ (10 mM) with 0.2 % Triton X-100 (F_{max}), respectively.

3.2.4. Measurements of $[Ca^{2+}]_c$ in single HEK-PR1 cells

The protocol for measuring $[Ca^{2+}]_c$ in single fura2-loaded HEK-PR1 cells is similar to that described in Section 2.2.4. However, for HEK-PR1cells, HBS buffer was used. HBS had the following composition (mM): NaCl 135, KCl 5.9, $MgCl_2$ 1.2, $CaCl_2$ 1.5, HEPES 11.6 and glucose 11.5, pH 7.3. $CaCl_2$ was omitted from Ca^{2+}-free HBS.

3.2.5. cAMP measurements using column chromatography

cAMP measurements were performed under conditions that replicate those used for measurements of $[Ca^{2+}]_c$. HEK-PR1 cells were grown in 24-well plates until ~90% confluent, [^{3}H]-adenine (2 µCi/well) was then added to the culture medium (DMEM-F12 containing 10% FBS). After 2 h at 37^{o}C in 5% CO_2, the medium was removed.

Cells were then washed with HBS, and used for experiments in HBS at 20°C. Because many cells extrude cAMP into the extracellular medium (Copsel *et al.*, 2011), reactions were terminated by first removing the medium and then adding ice-cold trichloroacetic acid (5%, 1 ml). After 30 min on ice, the cell lysate (1 ml) was transferred to a Dowex column at 20°C (1 ml, Dowex 50 WX4-400 equilibrated with 1 M HCl). The eluate contains [^{3}H] ATP and [^{3}H] ADP, but [^{3}H] cAMP is retained on the Dowex column. Each Dowex column was washed with H_2O (2 ml) and the eluate pooled with the initial run-through fraction. [^{3}H]cAMP was then eluted from the Dowex column using H_2O (8 ml) and loaded onto a alumina column (0.5 g/column, alumina equilibrated with 10 ml 1M imidazole-HCl pH 7.5, then 8 ml of 0.1 M imidazole-HCl pH 7.5), from which [^{3}H]cAMP was then eluted with 0.1 M imidazole pH 7.5 (4 ml) (Pantazaka *et al.*, 2013; Salomon *et al.*, 1974). Ultra-gold scintillant (5 ml) was added to each scintillation vial containing eluate from the Dowex or alumina columns. The activity of the eluates was determined by liquid scintillation counting. Amounts of ^{3}H-cAMP were expressed as percentages of the sum of the activities recovered in the ^{3}H-cAMP, ^{3}H-ADP and ^{3}H-ATP fractions.

3.2.4 Analysis

Concentration-effect relationships were fitted to Hill equations with a variable Hill slope (*h*) using Prism version 5 (GraphPad, San Diego, CA, USA):

$$R = \frac{R_{Max} - R_{Min}}{1 + 10^{(\log EC_{50} - \log[C]).h}} \qquad \text{equation (3.2)}$$

where, R is the response (e.g., $[Ca^{2+}]_c$) detected with the drug concentration, C (in M). R_{Max} and R_{Min} are the responses predicted by extrapolation of the fitted curve to an infinite concentration of C (R_{Max}) and no C (R_{Min}). EC50 is the concentration of C that evokes the half-maximal response, from which the pEC50 value was determined (pEC_{50} = -logEC_{50}). For most analyses, the curves were fitted without restraining R_{Max}, R_{Min} or *h*. Concentration-effect relationships were fitted to the results from individual experiments before pooling parameters (R_{max}, *h*, pEC_{50}, etc) for statistical analyses. Results are shown as means ± SEM. Statistical comparison of sensitivities used pEC_{50} values. Because the experiments were performed over a period of 2 years, there was some variability in CCh-evoked Ca^{2+} signals. Therefore, each experiment was performed with its control experiments and the statistical significance test has also been

performed between each experiment and its corresponding control. For multiple comparisons one-way analysis of variance and Tukey multiple comparison test and for comparing two samples, paired t-test was used.

3.3. Results

3.3.1. PTH(1-34) potentiates CCh-evoked Ca^{2+} responses

In populations of HEK-PR1 cells expressing M_3R, CCh, an agonist of muscarinic acetylcholine receptors (M_3R), was used to activate PLC, formation of IP_3 and release of Ca^{2+} from intracellular stores via IP_3R. 1,2-bis(o-aminophenoxy) ethane-N,N,N',N'-tetraacetic acid (BAPTA, 10 mM), a Ca^{2+}-chelating agent, was added before stimulation with a maximal CCh concentration (1 mM) to ensure that the increases in $[Ca^{2+}]_c$ were due to the Ca^{2+} release from intracellular stores. The increase in $[Ca^{2+}]_c$ evoked by CCh returned to the basal levels within ~60s. After the increased $[Ca^{2+}]_c$ had returned to the resting level, the addition of PTH(1-34) (100 nM) in the continuous presence of CCh, showed a further release of Ca^{2+} (Fig. 3.3A). These results are in agreement with previous studies (Tovey *et al.*, 2008; Tovey *et al.*, 2003). A similar protocol was used to examine the PTH(1-34) concentration-dependence. The results show that the maximal potentiation of CCh-evoked Ca^{2+} release with PTH(1-34) occurred with a half-maximally effective concentration (pEC_{50}) of 7.0 ± 0.01 (Fig. 3.3B). Similar results have been published (Tovey *et al.*, 2008; Tovey *et al.*, 2003).

In the presence of BAPTA (10 mM), stimulation of HEK-PR1 cells with PTH(1-34) (100 nM) showed no increase in $[Ca^{2+}]_c$. However, subsequent addition of a maximal concentration of CCh evoked an increase in $[Ca^{2+}]_c$ (Fig. 3.3C). Figure 3.3D shows the CCh dose-response curve obtained with or without PTH(1-34) (100nM) pre-treatment. PTH(1-34) increased both the maximal amplitude and the sensitivity of the response to CCh. The pEC_{50} for CCh was increased from 4.4 ± 0.1 to 5.1 ± 0.1, and the maximal amplitude of the increase in $[Ca^{2+}]_c$ increased from 131 ± 26 to 405 ± 83 nM in the presence of PTH(1-34) (Fig. 3.3D). In subsequent experiments 20 µM CCh was routinely used to obtain submaximal levels of Ca^{2+} release. These results are consistent with earlier studies (Short & Taylor 2000).

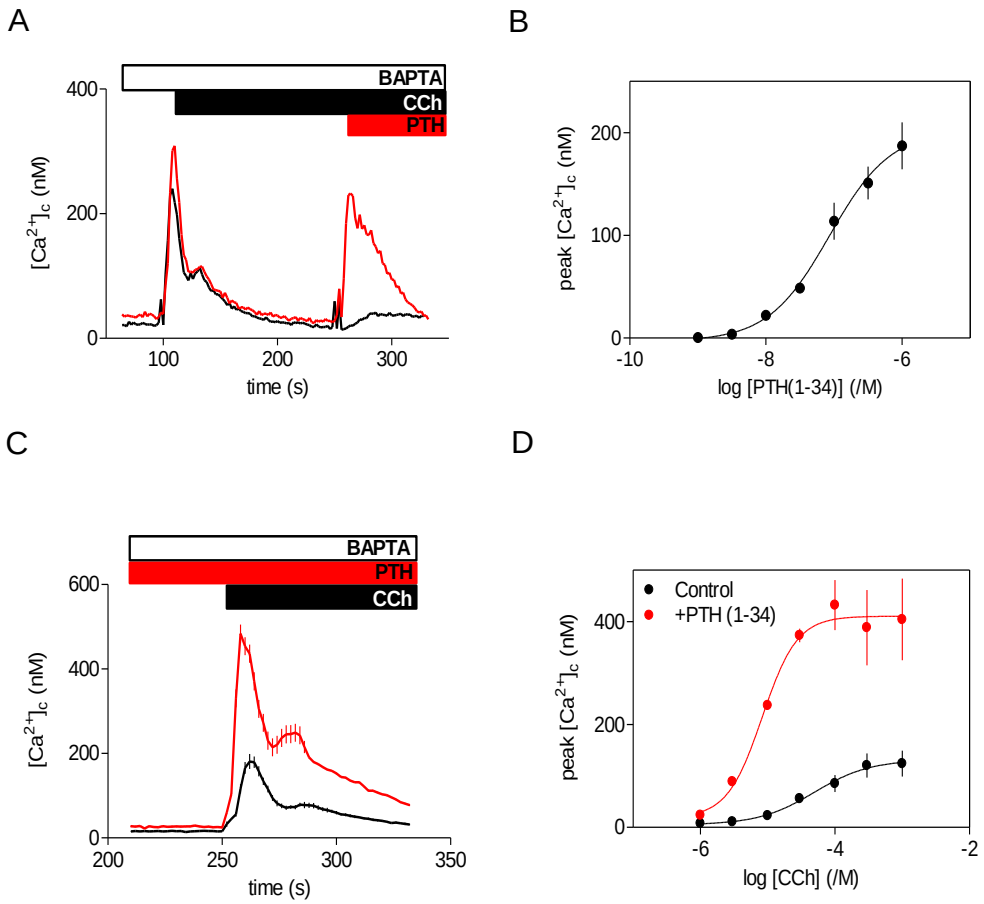

Figure 3.3. **PTH(1-34) potentiates CCh-stimulated Ca^{2+} signals.** (**A**) In a population of HEK-PR1 cells, the typical trace shows transient release of Ca^{2+} from intracellular stores upon stimulation with a maximal CCh (1 mM) concentration (black, the increase in $[Ca^{2+}]_i$ at 250 sec is an CCh addition artefact). In the continued presence of CCh (1 mM), PTH(1-34) (100 nM) stimulated a further Ca^{2+} release (red). (**B**) The concentration-dependent effect of PTH(1-34) on the peak Ca^{2+} signals ($[Ca^{2+}]_c$) evoked in the continuous presence of CCh (1 mM). (**C**) Typical trace shows HEK PR1 cells stimulated with PTH(1-34) (100 nM) (red) or HBS alone for 1 min before addition of CCh (1 mM) (black). (**D**) Concentration-dependent effect of CCh on the peak Ca^{2+} signals ($[Ca^{2+}]_c$) evoked in the presence or absence of PTH (100 nM). In each experiment BAPTA (10 mM) was added 30 s before the first addition of CCh or PTH(1-34). Results (A, C) are means ± SEM for 3 wells from one experiment, typical of 3 similar experiments. Results (B, D) are means SEM from 3 independent experiments.

3.3.2. Sustained stimulation with PTH(1-34) increases the sensitivity to PTH, but reduces the amplitude potentiation of CCh-evoked Ca^{2+} responses

In HEK-PR1 cells, (Tovey *et al.*, 2008) showed that PTH stimulates cAMP formation, and it was suggested that the cyclic nucleotide was directly delivered to IP_3R within hyperactive AC-IP_3R junctions (Section. 3.1.8). This, along with the evidence that binding of PTH(1-34) to PTH_1R at the plasma membrane stimulates internalisation of PTH_1R-AC signalling complexes, which then continues cAMP formation via AC for sustained durations (Ferrandon *et al.*, 2009), persuaded me to examine the effect of prolonged PTH(1-34) stimulation on CCh-evoked Ca^{2+} responses.

In a population of HEK-PR1 cells, acute (1 min) or sustained (60 min) stimulation with PTH(1-34) potentiated the Ca^{2+} signals evoked by submaximal (20 μM) (Fig. 3.4A) and maximal (1 mM) (Fig. 3.4B) concentrations of CCh in Ca^{2+}-free medium. Figure 3.4C, D shows the PTH(1-34) concentration-effect curve obtained after varying the duration of pre-treatment with PTH(1-34) before the addition of maximal or sub-maximal CCh concentrations in the presence of BAPTA. These results show that PTH(1-34) potentiated CCh-evoked Ca^{2+} responses after acute as well as sustained stimulation. However, in comparison with the acute effect, sustained exposure to PTH(1-34) reduced the maximal amplitude of the CCh-evoked Ca^{2+} signals by ~50%, whereas it increased the sensitivity to PTH(1-34) by almost 10-fold (Fig. 3.4C, D, Table 3.5).

The reduction in CCh-evoked Ca^{2+} signals after sustained stimulation with PTH(1-34) was evident after 15 min, and remained reduced after extending the incubation with PTH(1-34) to 60 min. The ~50% decrease in the maximal $\Delta[Ca^{2+}]_c$ release after sustained stimulation with PTH(1-34) was observed, whether maximal (1 mM) or submaximal (20 μM) concentrations of CCh were used to evoke Ca^{2+} release (Table 3.5). In most subsequent experiments, submaximal concentrations of CCh were used for the stimulation of Ca^{2+} release. It was found that 2.5 mM BAPTA was sufficient to chelate extracellular Ca^{2+} without affecting the initial peak Ca^{2+} signals, whereas 10 mM BAPTA reduced their amplitude (not shown). In most subsequent experiments 2.5 mM BAPTA was used. Acute stimulation with PTH(1-34) potentiates the Ca^{2+} signals evoked by CCh (Tovey *et al.*, 2008), but the Ca^{2+} responses obtained

after sustained PTH(1-34) stimulation have not previously been reported. Subsequent experiments focus on the effect of sustained stimulations with PTH.

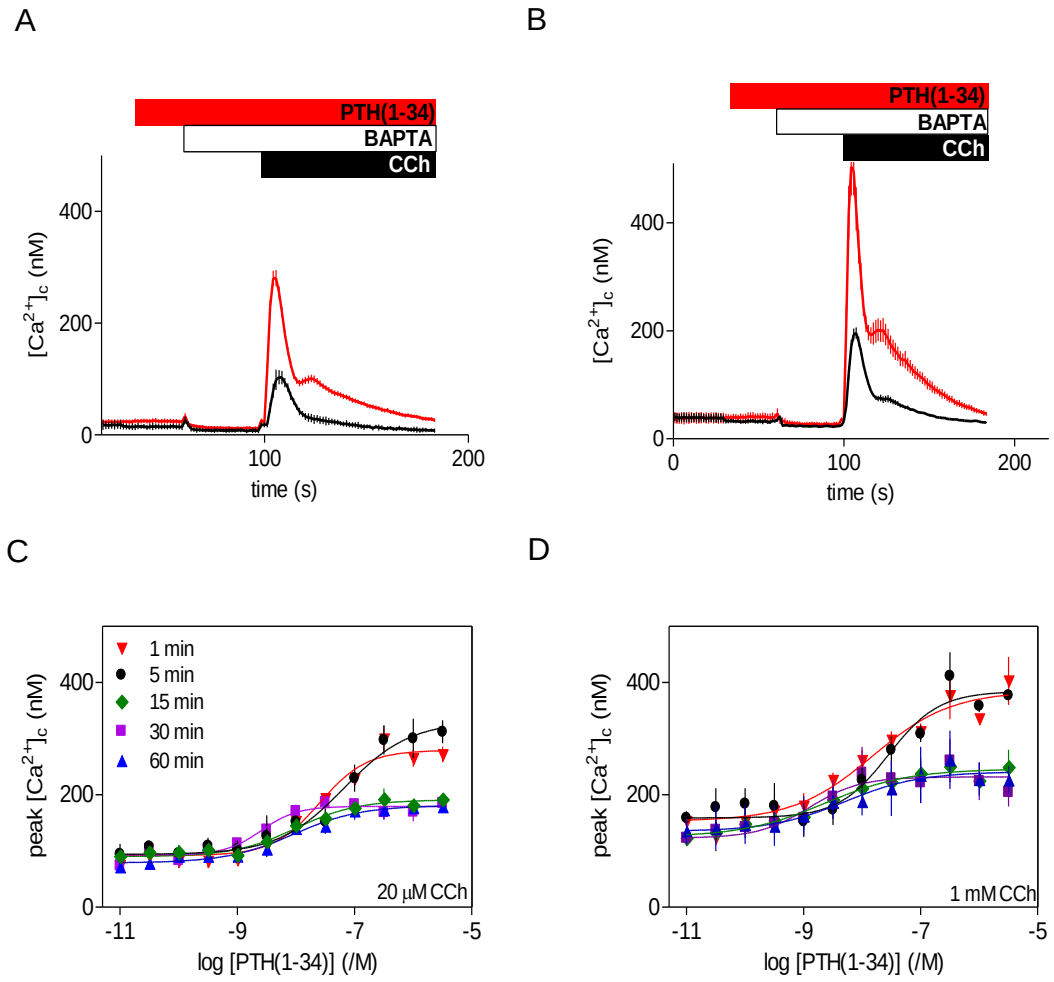

Figure 3.4. **Sustained PTH(1-34) stimulation reduces potentiation of CCh-evoked Ca^{2+} signals.** (**A**, **B**) Typical changes in $[Ca^{2+}]_c$ signals from a population of HEK-PR1 cells stimulated with a submaximal (20 µM, **A**) or maximal concentration (1 mM, **B**) of CCh alone, or with PTH(1-34) (100 nM, added 1 min before CCh). Results are means ± SEM for 3 wells from a single experiment. (**C**, **D**) Concentration-dependent effects of PTH(1-34), given for the indicated times, on the Ca^{2+} signals (peak $[Ca^{2+}]_c$) evoked by submaximal (20 µM, **C**) or maximal (1 mM, **D**) CCh concentrations. In each experiment, BAPTA (2.5 mM) was added 30 s before addition of CCh to chelate extracellular Ca^{2+}. The codes apply to both panels. Results (C, D) are means ± SEM from 4 independent experiments. Significant differences are given in Table 3.5.

	CCh (1 mM)		CCh (20 µM)	
PTH(1-34)	Maximal $\Delta[Ca^{2+}]_c$ (nM)	pEC_{50}	Maximal $\Delta[Ca^{2+}]_c$ (nM)	pEC_{50}
1 min	234 ± 29	7.8 ± 0.1	230 ± 10	7.5 ± 0.2
5 min	228 ± 9	7.6 ± 0.1	179 ± 37	7.1 ± 0.0
15 min	120 ± 7*	8.7 ± 0.1*	94 ± 7*	7.9 ± 0.1*
30 min	105 ± 30*	8.8 ± 0.1*	142 ± 38*	8.8 ± 0.1*
60 min	110 ± 16*	8.2 ± 0.2*	108 ± 07*	8.1 ± 0.2*

Table 3.5. **Acute or sustained stimulation with PTH(1-34) potentiates CCh-evoked Ca^{2+} signals**. Effect of stimulation with PTH(1-34) for different time durations, on the maximal $\Delta[Ca^{2+}]_c$ signals evoked by submaximal (20µM) or maximal (1mM) CCh concentrations, and on the sensitivity to PTH(1-34). Maximal $\Delta[Ca^{2+}]_c$ describes the difference between the peak Ca^{2+} signal evoked by CCh alone and that evoked by CCh in the presence of a maximally effective concentration of PTH(1-34). Results are means ± SEM from ≥ 3 independent experiments. $^*P < 0.05$ with one-way analysis of variance and Tukey multiple comparisons test.

3.3.3. Sustained or acute PTH(1-34) stimulation potentiates CCh-evoked Ca^{2+} responses in single HEK-PR1 cells.

The results from cell populations (Fig. 3.4, Table 3.5) are further validated by analyses of single HEK-PR1 cells. The increase in the peak $[Ca^{2+}]_c$ signal evoked by a maximal concentration of CCh (1 mM) was 176 ± 12 nM (Fig. 3.5D). These responses were further potentiated when measured after acute (1 min) or sustained (60 min) stimulation with PTH(1-34) (Fig. 3.5A, B). The peak increase in $[Ca^{2+}]_c$ signals evoked by maximal CCh (1 mM) after acute PTH(1-34) (100 nM) stimulation (372 ± 9 nM) (Fig. 3.5D) was significantly higher than the response after sustained stimulation with PTH(1-34) (243 ± 11 nM) (Fig. 3.5D).

The percentage of cells that responded after acute or sustained PTH(1-34) stimulation is 100% and 99% respectively of the cells that responded to the first maximal CCh stimulation (Fig. 3.5C).

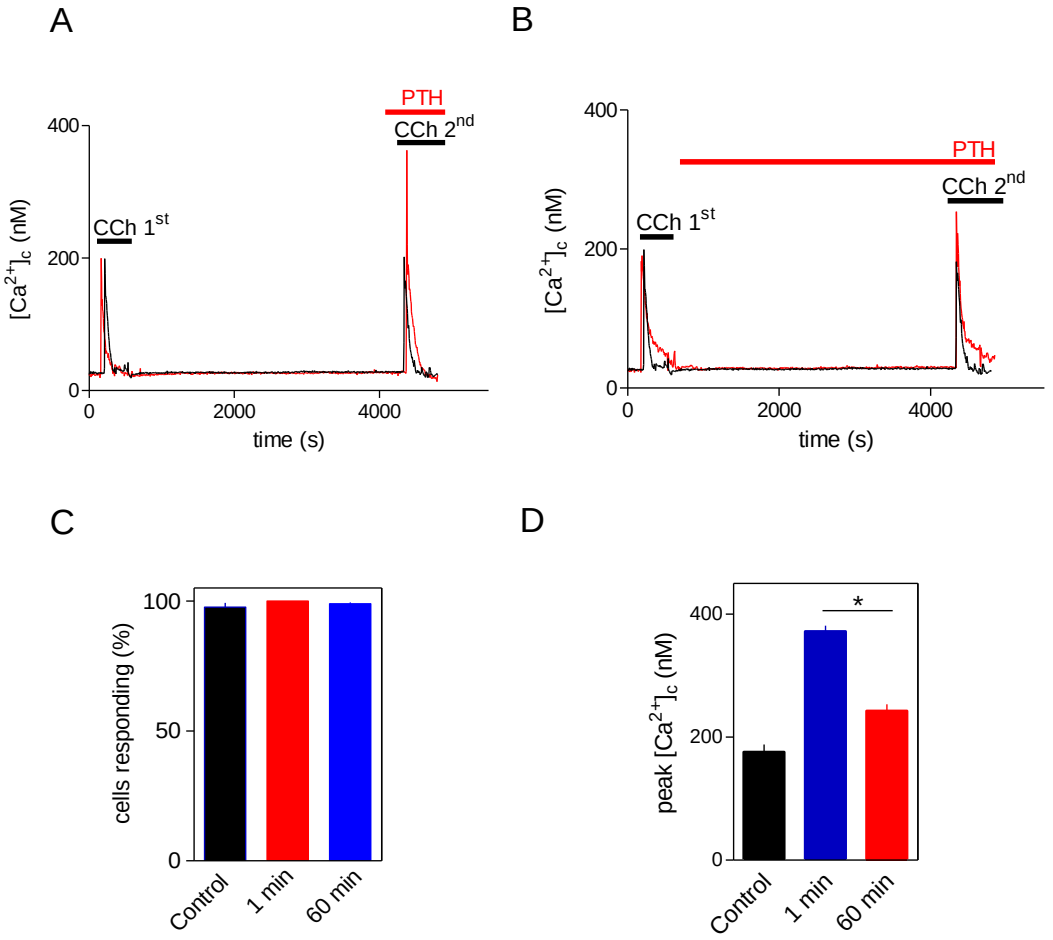

Figure 3.5. **PTH(1-34) potentiates CCh-evoked Ca^{2+} signals in single HEK-PR1 cells.** (**A**, **B**) Typical change in $[Ca^{2+}]_c$ from a single HEK-PR1 cell stimulated with CCh (1 mM, first challenge) alone or with PTH (100 nM, added 1 min (**A**) or 60 min (**B**) before CCh (1 mM, second challenge). In these experiments normal HBS was replaced with nominally Ca^{2+}-free HBS 5 min before addition of CCh. Results are from a single HEK-PR1 cell, typical of ≥ 195 cells analysed in 3 independent experiments. (**C**) Percentage of the cells in which the first stimulation with CCh (1 mM) evoked a detectable increase $[Ca^{2+}]_c$ (control) and percentage of cells that responded to addition of CCh with PTH(1-34) after a 1-min (red) or 60-min (blue) pre-incubation with PTH(1-34). (**D**) Summary results show the effects of 1-min or 60-min stimulation with PTH(1-34) (100 nM) on the peak increase in $[Ca^{2+}]_c$ evoked by CCh (1 mM) for each individual cell. Results (C, D) are means ± SEM from 3 coverslips, with ~65 cells analysed on each. Results (D) are means ± SEM from 3 independent experiments. $^{*}P <$ 0.05 with one-way analysis of variance and Tukey multiple comparisons test.

3.3.4. Potentiation of CCh-evoked Ca^{2+} responses by PTH(1-34) is mediated by cAMP

At the highest concentrations used (≥ 300 nM), PTH(1-34) evoked small (< 40 nM) increases in $[Ca^{2+}]_c$ in populations of HEK-PR1 cells (Fig. 3.6A) (Jobert *et al.*, 1997). These Ca^{2+} signals were also observed after inhibition of AC by SQ/DDA, PDE by IBMX, PKA by H89 or Epac 1/2 by ESI-09 (Fig. 3.6B-E). PTH(1-34), alone or with SQ/DDA, IBMX, H89 and ESI-09, gave similar increases in peak $[Ca^{2+}]_c$. Previously published data suggests that stimulation with PTH(1-34) evokes Ca^{2+} signals, which might be due to activation of Gs, Gq or both signalling pathways (Cupp *et al.*, 2013). This suggested that the results in figure 3.6, could be due to activation of either of these signalling pathways.

To investigate whether PTH(1-34) stimulates Ca^{2+} signals by activating Gq or Gs pathways, the effects of different PTH analogues were assessed. The selection of analogues was based on their specific mode of signalling after binding to PTH_1R. Tyr^1PTH(1-34) and PTH(2-38) are full agonists for activation of AC (Table 3.1). PTH(1-34) and PTHrP(1-34) are full agonists for activation of both AC and PLC (Pines *et al.*, 1996; Tsukazaki *et al.*, 1996). PTH(1-31) is a full agonist for activation of AC and a strong partial agonist for activation of PLC (Sneddon *et al.*, 2004; Whitfield *et al.*, 1995), though a recent study in CHO cells expressing PTH_1R suggests that PTH(1-31) was similar to PTH(1-34) in its ability to stimulate both AC and PLC (Cupp *et al.*, 2013; Takasu *et al.*, 1999) (Table 3.1).

Results shown in Figure 3.6A indicate that high concentrations of PTH(1-31), PTHrP(1-34) and PTH(1-34), which are reported to activate PLC, evoked small increases in $[Ca^{2+}]_c$. By contrast, PTH(1-34) potentiates CCh-evoked Ca^{2+} responses at much lower concentrations (Fig. 3.4C, D, 3.7A). The analogues which stimulate only AC, PTH(2-38) and Tyr^1PTH(1-34), alone did not evoke increases in $[Ca^{2+}]_c$ at any concentration (Fig. 3.7A). Acute stimulation with Tyr^1PTH(1-34) or PTH(2-38) potentiated the maximal $\Delta[Ca^{2+}]_c$ evoked by CCh (20 µM) to the same extent as PTH(1-34) (Fig. 3.7A, Table 3.6). The levels of maximal ΔcAMP produced by the three analogues were also comparable (Fig. 3.7B, Table 3.6). Furthermore, the relationship between the change in intracellular cAMP concentration and the potentiated Ca^{2+} signals were similar for the three analogues (Fig. 3.7C).

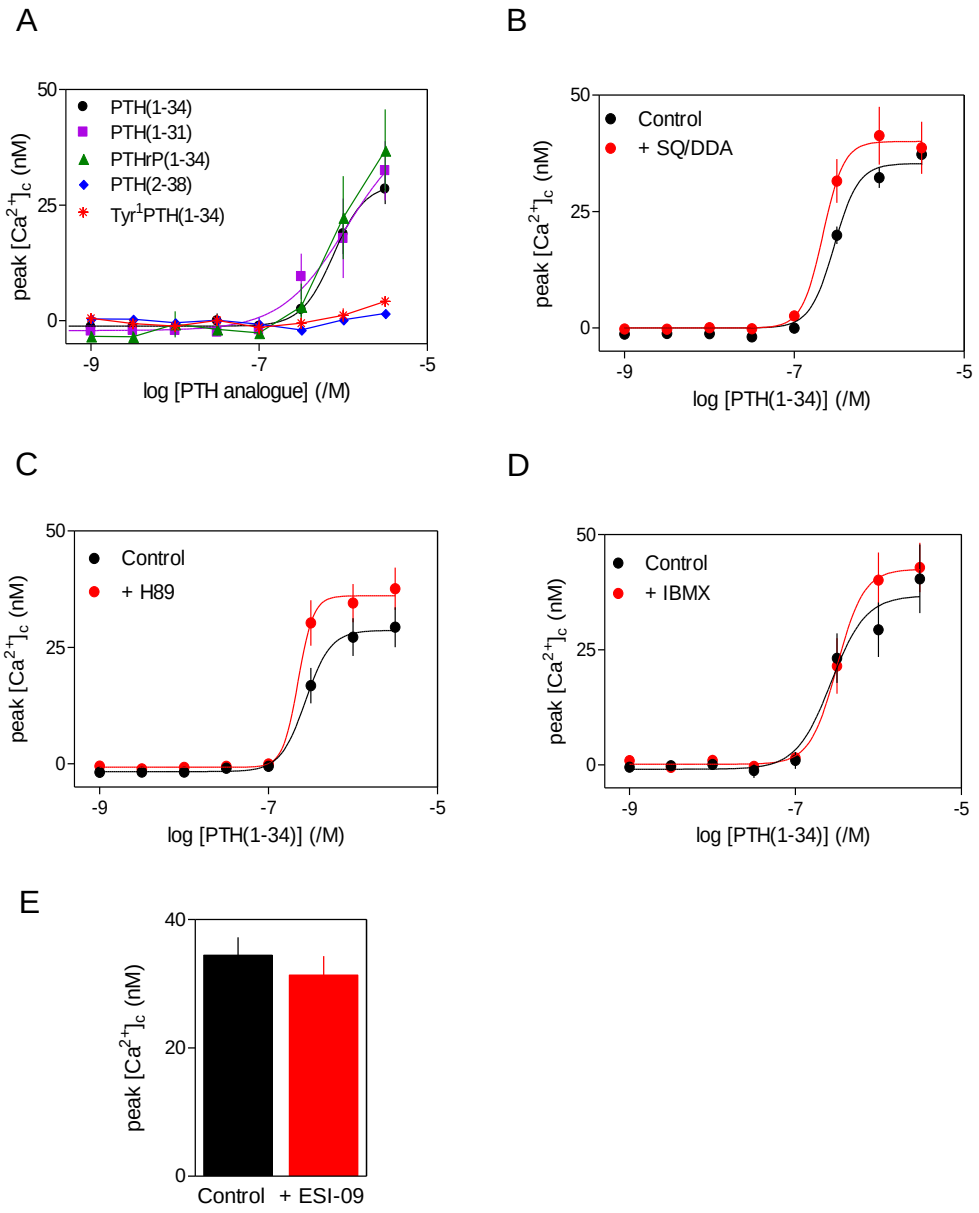

Figure 3.6. **Direct effects of PTH analogues on Ca^{2+} signals** (**A**) HEK-PR1 cells were stimulated with PTH analogues for 1 min. Results show concentration-dependent effects of PTH analogues alone on the peak increase in $[Ca^{2+}]_c$. (**B-D)** HEK-PR1 cells were incubated with SQ22536 (1 mM) and DDA (200 µM) (**B**, SQ/DDA, 20 min) to inhibit AC, H89 (**C**, 10 µM, 20 min) to inhibit PKA, or IBMX (**D**, 1 mM, 5 min) to inhibit cyclic nucleotide phosphodiesterases before addition of the indicated concentrations of PTH(1-34). Results show the peak increase $[Ca^{2+}]_c$ evoked by addition of PTH(1-34). (**E**) Cells were incubated with ESI-09 (10 µM, 5 min) to inhibit Epac. Results show the peak increase $[Ca^{2+}]_c$ evoked by 3 µM PTH(1-34) alone or with ESI-09. Results (A-E) are means ± SEM from ≥3 independent experiments.

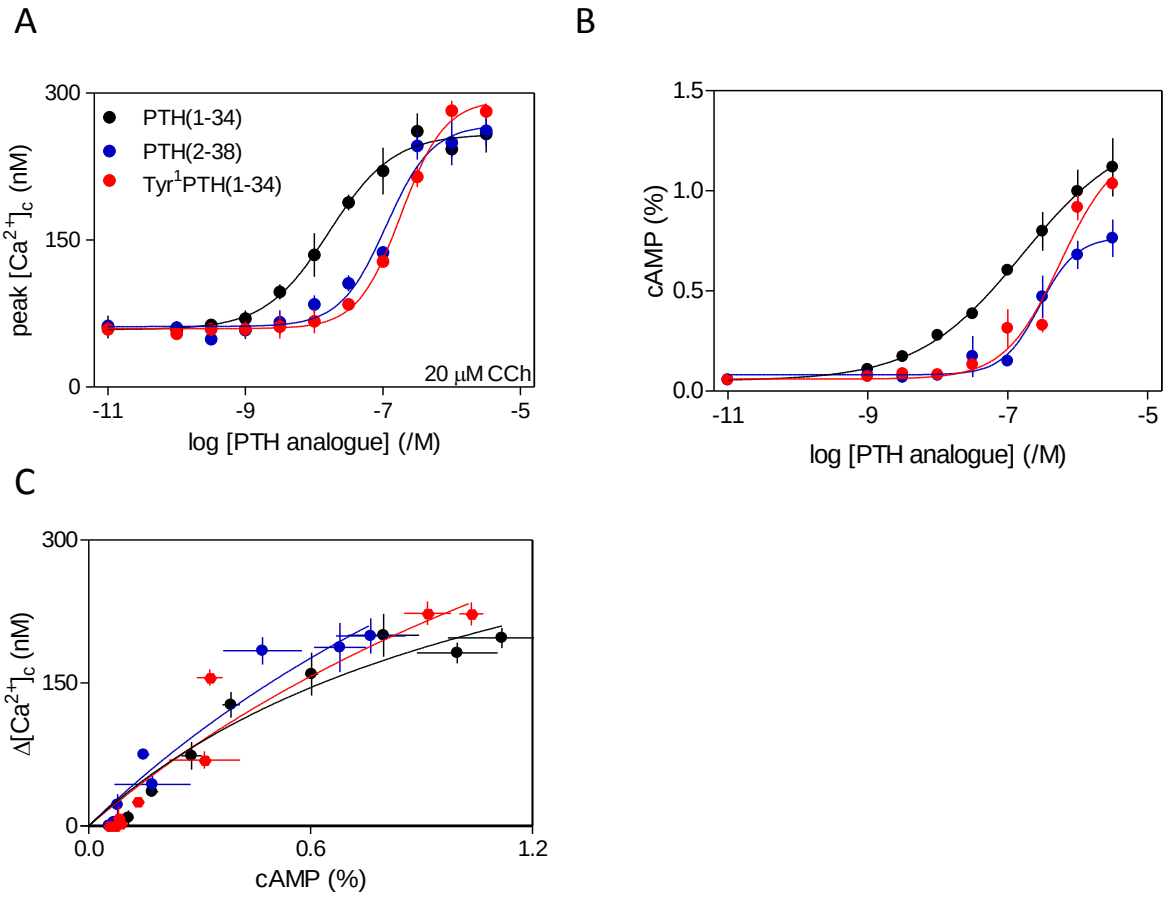

Figure 3.7. **cAMP mediates potentiation of CCh-evoked Ca^{2+} signals by PTH(1-34).** **(A)** Populations of HEK-PR1 cells were stimulated with PTH analogues for 1 min before CCh (20 µM) addition in the presence of BAPTA (2.5 mM). Results show concentration- dependent effects of PTH analogues on the peak increase in $[Ca^{2+}]_c$ evoked by CCh (20 µM). (**B**) Effects of PTH analogues on intracellular cAMP measured after 1 min under conditions identical to those used for measurements of peak $[Ca^{2+}]_c$ signals. Results show ^{3}H-cAMP as a percentage of ^{3}H-ATP, ^{3}H-ADP and ^{3}H-cAMP. (**C**) Results from (A) and (B) were used to establish the non linear regression relationship between cAMP and the potentiated CCh-evoked increases in $[Ca^{2+}]_c$ for cells stimulated with the indicated PTH analogues for 1 min, therefore each line corresponds the same. Results in A and B are means ± SEM from ≥ 3 experiments.

	$\Delta[Ca^{2+}]_c$		ΔcAMP	
	pEC_{50}	Maximal $\Delta[Ca^{2+}]_c$ (nM)	pEC_{50}	Maximal ΔcAMP (%)
Tyr^1PTH (1-34)	6.7 ± 0.03	233 ± 10	6.1 ± 0.20	1.3 ± 0.2
PTH (1-34)	7.7 ± 0.10	205 ± 13	7.0 ± 0.10	1.1 ± 0.1
PTH (2-38)	6.9 ± 0.10	216 ± 21	6.5 ± 0.04	0.7 ± 0.1

Table 3.6. **Acute stimulation with PTH analogues stimulates cAMP formation and potentiates Ca^{2+} signals**. Effect of stimulation with PTH analogues (1 min) on the maximal $\Delta[Ca^{2+}]_c$ and ΔcAMP signals evoked by CCh (20 µM) and their sensitivities to PTH analogues. Maximal ΔcAMP describes the difference between the basal level of cAMP and that detected after maximal stimulation (as % of ATP). Results show means ± SEM from ≥ 3 experiments.

3.3.5. Sustained stimulation with NKH477 and 8-Br-cAMP reduce the potentiation of CCh-evoked Ca^{2+} responses

A decrease in the maximal $\Delta[Ca^{2+}]_c$ evoked by CCh after prolonged PTH(1-34) stimulation (Fig. 3.4, Table 3.5) could be a consequence of a change in signalling from internalized PTH_1R (Ferrandon *et al.*, 2009) or a consequence of a sustained increase in intracellular cAMP concentration. These possibilities were explored using two approaches. Firstly, by directly stimulating AC with NKH477. Secondly, by delivering cAMP directly into the cell, in the form of 8-Br-cAMP, a membrane-permeable cAMP analogue.

Forskolin is often used to activate AC (Hosono *et al.*, 1992), but it is relatively insoluble in water. Hence NKH477 was used as it is cell-permeable, more water-soluble than forskolin (Hosono *et al.*, 1992), and more potent than forskolin in stimulating AC (Toya *et al.*, 1998).

An unavoidable limitation in performing these experiments is that PTH(1-34) quickly stimulates AC via PTH_1R, whereas NKH477 or 8-Br-cAMP activate AC more

slowly because they must first diffuse across the plasma membrane. Two-minute stimulations with 8-Br-cAMP did not show potentiation of CCh-evoked Ca^{2+} responses (not shown), presumably because this provides insufficient time for 8-Br-cAMP to reach intracellular targets. For NKH477 and 8-Br-cAMP, 2 or 5 min respectively were identified as the shortest stimulation times after which there was potentiation of CCh-evoked Ca^{2+} responses (Fig. 3.8A, 3.9C, Table 3.7, 3.8).

In populations of HEK-PR1 cells, acute or sustained stimulation with NKH477, 8-Br-cAMP or PTH(1-34) potentiated the increase in the peak $[Ca^{2+}]_c$ signals evoked by CCh (Fig. 3.9). Sustained stimulation with NKH477 or PTH(1-34) showed a significant decrease (~50%) in the maximal $\Delta[Ca^{2+}]_c$ signals and a ~10-fold increase in sensitivity to NKH477 or PTH(1-34) compared to acute stimulation (Fig. 3.9A, B, Table 3.8). However, after prolonged stimulation with 8-Br-cAMP, the sensitivity to 8-Br-cAMP was unchanged but there was a significant decrease (~50%) in the maximal $\Delta[Ca^{2+}]_c$ signals relative to acute stimulation (Fig. 3.9C, Table 3.8). With NKH477, levels of cAMP produced after acute or sustained stimulation were also measured under identical conditions to those used to measure Ca^{2+} signals. However, maximal ΔcAMP and pEC_{50} values could not be calculated because even 1 mM NKH477 failed to achieve a maximal response (Fig. 3.8B). Furthermore, the relationship between the change in intracellular cAMP concentration and the potentiated Ca^{2+} signals was established (Fig. 3.8C). This analysis was designed to assess whether the underlying relationship between cAMP and how enhanced $Ca2^{+}$ signals differed when different stimuli and/or timings were used to evoke cAMP formation.. From these results, it is clear that whether AC is activated directly by NKH477 or via PTH_1R, sustained activation produces more cAMP than brief stimulation, but lesser potentiation of CCh-evoked Ca^{2+} signals (Fig. 3.8A, Table 3.7).

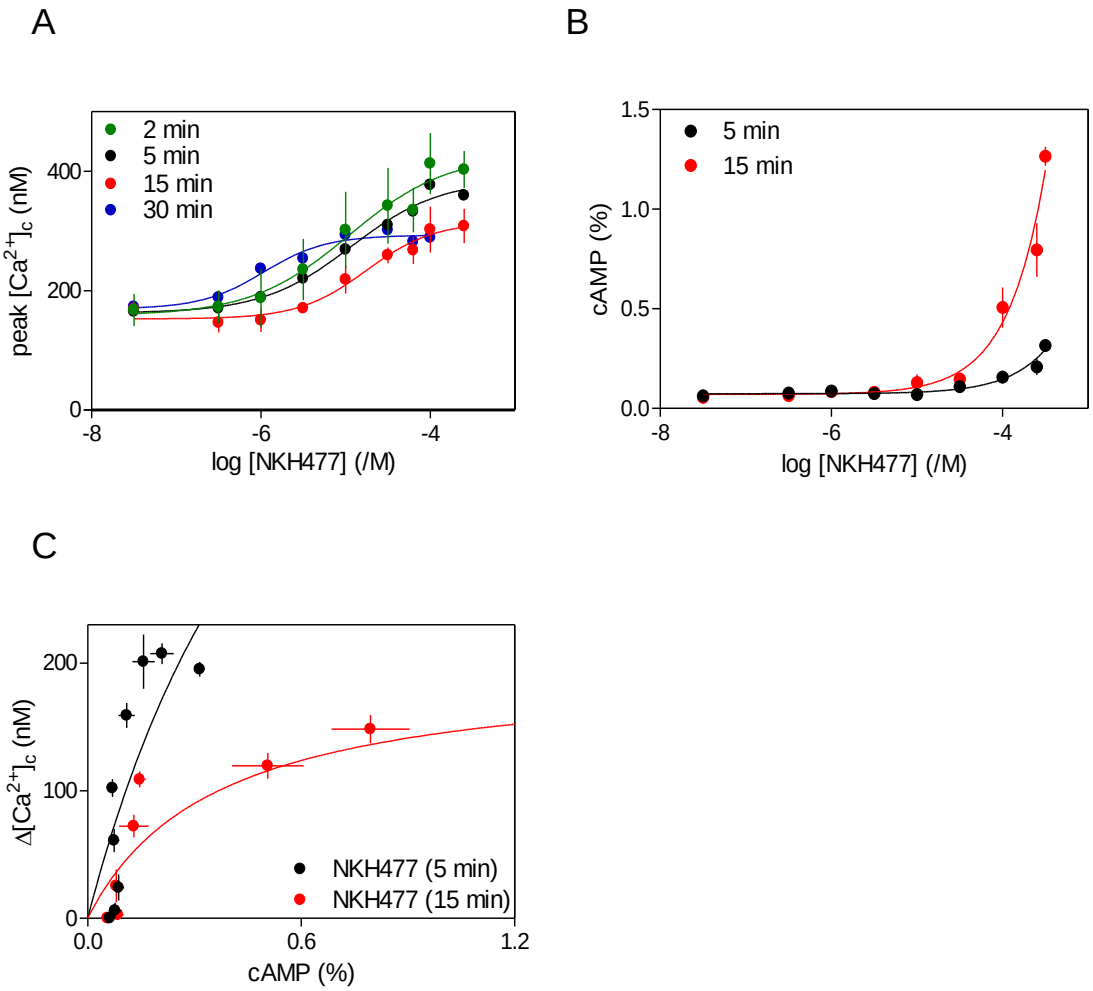

Figure 3.8. **Sustained stimulation with NKH477 reduces potentiated CCh-evoked Ca^{2+} signals.** (**A**) Populations of HEK-PR1 cells were stimulated with NKH477 for the indicated time before analysing CCh (20 µM)-evoked Ca^{2+} signals in the presence of BAPTA (2.5 mM). Results show concentration-dependent effects of NKH477 on the increase in peak $[Ca^{2+}]_c$ signals evoked by CCh. (**B**) Effects of NKH477 on intracellular cAMP measured after 5 or 15 min under conditions identical to those used for measurements of $[Ca^{2+}]_c$. Results show ^{3}H-cAMP as a percentage of ^{3}H-ATP, ^{3}H-ADP and ^{3}H-cAMP. Results (A, B) are means ± SEM from 3 independent experiments. (**C**) Results from (A) and (B) were used to establish the non linear regression relationship between cAMP and the potentiated CCh-evoked increases in $[Ca^{2+}]_c$ for cells stimulated with NKH477 for 5 min or 15 min, therefore each line corresponds the same.

NKH477	pEC_{50}	Maximal $\Delta[Ca^{2+}]_c$ (nM)
2 min	5.0 ± 0.3	257 ± 3
5 min	5.0 ± 0.1	225 ± 9
15 min	5.0 ± 0.1	155 ± 10*
30 min	6.0 ± 0.1*	124 ± 24*

Table 3.7. **Acute or sustained stimulation with NKH477 potentiates Ca^{2+} signals**. Effect of stimulation with NKH477 for different times on the maximal $\Delta[Ca^{2+}]_c$ signals evoked by CCh (20 µM) and the sensitivity to NKH477. Results are means ± SEM from ≥ 3 independent experiments. $^*P < 0.05$ with one-way analysis of variance and Tukey multiple comparisons test.

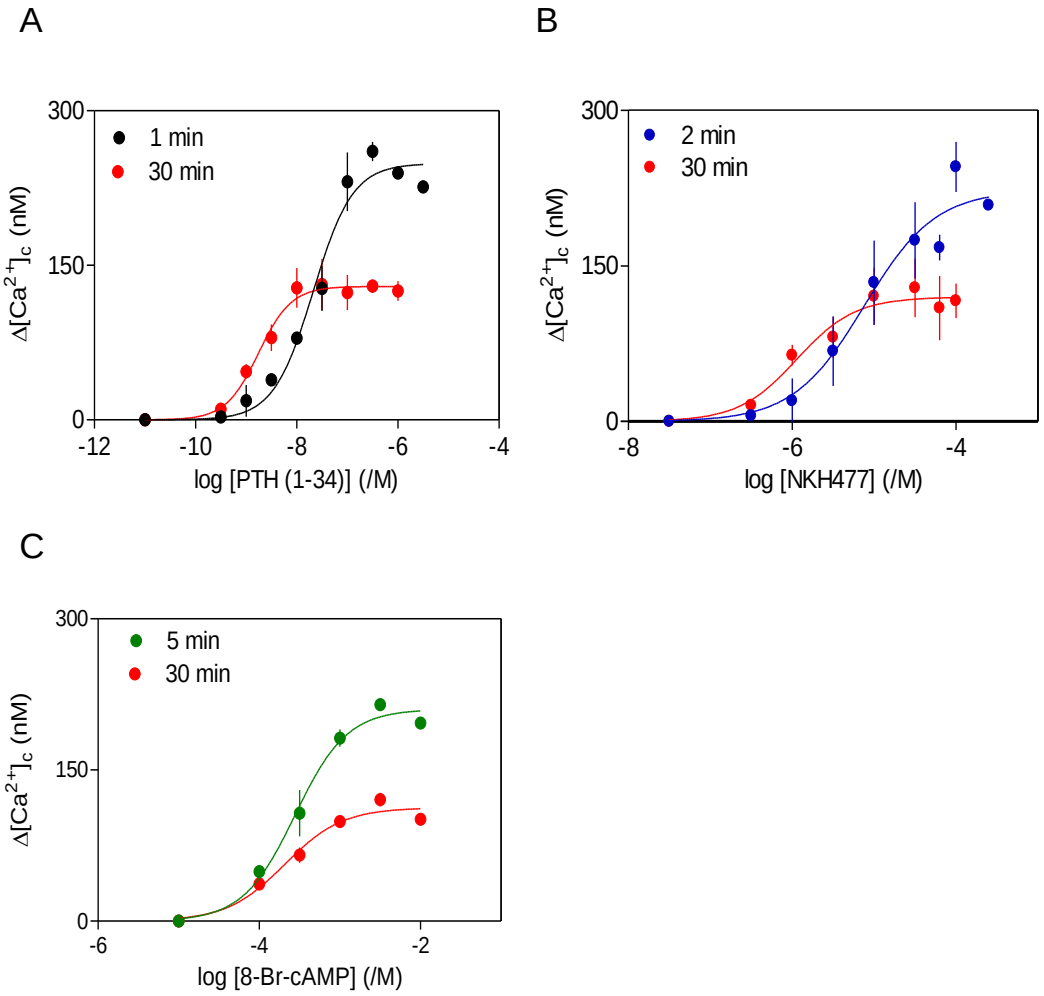

Figure 3.9. **Diminished potentiation of CCh-evoked Ca^{2+} signals after acute or sustained stimulation with NKH477, 8-Br-cAMP or PTH(1-34).** (**A-C**) Populations of HEK-PR1 cell were stimulated with PTH(1-34) for 1 or 30 min (**A**), NKH477 for 2 or 30 min (**B**) or 8-Br-cAMP for 5 or 30 min (**C**), before analysing CCh (20 µM)-evoked Ca^{2+} signals in the presence of BAPTA (2.5 mM). Results show peak increases in $[Ca^{2+}]_c$ evoked by the each of these stimulants after subtracting the response evoked by CCh (20 µM) alone. Results (A-C) are means ± SEM from 3 independent experiments.

	PTH(1-34)		NKH477		8-Br-cAMP	
	$\Delta[Ca^{2+}]_c$ (nM)	pEC_{50}	$\Delta[Ca^{2+}]_c$ (nM)	pEC_{50}	$\Delta[Ca^{2+}]_c$ (nM)	pEC_{50}
1 min	251 ± 2	7.6 ± 0.1	ND	ND	ND	ND
2 min	ND	ND	221 ± 10	5.1 ± 0.3	ND	ND
5 min	ND	ND	ND	ND	211 ± 5	3.5 ± 0.1
30 min	132 ± 12	8.7 ± 0.1	121 ± 26	5.9 ± 0.1	113 ± 7	3.7 ± 0.1

Table 3.8. **Responses to CCh after acute and sustained stimulation of production of intracellular cAMP.** Peak increases in $[Ca^{2+}]_c$ evoked by CCh (20 µM) were recorded after parallel incubations for the periods indicated with PTH(1-34), NKH477 or 8-Br-cAMP. Results show the maximal $\Delta[Ca^{2+}]_c$ after subtracting the responses evoked by CCh (20µM) alone and the sensitivity for each stimulus. Results are means ± SEM, from 3 independent experiments.

3.3.6. Sustained stimulation with PTH(1-34), NKH477 and 8-Br-cAMP in combination produce non-additive effects

Acute or sustained stimulation with PTH(1-34), NKH477 and 8-Br-cAMP caused similar potentiation of CCh-evoked Ca^{2+} signals (Fig. 3.9, Table 3.8). Additionally, in a previous study, acute stimulation with PTH(1-34) and 8-Br-cAMP in combination showed non-additive effects (Tovey *et al.*, 2008). These observations prompted me to assess whether acute or sustained stimulation of HEK-PR1 cells with these agents, in combination, would affect the peak increase in $[Ca^{2+}]_c$ signals and thus overcome the decrease in maximal Ca^{2+} signals observed after prolonged stimulation with PTH(1-34) (Fig. 3.9A)

In populations of HEK-PR1 cells, acute stimulation with PTH(1-34), NKH477 and 8-Br-cAMP in combination showed similar potentiation of CCh-evoked Ca^{2+} responses (Fig. 3.10, Table 3.9). The peak increases in Ca^{2+} signals evoked by CCh were similar after acute stimulations with combinations of these agonists. Similarly, sustained stimulation with PTH(1-34), NKH477 and 8-Br-cAMP in combination

showed similar potentiation of CCh-evoked Ca^{2+} signals. However, these responses were significantly lower than the Ca^{2+} responses observed after acute stimulations with the same stimulant (Fig. 3.10, Table 3.9).

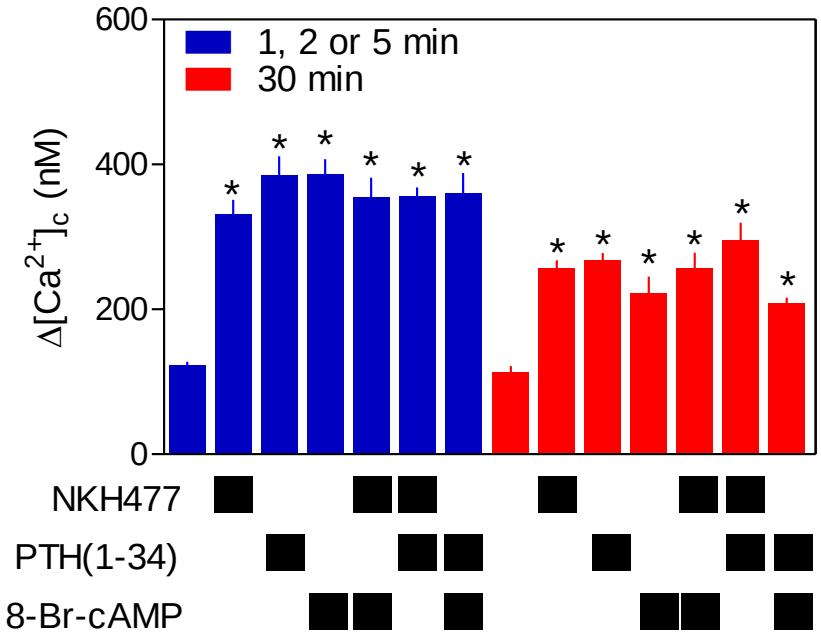

Figure 3.10. **Acute or sustained stimulation with PTH(1-34), NKH477 and 8-Br-cAMP alone or in combination, have similar non additive effects on CCh-evoked Ca^{2+} signals.** Populations of HEK-PR1 cells were stimulated with the indicated combinations of PTH(1-34) (1 µM, 1 or 30 min), NKH477 (200 µM, 2 min or 30 min) and 8-Br-cAMP (10 mM, 5 or 30 min), before measuring potentiation of CCh (20 µM)-evoked Ca^{2+} signals in the presence of BAPTA (2.5 mM). Results show the peak $[Ca^{2+}]_c$ signals evoked by CCh (20 µM). Results are means ± SEM from 3 independent experiments. The statistical analysis was between the acute stimulation (1, 2 or 5 min and sustained stimulation (30 min) for each combination stimuli. $^{*}P < 0.05$ with paired Student's t-test (comparing matched stimuli for acute and sustained stimulation).

	Maximal $\Delta[Ca^{2+}]_c$ (nM)	
	1, 2, or 5 min	30 min
Control	122 ± 6	113 ± 9
NKH477	331 ± 20	256 ± 12*
PTH(1-34)	385 ± 26	268 ± 10*
8-Br-cAMP	386 ± 21	222 ± 24*
8-Br-cAMP + NKH477	355 ± 27	257 ± 22*
NKH477 + PTH(1-34)	356 ± 12	295 ± 25*
PTH(1-34) + 8-Br-cAMP	360 ± 28	208 ± 08*

Table 3.9. **CCh-evoked Ca^{2+} signals after stimulation with PTH(1-34), NKH477 and 8-Br-cAMP, alone or in combination.** Effect of PTH(1-34) (1 or 30 min), NKH477 (2 or 30 min) and 8-Br-cAMP (5 or 30 min) alone or in combination as indicated on the maximal $\Delta[Ca^{2+}]_c$ signals evoked by CCh (20µM), measured from populations of HEK-PR1 cells. Results are means ± SEM from 3 independent experiments. $^*P < 0.05$ relative to paired comparisons at 1, 2, or 5 min as appropriate. Paired Student's t-test was used for the analysis.

3.3.7. Protein kinase A is not required for PTH(1-34) to potentiate CCh-evoked Ca^{2+} signals

In populations of HEK-PR1cells H89, an inhibitor of PKA (Lochner *et al.*, 2006), was used to assess whether PKA inhibition affects acute or sustained stimulation with PTH(1-34). The results show that inhibition of PKA with H89 did not affect the CCh-evoked Ca^{2+} signals after acute or sustained stimulation with PTH(1-34). Furthermore, H89 did not change the increase in sensitivity and decrease in maximal responses observed after sustained stimulation with PTH(1-34). (Fig. 3.11A, B, D, Table 3.10). Likewise, PKA inhibition did not affect levels of cAMP produced after acute or sustained stimulations with PTH(1-34). The maximal intracellular ΔcAMP produced

after stimulation with PTH(1-34) and H89 for 1 or 60 min was 95 ± 0.1 and 98 ± 0.2%, respectively, of the levels detected in matched control cells (n = 3) (Fig. 3.11C). That inhibition of PKA using H89 does not affect levels of intracellular cAMP formation has been observed previously (Chijiwa *et al.*, 1990).

These results agree with previous studies of HEK-PR1 cells where inhibition of PKA using H89 reduced PTH(1-34)-, FK- and 8-Br-cAMP- induced protein phosphorylation without affecting potentiation of CCh-evoked Ca^{2+} signals (Tovey *et al.*, 2008). It seems reasonable to suppose, because I used identical treatments with H89, that PKA was also effectively inhibited in the experiments described here, although it would be useful to re-confirm the inhibition.

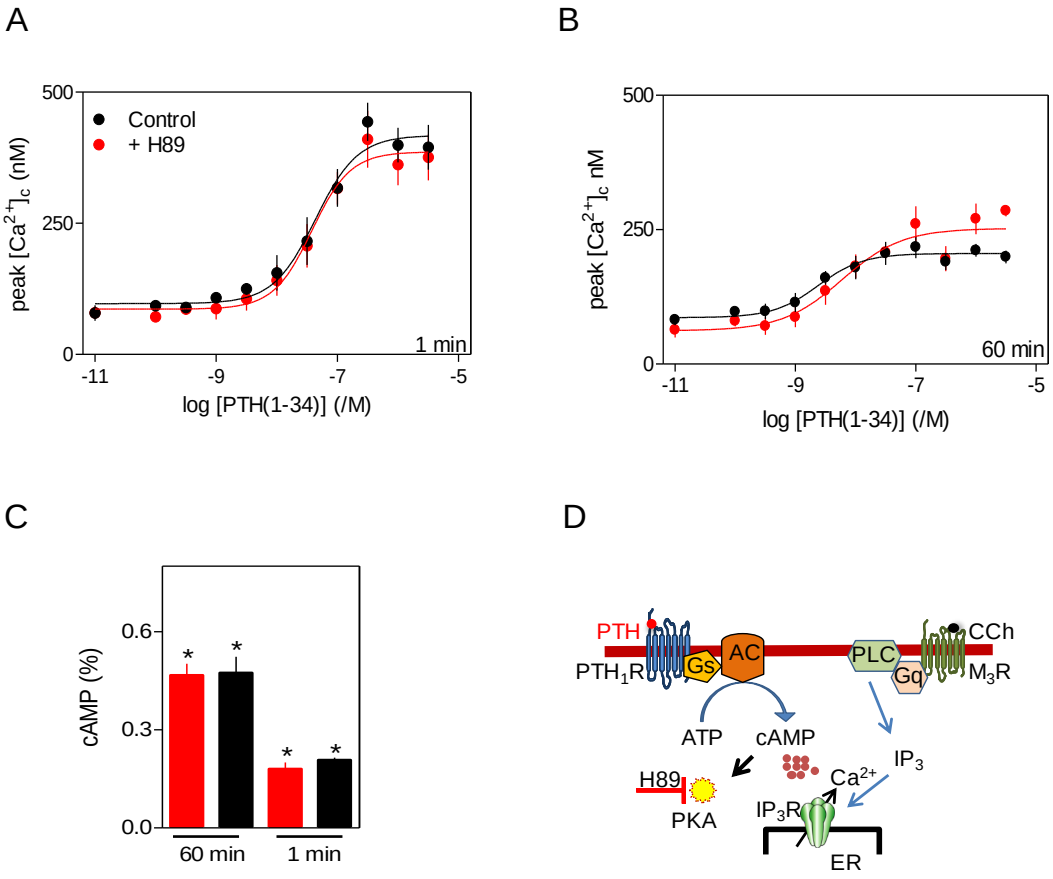

Figure 3.11. **PKA is not involved in CCh-evoked Ca^{2+} signals and cAMP production potentiated by PTH(1-34).** (**A**, **B**) Populations of HEK-PR1 cells were incubated with H89 (10 µM, 20 min) before stimulation with PTH(1-34) for 1 or 60 min. The CCh (20 µM)-evoked Ca^{2+} responses were then assessed in the presence of BAPTA (2.5 mM). Results show concentration-dependent effects of acute (**A**) or sustained (**B**) stimulation with PTH(1-34) and H89 treatment on peak increases in $[Ca^{2+}]_c$ evoked by CCh (20 µM) in the continuous presence of BAPTA (2.5 mM). (**C**) Effects of PTH(1-34) (3 µM) with or without incubation with H89 (10 µM, 20 min), on intracellular cAMP measured after 1 min or 60 min stimulation. These cAMP measurements were done under conditions identical to those used for the measurements of $[Ca^{2+}]_c$. Results show ^{3}H-cAMP as a percentage of ^{3}H-ATP, ^{3}H-ADP and ^{3}H-cAMP. The statistical analysis was done in between the acute stimulation (1 min) and sustained stimulation (60 min) for each combination stimuli. $^*P < 0.05$ with paired Student's t-test (comparing matched stimuli for acute and sustained stimulation). (**D**) PTH(1-34)-potentiated CCh-evoked Ca^{2+} release is not affected by PKA inhibition using H89. Results (A-C) are means ± SEM from ≥ 3 independent experiments.

	1 min		60 min	
	pEC_{50}	Maximal $\Delta[Ca^{2+}]_c$ (nM)	pEC_{50}	Maximal $\Delta[Ca^{2+}]_c$ (nM)
Control	7.4 ± 0.20	364 ± 29	8.5 ± 0.20*	153 ± 14*
H89	7.4 ± 0.40	322 ± 40	8.3 ± 0.20*	171 ± 33*

Table 3.10. **PKA inhibition does not affect the potentiation by PTH(1-34) of CCh-evoked Ca^{2+} signals** Effect of PTH(1-34), for 1 or 60 min, with H89 (10 µM, 20 min) pre-treatment on the maximal $\Delta[Ca^{2+}]_c$ signals evoked by CCh (20 µM) and on the sensitivity to PTH(1-34). Results are means ± SEM from 3 independent experiments. $^*P < 0.05$ relative to paired comparisons at 1 min. Paired Student's t-test was used for the analysis.

3.3.8. Protein kinase A is not required for NKH477 or 8-Br-cAMP to potentiate CCh-evoked Ca^{2+} signals

Results shown in figure 3.9 and the table 3.8 show that acute or sustained stimulation with PTH(1-34), NKH477 or 8-Br-cAMP similarly potentiate CCh-evoked Ca^{2+} signals. Furthermore, PKA is not involved in mediating the effects of acute or sustained stimulation with PTH(1-34) on the Ca^{2+} signals evoked by CCh (Fig. 3.11A, B, Table 3.10). Incubation of HEK-PR1 cells with H89 before brief or sustained stimulation with NKH477 or 8-Br-cAMP did not affect the increase in peak $\Delta[Ca^{2+}]_c$ signals evoked by CCh (Fig. 3.12, Table 3.11). These results suggest that PKA is not involved in NKH477- or 8-Br-cAMP- potentiated Ca^{2+} responses. No effect of PKA inhibition on acute stimulation with forskolin and 8-Br-cAMP potentiated Ca^{2+} signals has been observed previously (Tovey *et al.*, 2008). As described previously (Section 3.3.7), the treatment with H89 has been shown to effectively inhibit PKA (Lochner *et al.*, 2006), but my conclusion would be stronger if supported by additional inhibitors of PKA and a direct demonstration of their effective inhibition of PKA.

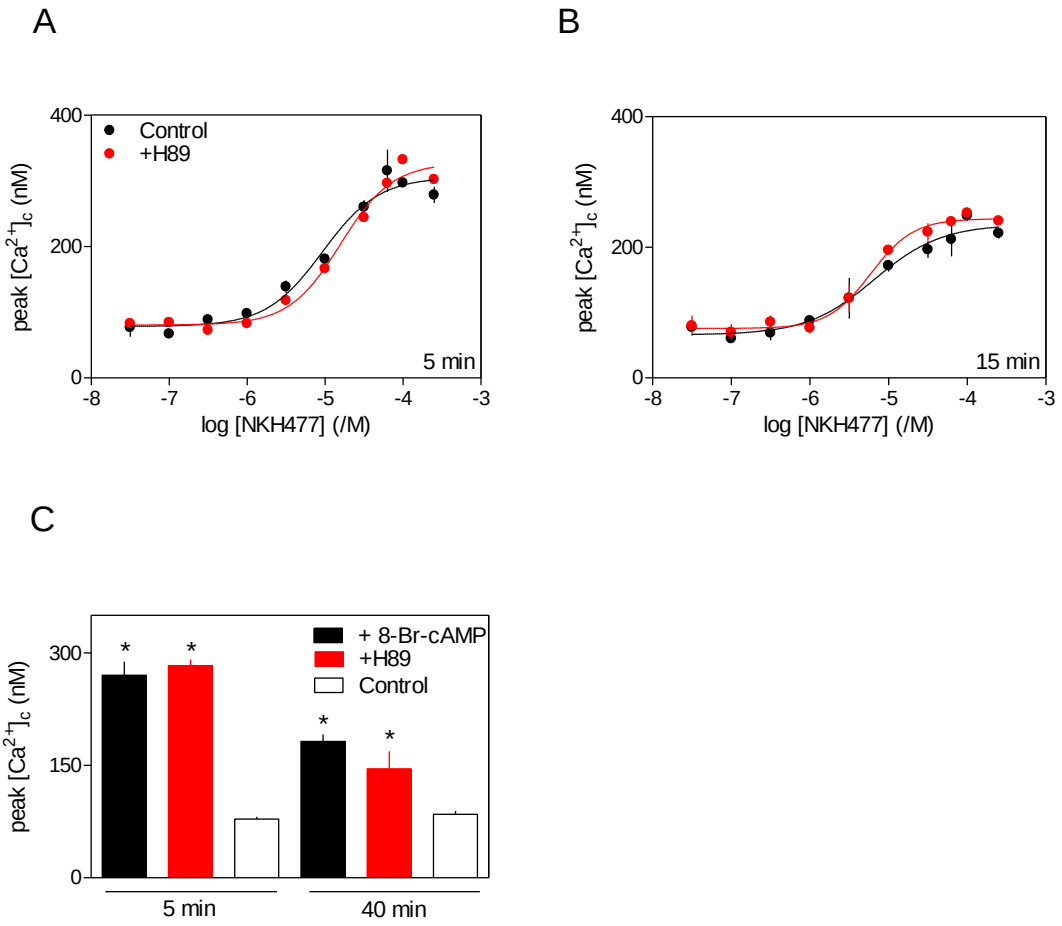

Figure 3.12. **PKA is unlikely to be involved in potentiation of CCh-evoked Ca^{2+} signals by NKH477 or 8-Br-cAMP.** (**A**, **B**) Populations of HEK-PR1 cells were incubated with H89 (10 µM, 20 min) before stimulation with NKH477 (5 or 15 min) or 8-Br-cAMP (10 mM, 5 or 40 min). The CCh (20 µM)-evoked Ca^{2+} signals were then assessed in the presence of BAPTA (2.5 mM). Results show the concentration-dependent effects of NKH477 (**A**, **B**) or 8-Br-cAMP (**C**) with or without H89 on the potentiated peak $[Ca^{2+}]_c$ signals evoked by CCh. Results are means ± SEM from 3 independent experiments. The statistical analysis was done in between the acute stimulation (5 min) and sustained stimulation (40 min) for each combination stimuli. $^{*}P < 0.05$ with paired Student's t-test (comparing matched stimuli for acute and sustained stimulation).

	5 min		15 min	
	pEC_{50}	Maximal $\Delta[Ca^{2+}]_c$ (nM)	pEC_{50}	Maximal $\Delta[Ca^{2+}]_c$ (nM)
Control	5.0 ± 0.1	225 ± 9	5.0 ± 0.1	155 ± 10*
H89	4.8 ± 0.1	245 ± 7.0	5.2 ± 0.1	171 ± 9.0*

Table 3.11. **PKA inhibition does not affect the potentiation of CCh-evoked Ca^{2+} signals by NKH477**. Effect of stimulation with NKH477 (5 or 15 min) alone or with H89 (10 µM, 20 min) pre-treatment on the maximal $\Delta[Ca^{2+}]_c$ signals evoked by CCh (20 µM) and on the sensitivity to NKH477, measured from populations of HEK-PR1 cells. Results are means ± SEM from 3 independent experiments. $^{*}P < 0.05$ relative to paired comparisons at 5 min. Paired Student's t-test was used for the analysis.

3.3.9. Potentiation of CCh-evoked Ca^{2+} signals by PTH(1-34) is independent of Epac.

ESI-09 is a new membrane-permeant antagonist of Epac 1/2 (Chen *et al.*, 2013). Thus, it was necessary to optimise the concentration and incubation times to avoid directly affecting CCh-evoked Ca^{2+} signals. Populations of HEK-PR1 cells were incubated with different concentrations of ESI-09 before measuring the peak increase in $[Ca^{2+}]_c$ evoked by CCh. Pre-treatment with ESI-09 (10-50 µM) for 15 min inhibited CCh-evoked Ca^{2+} signals (Fig. 3.13A). A brief (5 min) treatment with ESI-09 (10 µM) had no significant effect on the $\Delta[Ca^{2+}]_c$ signals evoked by PTH(1-34) (3 µM) alone (Fig. 3.13B) or CCh compared to matched controls (Fig. 3.13B, Table 3.12).

These results confirm that use of high concentrations of ESI-09 (> 10µM) or prolonged treatment (> 5 min) is not practical because they directly inhibit CCh-evoked Ca^{2+} release (Fig. 3.13A). Others have also recently reported non-specific effects of ESI-09 (Rehmann, 2013). Subsequently, ESI-09 (10 µM, 5 min) was used to confirm whether inhibition of Epac 1/2 affects the acute potentiation by PTH(1-34) of the CCh-evoked increase in $[Ca^{2+}]_c$ (Fig. 3.13C, Table 3.12). Since ES1-09 inhibits Ca^{2+} signals

evoked by CCh beyond 5 min incubation, sustained PTH(1-34) stimulation experiments could not be performed.

Inhibition of Epac 1/2 had no effect on the potentiation of CCh-evoked Ca^{2+} signals by acute stimulation with 8-Br-cAMP. ESI-09 did not affect the increase in peak $[Ca^{2+}]_c$ evoked by CCh (Fig. 3.13D, Table3.12). These results suggest that Epacs 1/2 are not involved in the potentiation of CCh-evoked Ca^{2+} signals by PTH(1-34) or 8-Br-cAMP (Tovey *et al.*, 2008). The conclusion is weakened by the limited opportunity to explore higher concentrations of ESI-09 or more prolonged incubations, but it is consistent with evidence that an effective and selective agonist of Epac does not mimic the effects of 8-Br-cAMP on CCh-evoked Ca^{2+} signals (Tovey *et al.*, 2008) Both analyses would be stronger if supported by direct measurements of the ligands on Epac activity.

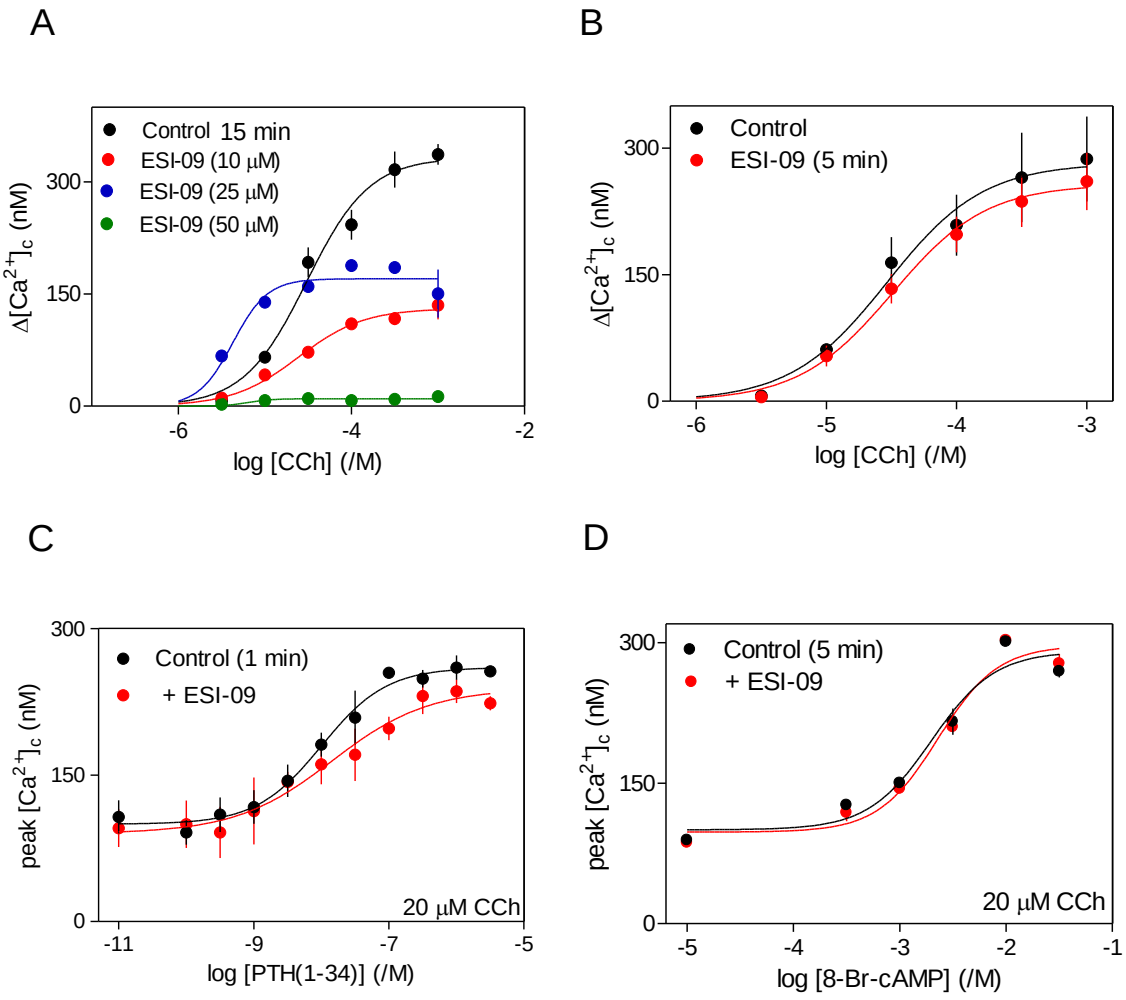

Figure 3.13. **Epac is probably not involved in potentiation of CCh-evoked Ca^{2+} signals by PTH(1-34) and 8-Br-cAMP.** (**A**) Populations of HEK-PR1 cells were incubated with the Epac 1/2 antagonist ESI-09 (10, 25, 50 µM, 15 min) before addition of the indicated concentrations of CCh in Ca^{2+}-free HBS. Results show the increase in $[Ca^{2+}]_c$ evoked by CCh. Results are means ± SD from 2 independent experiments. (**B**) Cells were incubated with ESI-09 (10 µM, 5 min) before addition of increasing CCh concentrations. Results show the increases in $[Ca^{2+}]_c$ evoked by CCh in the presence of BAPTA (2.5 mM). (**C, D**) Cells were incubated with ESI-09 (10 µM, 5 min) before stimulation with PTH(1-34) (1 min) (**C**) and 8-Br-cAMP (5 min) (**D**). Results show peak $[Ca^{2+}]_c$ evoked by CCh (20 µM) in the presence of BAPTA (2.5 mM). Results (B-D) are means ± SEM from 3 independent experiments.

	pEC_{50}	Maximal $\Delta[Ca^{2+}]_c$ (nM)
CCh		
Control	4.5 ± 0.0	283 ± 82
+ ESI-09	4.5 ± 0.1	257 ± 38
PTH(1-34) (1 min)		
Control	7.9 ± 0.1	161 ± 14
+ ESI-09	7.8 ± 0.1	150 ± 18
8-Br-cAMP (5 min)		
Control	2.7 ± 0.1	190 ± 06
+ ESI-09	2.6 ± 0.1	198 ± 16

Table 3.12. **An inhibitor of Epac 1/2 does not affect potentiation by PTH(1-34) or 8-Br-cAMP of CCh-evoked Ca^{2+} signals.** Effect of stimulation with CCh, PTH(1-34) (1 min) and 8-Br-cAMP (5 min) alone or with ESI-09 (10 µM, 5 min) pretreatment on the maximal $\Delta[Ca^{2+}]_c$ signals evoked by either different CCh concentrations or CCh (20 µM) when stimulated with PTH(1-34) or 8-Br-cAMP. The table shows the sensitivity to CCh, PTH(1-34) or 8-Br-cAMP under the different conditions. Results are means ± SEM from 3 independent experiments.

3.4. Discussion

Acute or sustained stimulation with PTH(1-34) potentiated Ca^{2+} responses evoked by CCh (Fig. 3.4, Table 3.5). However, the maximal Ca^{2+} signal was reduced by ~50%, and the sensitivity to PTH(1-34) was increased by ~10-fold after sustained stimulation. From experiments performed in single HEK-PR1 cells, it was confirmed that the decrease in maximal Ca^{2+} response after prolonged incubation with PTH(1-34) was not due to fewer cells responding in populations of HEK-PR1 cells. Instead, it was because of a reduction in Ca^{2+} signals within individual cells (Fig. 3.5).

Results in figures 3.6 and 3.7 and table 3.6 provide persuasive evidence that cAMP mediates the ability of acute or sustained stimulation with PTH(1-34) to potentiate Ca^{2+} signals evoked by CCh. PTH(1-34) and analogues (PTH(2-38) and Tyr^{1}PTH(1-34)) that only stimulate AC (Table 3.1) (Cupp *et al.*, 2013) showed potentiation of CCh-evoked Ca^{2+} signals at lower concentrations of PTH (higher pEC_{50}) (Fig. 3.7A, Table 3.6) than were required to stimulate cAMP accumulation (Fig. 3.7B). Previously, PTH(3-34), which was thought to allow selective activation of Gq (Fujimori *et al.*, 1991; but see Takasu *et al.*, 1999), was used to suggest that PTH(1-34) evokes its effects on Ca^{2+} signalling via the AC signalling pathway (Tovey *et al.*, 2008). However, a recent study challenges the utility of PTH(3-34). In CHO cells stably expressing PTH_1R, PTH(3-34) stimulated AC (though with very low potency), but not PLC (Cupp *et al.*, 2013). In the same study, PTH(2-38) and Trp^{1}PTH(1-34) were as effective as PTH(1-34) in stimulating AC, but they failed to activate PLC (Cupp *et al.*, 2013). Selective activation of AC by PTH(2-38) and Trp^{1}PTH(1-34) is consistent with evidence that N-terminal modifications to PTH attenuate coupling to PLC (Cupp *et al.*, 2013; Takasu *et al.*, 1999). Collectively, these and published results (Tovey *et al.*, 2008) suggest that cAMP mediates the effects of PTH(1-34) on CCh-evoked Ca^{2+} signals.

Even so, the Ca^{2+} signals evoked by high concentrations of PTH(1-34) (Fig. 3.6A) are likely to result from direct stimulation of PLC (Section 3.1.4-6). The inability to detect IP_3 formation under these conditions (Short *et al.*, 2000; Tovey *et al.*, 2008; Tovey *et al.*, 2013) is unsurprising when the Ca^{2+} signals are so small (Fig. 3.6A) and they are detected under conditions where there is also maximal potentiation of IP_3-evoked Ca^{2+} release by cAMP.

In addition, data obtained using NKH477 (Fig. 3.8, Table 3.7) and 8-Br-cAMP (Fig. 3.9, Table 3.8), mimicked the responses evoked by PTH(1-34) and the maximal effects of acute or sustained exposure to PTH(1-34). NKH477 and 8-Br-cAMP in combination were non-additive (Fig. 3.10, Table 3.9). This further supports the conclusion that cAMP is the only signal linking PTH_1R to sensitization of IP_3R. Previously, it has been shown that G protein βγ subunits stimulate IP_3R directly and thus cause release of Ca^{2+} (Zeng *et al.*, 2003). However, PTH(1-34) cannot work via this pathway because PTH(1-34) alone does not cause release of Ca^{2+} specifically at lower concentrations (Fig. 3.6A)

There is no evidence to suggest that PKA (Fig. 3.11, 3.12, Table 3.10, 3.11) or Epacs (Fig. 3.13, Table 3.12) are required for PTH(1-34), NKH477 or 8-Br-cAMP to potentiate the Ca^{2+} signals evoked by CCh. Under conditions when H89 has previously been shown to inhibit PKA-evoked protein phosphorylation, it had no effect on the potentiation of CCh-evoked Ca^{2+} signals evoked by PTH(1-34) (Tovey *et al.*, 2008). H89 is not a specific inhibitor of PKA (Davies *et al.*, 2000) but its off-target effects are less problematic when the conclusion rests on a lack of effect on the cellular response (potentiation of CCh-evoked Ca^{2+} signals). Nevertheless, the conclusion that cAMP affects IP_3R without requiring activation of PKA is important, and it would be stronger for additional evidence (Tovey *et al.*, 2008). There are other inhibitors of PKA (e.g. KT5720 and PKI) (Davies *et al.*, 2000) and there are peptides that disrupt association of PKA with its anchoring proteins (AKAPs). While each of these tools has its limitations and/or practical difficulties, they could be use to reinforce the evidence excluding a role for PKA providing their effectiveness is verified.

Only Epac1 has been detected in HEK-PR1 cells (Qiao *et al.*, 2002; Tovey *et al.*, 2008). Previously, stimulation of HEK-PR1 cells with 8-Br-2'- *O*- methyleadenosine-3',5- cAMP, which selectively activates Epac1/2 (Christensen *et al.*, 2003), had no effect on CCh-evoked Ca^{2+} signals, whereas 8-Br-cAMP potentiated them (Tovey *et al.*, 2008). These results were supported by using a competitive antagonist of Epac1/2, ESI-09 (Fig. 3.13, Table 3.12) (Almahariq *et al.*, 2013). ESI-09 may be ineffective if high concentrations of cAMP are locally delivered to IP_3R from AC (Section 3.1.8) (Tovey *et al.*, 2008). However, 8-Br-cAMP (which is uniformly dispersed in the cytosol) potentiated the Ca^{2+} signals evoked by CCh, and this response was also unaffected by ESI-09 (Fig. 3.13D, Table 3.12). I have not, however, directly demonstrated that Epac-1 was effectively inhibited by this treatment with ESI-09.

These results indicate that PKA and Epac are unlikely to be required in the potentiation by acute or sustained stimulation with PTH(1-34) of Ca^{2+} signals evoked by CCh. Nor are these two conventional targets of cAMP likely to mediate the Ca^{2+} signals evoked directly by higher concentrations of PTH(1-34) (Fig. 3.6C, E). Evidence that PTH analogues that stimulate only AC do not directly evoke Ca^{2+} signals (Fig. 3.6A, 3.7A, Table 3.6) strongly suggests that cAMP/Epac-mediated activation of PLC_{ε} (Schmidt *et al.*, 2001) does not contribute to PTH(1-34)-evoked Ca^{2+} signals. In addition to PKA and Epacs there are few other kinases for example phosphatidylinositol-3-kinase and Akt which could also be activated by sustained stimulation of PTH_1R by PTH(1-34) (Yamamoto *et al.*, 2007). However, it is very unlikely that Akt and phosphatidylinositol-3-kinase can contribute in sustained stimulation with PTH(1-34) potentiated CCh-evoked Ca^{2+} signals. As acute or sustained stimulation with 8-Br-cAMP (Fig. 3.9) and direct activation of AC using NKH477 (Fig. 3.8) were also similar to the responses evoked by PTH(1-34) and the maximal effect of sustained exposure to each stimulus were non-additive (Fig. 3.10)

In summary, I conclude that in HEK-PR1 cells, both acute and sustained stimulation with PTH(1-34) potentiates CCh-evoked Ca^{2+} release However, the maximal Ca^{2+} release after sustained stimulation with PTH(1-34) is almost half that observed after acute stimulation. I also conclude that potentiation of CCh-evoked Ca^{2+} signals by acute or sustained stimulation with PTH(1-34) is entirely mediated by cAMP, which sensitizes IP_3R to IP_3 without need for activation of PKA or Epacs. The mechanisms underlying the decrease in the maximal Ca^{2+} release after sustained stimulation with PTH(1-34) are explored in chapter 4.

Chapter 4. AC-IP_3R junctions mediate sustained potentiation of Ca^{2+} signals by PTH

4.1. Introduction

In Chapter 3, I demonstrated that acute or sustained stimulation with PTH(1-34) potentiates CCh-evoked Ca^{2+} signals, but the maximal Ca^{2+} release is almost 50% less and the sensitivity to PTH is ~10-fold higher after sustained stimulation. Both the acute and sustained effects of PTH(1-34) on CCh-evoked Ca^{2+} signals are mediated by cAMP, but they are independent of PKA and Epac.

Earlier work suggested that the potentiation of IP_3-evoked Ca^{2+} release was probably due to cAMP binding directly to IP_3R, or to proteins associated with IP_3R, to increase their sensitivity to IP_3. The mechanisms underlying the long-term response to PTH(1-34) has not previously been addressed; it is the topic of this chapter I anticipated three potential mechanism underlying the decrease in maximal Ca^{2+} responses after sustained stimulation with PTH(1-34).

1) A leak of Ca^{2+} from intracellular stores might reduces the effect of IP_3 on $[Ca^{2+}]_c$ (Huang *et al.*, 1998; Tovey *et al.*, 2003; Tovey *et al.*, 2013).

2) Internalization of a PTH_1R-coupled-AC signalling complex (Ferrandon *et al.*, 2009) might disrupt effective regulation of IP_3R by cAMP.

3) A decrease in CCh-evoked IP_3 formation after sustained stimulation with PTH(1-34) might attenuate the direct stimulation of IP_3R.

These alternatives are explored in this chapter, together with an assessment of whether sustained responses to PTH(1-34) are mediated by the hyperactive AC-IP_3R junctions proposed in earlier work to mediate the acute effects of PTH(1-34) (Tovey *et al.*, 2008).

4.2. Materials and Methods

4.2.1. Materials

The Forster Resonance Energy Transfer (FRET)-based IP_3-biosensor plasmid was from Professor Colin Taylor (University of Cambridge, U.K). Properties of the IP_3-biosensor have been reported previously (Tovey *et al.*, 2013). Lipofectamine LTX reagent with

PLUS^{TM} reagent was from Invitrogen Ltd (Renfrew, Renfrewshire, UK). Most the materials used in this chapter are listed in Table 3.2.

4.2.2. IP_3 measurements in HEK-PR1 cells

In single HEK-PR1 cells, the cytosolic IP_3 concentration was measured using a FRET-based IP_3-sensor. This IP_3-biosensor is based on the IP_3-binding core (IBC) of IP_3R1 (Tovey *et al.*, 2013). The details of the plasmid preparation and the properties of the biosensor have been described previously (Tovey *et al.*, 2013). The biosensor consists of the IBC attached via short linkers to enhanced yellow fluorescent protein (YFP) at its C-terminal and enhanced cyan fluorescent protein (CFP) at its N terminal. The binding of IP_3 at IBC causes changes in CFP and YFP emission, which was collected each second. In results increase in CFP and YFP ratio was considered as decrease in FRET and hence, overall increase in IP_3 concentration. HEK-PR1 cells were grown in 6-well plates (up to 60% confluence) on poly-L-lysine-coated round coverslips (22-mm diameter). Cells were grown for 48 h before transfecting with the plasmid encoding the IP_3-sensor using Lipofectamine LTX reagent with PLUS^{TM} reagent. For each well, a transfection cocktail was prepared consisting of 6 µl of Lipofectamine LTX, 2.5 µl PLUS^{TM} reagent, 1 µg of the IP_3 sensor plasmid and 200 µl of Opti-MEM reduced-serum medium. After a 5-min incubation, the transfection cocktail (209.5 µl) was added to each well containing 2 ml of culture medium. Cells were further grown for 48 h at 37 ^{o}C in 5% CO_2 before measuring the CFP/YFP FRET ratio, reflecting changes in intracellular IP_3 concentration. These measurements were done under conditions that match those used to measure $[Ca^{2+}]_{c.}$ An Olympus IX71 inverted fluorescence microscope equipped with a 40x objective and a 440/520 nm dual band-pass dichroic mirror was used to record fluorescence using widefield excitation at 440 nm and simultaneous collection of YFP (520-550 nm) and CFP (455-485 nm) emissions using an Olympus U-SIP split imaging TV port fitted with a 505-nm dichroic mirror. Split images were obtained at 1-s intervals using a Luca EMCCD camera (Andor Technology, Belfast, UK). YFP and CFP emissions were background corrected. The background was collected from non-transfected cells present in the field. IP_3 binding causes an increase in CFP/YFP ratio, which was indicative of decreased FRET. The FRET ratios are presented as CFP emission/YFP emission. The transfection efficiency was ~65%, and 52 ± 2% (n = 17 coverslips) of transfected cells responded to the first

CCh (1 mM) challenge with detectable FRET changes. Only these responsive cells were included in analyses of the effects of PTH(1-34).

The methods used to measure $[Ca^{2+}]_c$ and cAMP were described in Chapter 3 (Section 3.2).

4.3. Results

4.3.1. Decreased Ca^{2+} signals after sustained stimulation with PTH(1-34) do not involve a Ca^{2+} leak from intracellular stores

The maximal $\Delta[Ca^{2+}]_c$ signals evoked by CCh after sustained stimulation with PTH(1-34) were ~50% smaller than those detected after acute stimulation with PTH(1-34) (Fig. 3.4A, B, Table 3.5). This might be a consequence of Ca^{2+} leaking from stores in the sustained presence of PTH(1-34). Therefore, ionomycin was used to define the amount of Ca^{2+} within intracellular stores (Tovey *et al.*, 2013) after sustained or acute stimulation of fluo-4-loaded HEK-PR1 cells with PTH(1-34).

Ionomycin, a Ca^{2+} ionophore, is frequently used to modify intracellular Ca^{2+} concentration and to calibrate fluorescent Ca^{2+} indicators (Liu *et al.*, 1978). Addition of ionomycin, in the presence of BAPTA, after sustained (30 min) or acute (1 min) stimulation with PTH(1-34) shows that there was no effect of PTH(1-34) on the Ca^{2+} signals evoked by ionomycin. The peak increase in $[Ca^{2+}]_c$ evoked by ionomycin after acute or sustained stimulation with PTH(1-34) was 377 ± 22 nM and 399 ± 9 nM, respectively (Fig. 4.1A). To confirm that the ionomycin-evoked Ca^{2+} signals do not saturate the Ca^{2+} indicator, at the end of the experiment the increase in fluo-4 fluorescence evoked by the addition of extracellular $CaCl_2$ was measured. The results show that fluo-4 fluorescence after addition of extracellular $CaCl_2$ was significantly higher than that evoked by ionomycin in Ca^{2+}-free HBS (Fig. 4.1B). These results confirm that the indicator was not saturated when ionomycin-evoked Ca^{2+} signals were measured.

After stimulation with PTH(1-34) and CCh, the residual Ca^{2+} content of the stores was also measured using a similar protocol. These experiments were performed in parallel to the ionomycin experiments to allow direct comparisons. After prolonged incubation with PTH(1-34), the Ca^{2+} remaining in the intracellular stores was greater

(increase in $[Ca^{2+}]_c$ was 181 ± 12 nM) than for cells briefly incubated with PTH(1-34) (97 ± 4 nM) (Fig. 4.1A). The results from cells stimulated with PTH(1-34) and CCh clearly show that the decrease in maximal $[Ca^{2+}]_c$ signals after sustained stimulation with PTH(1-34) (Fig. 3.4, Table 3.4) is not because of enhanced Ca^{2+} leaks from the intracellular stores.

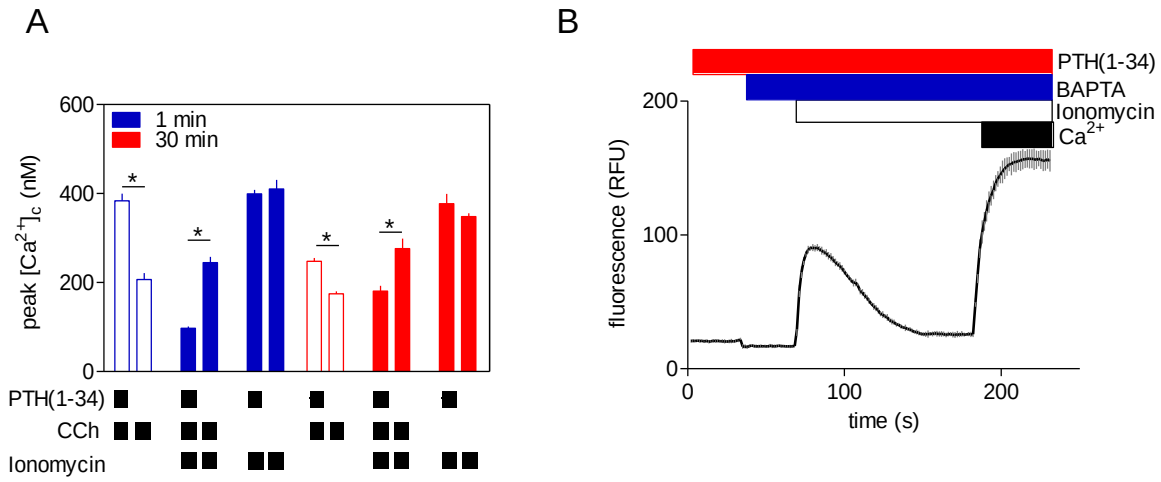

Figure 4.1. **Effects of sustained stimulation with PTH(1-34) on the Ca^{2+} contents of the intracellular stores.** (**A**) Populations of HEK-PR1 cells were pre-treated with PTH(1-34) (100 nM) for 1 or 30 min before addition of CCh (20 µM) (open bars) or ionomycin (1 µM) (solid bars), or first CCh (20 µM) followed by ionomycin (solid bars) in the continuous presence of BAPTA (2.5 mM). Results show CCh- or ionomycin-evoked peak increases in $[Ca^{2+}]_c$ after each treatment. Results are means ± SEM from 3 experiments. $^{*}P < 0.05$ relative to paired comparisons with the controls. Students paired t-test was used for analysis. . (**B**) HEK-PR1 cells were incubated with PTH(1-34) for 30 min before addition of BAPTA (2.5 mM), then ionomycin (1 µM) and lastly extracellular Ca^{2+} (10 mM) was added to check for indicator saturation. Results show typical traces from 5 wells in 1 experiment. Relative fluorescence units (RFU).

4.3.2. Decreased Ca^{2+} signals after sustained stimulation with PTH do not involve PTH_1R internalization

PTH binding to PTH_1R stimulates PTH_1R β-arrestin/dynamin-mediated internalization (van der Lee *et al.*, 2013). It has also been observed that brief stimulation with PTH(1-

34) evokes persistent signalling from internalized PTH_1R-coupled AC (Ferrandon *et al.*, 2009) (Section 3.1.7). PTH(1-34), PTHrP(1-36), PTH(2-38) and Tyr^1PTH(1-34) were used to assess whether internalization of PTH_1R might contribute to the different effects of PTH(1-34) on CCh-evoked Ca^{2+} signals after brief and sustained exposure to PTH. These analogues were selected based on their ability to promote internalization of PTH_1R after PTH binding and/or show persistent signalling from internalized PTH_1R-coupled AC. PTH(1-34) shows both internalization and continuous signalling, PTH(2-38) does not promote internalization, Tyr^1PTH(1-34) acts as a weak partial agonist in promoting internalization, and PTHrP(1-36) is internalized, but does not persistently signal (Cupp *et al.*, 2013; Ferrandon *et al.*, 2009).

The results demonstrate that each of these PTH analogues showed an increased sensitivity to PTH and a decrease in the maximal $\Delta[Ca^{2+}]_c$ signals evoked by CCh (20 μM) after sustained, relative to acute, stimulation (Fig. 4.2A, C, 4.3A, C, Table 4.1). However, the levels of intracellular cAMP produced after acute or sustained stimulation with each of these analogues were not similar (Fig. 4.2B, D, 4.3B, D, Table 4.2). Tyr^1PTH(1-34) and PTH(1-34) showed a significant increase in both the levels of cAMP produced and the sensitivity to PTH after sustained, relative to acute, stimulation (Fig. 4.2B, D, Table 4.2). Whereas, PTH(2-38) and PTHrP(1-36) did not show a significant increase in the amount of cAMP produced after prolonged stimulation. PTH(2-38) showed a significant increase in sensitivity to PTH after prolonged stimulation, whereas PTHrP did not (Fig. 4.3B, D, Table 4.2). These results, which rely heavily on published properties of the analogues used, suggest that internalization of PTH_1R after sustained or acute stimulation is unlikely to be associated with the effect of PTH on CCh-evoked Ca^{2+} signals.

Results shown in figures 4.2 and 4.3 were used to assess the relationship between the change in intracellular cAMP concentration and the corresponding potentiated Ca^{2+} signals after acute or sustained stimulation with PTH analogues (Fig. 4.4). These cAMP and Ca^{2+} relationship graphs suggested that there is a disparity between the amount of cAMP produced and the corresponding increase in Ca^{2+} signals for each PTH analogue (Fig. 4.4).

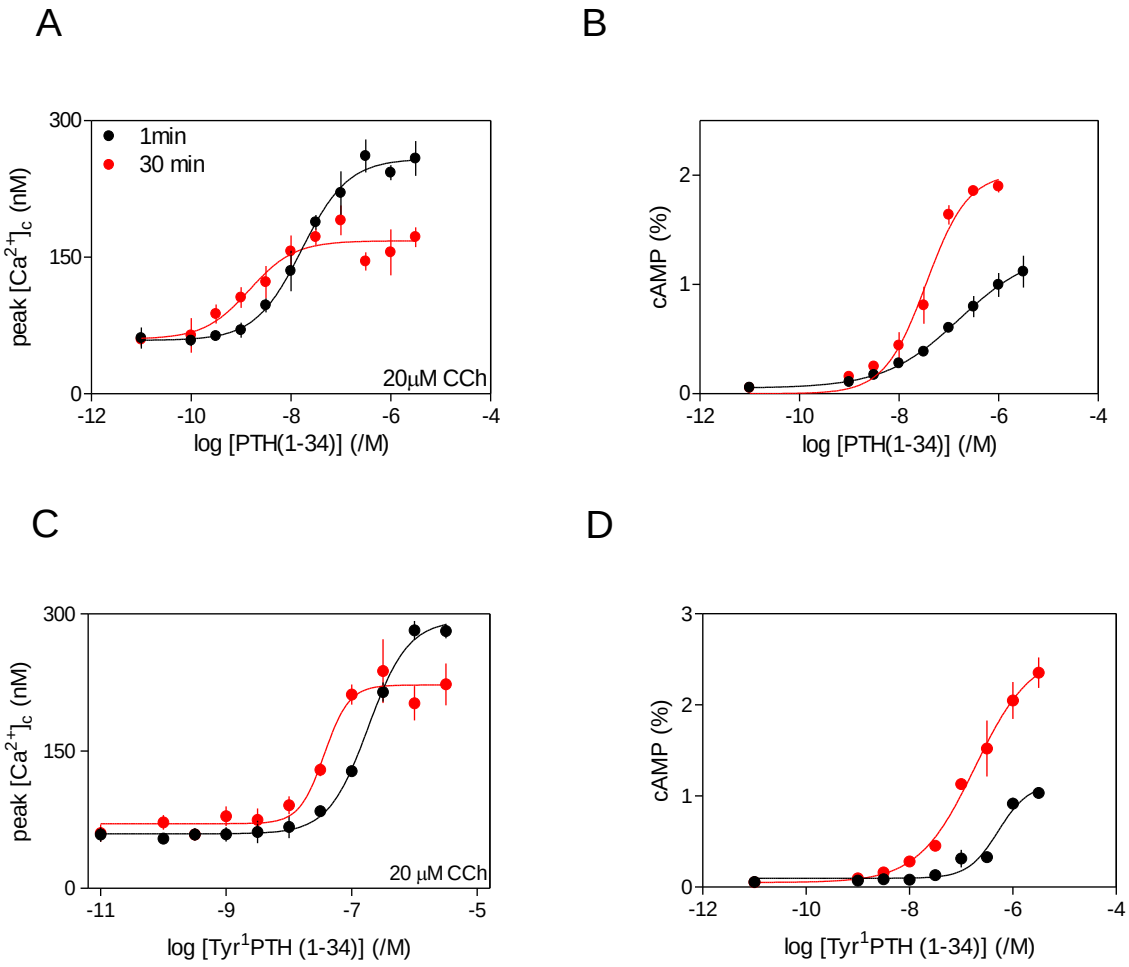

Figure 4.2. **Sustained stimulation with PTH analogues potentiates CCh-evoked Ca^{2+} signals.** (**A**, **C**) Populations of HEK-PR1 cells were stimulated with PTH analogues for 1 or 30 min. The CCh (20 µM)-evoked Ca^{2+} responses were then assessed in the presence of BAPTA (2.5 mM). Results show concentration-dependent effects of PTH analogues on the peak Ca^{2+} signals evoked by CCh. (**B**, **D**) Effects of PTH analogues on intracellular cAMP measured after 1 or 30 min under conditions identical to those used for measurements of $[Ca^{2+}]_c$. Results show ^{3}H-cAMP as a percentage of ^{3}H-ATP, ^{3}H-ADP and ^{3}H-cAMP. Results are means ± SEM from ≥ 3 experiments. The code applies to all panels.

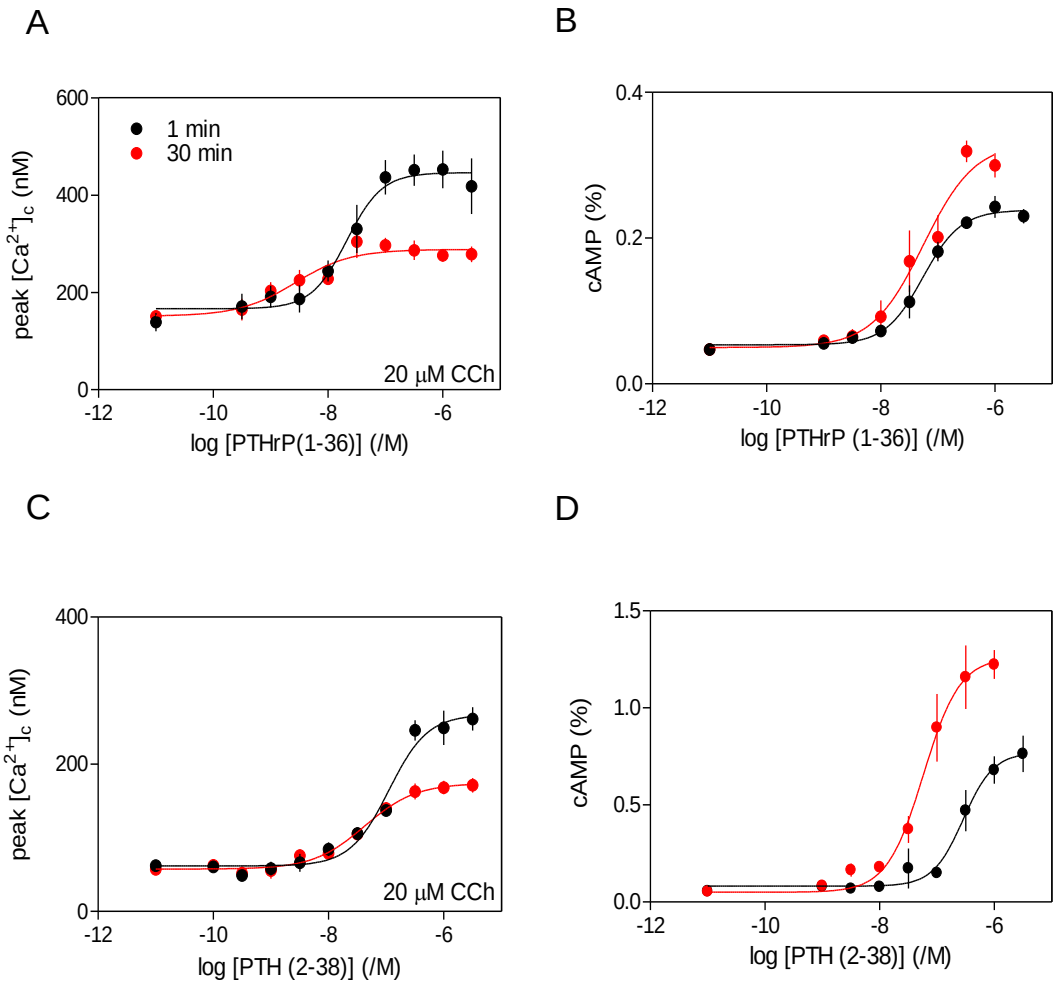

Figure 4.3. **Sustained or acute stimulation with PTH analogues potentiates CCh-evoked Ca^{2+} signals.** (**A**, **C**) Populations of HEK-PR1 cells were stimulated with PTH analogues for 1 min or 30 min. The CCh (20 µM)-evoked Ca^{2+} responses were then assessed in the presence of BAPTA (2.5 mM). Results show concentration-dependent effects of the PTH analogues on the peak Ca^{2+} signals evoked by CCh. (**B**, **D**) Effects of PTH analogues on intracellular cAMP measured after 1 min or 30 min under conditions identical to those used for measurements of $[Ca^{2+}]_c$. Results show ^{3}H-cAMP as a percentage of ^{3}H-ATP, ^{3}H-ADP and ^{3}H-cAMP. Results are means ± SEM from ≥ 3 experiments. The code applies to all panels.

	1 min		30 min	
	pEC_{50}	Maximal $\Delta[Ca^{2+}]_c$ (nM)	pEC_{50}	Maximal $\Delta[Ca^{2+}]_c$ (nM)
PTHrP(1-36)	7.6 ± 0.1	281 ± 34	8.6 ± 0.2*	139 ± 2*
PTH(2-38)	6.9 ± 0 .1	216 ± 21	7.3 ± 0.1*	115 ± 13*
Tyr^1PTH(1-34)	6.7 ± 0.03	233 ± 10	7.4 ± 0.1*	148 ± 6*
PTH(1-34)	7.7 ± 0.1	205 ± 13	8.8 ± 0.2*	105 ± 13*

Table 4.1. **PTH analogues potentiate CCh-evoked Ca^{2+} signals in HEK-PR1 cells.** Effect of stimulation with PTH analogues for 1 or 30 min on the maximal Ca^{2+}signals evoked by CCh (20 µM) and on the sensitivity to PTH(1-34), measured from populations of HEK-PR1 cells. Results are means ± SEM from 3 independent experiments. $^*P < 0.05$ relative to paired comparisons at 1 min using paired Student's t-test. Results are means ± SEM from 3 independent experiments.

	1 min		30 min	
	pEC_{50}	Maximal ΔcAMP (%)	pEC_{50}	Maximal ΔcAMP (%)
PTHrP(1-36)	7.3 ± 0.1	0.2 ± 0.01	7.3 ± 0.2	0.3 ± 0.01
PTH(2-38)	6.5 ± .04	0.7 ± 0.1	7.2 ± 0.1*	1.2 ± 0.1
Tyr^1PTH(1-34)	6.1 ± 0.2	1.3 ± 0.2	6.7 ± 0.2*	2.6 ± 0.1*
PTH(1-34)	7.0 ± 0.1	1.1 ± 0.1	7.5 ± 0.2*	1.9 ± 0.03*

Table 4.2. **PTH analogues evoke cAMP formation in HEK-PR1 cells.**
Effects of stimulation with PTH analogues for 1 or 30 min on the maximal intracellular cAMP accumulation and sensitivity to PTH. Results are means ± SEM from 3 independent experiments. $^*P < 0.05$ relative to paired comparisons at 1 min using paired Student's t-test. Results are means ± SEM from 3 independent experiments.

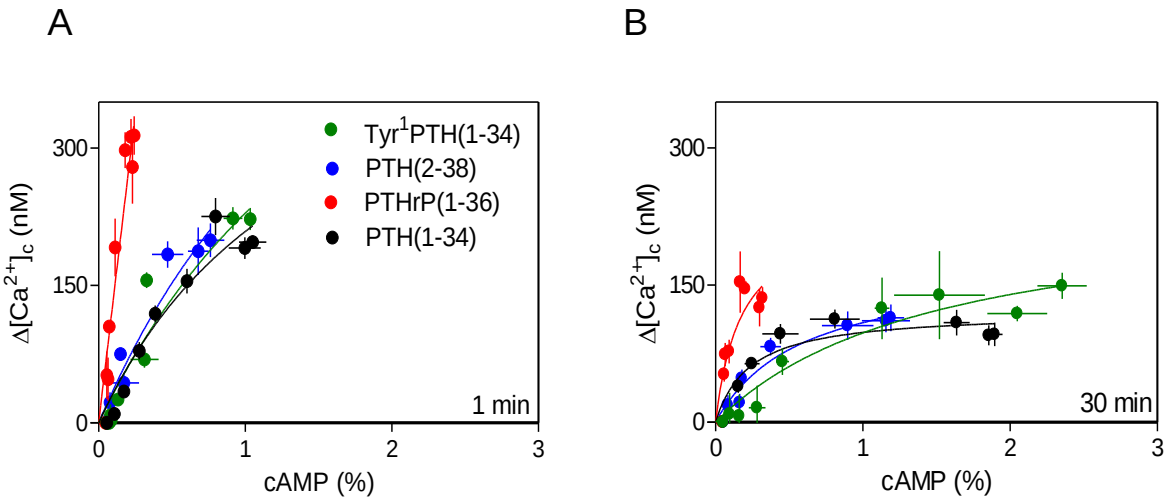

Figure 4.4. **Relationship between Ca^{2+} and cAMP for HEK-PR1 cells stimulated with analogues of PTH.** Results from figures 4.2 and 4.3 were used to establish the a non linear regression relationship between cAMP and the potentiated CCh-evoked increase in $[Ca^{2+}]_c$ for cells stimulated with the indicated PTH analogues for 1 min (**A**) or 30 min (**B**), therefore each line corresponds the same.

4.3.3. Sustained stimulation with PTH(1-34) decreases CCh-evoked IP_3 formation

The 50% decrease in maximal $\Delta[Ca^{2+}]_c$ signals seen after sustained stimulation with PTH(1-34) compared to acute stimulation (Fig. 3.4A, B, Table 3.4) could be a consequence of a decrease in IP_3 formation. Hence, I measured CCh-evoked IP_3 formation after acute and sustained stimulation with PTH(1-34). A dual-simulation protocol was established for these experiments. HEK-PR1 cells were stimulated twice with CCh separated by an interval of 30 min. The results show that the first stimulation with a maximal CCh concentration (1 mM) increased ΔFRET ratio by 10 ± 1%. After 3 washes with HBS and 30-min recovery interval, the second stimulation with submaximal (30 µM) CCh showed a 4 ± 0.1% increase in ΔFRET ratio (Fig. 4.5). The increase in FRET ratio evoked by a maximal CCh concentration is significantly different from that evoked by a submaximal CCh concentration. Furthermore, the FRET changes evoked by 30 µM CCh were unaffected by previous exposure to 1 mM CCh (Fig. 4.5B). These results demonstrate that my protocol allows change in cytosolic IP_3 to be measured, and that 30 µM CCh does not saturate the signals (Fig. 4.5B). This paired analysis method reduced the variability arising from the limited dynamic range of the sensor.

The dual simulation protocol was used to determine the effects of PTH(1-34). The first stimulation with a maximal CCh concentration was used to identify responsive cells, prior to a second stimulation with a submaximal concentration of CCh after treatment with PTH(1-34) for 1 min (Fig. 4.6A) or 30 min (Fig. 4.6B). The results show that pretreatment with PTH(1-34) for 30 min significantly reduced the responses to CCh relative to 1 min stimulation (Fig. 4.6A, B). The ΔFRET ratio was 0.7 ± 1 % after a 30-min stimulation with PTH(1-34) (Fig. 4.6D, E), whereas it was 4 ± 1% after a 1-min pretreatment with PTH(1-34) (Fig. 4.6C, E). However, in both experiments the first stimulation with CCh (1 mM) showed similar responses 9 ± 1% (Fig. 4.6D) and 8 ± 1% (Fig. 4.6C, E). It is unlikely that the increase in cAMP evoked by PTH directly reduced the sensitivity of the sensor because earlier analyses have shown that cAMP does not affect IP_3 binding to IP_3R (from which the sensor was derived) (Tovey *et al.*, 2008). Nevertheless, it would be useful to confirm that the behaviour of the sensor is not itself affected by any consequences of stimulating PTH_1R. These results demonstrate that

sustained stimulation with PTH(1-34) reduced the ability of CCh to evoke an increase in cytosolic IP_3 concentration.

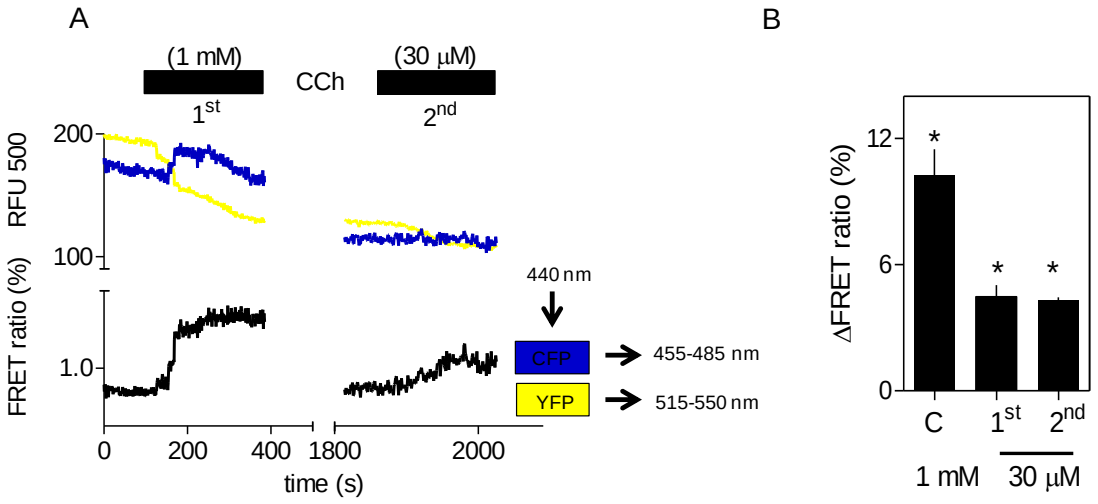

Figure 4.5. **Stimulation with CCh evoked changes in cytosolic IP_3 concentration.** (**A**) Typical trace from a single HEK-PR1 cell showing CFP and YFP emission and the resultant changes in the FRET ratio (CFP/YFP) of an IP_3 biosensor reflecting changes in intracellular IP_3 concentration. Cells were stimulated twice, first with CCh (1 mM, 3 min) (1^{st} stimulus) and then with CCh (30 µM, 3 min) (2^{nd} stimulus) after a 30 min interval. The typical trace is representative of 3 coverslips. The excitation and emission wavelengths used are shown alongside the graph. Inset illustrates the wavelengths used to collect each image. (**B**) Summary results show ΔFRET ratio (= observed / basal signal) for ~28 control cells. Results (B) are means ± SEM from ≥ 3 coverslips. $^{*}P <$ 0.05 relative to paired comparisons between C and 1^{st} bar or C and 2^{nd} bar as appropriate. Paired Student's t-test was used for the analysis.

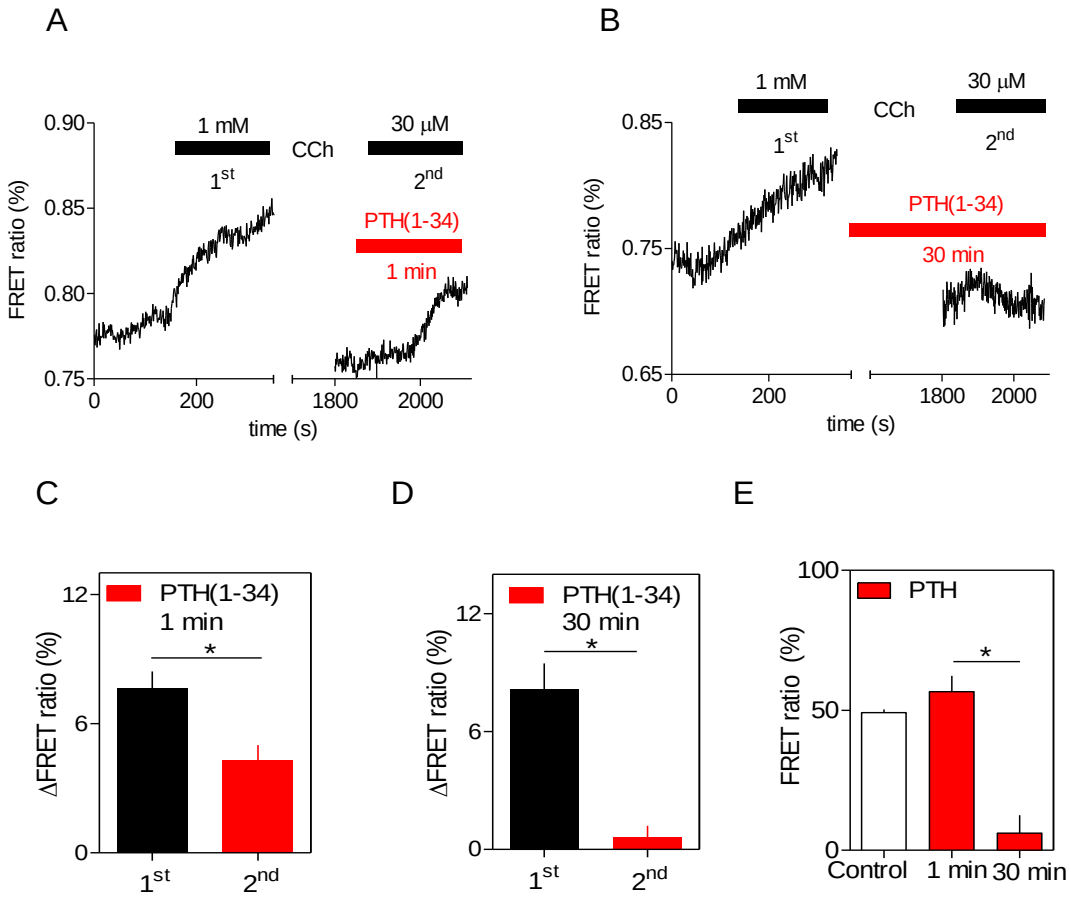

Figure 4.6. **Sustained stimulation with PTH(1-34) inhibits the CCh-evoked increase in cytosolic IP_3 concentration**. (**A**, **B**) Typical traces showing the increase in FRET ratio after stimulation with CCh (1 mM) (1^{st}), and CCh (30 µM) (2^{nd}) after a intervening pre-treatment with PTH(1-34) (100 nM) for 1 min (**A**) or 30 min (**B**). The traces in are representative of 5 (A) and 7 (B) coverslips. (**C**, **D**) Summary results show ΔFRET ratio (= observed / basal signal) for cells pretreated with PTH(1-34) for 1 min (~ 36 cells) (**C**) or 30 min (~34 cells) (**D**). Results (C, D) are means ± SEM from ≥ 3 coverslips. (**E**) For each cell, ΔFRET measurements for the first (1^{st}, 1 mM CCh) and second stimulus (2^{nd}, 30 µM CCh) were used to calculate the ratio of the $1^{st}/2^{nd}$ responses for the indicated treatments. $^{*}P < 0.05$ relative to paired comparisons with the controls. Students paired t-test was used for analysis.

4.3.4. Super-saturating cAMP junctions mediate sustained potentiation of CCh-evoked Ca^{2+} signals by PTH(1-34)

Previously, it was shown that global inhibition of cAMP formation by inhibiting AC with SQ/DDA, and of cAMP degradation by inhibiting PDE by IBMX (Morgan *et al.*, 1993) did not affect the potentiation of CCh-evoked Ca^{2+} signals evoked by acute stimulation with PTH(1-34). Hence, these signals were proposed to be mediated by AC-IP_3R signalling junctions, within which super-saturating concentrations of cAMP reach IP_3R (Tovey *et al.*, 2008) (Section 3.1.8). Furthermore, from a comparison of the responses of intact cells to PTH and 8-Br-cAMP and of permeabilized cells to cAMP, the calculated global intracellular cAMP was estimated to ~1000-fold too low to affect IP_3R. These results further supported the suggestion that cAMP was locally delivered to IP_3Rs. It is not yet clear whether similar local delivery of cAMP contributes to the sustained responses to PTH.

Subsequent, experiments assess whether the sustained effects of PTH(1-34) on CCh-evoked Ca^{2+} signals are mediated by cAMP junctions. The results indicate that acute or sustained stimulation with PTH(1-34) potentiates the increase in $[Ca^{2+}]_c$. These responses were not affected by inhibition of cAMP formation via AC with SQ/DDA (Seifert *et al.*, 2012). The maximal $\Delta[Ca^{2+}]_c$ responses after acute stimulation with PTH(1-34) in the presence of SQ/DDA were significantly higher, and the sensitivity to PTH(1-34) was significantly lower (~10-fold) in comparison to sustained stimulation with PTH(1-34) (Fig. 4.7A, B, Table4.4). However, intracellular cAMP formation was significantly reduced by the SQ/DDA treatment. For both acute and sustained stimulation with PTH(1-34), SQ/DDA reduced the amount of cAMP produced by ~70% relative to the matched controls (Fig. 4.7C, D, Table 4.5). The lack of effect of SQ/DDA on Ca^{2+} signals could be a limitation of the method used to measure the Ca^{2+} responses. However, an analysis that assumed that uniformly distributed cAMP regulates IP_3R shows that 70% inhibition of AC by SQ/DDA should allow readily detectable inhibition of the effects of PTH(1-34) on CCh-evoked Ca^{2+} responses (Fig. 4.8). These results are in line with a previous study, where it was shown that global inhibition of cAMP formation by inhibition of AC did not affect the potentiation of CCh-evoked Ca^{2+} signals by acute stimulation with PTH(1-34) (Tovey *et al.*, 2008).

My results suggest that the effect of sustained stimulation with PTH(1-34) on Ca^{2+} signals are also insensitive to substantial inhibition of AC. This is consistent with the sustained responses to PTH(1-34) also being mediated by hyperactive AC-IP_3R signalling junctions, wherein cAMP is locally delivered at super-saturating concentration to IP_3Rs. This interpretation is discussed further in Section 4.4.

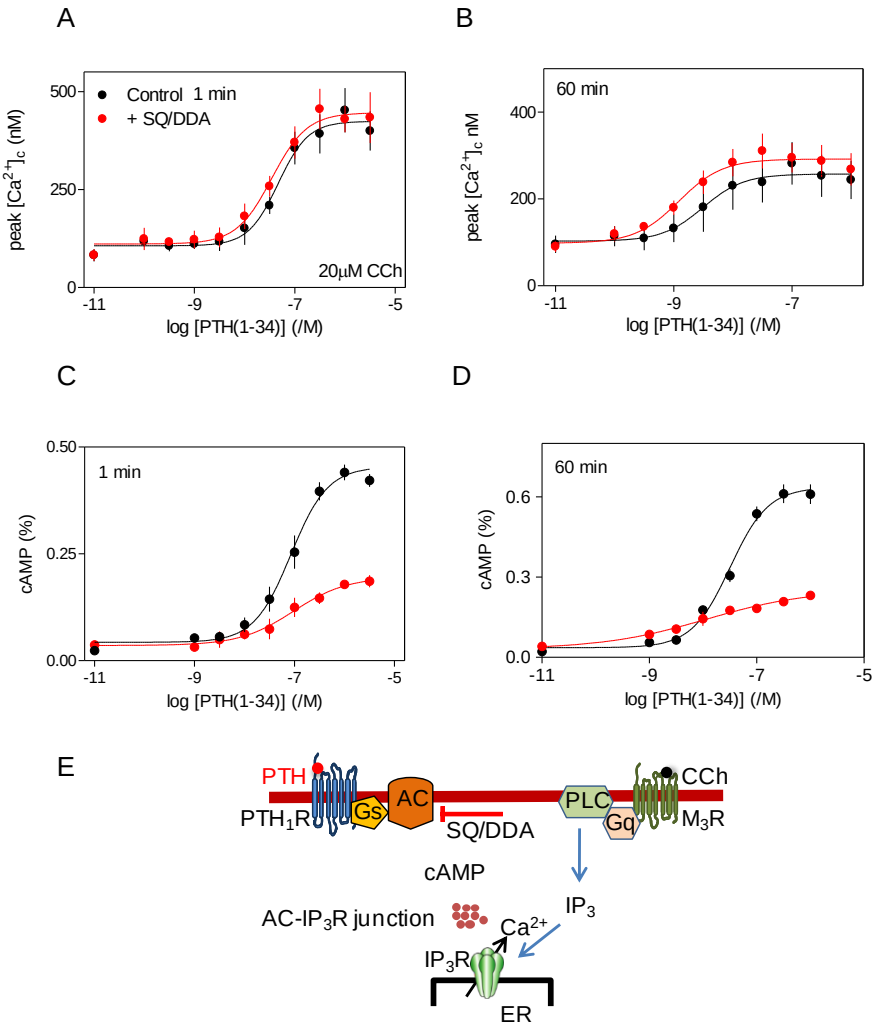

Figure 4.7. **Effects of inhibition of AC on the cAMP produced and potentiation of CCh-evoked Ca^{2+} signals by PTH(1-34)** (**A**, **B**) Populations of HEK-PR1 cells were incubated with SQ 22536 (1 mM) and DDA (200 µM) (SQ/DDA, 20 min) before stimulation with PTH(1-34) for 1 or 60 min. The effects of CCh (20µM) on Ca^{2+} signals in the presence of BAPTA (2.5 mM) were then assessed. Results show the concentration-dependent effects of PTH(1-34) after stimulation with it for 1 min (**A**) or 60 min (**B**) and the effects of SQ/DDA treatment. The peak increase in $[Ca^{2+}]_c$ evoked by CCh are shown. (**C**, **D**) Concentration-dependent effects of a 1-min (**C**) or 60-min (**D**) stimulation with PTH(1-34) with or without SQ/DDA on intracellular cAMP measured under identical conditions to those used to measure peak $[Ca^{2+}]_c$. Results show ^{3}H-cAMP as a percentage of ^{3}H-ATP, ^{3}H-ADP and ^{3}H-cAMP. Results are means ± SEM from 3 independent experiments. The codes in panel A applies to all panels. (**E**) Potentiation of PTH(1-34) on the Ca^{2+} signals evoked by CCh are not affected by inhibition of AC with SQ/DDA.

	1 min		60 min	
	pEC_{50}	Maximal $\Delta[Ca^{2+}]_c$ (nM)	pEC_{50}	Maximal $\Delta[Ca^{2+}]_c$ (nM)
Control	7.4 ± 0.2	364 ± 29	8.5 ± 0.20*	153 ± 14*
SQ/DDA	7.5 ± 0.1	341 ± 43	8.9 ± 0.10*	193 ± 32*

Table 4.3. **Inhibition of AC does not affect the potentiation of CCh-evoked Ca^{2+} signals by PTH(1-34)**. Effects of stimulation with PTH(1-34) for 1 or 60 min with SQ22536 (1 mM) and DDA (200 µM) (SQ/DDA, 20 min) pretreatment on the maximal Ca^{2+} signals evoked by CCh (20 µM) and on sensitivity to PTH(1-34). Results are means ± SEM from 3 independent experiments. $^{*}P < 0.05$ relative to paired comparisons at 1 min. Students paired t-test was used for analysis.

	1 min		60 min	
	pEC_{50}	Maximal ΔcAMP (%)	pEC_{50}	Maximal ΔcAMP (%)
Control	7.1 ± 0.1	0.4 ± 0.01	7.5 ± 0.01	0.6 ± 0.01
SQ/DDA	7.2 ± 0.5	0.16 ± 0.01*	7.9 ± 0.4	0.18 ± 0.03*

Table 4.4. **Inhibition of AC reduces PTH(1-34)-evoked cAMP formation.** Effects of stimulation with PTH(1-34) for 1 or 60 min with SQ22536 (1 mM) and DDA (200 µM) (SQ/DDA, 20 min) pretreatment on the maximal amount of intracellular cAMP accumulation, and the sensitivity to PTH(1-34). Results are means ± SEM from 3 independent experiments. $^{*}P < 0.05$ relative to paired comparisons with the controls. Students paired t-test was used for analysis.

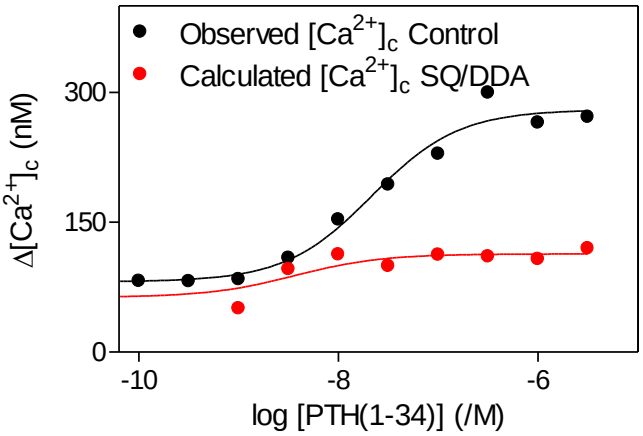

Figure 4.8**. Effect of inhibiting AC on Ca^{2+} signals modulated by globally delivered cAMP should be readily detectable** Results in figure 4.9E show the relationship between ΔcAMP and the potentiation of CCh-evoked Ca^{2+} signals for each concentration of PTH(1-34). Assuming (for Ca^{2+} signals regulated by globally distributed cAMP) that this relationship between cAMP and $[Ca^{2+}]_c$ is unaffected by inhibition of AC, allows the effects of SQ/DDA on potentiation of CCh-evoked Ca^{2+} signals by PTH(1-34) to be predicted. From figure 4.7C, I can compute the effects of SQ/DDA on the cAMP produced in response to each concentration of PTH(1-34); and from figure 4.7A I can compute the effect of each increase in cAMP on the potentiated Ca^{2+} signal. The results demonstrate that if the effects of PTH(1-34) were mediated by a global cAMP signal, SQ/DDA would cause an easily resolved inhibition of the potentiated Ca^{2+} signals.

Inhibition of PDE with IBMX significantly increased the levels of cAMP detected after acute or sustained stimulation with PTH(1-34), whereas the potentiation of CCh-evoked Ca^{2+} responses by PTH(1-34) was unchanged. The results show that during acute or sustained stimulation with PTH(1-34), IBMX increased the levels of cAMP by ~2-fold and ~15-fold respectively, relative to matched controls (Fig. 4.9C. D, Table 4.7). The peak increase in $[Ca^{2+}]_c$ signals evoked by CCh after acute or sustained stimulation with PTH(1-34) and IBMX were similar to the matched controls (Fig. 4.9A, B). The maximal $\Delta[Ca^{2+}]_c$ was significantly higher after acute compared to sustained stimulation with PTH(1-34) and IBMX (Table 4.6). However, the sensitivity to PTH(1-34) after sustained stimulation with PTH(1-34) and IBMX was ~10-fold higher

compared to the matched controls without IBMX, and ~20-fold higher relative to acute stimulation (Table 4.6). There was no such effect of IBMX on the sensitivity of the acute response to PTH(1-34) (Fig. 4.9A).

For each stimulation condition, the amount of cAMP produced can be related to the associated potentiation of the CCh-evoked Ca^{2+} signal. The results (Fig. 4.9E, F) show that there is huge disparity between the amount of cAMP and the corresponding Ca^{2+} signals for responses evoked by PTH(1-34) with and without IBMX. These results demonstrate that there is no consistent relationship between global levels of intracellular cAMP and the potentiation of CCh-evoked Ca^{2+} signals.

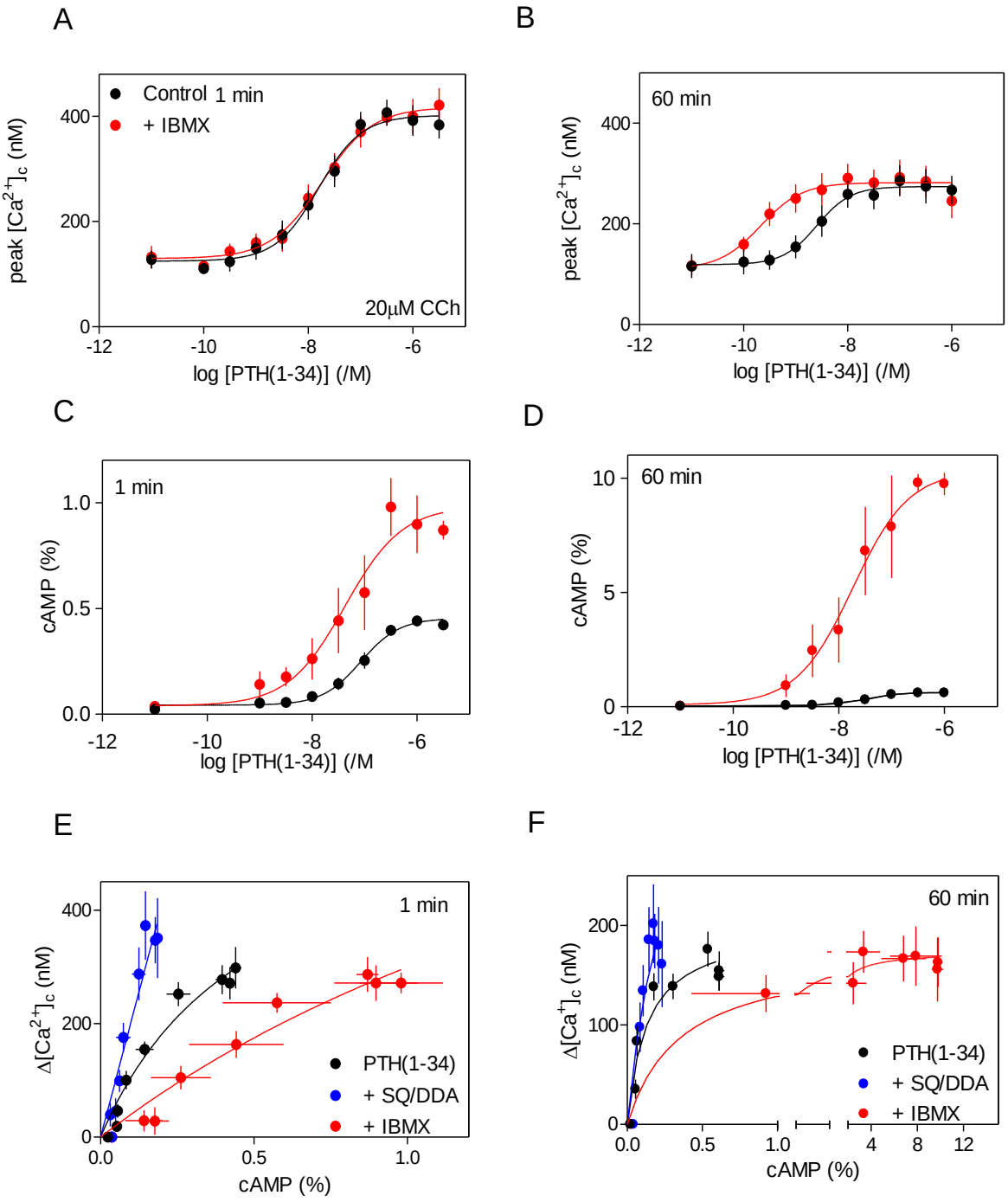

Figure 4.9. **Effects of inhibition of PDEs on the potentiation of CCh-evoked Ca^{2+} signals by acute and sustained stimulation with PTH(1-34).** The figure legend is on the following page

Figure 4.9 Legend, **(A, B)** Populations of HEK-PR1 cells were incubated with IBMX (1 mM, 5 min) before stimulation with PTH(1-34) for 1 or 60 min. The effect of CCh (20 μM) on Ca^{2+} signals in Ca^{2+}-free HBS were then assessed. Results show the concentration-dependent effects of PTH(1-34) after incubation for 1 min (**A**) or 60 min (**B**) with and without IBMX (1 mM, 5 min) on the peak increase in $[Ca^{2+}]_c$ evoked by CCh in the presence of BAPTA (2.5 mM). (**C**, **D**) Concentration-dependent effect of 1-min (**C**) or 60-min (**D**) stimulation with PTH(1-34) and IBMX on intracellular cAMP measured under identical condition to those used to measure $[Ca^{2+}]_c$. Results show ^{3}H-cAMP as a percentage of ^{3}H-ATP, ^{3}H-ADP and ^{3}H-cAMP. Results (A-D) are means ± SEM from 3 independent experiments. The codes in panel A apply to panels B-D. (**E**, **F**) Comparison of the CCh-evoked increases in $[Ca^{2+}]_c$ and intracellular cAMP during 1 min (data from Fig. 4.7A,C, Fig. 4.9A,C) (**E**) or 60 min (data from Fig. 4.7B, D, Fig. 4.9B, D) (**F**) stimulation with PTH(1-34) allowed to establish the a non linear regression relationship between the two to be defined for the different stimulation conditions (from Fig. 4.7), thus each line corresponds the same.

	1 min		60 min	
	pEC_{50}	Maximal $\Delta[Ca^{2+}]_c$ (nM)	pEC_{50}	Maximal $\Delta[Ca^{2+}]_c$ (nM)
Control	7.4 ± 0.2	364 ± 29	8.5 ± 0.2*	153 ± 14*
IBMX	7.7 ± 0.1	300 ± 26	9.6 ± 0.1*	177 ± 18*

Table 4.5. **Inhibition of PDEs does not affect PTH(1-34)-potentiated Ca^{2+} signals.** Effect of stimulation with PTH(1-34) for 1 or 60 min, with IBMX (1 mM, 5 min) pretreatment, on the maximal Ca^{2+} signals evoked by CCh (20 μM) and on the sensitivity to PTH(1-34). Results are means ± SEM from 3 independent experiments. $^*P < 0.05$ relative to paired comparisons at 1 min. Students paired t-test was used for analysis.

	1 min		60 min	
	pEC_{50}	Maximal ΔcAMP (%)	pEC_{50}	Maximal ΔcAMP (%)
Control	7.1 ± 0.1	0.4 ± 0.01	7.5 ± .01*	0.6 ± 0.01*
IBMX	7.4 ± 0.3	0.8 ± 0.1	7.7 ± 0.1	9 ± 0.02*

Table 4.6. **Inhibition of PDEs increases the accumulation of cAMP evoked by PTH(1-34).** Effect of stimulation with PTH(1-34) for 1 or 60 min with IBMX (1 mM, 5 min) pretreatment, on the accumulation of intracellular cAMP, and the sensitivity to PTH. Results are means ± SEM from 3 independent experiments. $^{*}P < 0.05$ relative to paired comparisons at 1 min. Students paired t-test was used for the analysis.

Acute potentiation of CCh-evoked Ca^{2+} signals by PTH(1-34) was unaffected by simultaneous inhibition of both AC (with SQ/DDA) and PDE (with IBMX) (Fig. 4.10A). However, during sustained stimulation the increase in the sensitivity to PTH(1-34) evoked by IBMX (Fig. 4.9B) was partially reversed by inhibition of AC (Fig. 4.10B). cAMP levels were also measured under similar conditions. Sustained stimulation with PTH(1-34) in the presence of SQ/DDA and IBMX showed only an ~3-fold increase in the level of cAMP compared to the level observed after stimulation with PTH(1-34) alone. Stimulation with PTH(1-34) and IBMX showed an ~10-fold increase in the level of intracellular cAMP (Fig. 4.10C, Table 4.9). Significant decreases in cAMP accumulation after inhibition of AC and PDEs in combination probably underlie the decrease in the sensitivity to PTH(1-34) (4.10B). However, these results suggested that the most likely potentiation of CCh-evoked Ca^{2+} signals by sustained stimulation with PTH(1-34) and IBMX is mediated by cAMP junctions. This interpretation is discussed further in Section 4.4.

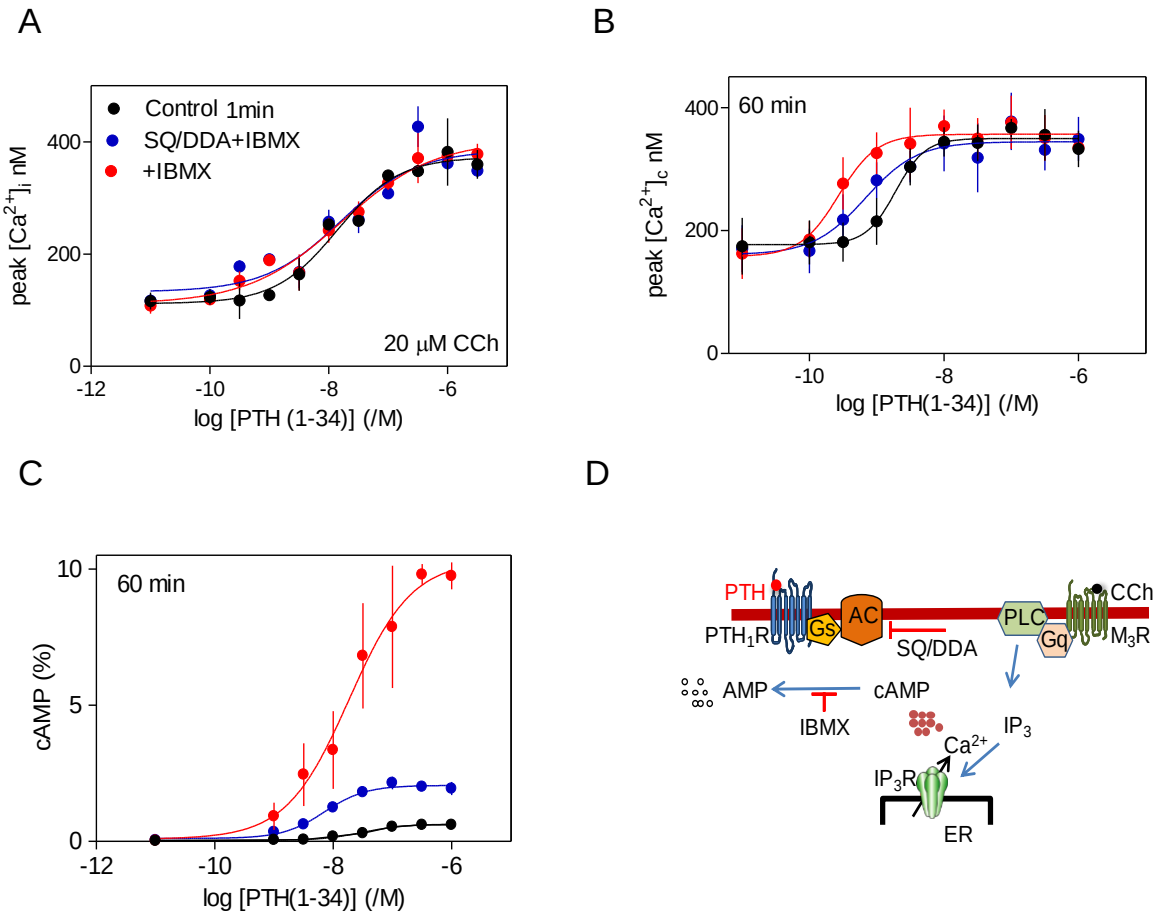

Figure 4.10. **Effect of inhibiting AC and PDE in combination on PTH(1-34)-potentiation of Ca^{2+} signals and cAMP formation.** (**A**, **B**) Populations of HEK-PR1cells were incubated with SQ 22536 (1 mM) and DDA (200 µM) (SQ/DDA, 20 min) and IBMX (1 mM, 5 min) before stimulation with PTH(1-34) for 1 or 60 min. The effects of CCh on Ca^{2+} signal were measured in the presence of BAPTA (2.5 mM). Results (**A**) and (**B**) show the concentration-dependent effects of stimulation with PTH(1-34) for 1-min or 60-min respectively in the presence of IBMX and SQ/DDA (**C**) Concentration-dependent effects of 60-min stimulation with PTH(1-34) in the presence of IBMX and SQ/DDA, on intracellular cAMP measured under identical conditions to those used to measure $[Ca^{2+}]_c$. Results show ^{3}H-cAMP as a percentage of ^{3}H-ATP, ^{3}H-ADP and ^{3}H-cAMP. The codes in panel A apply to all panels. Results are means ± SEM from 3 independent experiments.

The ability of IBMX to increase the sensitivity to PTH(1-34) during sustained stimulation with PTH(1-34) was unaffected by H89 (Fig. 4.11, Table 4.8). These results further suggest that PKA activity is probably not involved in the Ca^{2+} responses evoked by sustained stimulation with PTH(1-34).

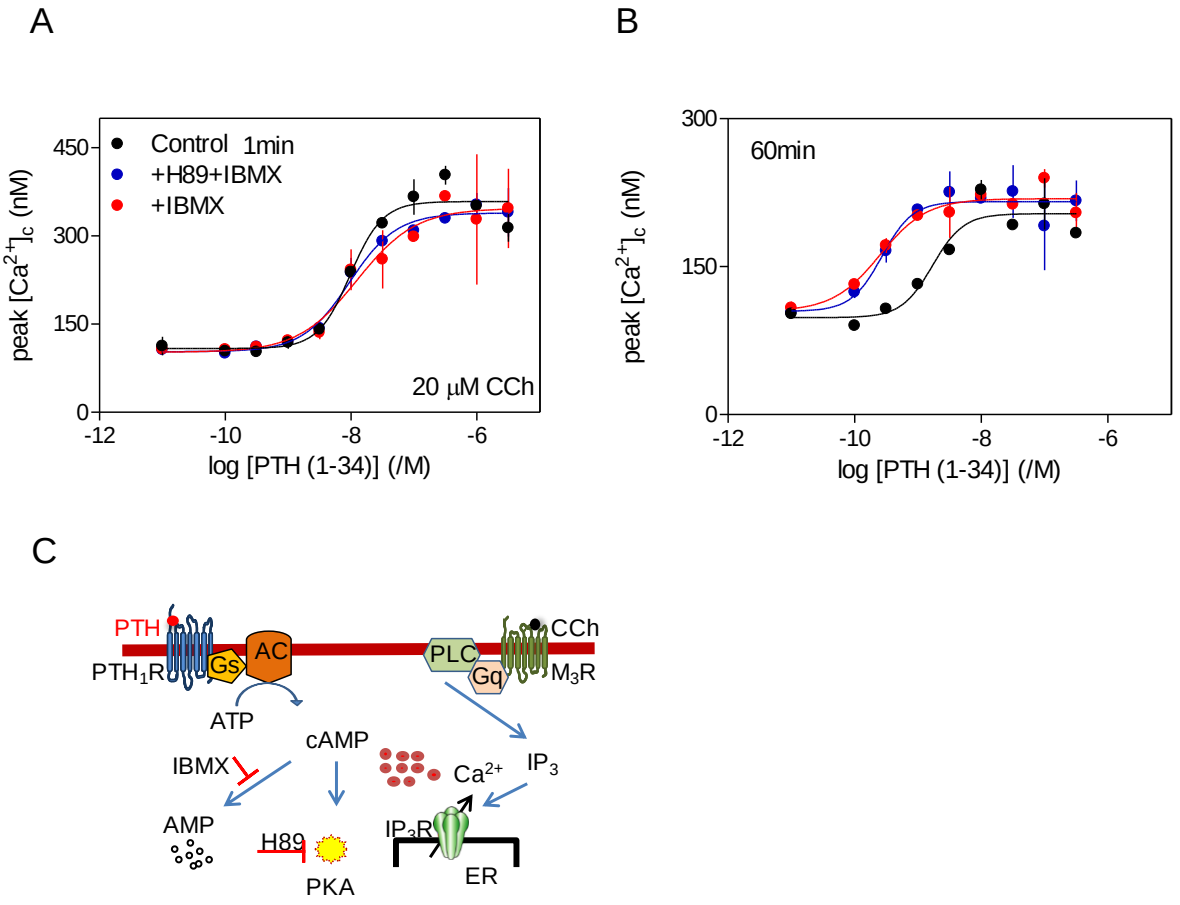

Figure 4.11. **Effect of inhibiting PKA and PDE in combination on PTH(1-34) potentiation of Ca^{2+} signals and cAMP production.** (**A**, **B**) Populations of HEK-PR1cells were incubated with H89 (10 µM, 20 min) and IBMX (1 mM, 5 min) before stimulation with PTH(1-34) for 1 or 60 min. The effects of CCh on Ca^{2+} signals in Ca^{2+}-free conditions were then assessed. Results show the concentration-dependent effects of 1-min (**A**) or 60-min (**B**) stimulation with PTH(1-34) alone or with IBMX and H89 on the peak $[Ca^{2+}]_c$ evoked by CCh (20 µM) in the presence of BAPTA (2.5 mM). Codes in panel A apply to panel B. Results are means ± SEM from 3 independent experiments.

	1 min		60 min	
	pEC_{50}	Maximal $\Delta[Ca^{2+}]_c$ (nM)	pEC_{50}	Maximal $\Delta[Ca^{2+}]_c$ (nM)
Control	7.9 ± 0.05	259 ± 28	8.8 ± 0.03	146 ± 20
IBMX	7.7 ± 0.10	300 ± 26	9.6 ± 0.10*	177 ± 18
IBMX +SQ/DDA	7.8 ± 0.10	259 ± 08	9.2 ± 0.05*	178 ± 14
IBMX + H89	7.9 ± 0.2	246 ± 37	9.6 ± 0.10*	112 ± 03

Table 4.7. **Inhibition of PDE, AC and PKA in combination does not affect PTH(1-34) potentiation of Ca^{2+} signals.** Effects of stimulation with PTH(1-34) for 1 or 60 min with IBMX (1 mM, 5 min), H89 (10 µM, 20 min) or SQ22536 (1 mM) and DDA (200 µM) (SQ/DDA, 20 min) pretreatment, alone or in combination, on the maximal Ca^{2+} signals evoked by CCh (20µM) and the sensitivity to PTH(1-34). Results are means ± SEM from 3 independent experiments. $^{*}P < 0.05$ relative to paired comparisons with time-matched control. Students paired t-test was used for the analysis.

	1 min		60 min	
	pEC_{50}	Maximal ΔcAMP (%)	pEC_{50}	Maximal ΔcAMP (%)
Control	7.1 ± 0.1	0.4 ± 0.01	7.5 ± 0.01	0.6 ± 0.01
IBMX	7.4 ± 0.3	0.8 ± 0.1	7.7 ± 0.1	9 ± 0.02 *
IBMX + SQ/DDA	ND	ND	8.1 ± 0.05*	1.9 ± 0.2*

Table 4.8. **Inhibition of PDE and AC in combination affects PTH(1-34)-evoked cAMP accumulation.** Effects of stimulation with PTH(1-34) for 1 or 60 min with IBMX (1 mM, 5 min) or SQ22536 (1 mM) and DDA (200 µM) (SQ/DDA, 20 min) pretreatment, alone or in combination, on the maximal cAMP accumulation and sensitivity to PTH(1-34). Results are means ± SEM from 3 independent experiments. $^{*}P < 0.05$ relative to paired comparisons to matched controls. Students paired t-test was used for the analysis. ND, not determined.

4.3.5. Potentiation of CCh-evoked Ca^{2+} signals by NKH477 is mediated by cAMP junctions

Acute or sustained stimulation with NKH477 potentiated Ca^{2+} responses evoked by CCh in a similar fashion to the acute or sustained stimulation with PTH(1-34) (Fig. 3.9, Table 3.7). Inhibition of AC reduced the cAMP accumulation detected after acute or sustained stimulation with NKH477 (Fig. 4.12C, D). But the peak increase in $[Ca^{2+}]_c$ evoked by CCh after acute or sustained stimulation with NKH477 was unaffected by AC inhibition using SQ/DDA relative to matched controls (Fig. 4.12A, B). Furthermore, the maximal $\Delta[Ca^{2+}]_c$ signals recorded after acute stimulation with NKH477 and SQ/DDA (Fig. 4.12A, Table 4.10) were significantly higher than those recorded after sustained stimulation (Fig. 4.12B, Table 4.10).

Inhibition of PDE with IBMX before acute or sustained stimulation with NKH477 significantly increased the levels of cAMP accumulation compared to matched controls without IBMX (Fig. 4.13C, D). However, the maximal potentiation of $\Delta[Ca^{2+}]_c$ for CCh-evoked Ca^{2+} signals remained similar after acute or sustained stimulation with NKH477 and IBMX relative to matched controls (Fig. 4.13A, B). IBMX caused the sensitivity to NKH477 to increase ~3-fold during sustained stimulation (Fig. 4.13B,

Table 4.9). These results, in addition to the results in figures 4.12 and 4.13 and Table 4.9, suggest that NKH477 potentiated Ca^{2+} responses are also most likely mediated by cAMP junctions (Tovey *et al.*, 2008). This interpretation is discussed further in Section 4.4.

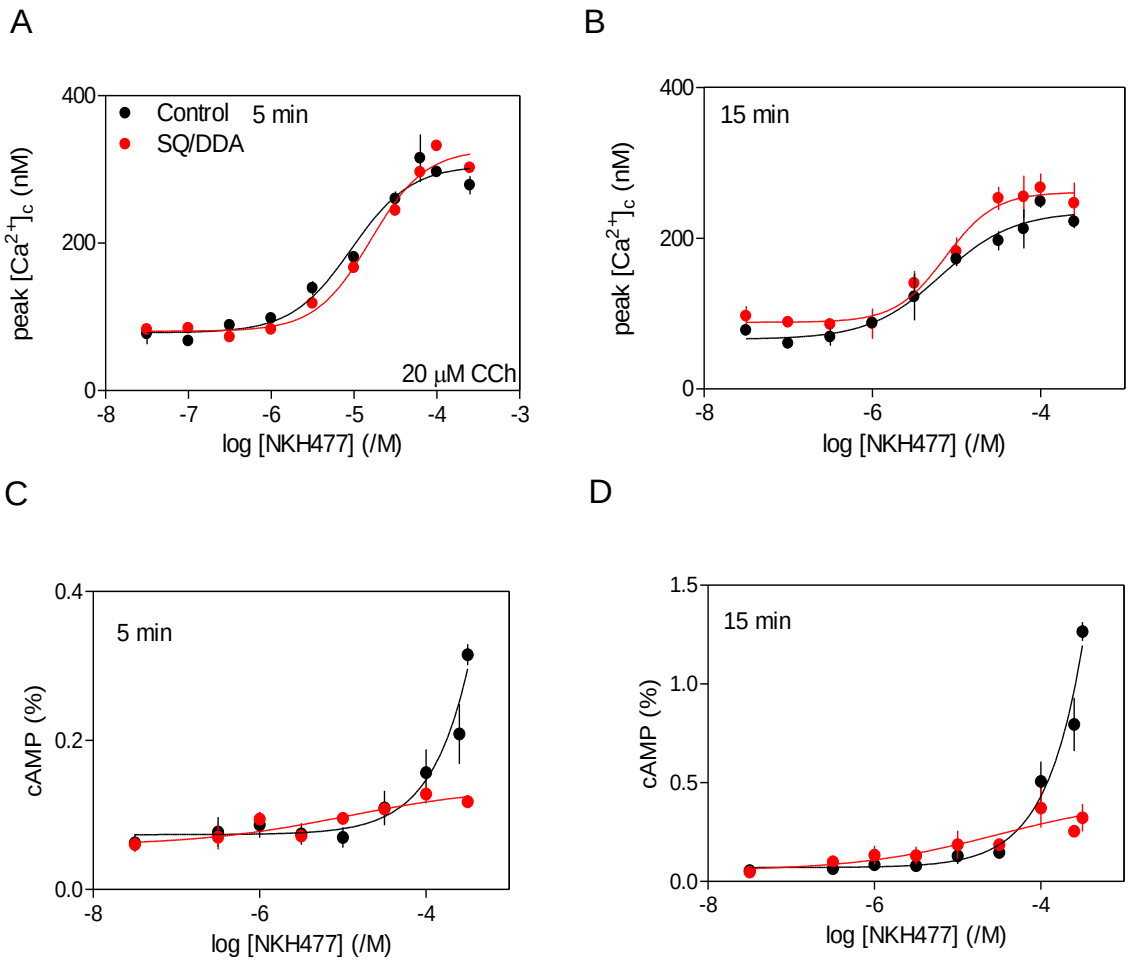

Figure 4.12. **Effects of inhibition of AC on the responses to NKH477.** (**A**, **B**) Populations of HEK-PR1 cells were incubated with SQ 22536 (1 mM) and DDA (200 μM) (SQ/DDA, 20 min) before stimulation with NKH477 for 5 or 15 min. The effects of CCh on the Ca^{2+} signals were assessed in the presence of BAPTA (2.5 mM). Results show the concentration-dependent effects of 5-min (**A**) or 15-min (**B**) stimulation with NKH477 on the peak $[Ca^{2+}]_c$ evoked by CCh (20 μM). (**C**, **D**) The concentration-dependent effects of a 5-min (**C**) or 15-min (**D**) stimulation with NKH477 and SQ/DDA on the intracellular cAMP measured under identical conditions to those used to measure $[Ca^{2+}]_c$. Results show ^{3}H-cAMP as a percentage of ^{3}H-ATP, ^{3}H-ADP and ^{3}H-cAMP. The codes in panel A apply to all the panels. Results are means ± SEM from 3 independent experiments.

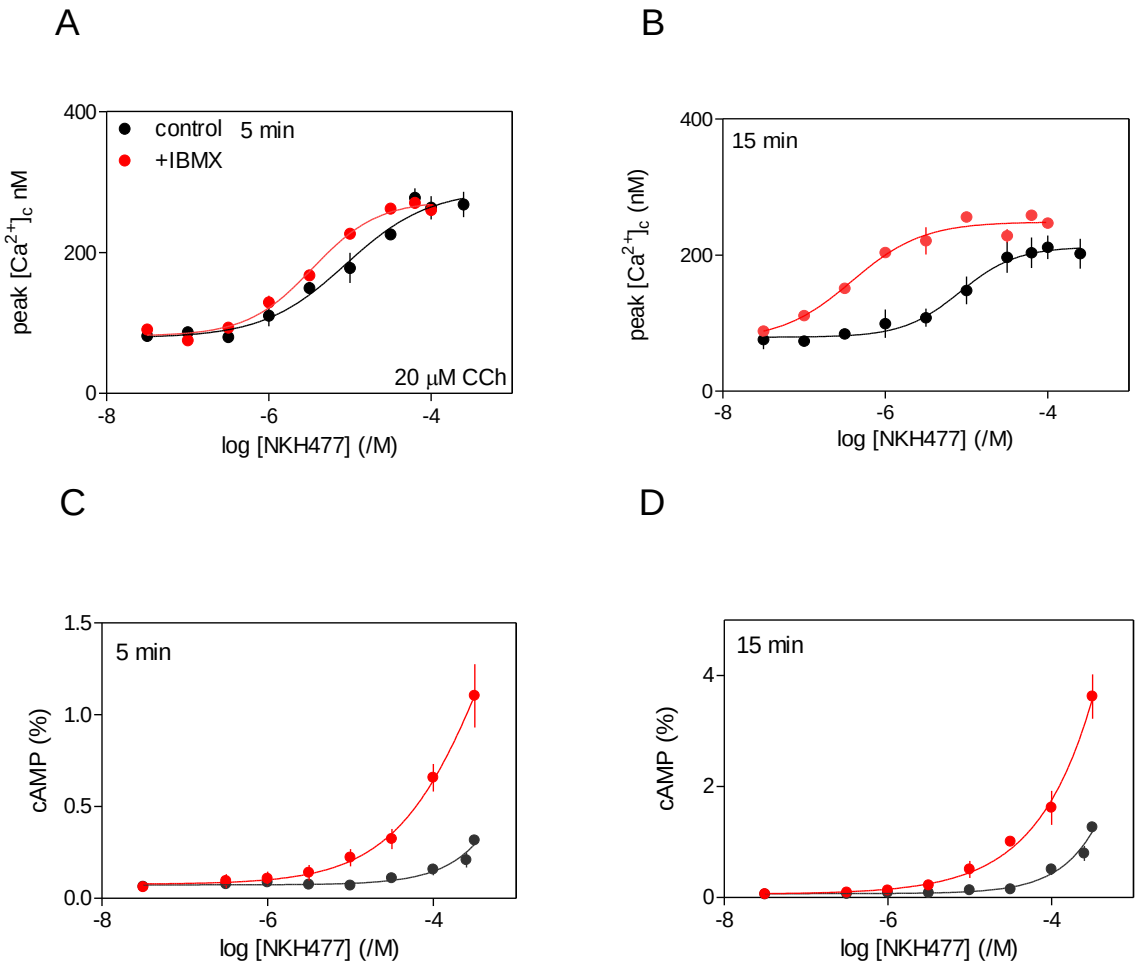

Figure 4.13. **Effects of inhibition of PDEs on potentiation of CCh-evoked Ca^{2+} signals by NKH477.** (**A**, **B**) Populations of HEK-PR1 cells were incubated with IBMX (1 mM, 5 min) before stimulation with NKH477 for 5 or 15 min. The effects of CCh on the Ca^{2+} signals evoked in Ca^{2+}-free HBS were then assessed. Results show the concentration-dependent effects of a 5-min (**A**) or 15-min (**B**) stimulation with NKH477 on the peak $[Ca^{2+}]_c$ evoked by CCh in the presence of BAPTA (2.5 mM). (**C**, **D**) Concentration-dependent effects of a 5-min (**C**) or 15-min (**D**) stimulation with NKH477 and IBMX on the intracellular cAMP measured under identical conditions to those used to measure $[Ca^{2+}]_c$. Results show ^{3}H-cAMP as a percentage of ^{3}H-ATP, ^{3}H-ADP and ^{3}H-cAMP. Codes in panel A apply to all panels. Results are means ± SEM from 3 independent experiments.

	5 min		15 min	
	pEC_{50}	Maximal $\Delta[Ca^{2+}]_c$ (nM)	pEC_{50}	Maximal $\Delta[Ca^{2+}]_c$ (nM)
Control	5.0 ± 0.10	225 ± 09	5.0 ± 0.10	155 ± 0.1
SQ/DDA	5.1 ± 0.20	234 ± 12	5.1 ± 0.01	172 ± 16
IBMX	5.5 ± 0.02	192 ± 3.0	6.0 ± 0.01*	156 ± 10

Table 4.9. **Effect of inhibiting PDE and AC on the potentiation of CCh-evoked Ca^{2+} signals by NKH477.** Effect of stimulation with NKH477, for 5 or 15 min, with IBMX (1 mM, 5 min) or SQ22536 (1 mM) and DDA (200 µM) (SQ/DDA, 20 min) pretreatment on the maximal Ca^{2+} signals evoked by CCh (20 µM) and on the sensitivity to NKH477. Results are means ± SEM from 3 independent experiments. $^{*}P < 0.05$ relative to paired comparisons to time matched control. Students paired t-test was used for the analysis.

4.4. Discussion

Previous work demonstrated that acute stimulation of PTH_1R by PTH(1-34) stimulates AC and that the cAMP formed then potentiates the Ca^{2+} signals evoked by CCh (Tovey *et al.*, 2008). My results are consistent with this scheme (Fig. 3.4). Several lines of evidence suggest that the response to PTH(1-34) is entirely mediated by cAMP, but that it is unlikely to be due to cAMP uniformly distributed in the cytosol. The most important evidence can be summarised as follows:

1. For different stimuli that cause activation of AC, there was no consistent relationship between the increase in cAMP accumulation and the potentiation of CCh-evoked Ca^{2+} signals (Meena *et al.*, 2015; Tovey *et al.*, 2008).
2. Manipulations of cAMP accumulation by inhibition of PDE, AC or expression of AC subtypes, did not consistently affect the response to CCh (Meena *et al.*, 2015; Tovey *et al.*, 2008). The most important evidence came from SQ/DDA, which caused substantial (>70%) inhibition of PTH(1-34)-evoked accumulation

of cAMP without affecting the ability of any PTH(1-34) concentration to potentiate responses to CCh (Fig. 4.7, Table 4.3, 4.4).

3. AC6 and IP_3R2 were shown to be specifically associated in HEK cells and siRNA-mediated knockdown of either had some selective effect on the ability of PTH(1-34) to potentiate CCh-evoked Ca^{2+} signals (Tovey *et al.*, 2008).

These results, many of which have been confirmed by my experiments (Fig. 3.4, 3.6, 4.7, Table 3.4, 3.5,4.3, 4.4), provide evidence that the cAMP that regulates IP_3Rs is not uniformly distributed in the cytosol. Similarly spatially organised cAMP signals have been reported in many other systems (Rich *et al.*, 2001). The SQ/DDA results, suggest an additional layer of complexity because these inhibit AC (by ~70%) and yet they have no effect on the ability of even a submaximal concentrations of PTH(1-34) to potentiate CCh-evoked Ca^{2+} signals. This observation lead to the proposal that cAMP might be delivered to IP_3R in signalling junctions, within which, cAMP locally saturates associated IP_3R. The concentration dependent effects of PTH(1-34) would then come from graded recruitment of these junctions (Fig.4.7, 4.8, 4.9). It is possible that a minor subtype of AC that is unaffected by SQ/DDA contributes disproportionately to the regulation of IP_3R while not significantly contributing to the overall level of cAMP (Seifert *et al.*, 2012). The 70% inhibition of AC by SQ/DDA might then report the behaviour of irrelevant subtypes of AC. A similar problem might arise if SQ/DDA does not again access to the AC that regulates IP_3Rs.

However, previously when the expression of Gαs was decreased using siRNA, the CCh-evoked Ca^{2+} responses were typical in HEK-PR1 cells, FK potentiated them and also the response to FK was not affected by inhibition of AC, while the sensitivity to PTH was decreased by inhibition of AC using SQ/DDA in similar cells. These results demonstrate that when the safety margin for signalling between IP_3R and PTH_1R was entirely eroded by reducing expression of Gαs, the requirement for AC activity was revealed. This further validates that cAMP mediates the effects of PTH on IP_3R (Tovey *et al.*, 2008). Despite all these results, if the existence of hyperactive junctions is not persuasive, the existence of some preferred pool of cAMP that regulates IP_3R cannot be avoided. Further, this evidence shows that potentiation of CCh-evoked Ca^{2+} signals by PTH(1-34) requires local communication between AC and IP_3R motivated my analysis of sustained responses to PTH(1-34) during which functional PTH_1R-AC-complex are supposed to be internalized. The proposed or hypothesised primary site for the formation of AC-IP_3R junctions was near PM (Tovey *et al.*, 2008)

and it was interesting to find what exactly happens when the primary site for cAMP synthesis (which is supposed to be near the PM) would change with the internalisation of PTH_1R-AC complex during sustained PTH(1-34) stimulation.

Sustained stimulation with PTH(1-34) potentiates Ca^{2+} signals evoked by CCh almost 50% less, than acute stimulation (Fig. 3.4, Table. 3.5). I anticipated three potential mechanisms which may contribute to the decrease in maximal Ca^{2+} release after sustained stimulations with PTH(1-34).

1. At higher concentrations (>300 nM) PTH(1-34) stimulates PLC (Table. 3.1). This leads to IP_3 formation which could cause a leak of Ca^{2+} from intracellular stores via IP_3R, during sustained stimulation with PTH(1-34) (Fig. 4.1A, Table. 4.1) (Bisello *et al.*, 2002; Castro *et al.*, 2002; Cupp *et al.*, 2013; van der Lee *et al.*, 2013). However, the PTH analogues which do not stimulate the PLC pathway, like PTH(2-38) and Tyr^1PTH(1-34) (Fig. 3.6, Table 3.11) (Cupp *et al.*, 2013), also showed lesser Ca^{2+} release after sustained stimulation. In addition I also checked store content using ionomycin and this remained unaltered (Huang *et al.*, 1998; Tovey *et al.*, 2003; Tovey *et al.*, 2013).
2. Binding of PTH(1-34) to PTH_1R could cause internalization of the PTH_1R (Section. 3.1.6). Different PTH analogues: PTH(1-34), PTH(2-38), PTHrP(1-36), Tyr^1PTH(1-34) (Table 3.1) were used to confirm this probability. The results in figure 4.2A, C, figure 4.3A, C, and Table. 4.2 suggest that internalization of PTH_1R is not associated with the decrease in maximal Ca^{2+} response after sustained stimulation with PTH(1-34). However, this experiment needs to be confirmed probably by over expressing GFP-tagged-PTH_1R in HEK-wt cells and subsequently tracking PTH_1R before and after PTH treatment under the confocal microscope. Besides, the association of PTH_1R internalization with the increased levels of cAMP produced cannot be averted (Fig. 4.2B, D, 4.3B, D, Table. 4.3). Probably the increase in cAMP levels is due to a) continuous activation of AC, and/or b) a decrease in cAMP degradation via PDEs. Perhaps internalized PTH_1R-coupled-AC complex (Ferrandon *et al.*, 2009) changes the location of cAMP formation, which is not accessible to PDEs. However, PKA has been reported to stimulate PDEs and thereby regulate intracellular cAMP concentrations (Brown *et al.*, 2012), but seems like not much effective in this setting.
3. Higher levels of cAMP accumulation during sustained stimulation with PTH(1-34) (Fig. 4.2B, 4.7D, 4.9D Tables. 4.3, 4.5, 4.7) could also affect CCh-evoked IP_3

formation or increase degradation of IP_3 and thereby decrease maximal Ca^{2+} release. From results in figure 4.6 it is suggested that the decrease in CCh-evoked IP_3 formation after sustained stimulation with PTH(1-34) is the potential cause for decrease maximal $[Ca^{2+}]_c$, rather than leak of Ca^{2+} from intracellular stores or internalization of PTH_1R.

Sustained stimulation with PTH(1-34) potentiated CCh-evoked Ca^{2+} signals and the sensitivity to PTH(1-34) was increased by~10 fold in comparison to acute stimulation (Fig. 3.4, Table. 3.5). Possibly it could be due to an increase in the sensitivity of cAMP accumulation to PTH(1-34) (Fig. 4.2, Table. 4.3). As the sensitivity to PTH(1-34) further increases when the cAMP levels were assessed after inhibition of PDEs and significantly reversed back when PDEs and ACs were inhibited together (Fig. 4.9, 4.10, Table 4.5, 4.6, 4.7), these results further confirm that higher cAMP levels are responsible for the increase in sensitivity to PTH(1-34). Also, PKA cannot be associated with it as sustained stimulation with PTH(1-34) potentiated CCh-evoked Ca^{2+} signals were normal after inhibition of PDEs and PKA together, the sensitivity to PTH remain unchanged (Fig. 4.11, Table 4.7).

Acute and sustained Ca^{2+} responses to PTH analogues (Table 3.1) were similar to those evoked by PTH(1-34) (Fig. 4.4, 4.3, Table. 4.2). Furthermore, acute and sustained responses to 8-Br-cAMP or direct activation of AC mimicked the responses evoked by PTH(1-34), and the maximal effects of sustained exposure to each stimulus were non-additive (Fig. 3.9, 3.10, Table. 3.7, 3.8). Therefore, I conclude that attenuated potentiation of CCh-evoked Ca^{2+} signals during sustained exposure to PTH(1-34) is mediated by a sustained increase in cytosolic cAMP that perhaps does not require PKA or internalization of PTH_1R signalling complexes. Previously, it was reported that PKA can inhibit the activation of PLC-β2 via Gβγ subunits by phosphorylating PLC (Liu *et al.*, 1996) and hence can affect the intracellular IP_3 concentrations. However, this possibility seems unlikely because the inhibition of PKA did not affect sustained stimulation with PTH(1-34) potentiated CCh-evoked Ca^{2+} signals.

The insensitivity of sustained responses to PTH(1-34) (Fig. 4.7, Table. 4.4) and NKH477 (Fig. 4.12, Table. 4.10) to substantial inhibition of AC suggests that similar to acute stimulation with PTH(1-34) potentiated CCh-evoked Ca^{2+} signals, most likely these responses are also mediated by cAMP junctions, wherein globally distributed cAMP is not involved in the sustained stimulation with PTH(1-34) potentiated Ca^{2+} signals, rather these signals are also regulated by local supersaturating cAMP

concentrations. However, these results would be more informative in proving AC involvement if a HEK-PR1 cell line with reduced expression of Gαs by means of siRNA could be used (Tovey *et al.*, 2008). I conclude, and despite evidence that sustained stimulation with PTH(1-34) evokes internalization of functional AC signalling complexes (Ferrandon *et al.*, 2009), that PTH_1R retains its ability to signal via hyperactive AC-IP_3R signalling junctions during sustained stimulation. Sustained stimulation with PTH(1-34) in the presence of IBMX caused the global concentration of intracellular cAMP to increase to levels sufficient to sensitize IP_3R without the usual need for junctional delivery of cAMP. This was evident from the increased sensitivity to PTH(1-34) (Fig. 4.9, Table. 4.6) and NKH477 (Fig. 4.13, Table. 4.10) after sustained stimulation in the presence of IBMX, and its partial reversal by inhibition of AC with SQ/DDA (Fig. 4.10, Table. 4.8). These results demonstrate that SQ/DDA can, under these experimental conditions, attenuate the effects of PTH(1-34) on CCh-evoked Ca^{2+} signals and reinforces my conclusion that hyperactive cAMP signalling junctions normally mediate the effects of PTH(1-34) (Fig. 3.4). On the other hand, the increase in sensitivity in the presence of IBMX for sustained durations could be because under these conditions, cAMP may be sensitising both junctional and extra junctional IP_3Rs, and perhaps the recruitment of the extra junctional IP_3R will be the first to be affected by inhibition of ACs, whereas junctional signalling remains functional (Fig. 4.14). As results in Figure 4.10 and Table 4.7 show; inhibition of PDEs and ACs together reversed the increased sensitivity to PTH(1-34) shown in the presence of IBMX. However sensitivity was still higher in comparison to its controls (Fig. 4.10, Table 4.7).

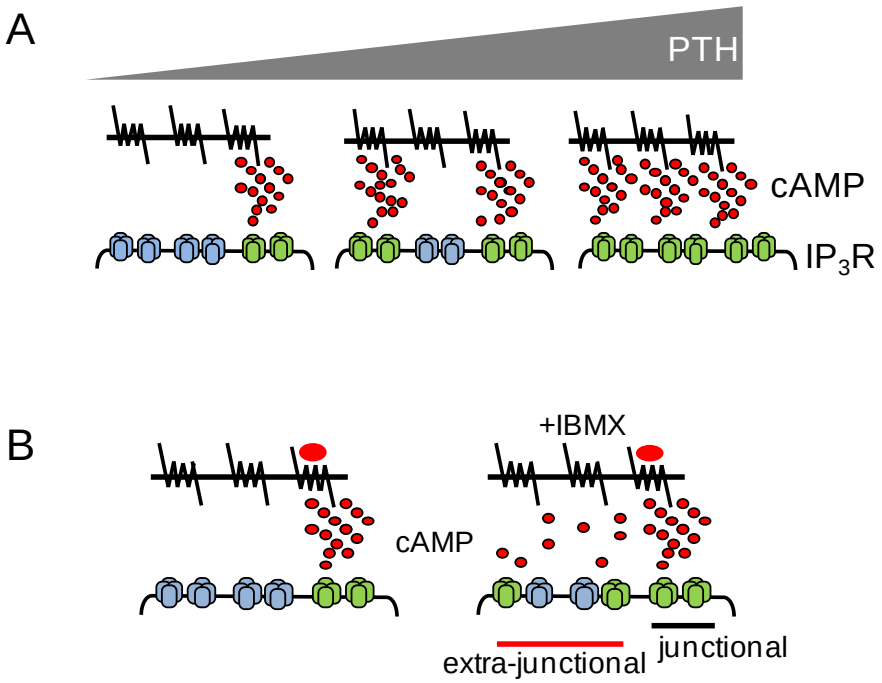

Figure. 4.14. (**A**) Communication between IP_3R and PTH_1R-AC complex is anticipated to be mediated by local delivery of supramaximal cAMP concentration from AC to IP_3Rs within junctional complexes. The implication is that the concentration-dependent effects of PTH are then mediated by recruitment of these all-or-nothing junctions, rather than from graded activity within each (Meena *et al.*, 2015; Tovey *et al.*, 2008). (**B**) Usually cAMP is delivered to IP_3R within signalling junctions (left panel), but the substantial accumulation of cAMP during sustained stimulation with PTH and IBMX (right panel) attains global intracellular cAMP concentrations enough to sensitize IP_3Rs beyond active junctions (Meena *et al.*, 2015).

Although the global increase in cAMP increased the sensitivity to PTH(1-34) (Fig. 4.9) and NKH477 (Fig. 4.12), it had no effect on the maximal response, which remained smaller than that evoked by acute stimulation. This occurred despite there being no loss of Ca^{2+} from intracellular stores during sustained activation of AC. This observation demonstrates that ineffective delivery of cAMP to IP_3R during sustained stimulation does not the cause the diminished potentiation of CCh-evoked Ca^{2+} signals. Instead, sustained increases in intracellular cAMP reduce the amounts of IP_3 produced after CCh stimulation. So far it is not addressed whether this results from decreased production or enhanced degradation of IP_3. However, the diminished responses to CCh

during sustained stimulation with PTH(1-34) are mediated by cAMP, probably independently of PKA and dependent on delivery of cAMP within hyperactive signalling junctions.

Chapter. 5. Conclusions

Ca^{2+} and cAMP are ubiquitous intracellular messengers that regulate nearly all aspects of cellular activity (Bruce *et al.*, 2003; Siso-Nadal *et al.*, 2009; Willoughby *et al.*, 2007). The versatility of cAMP and Ca^{2+} is achieved by the complex spatial and temporal organization of their concentration changes within cells. This intricacy allows signals delivered to different parts of a cell to trigger various responses (Dyachok *et al.*, 2006; Gorbunova *et al.*, 2002; Mongillo *et al.*, 2006; Zaccolo *et al.*, 2006). In addition, cross-talk between cAMP and Ca^{2+} adds further versatility, and allows cells to process information arriving from various receptors (Bruce *et al.*, 2003; Gerbino *et al.*, 2005; Lefkimmiatis *et al.*, 2009; Tovey *et al.*, 2008). These properties: cross-talk between second messengers and spatiotemporal complexity, allow cells to respond appropriately and specifically to different environmental signals using a limited range of intracellular signals.

Hitherto, the effects of cAMP were suggested to be mediated by three families of proteins: Epacs, PKA and CNGC. Each of these cAMP targets has a conserved cAMP-binding domain, where cAMP binds and activates the protein (Rehmann *et al.*, 2007). However, the work reported in chapters 3 and 4 is associated with understanding a new mode of cAMP signalling, which involves a local and direct interaction between the cAMP produced by a specific AC and IP_3R (Meena *et al.*, 2015). This regulation of IP_3R by cAMP occurs in the absence of an obvious cAMP-binding motif within the primary sequences of IP_3Rs. The latter is not unexpected because regulation of IP_3Rs requires unusually high concentrations of cAMP (Tovey *et al.*, 2008; Tovey *et al.*, 2013). The conclusions from Chapter 3 and 4 can be summarised as follows:

1. Both acute and sustained stimulation with PTH(1-34) potentiate CCh-evoked Ca^{2+} signals. However, in comparison to acute stimulation, the maximal Ca^{2+} release was about 50% lower and the sensitivity to PTH(1-34) was about 10-fold greater after sustained stimulation with PTH(1-34) (Meena *et al.*, 2015).
2. Both acute and sustained stimulation with PTH(1-34) are entirely mediated by cAMP, and probably independent of PKA and Epacs (Meena *et al.*, 2015). The independence of PKA is most convincing for the acute responses to PTH(1-34).
3. Sustained stimulation with PTH(1-34) has no effect on the basal leak of Ca^{2+} from intracellular stores, nor does internalisation of PTH_1R contribute to the diminished response. The most likely reason for the diminished potentiation of

CCh-evoked Ca^{2+} release after sustained stimulation with PTH(1-34) is that after this treatment CCh causes a reduced accumulation of IP_3. The mechanism for this diminished intracellular accumulation of IP_3 is unresolved, but it is likely to be caused by cAMP (Meena *et al.*, 2015).

4. The increase in sensitivity to PTH(1-34) after sustained stimulation was solely due to the more substantial formation of cAMP after sustained stimulation (Meena *et al.*, 2015).
5. My results are consistent with a model in which PTH(1-34) via PTH_1R stimulates AC and locally delivers cAMP at supersaturating concentrations to associated IP_3Rs, thereby increasing their sensitivity to IP_3 and so potentiating the Ca^{2+} signals evoked by CCh (Tovey *et al.*, 2008). This junctional delivery of cAMP is maintained during sustained stimulation with PTH(1-34), but prolonged activity of the junction leads to an inhibition of IP_3 production. These cAMP junctions allow fast and robust signalling from AC to its targets, and without the need for PKA. I suggest that cAMP junctions deliver cAMP directly to both IP_3R and to a target (possibly PLC or an enzyme that degrades IP_3) responsible for diminished IP_3 accumulation (Meena *et al.*, 2015).

An important question is where does cAMP bind to regulate IP_3R? It may bind either directly to IP_3R or to a protein tightly associated with IP_3R for example NHERF 1 or 2, both of which are expressed in HEK-PR1 cells (Wang *et al.*, 2010) and favour coupling via Gq or Gi/o to PLCβ (Wang *et al.*, 2007). However, there are problems involved with identifying the cAMP-binding site:

a) It has low affinity for cAMP, which limits possibilities to use native proteins for P^{32}-cAMP binding, pull-down with immobilised cAMP, or photo-affinity labelling.

b) The lack of sequence similarity between IP_3R and consensus cAMP-binding sites, and no apparent relationship with low-affinity cAMP-binding sites for example PDEs. The best way to address this issue may be by performing structure-activity relationship studies with cAMP analogues on IP_3-evoked Ca^{2+} release in permeabilized cells. These experiments would help to define recognition properties of the cAMP-binding site. In addition they may also help in ruling out a role for PKA and Epacs.

In a parallel study of human aortic smooth muscle cells, the IP_3-mediated Ca^{2+} signals evoked by activation of H_1 histamine receptors were attenuated by prostaglandin E_2 (PGE_2). PGE_2 stimulated cAMP formation and thereby inhibition of Ca^{2+} signals (Pantazaka *et al.*, 2013). This PGE_2-mediated inhibition of IP_3-evoked Ca^{2+} release was partially reversed by inhibition of PKA, although the data are not yet compelling (unpublished work from Pantazaka et al). It is noteworthy, that these effects of PGE_2 appear also to require delivery of cAMP within junctions analogous to those proposed to mediate sensitization of IP_3Rs. These results suggest that local delivery of cAMP can lead to diminished accumulation of IP_3 in other cells too. The role of PKA in this effect remains somewhat ambiguous, as it does to some extent in the experiments with PTH(1-34). The issue needs to be re-examined with better tools than H89. These might include KT5720 and myristoylated PKI (Davies *et al.*, 2000) or by using transfected PKI or the mutant regulator PKA subunit RevAB, which does not bind to cAMP (Morgan *et al.*, 2014). Future studies need therefore to determine unambiguously whether PKA contributes to the inhibition of IP_3 accumulation evoked by the sustained stimulation with PTH(1-34) and to resolve the target (formation of IP_3 or its metabolism).

It is possible that mechanisms additional to the reduced accumulation of IP_3 may also contribute to the smaller CCh-evoked Ca^{2+} signals after sustained stimulation with PTH(1-34). PKA can increase removal of Ca^{2+} from cytosol by activating Ca^{2+} pumps (Tada *et al.*, 1998) or the Na^{2+}/Ca^{2+} exchanger (Karashima *et al.*, 2007). These possibilities need also to be addressed.

Previously using immunoprecipitation assay and siRNA techniques it has been proved that specifically AC6 and IP_3R2 are involved in forming junctions (Tovey *et al.*, 2008). In addition to this, the existence of junctional communication among various intracellular molecules has also been observed in other cell types like a) excitation-contraction coupling in striated muscle, where voltage-sensing dihydropyridine receptors in the PM modulate the opening of RyR in the ER across a narrow junctional complex. Coupling of these proteins is developed from chemical coupling mediated by Ca^{2+} (cardiac muscles) to conformational coupling between two side by side protein (skeletal muscles) (Di Biase *et al.*, 2005), b) Neuromuscular junctions of focally inverted skeletal muscles, where release of acetylcholine from presynaptic terminals saturates postsynaptic receptors and leads to all-or-nothing contraction of the myofibril (Fig. 5.1). Graded contraction of the muscle then results from graded recruitment of

these all-or -nothing fibrillar responses. Similar to these junctions, AC-IP_3R junctions work in an all or nothing mode of signalling.

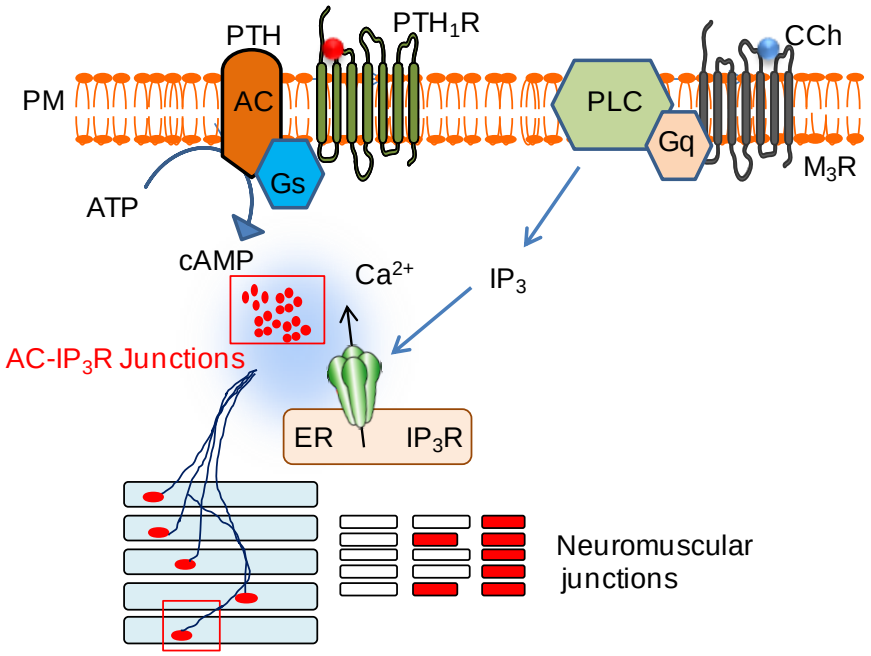

Figure 5.1. **AC-IP_3R junctions may be similar to neuromuscular junctions in delivering supersaturating concentrations of stimulus to a target.** Direct delivery of cAMP to IP_3R within 'signalling junctions' (red box) increases the sensitivity of IP_3Rs to IP_3. This potentiates the Ca^{2+} release evoked by IP_3 formed in response to the activation of M_3R. The all-or-nothing mode of activation of these AC-IP_3R signalling junctions is analogous to the behaviour of focally innervated skeletal muscle (lower panel), where release of acetylcholine at the neuromuscular junction (bottom) evokes all-or-nothing contraction of individual myofibrils. Graded contraction of the muscle fibre results from recruitment of contracting myofibrils (right panels at bottom). Image redrawn from Meena *et al.*, 2015.

Even though the proposed AC-IP_3R junctions show similarities with neuromuscular junctions, their existence and/or assembly after sustained stimulation with PTH(1-34) needs to be confirmed at the molecular level. The key questions to be addressed are a) How exactly communication is taking place between these junctions, what is the structural assembly of AC-IP_3R junctions? b) Which proteins or

intracellular organelles are actually taking part in the formation of AC-IP_3R junctions? c) Are these junctions ACs and IP_3Rs subtype specific? d) Whether these junctions are intracellular physical entities or do they assemble on demand for certain time durations? Only after resolving all these puzzles can the existence of AC-IP_3R junctions be fully elucidated. Nevertheless, experimental results from Chapter 3 and 4 fully supports the hypothesis that "sustained stimulations with PTH(1-34) potentiated CCh-evoked Ca^{2+} signals are mediated by AC-IP_3R junctions" (Meena *et al.*, 2015).

References

Abou-Samra AB, Juppner H, Force T, Freeman MW, Kong XF, Schipani E, Urena P, Richards J, Joseph V. Bonventre JV, Potts JT, Kronenberg MH , Segre GV (1992). Expression cloning of a common receptor for parathyroid hormone and parathyroid hormone-related peptide from rat osteoblast-like cells: a single receptor stimulates intracellular accumulation of both cAMP and inositol trisphosphates and increases intracellular free calcium. *Proc Natl Acad Sci U S A* 89: 2732-2736.

Adams AE, Bisello A, Chorev M, Rosenblatt M, Suva LJ (1998). Arginine 186 in the extracellular N-terminal region of the human parathyroid hormone 1 receptor is essential for contact with position 13 of the hormone. *Mol Endocrinol* 12: 1673-1683.

Adkins CE, Taylor CW (1999). Lateral inhibition of inositol 1,4,5-trisphosphate receptors by cytosolic Ca^{2+}. *Curr Biol* 9: 1115-1118.

Adrogue HJ (1992). Glucose homeostasis and the kidney. *Kidney Int* 42**:** 1266-1282.

Ahmed AM (2002). History of diabetes mellitus. *Saudi Med J* 23**:** 373-378.

Aizawa T, Komatsu M, Asanuma N, Sato Y, Sharp GW (1998). Glucose action 'beyond ionic events' in the pancreatic β cell. *Trends Pharmacol Sci* 19: 496-499.

Almahariq M, Tsalkova T, Mei FC, Chen H, Zhou J, Sastry SK, Schwede F, Cheng X. (2013). A novel EPAC-specific inhibitor suppresses pancreatic cancer cell migration and invasion. *Mol Pharm* 83: 122-128.

Asfari M, Janjic D, Meda P, Li G, Halban PA, Wollheim CB (1992). Establishment of 2-mercaptoethanol-dependent differentiated insulin-secreting cell lines. *Endocrinology* 130: 167-178.

Ashcroft FM (2007). The Walter B. Cannon Physiology in Perspective Lecture, 2007. ATP-sensitive K^+ channels and disease: from molecule to malady. *Am. J. Physiol* 293: E880-E889.

Babcock DF, Herrington J, Goodwin PC, Park YB, Hille B (1997). Mitochondrial participation in the intracellular Ca^{2+} network. *J Cell Biol* 136: 833-844.

Babich M, Choi H, Johnson RM, King KL, Alford GE, Nissenson RA (1991). Thrombin and parathyroid hormone mobilize intracellular calcium in rat osteosarcoma cells by distinct pathways. *Endocrinology* 129: 1463-1470.

Banting FG, Best CH, Collip JB, Campbell WR, Fletcher AA (1922). Pancreatic Extracts in the Treatment of Diabetes Mellitus. *Can Med Assoc J* 12**:** 141-146.

Barry EL, Gesek FA, Yu AS, Lytton J, Friedman PA (1998). Distinct calcium channel isoforms mediate parathyroid hormone and chlorothiazide-stimulated calcium entry in transporting epithelial cells. *J Membr Biol* 161: 55-64.

Baughman JM, Perocchi F, Girgis HS, Plovanich M, Belcher-Timme CA, Sancak Y, Bao XR, Strittmatter L, Goldberger O, Bogorad RL, Koteliansky V, Mootha VK (2011). Integrative genomics identifies MCU as an essential component of the mitochondrial calcium uniporter. *Nature* 476: 341-345.

Beavo JA, Brunton LL (2002). Cyclic nucleotide research -- still expanding after half a century. *Nat Rev Mol Cell Biol* 3: 710-718.

Beebe SJ, Oyen O, Sandberg M, Froysa A, Hansson V, Jahnsen T (1990). Molecular cloning of a tissue-specific protein kinase (C gamma) from human testis--representing a third isoform for the catalytic subunit of cAMP-dependent protein kinase. *Mol Endocrinol* 4: 465-475.

Behar V, Bisello A, Bitan G, Rosenblatt M, Chorev M (2000). Photoaffinity cross-linking identifies differences in the interactions of an agonist and an antagonist with

the parathyroid hormone/parathyroid hormone-related protein receptor. *J Biol Chem* 275: 9-17.

Behar V, Pines M, Nakamoto C, Greenberg Z, Bisello A, Stueckle SM, Bessalle R, Usdin TB, Chorev M, Rosenblatt M, Suva LJ (1996). The human PTH2 receptor: binding and signal transduction properties of the stably expressed recombinant receptor. *Endocrinology* 137: 2748-2757.

Belfiore A, Frasca F, Pandini G, Sciacca L, Vigneri R (2009). Insulin receptor isoforms and insulin receptor/insulin-like growth factor receptor hybrids in physiology and disease. *Endocr Rev* 30**:** 586-623.

Bergwitz C, Gardella TJ, Flannery MR, Potts JT, Jr., Kronenberg HM, Goldring SR, Jüppner H (1996). Full activation of chimeric receptors by hybrids between parathyroid hormone and calcitonin. Evidence for a common pattern of ligand-receptor interaction. *J Biol Chem* 271: 26469-26472.

Berridge MJ (1997). Elementary and global aspects of calcium signalling. *J Exp Biol* 200: 315-319.

Berridge MJ (2009). Inositol trisphosphate and calcium signalling mechanisms. *Biochim Biophys Acta* 1793: 933-940.

Berridge MJ, Bootman MD, Roderick HL (2003). Calcium signalling: dynamics, homeostasis and remodelling. *Nat Rev Mol Cell Biol* 4: 517-529.

Berridge MJ, Irvine RF (1989). Inositol phosphates and cell signalling. *Nature* 341: 197-205.

Berridge MJ, Lipp P, Bootman MD (2000). The versatility and universality of calcium signalling. *Nature Reviews: Mol Cell Biol* 1: 11-21.

Bers DM (2002). Cardiac excitation-contraction coupling. *Nature* 415: 198-205.

Bertram R, Pernarowski M (1998). Glucose diffusion in pancreatic islets of Langerhans. *Biophys J* 74: 1722-1731.

Bertram R, Sherman A, Satin LS (2010). Electrical bursting, calcium oscillations, and synchronization of pancreatic islets. *Adv Exp Med Biol* 654: 261-279.

Best JM, Kamp TJ (2012). Different subcellular populations of L-type Ca^{2+} channels exhibit unique regulation and functional roles in cardiomyocytes. *J Mol Cell Cardiol* 52: 376-387.

Best L, Elliott AC, Brown PD (2007). Curcumin induces electrical activity in rat pancreatic β -cells by activating the volume-regulated anion channel. *Biochem Pharmacol* 73: 1768-1775.

Bird GS, Burgess GM, Putney JW, Jr. (1993). Sulfhydryl reagents and cAMP-dependent kinase increase the sensitivity of the inositol 1,4,5-trisphosphate receptor in hepatocytes. *J Biol Chem* 268: 17917-17923.

Bird GS, Putney JW, Jr. (2005). Capacitative calcium entry supports calcium oscillations in human embryonic kidney cells. *J Physiol* 562: 697-706.

Bisello A, Chorev M, Rosenblatt M, Monticelli L, Mierke DF, Ferrari SL (2002). Selective ligand-induced stabilization of active and desensitized parathyroid hormone type 1 receptor conformations. *J Biol Chem* 277: 38524-38530.

Blondel O, Takeda J, Janssen H, Seino S, Bell GI (1993). Sequence and functional characterization of a third inositol trisphosphate receptor subtype, IP_3R-3, expressed in pancreatic islets, kidney, gastrointestinal tract, and other tissues. *J Biol Chem* 268: 11356-11363.

Boden SD, Kaplan FS (1990). Calcium homeostasis. *Orthop Clin North Am* 21: 31-42.

Bootman MD, Collins TJ, Peppiatt CM, Prothero LS, MacKenzie L, De Smet P, Travers M, Tovey SC, Seo JT, Berridge MJ, Ciccolini F, Lipp P (2001). Calcium signalling--an overview. *Semin Cell Dev Biol* 12: 3-10.

Brandman O, Liou J, Park WS, Meyer T (2007). STIM2 is a feedback regulator that stabilizes basal cytosolic and endoplasmic reticulum Ca^{2+} levels. *Cell* 131: 1327-1339.

Bratanova-Tochkova TK, Cheng H, Daniel S, Gunawardana S, Liu YJ, Mulvaney-Musa J, Schermerhorn T, Straub SG, Yajima H, Sharp GW (2002). Triggering and augmentation mechanisms, granule pools, and biphasic insulin secretion. *Diabetes* 51 Suppl 1: S83-90.

Braun M, Ramracheya R, Bengtsson M, Zhang Q, Karanauskaite J, Partridge C, Johnson PR, Rorsman P (2008). Voltage-gated ion channels in human pancreatic β-cells: electrophysiological characterization and role in insulin secretion. *Diabetes* 57: 1618-1628.

Bringhurst FR, Juppner H, Guo J, Urena P, Potts JT, Jr., Kronenberg HM, Abou-Samra AB, Segre GV (1993). Cloned, stably expressed parathyroid hormone (PTH)/PTH-related peptide receptors activate multiple messenger signals and biological responses in LLC-PK1 kidney cells. *Endocrinology* 132: 2090-2098.

Brini M, Carafoli E (2009). Calcium pumps in health and disease. *Physiol Rev* 89: 1341-1378.

Brini M, Ottolini D, Cali T, Carafoli E (2013). Calcium in health and disease. *Met Ions Life Sci* 13: 81-137.

Brittsan AG, Kranias EG (2000). Phospholamban and cardiac contractile function. *J Mol Cell Cardiol* 32: 2131-2139.

Brogard JM, Vetter T, Blickle JF (1992). [Discovery of pancreatic diabetes in Strasbourg]. *Diabete Metab* 18**:** 104-114

Brown EM (1993). Mechanisms underlying the regulation of parathyroid hormone secretion in vivo and in vitro. *Curr Opin Nephrol Hypertens* 2: 541-551.

Brown EM (2013). Role of the calcium-sensing receptor in extracellular calcium homeostasis. *Best Pract Res Clin Endocrinol Metab* 27: 333-343.

Brown EM, MacLeod RJ (2001). Extracellular calcium sensing and extracellular calcium signaling. *Physiol Rev* 81: 239-297.

Brown KM, Lee LC, Findlay JE, Day JP, Baillie GS (2012). Cyclic AMP-specific phosphodiesterase, PDE8A1, is activated by protein kinase A-mediated phosphorylation. *FEBS Lett* 586: 1631-1637.

Bruce JI, Shuttleworth TJ, Giovannucci DR, Yule DI (2002). Phosphorylation of inositol 1,4,5-trisphosphate receptors in parotid acinar cells. A mechanism for the synergistic effects of cAMP on Ca^{2+} signaling. *J Biol Chem* 277: 1340-1348.

Bruce JI, Straub SV, Yule DI (2003). Crosstalk between cAMP and Ca^{2+} signaling in non-excitable cells. *Cell Calcium* 34: 431-444.

Buck E, Zimanyi I, Abramson JJ, Pessah IN (1992). Ryanodine stabilizes multiple conformational states of the skeletal muscle calcium release channel. *J Biol Chem* 267: 23560-23567.

Buckley KA, Wagstaff SC, McKay G, Hipskind RA, Bilbe G, Gallagher JA, Bowler WB. (2001). Parathyroid hormone potentiates nucleotide-induced $[Ca^{2+}]_i$ release in rat osteoblasts independently of G_q activation or cyclic monophosphate accumulation. *J Biol Chem* 276: 9565-9571.

Burgess GM, Bird GS, Obie JF, Putney JW, Jr. (1991). The mechanism for synergism between phospholipase C- and adenylylcyclase-linked hormones in liver. Cyclic AMP-dependent kinase augments inositol trisphosphate-mediated Ca^{2+} mobilization without increasing the cellular levels of inositol polyphosphates. *J Biol Chem* 266: 4772-4781.

Cahalan MD (2009). STIMulating store-operated Ca^{2+} entry. *Nat Cell Biol* 11: 669-677.

Calcraft PJ, Ruas M, Pan Z, Cheng X, Arredouani A, Hao X, Tang J, Rietdorf K, Teboul L, Chuang KT, Lin P, Xiao R, Wang C, Zhu Y, Lin Y, Wyatt CN, Parrington J, Ma J, Evans AM, Galione A, Zhu MX (2009). NAADP mobilizes calcium from acidic organelles through two-pore channels. *Nature* 459: 596-600.

Calebiro D, Nikolaev VO, Gagliani MC, de Filippis T, Dees C, Tacchetti C, Persani L, Lohse MJ (2009). Persistent cAMP-signals triggered by internalized G-protein-coupled receptors. *PLoS Biol* 7: e1000172.

Calebiro D, Nikolaev VO, Persani L, Lohse MJ (2010). Signaling by internalized G-protein-coupled receptors. *Trends in Pharmacol Sci* 31: 221-228.

Cancela JM, Churchill GC, Galione A (1999). Coordination of agonist-induced Ca^{2+}-signalling patterns by NAADP in pancreatic acinar cells. *Nature* 398: 74-76.

Carafoli E (1991). Calcium pump of the plasma membrane. *Physiol Rev* 71: 129-153.

Care AD, Sherwood LM, Potts JT, Jr., Aurbach GD (1966). Perfusion of the isolated parathyroid gland of the goat and sheep. *Nature* 209: 55-57.

Carr DW, Stofko-Hahn RE, Fraser ID, Bishop SM, Acott TS, Brennan RG, Scott JD (1991). Interaction of the regulatory subunit (RII) of cAMP-dependent protein kinase with RII-anchoring proteins occurs through an amphiathic helix binding motif. *J Biol Chem* 266: 14188-14192.

Carter JD, Dula SB, Corbin KL, Wu R, Nunemaker CS (2009). A practical guide to rodent islet isolation and assessment. *Biol Proceeding Online* 11: 3-31.

Castro M, Dicker F, Vilardaga JP, Krasel C, Bernhardt M, Lohse MJ (2002). Dual regulation of the parathyroid hormone (PTH)/PTH-related peptide receptor signaling by protein kinase C and β-arrestins. *Endocrinology* 143: 3854-3865.

Caulfield MP, McKee RL, Goldman ME, Duong LT, Fisher JE, Gay CT, DeHaven PA, Levy JJ, Roubini E, Nutt RF, Chorev M, Rosenblatt M (1990). The bovine renal parathyroid hormone (PTH) receptor has equal affinity for two different amino acid sequences: the receptor binding domains of PTH and PTH-related protein are located within the 14-34 region. *Endocrinology* 127: 83-87.

Caumo A, Luzi L (2004). First-phase insulin secretion: does it exist in real life? Considerations on shape and function. *Am J Physiol Endocrinol Metab* 287: E371-385.

Chase LR, Aurbach GD (1967). Parathyroid function and the renal excretion of 3'5'-adenylic acid. *Proc Natl Acad Sci U S A* 58: 518-525.

Chen H, Ding C, Wild C, Liu H, Wang T, White MA, Cheng X, Zhou J (2013). Efficient synthesis of ESI-09, a novel non-cyclic nucleotide EPAC Antagonist. *Tetrahedron Lett* 54: 1546-1549.

Chen SR, Li X, Ebisawa K, Zhang L (1997). Functional characterization of the recombinant type 3 Ca^{2+} release channel (ryanodine receptor) expressed in HEK293 cells. *J Biol Chem* 272: 24234-24246.

Chen TH, Lee B, Yang C, Hsu WH (1996). Effects of caffeine on intracellular calcium release and calcium influx in a clonal β-cell line RINm5F. *Life Sci* 58: 983-990.

Cheng H, Beck A, Launay P, Gross SA, Stokes AJ, Kinet JP, Fleig A, Penner R (2007). TRPM4 controls insulin secretion in pancreatic β-cells. *Cell Calcium* 41: 51-61.

Chijiwa T, Mishima A, Hagiwara M, Sano M, Hayashi K, Inoue T, Naito K, Toshioka T, Hidaka H (1990). Inhibition of forskolin-induced neurite outgrowth and protein phosphorylation by a newly synthesized selective inhibitor of cyclic AMP-dependent protein kinase, N-[2-(p-bromocinnamylamino)ethyl]-5-isoquinolinesulfonamide (H-89), of PC12D pheochromocytoma cells. *J Biol Chem* 265: 5267-5272.

Chiono M, Mahey R, Tate G, Cooper DM (1995). Capacitative Ca^{2+} entry exclusively inhibits cAMP synthesis in C6-2B glioma cells. Evidence that physiologically evoked Ca^{2+} entry regulates Ca^{2+}-inhibitable adenylyl cyclase in non-excitable cells. *J Biol Chem* 270: 1149-1155.

Christakos S, Lieben L, Masuyama R, Carmeliet G (2014). Vitamin D endocrine system and the intestine. *Bonekey Rep* 3: 496.

Christensen AE, Selheim F, de Roooij J, Dremier S, Schwede F, Dao KK, Martinez A, Maenhaut C, Bos JL, Genieser HG, Døskeland SO (2003). cAMP analog mapping of epac1 and cAMP kinase. Discriminating analogs demonstrate that Epac and cAMP kinase act syneristically to promote PC12 cell neurite extension. *J Biol Chem* 278: 35394-35402.

Churchill GC, Okada Y, Thomas JM, Genazzani AA, Patel S, Galione A (2002). NAADP mobilizes Ca^{2+} from reserve granules, lysosome-related organelles, in sea urchin eggs. *Cell* 111: 703-708.

Clapham DE (1995). Calcium signaling. *Cell* 80: 259-268.

Clegg CH, Cadd GG, McKnight GS (1988). Genetic characterization of a brain-specific form of the type I regulatory subunit of cAMP-dependent protein kinase. *Proc Natl Acad Sci U S A* 85: 3703-3707.

Colegrove SL, Albrecht MA, Friel DD (2000). Quantitative analysis of mitochondrial Ca^{2+} uptake and release pathways in sympathetic neurons. Reconstruction of the recovery after depolarization-evoked $[Ca^{2+}]_i$ elevations. *J Gen Physiol* 115: 371-388.

Cooper DM, Mons N, Karpen JW (1995). Adenylyl cyclases and the interaction between calcium and cAMP signalling. *Nature* 374: 421-424.

Copello JA, Qi Y, Jeyakumar LH, Ogunbunmi E, Fleischer S (2001). Lack of effect of cADP-ribose and NAADP on the activity of skeletal muscle and heart ryanodine receptors. *Cell Calcium* 30: 269-284.

Copsel S, Garcia C, Diez F, Vermeulem M, Baldi A, Bianciotti LG, Russel FG, Shayo C, Davio C (2011). Multidrug resistance protein 4 (MRP4/ABCC4) regulates cAMP cellular levels and controls human leukemia cell proliferation and differentiation. *J Biol Chem* 286: 6979-6988.

Coronado R, Morrissette J, Sukhareva M, Vaughan DM (1994). Structure and function of ryanodine receptors. *Am J Physiol* 266: C1485-1504.

Cukkemane A, Seifert R, Kaupp UB (2011). Cooperative and uncooperative cyclic-nucleotide-gated ion channels. *Trends Biochem Sci* 36: 55-64.

Cupp ME, Nayak SK, Adem AS, Thomsen WJ (2013). Parathyroid hormone (PTH) and PTH-related peptide domains contributing to activation of different PTH receptormediated signaling pathways. *J Pharmacol Exp Ther*. 345:404-18.

Daaka Y, Luttrell LM, Lefkowitz RJ (1997). Switching of the coupling of the β2-adrenergic receptor to different G proteins by protein kinase A. *Nature* 390: 88-91.

Daunt M, Dale O, Smith PA (2006). Somatostatin inhibits oxidative respiration in pancreatic β-cells. *Endocrinology* 147: 1527-1535.

Davies SP, Reddy H, Caivano M, Cohen P (2000). Specificity and mechanism of action of some commonly used protein kinase inhibitors. *Biochem J* 351**:** 95-105.

de Rooij J, Rehmann H, van Triest M, Cool RH, Wittinghofer A, Bos JL (2000). Mechanism of regulation of the Epac family of cAMP-dependent RapGEFs. *J Biol Chem* 275: 20829-20836.

de Rooij J, Zwartkruis FJ, Verheijen MH, Cool RH, Nijman SM, Wittinghofer A, Bos JL (1998). Epac is a Rap1 guanine-nucleotide-exchange factor directly activated by cyclic AMP. *Nature* 396: 474-477.

De Stefani D, Patron M, Rizzuto R (2015). Structure and function of the mitochondrial calcium uniporter complex. *Biochim Biophys Acta* S0167-4889: 00127-5.

De Stefani D, Raffaello A, Teardo E, Szabo I, Rizzuto R (2011). A forty-kilodalton protein of the inner membrane is the mitochondrial calcium uniporter. *Nature* 476: 336-340.

Dean T, Linglart A, Mahon MJ, Bastepe M, Juppner H, Potts JT, Jr. Gardella TJ. (2006). Mechanisms of ligand binding to the parathyroid hormone (PTH)/PTH-related protein receptor: selectivity of a modified PTH(1-15) radioligand for GalphaS-coupled receptor conformations. *Mol Endocrinology* 20: 931-943.

Dean T, Vilardaga JP, Potts JT, Jr., Gardella TJ (2008). Altered selectivity of parathyroid hormone (PTH) and PTH-related protein (PTHrP) for distinct conformations of the PTH/PTHrP receptor. *Mol Endocrinology* 22: 156-166.

Dean WL, Chen D, Brandt PC, Vanaman TC (1997). Regulation of platelet plasma membrane Ca2+-ATPase by cAMP-dependent and tyrosine phosphorylation. *J Biol Chem* 272: 15113-15119.

Dellis O, Dedos S, Tovey SC, Rahman T-U-, Dubel SJ, Taylor CW (2006). Ca^{2+} entry through plasma membrane IP_3 receptors. *Science* 313: 229-233.

Derrickson BH, Mandel LJ (1997). Parathyroid hormone inhibits $Na^{(+)}$-$K^{(+)}$-ATPase through G_q/G_{11} and the calcium-independent phospholipase A2. *Am J Physiol* 272: F781-788.

DeSouza N, Reiken S, Ondrias K, Yang YM, Matkovich S, Marks AR (2002). Protein kinase A and two phosphatases are components of the inositol 1,4,5-trisphosphate receptor macromolecular signaling complex. *J Biol Chem* 277: 39397-39400.

Dessauer CW (2009). Adenylyl cyclase--A-kinase anchoring protein complexes: the next dimension in cAMP signaling. *Mol Pharmacol* 76: 935-941.

Di Biase V, Franzini-Armstrong C (2005). Evolution of skeletal type e-c coupling: a novel means of controlling calcium delivery. *Journal of Cell Biology* 171**:** 695-704.

Di Capite J, Ng SW, Parekh AB (2009). Decoding of cytoplasmic Ca^{2+} oscillations through the spatial signature drives gene expression. *Curr Biol* 19: 853-858.

Dobolyi A, Ueda H, Uchida H, Palkovits M, Usdin TB (2002). Anatomical and physiological evidence for involvement of tuberoinfundibular peptide of 39 residues in nociception. *Proc Natl Acad Sci U S A* 99: 1651-1656.

Dolmetsch RE, Xu K, Lewis RS (1998). Calcium oscillations increase the efficiency and specificity of gene expression. *Nature* 392: 933-936.

Drucker DJ (2006). The biology of incretin hormones. *Cell Metab* 3: 153-165.

Duckworth WC, Bennett RG, Hamel FG (1998). Insulin degradation: progress and potential. *Endocr Rev* 19**:** 608-624.

Dufer M, Haspel D, Krippeit-Drews P, Aguilar-Bryan L, Bryan J, Drews G (2004). Oscillations of membrane potential and cytosolic Ca^{2+} concentration in SUR1(-/-) β cells. *Diabetologia* 47: 488-498.

Dunlay R, Hruska K (1990). PTH receptor coupling to phospholipase C is an alternate pathway of signal transduction in bone and kidney. *Am J Physiol* 258: F223-231.

Dyachok O, Gylfe E (2001). Store-operated influx of Ca^{2+} in pancreatic β-cells exhibits graded dependence on the filling of the endoplasmic reticulum. *J Cell Sci* 114: 2179-2186.

Dyachok O, Isakov Y, Sagetorp J, Tengholm A (2006). Oscillations of cyclic AMP in hormone-stimulated insulin-secreting β-cells. *Nature* 439: 349-352.

Dyachok O, Tufveson G, Gylfe E (2004). Ca^{2+}-induced Ca^{2+} release by activation of inositol 1,4,5-trisphosphate receptors in primary pancreatic β-cells. *Cell Calcium* 36: 1-9.

Dyer JL, Liu Y, de la Huerga IP, Taylor CW (2005). Long lasting inhibition of adenylyl cyclase selectively mediated by inositol 1,4,5-trisphosphate-evoked calcium release. *J Biol Chem* 280: 8936-8944.

Efrat S (1999). Genetically engineered pancreatic β-cell lines for cell therapy of diabetes. *Ann N Y Acad Sci* 875: 286-293.

Eizirik DL, Korbutt GS, Hellerstrom C (1992). Prolonged exposure of human pancreatic islets to high glucose concentrations in vitro impairs the β-cell function. *J Clin Invest* 90**:** 1263-1268.

Elayat AA, el-Naggar MM, Tahir M (1995). An immunocytochemical and morphometric study of the rat pancreatic islets. *J Anat* 186**:** 629-637.

Fagan KA, Graf RA, Tolman S, Schaack J, Cooper DM (2000). Regulation of a Ca^{2+}-sensitive adenylyl cyclase in an excitable cell. Role of voltage-gated versus capacitative Ca^{2+} entry. *J Biol Chem* 275: 40187-40194.

Fagan KA, Mons N, Cooper DM (1998). Dependence of the Ca^{2+}-inhibitable adenylyl cyclase of C6-2B glioma cells on capacitative Ca^{2+} entry. *J Biol Chem* 273: 9297-9305.

Feinstein TN, Wehbi VL, Ardura JA, Wheeler DS, Ferrandon S, Gardella TJ, Vilardaga JP (2011). Retromer terminates the generation of cAMP by internalized PTH receptors. *Nat Chem Biol* 7: 278-284.

Ferrandon S, Feinstein TN, Castro M, Wang B, Bouley R, Potts JT, Vilardaga JP (2009). Sustained cyclic AMP production by parathyroid hormone receptor endocytosis. *Nat Chem Biol* 5: 734-742.

Ferrier J, Ward-Kesthely A, Heersche JN, Aubin JE (1988). Membrane potential changes, cAMP stimulation and contraction in osteoblast-like UMR 106 cells in response to calcitonin and parathyroid hormone. *Bone Miner* 4: 133-145.

Fesenko EE, Kolesnikov SS, Lyubarsky AL (1985). Induction by cyclic GMP of cationic conductance in plasma membrane of retinal rod outer segment. *Nature* 313: 310-313.

Fill M, Copello JA (2002). Ryanodine receptor calcium release channels. *Physiol Rev* 82(4): 893-922.

Findlay I, Dunne MJ (1985). Voltage-activated Ca^{2+} currents in insulin-secreting cells. *FEBS Lett* 189: 281-285.

Foskett JK, White C, Cheung KH, Mak DO (2007). Inositol trisphosphate receptor Ca^{2+} release channels. *Physiol Rev* 87: 593-658.

Fraser DR, Kodicek E (1973). Regulation of 25-hydroxycholecalciferol-1-hydroxylase activity in kidney by parathyroid hormone. *Nat New Biol* 241: 163-166.

Fridlyand LE, Tamarina N, Philipson LH (2010). Bursting and calcium oscillations in pancreatic β-cells: specific pacemakers for specific mechanisms. *Am J Physiol Endocrinol Metab* 299: E517-532.

Friedman PA, Gesek FA (1994). Hormone-responsive Ca^{2+} entry in distal convoluted tubules. *J Am Soc Nephrol* 4: 1396-1404.

Fritsch J, Edelman A, Balsan S (1988). Early effects of parathyroid hormone on membrane potential of rat osteoblasts in culture: role of cAMP and Ca^{2+}. *J Bone Miner Res* 3: 547-554.

Fu Z, Gilbert ER, Liu D (2013). Regulation of insulin synthesis and secretion and pancreatic B-cell dysfunction in diabetes. *Curr Diabetes Rev* 9**:** 25-53.

Fujimori A, Cheng S-L, Avioli LV, Civitelli R (1991). Dissociation of second messenger activation by parathyroid hormone fragments in osteosarcoma cells. *Endocrinology* 128: 3032-3039.

Galione A, Morgan AJ, Arredouani A, Davis LC, Rietdorf K, Ruas M, Parrington J. (2010). NAADP as an intracellular messenger regulating lysosomal calcium-release channels. *Biochem Soc Trans* 38: 1424-1431.

Gallagher EJ, Leroith D, Karnieli E (2010). Insulin resistance in obesity as the underlying cause for the metabolic syndrome. *Mt Sinai J Med* 77: 511-523.

Gambara G, Billington RA, Debidda M, D'Alessio A, Palombi F, Ziparo E, Genazzani AA, Filippini A (2008). NAADP-induced Ca^{2+} signaling in response to endothelin is via the receptor subtype B and requires the integrity of lipid rafts/caveolae. *J Cell Physiol* 216: 396-404.

Gamberucci A, Fulceri R, Pralong W, Banhegyi G, Marcolongo P, Watkins SL Benedetti A (1999). Caffeine releases a glucose-primed endoplasmic reticulum Ca^{2+} pool in the insulin secreting cell line INS-1. *FEBS Lett* 446: 309-312.

Gao T, Yatani A, Dell'Acqua ML, Sako H, Green SA, Dascal N, Scott JD, Hosey MM. (1997). cAMP-dependent regulation of cardiac L-type Ca^{2+} channels requires membrane targeting of PKA and phosphorylation of channel subunits. *Neuron* 19: 185-196.

Gardella TJ, Axelrod D, Rubin D, Keutmann HT, Potts JT, Jr., Kronenberg HM, Nussbaum SR (1991). Mutational analysis of the receptor-activating region of human parathyroid hormone. *J Biol Chem* 266: 13141-13146.

Gardella TJ, Juppner H, Wilson AK, Keutmann HT, Abou-Samra AB, Segre GV, Bringhurst FR, Potts JT Jr, Nussbaum SR, Kronenberg HM. (1994). Determinants of [Arg^2]PTH-(1-34) binding and signaling in the transmembrane region of the parathyroid hormone receptor. *Endocrinology* 135: 1186-1194.

Gardella TJ, Wilson AK, Keutmann HT, Oberstein R, Potts JT, Jr., Kronenberg M, Nussbaum SR (1993). Analysis of parathyroid hormone's principal receptor-binding region by site-directed mutagenesis and analog design. *Endocrinology* 132: 2024-2030.

Gerbino A, Ruder WC, Curci S, Pozzan T, Zaccolo M, Hofer AM (2005). Termination of cAMP signals by Ca^{2+} and Gαi via extracellular Ca^{2+} sensors: a link to intracellular Ca^{2+} oscillations. *J Cell Biol* 171**:** 303-312.

Gesek FA, Friedman PA (1992). On the mechanism of parathyroid hormone stimulation of calcium uptake by mouse distal convoluted tubule cells. *J Clin Invest* 90: 749-758.

Gesty-Palmer D, Chen M, Reiter E, Ahn S, Nelson CD, Wang S, Eckhardt AE, Cowan CL, Spurney RF, Luttrell LM, Lefkowitz RJ (2006). Distinct β-arrestin- and G protein-dependent pathways for parathyroid hormone receptor-stimulated ERK1/2 activation. *J Biol Chem* 281:10856-10864.

Gesty-Palmer D, Luttrell LM (2011). 'Biasing' the parathyroid hormone receptor: a novel anabolic approach to increasing bone mass? *Br J Pharmacol* 164: 59-67.

Giannini G, Sorrentino V (1995). Molecular structure and tissue distribution of ryanodine receptors calcium channels. *Med Res Rev* 15: 313-323.

Gilon P, Ravier MA, Jonas JC, Henquin JC (2002). Control mechanisms of the oscillations of insulin secretion in vitro and in vivo. *Diabetes* 51 Suppl 1: S144-151.

Giovannucci DR, Sneyd J, Groblewski GE, Yule DI (2000). Modulation of $InsP_3$ receptor properties by phosphorylation: targeting of PKA to $InsP_3$ receptors shapes oscillatory calcium signals in pancreatic acinar cells. *J Korean Med Sci* 15 Suppl: S55-56.

Gleason CE, Gonzalez M, Harmon JS, Robertson RP (2000). Determinants of glucose toxicity and its reversibility in the pancreatic islet β-cell line, HIT-T15. *Am J Physiol Endocrinol Metab* 279: E997-1002.

Glitsch MD, Bakowski D, Parekh AB (2002). Store-operated Ca^{2+} entry depends on mitochondrial Ca^{2+} uptake. *EMBO. J* 21: 6744-6754.

Gorbunova YV, Spitzer NC (2002). Dynamic interactions of cyclic AMP transients and spontaneous Ca^{2+} spikes. *Nature (London)* 418: 93-96.

Goren HJ (2005). Role of insulin in glucose-stimulated insulin secretion in β cells. *Curr Diabetes Rev* 1: 309-330.

Grant FD, Conlin PR, Brown EM (1990). Rate and concentration dependence of parathyroid hormone dynamics during stepwise changes in serum ionized calcium in normal humans. *J Clin Endocrinol Metab* 71: 370-378.

Grauschopf U, Lilie H, Honold K, Wozny M, Reusch D, Esswein A, Schäfer W, Rücknagel KP, Rudolph R (2000). The N-terminal fragment of human parathyroid hormone receptor 1 constitutes a hormone binding domain and reveals a distinct disulfide pattern. *Biochemistry* 39: 8878-8887.

Graves TK, Hinkle PM (2003). Ca^{2+}-induced Ca^{2+} release in the pancreatic β-cell: direct evidence of endoplasmic reticulum Ca^{2+} release. *Endocrinology* 144: 3565-3574.

Greenberg Z, Bisello A, Mierke DF, Rosenblatt M, Chorev M (2000). Mapping the bimolecular interface of the parathyroid hormone (PTH)-PTH1 receptor complex: spatial proximity between Lys(27) (of the hormone principal binding domain) and leu(261) (of the first extracellular loop) of the human PTH1 receptor. *Biochem* 39: 8142-8152.

Gromadzinska E, Lachowicz L, Walkowiak B, Zylinska L (2001). Calmodulin effect on purified rat cortical plasma membrane Ca^{2+}-ATPase in different phosphorylation states. *Biochim Biophys Acta* 1549: 19-31.

Grose JH, Scriver CR (1968). Parathyroid-dependent phosphaturia and aminoaciduria in the vitamin D-deficient rat. *Am J Physiol* 214: 370-377.

Grynkiewicz G, Poenie M, Tsien RY (1985). A new generation of Ca^{2+} indicators with greatly improved fluorescence properties. *J Biol Chem* 260: 3440-3450.

Guimond J, Mamarbachi AM, Allen BG, Rindt H, Hebert TE (2005). Role of specific protein kinase C isoforms in modulation of β1- and β2-adrenergic receptors. *Cell Signal* 17: 49-58.

Guo J, Iida-Klein A, Huang X, Abou-Samra AB, Segre GV, Bringhurst FR (1995). Parathyroid hormone (PTH)/PTH-related peptide receptor density modulates activation of phospholipase C and phosphate transport by PTH in LLC-PK1 cells. *Endocrinology* 136: 3884-3891.

Guo J, Liu M, Yang D, Bouxsein ML, Thomas CC, Schipani E, Bringhurst FR, Kronenberg HM (2010). Phospholipase C signaling via the parathyroid hormone (PTH)/PTH-related peptide receptor is essential for normal bone responses to PTH. *Endocrinology* 151: 3502-3513.

Guse AH, Lee HC (2008). NAADP: a universal Ca^{2+} trigger. *Sci Signal* 1: re10.

Gustafsson AJ, Ingelman-Sundberg H, Dzabic M, Awasum J, Nguyen KH, Ostenson CG, Tedeschi P, Woolcott O, Chiounan S, Lund PE, Larsson O,Islam MS

(2005). Ryanodine receptor-operated activation of TRP-like channels can trigger critical Ca^{2+} signaling events in pancreatic β-cells. *FASEB J* 19: 301-303.

Habener JF, Kemper B, Potts JT, Jr., Rich A (1975). Pre - proparathyroid hormone identified by cell - free translation of messenger RNA from hyperplastic human parathyroid tissue. *J Clin Invest* 56: 1328-1333.

Habener JF, Potts JT, Jr. (1979). Subcellular distributions of parathyroid hormone, hormonal precursors, and parathyroid secretory protein. *Endocrinology* 104: 265-275.

Habener JF, Rosenblatt M, Dee PC, Potts JT, Jr. (1979). Cellular processing of pre-proparathyroid hormone involves rapid hydrolysis of the leader sequence. *J Biol Chem* 254**:** 10596-10599.

Habener JF, Rosenblatt M, Kemper B, Kronenberg HM, Rich A, Potts JT, Jr. (1978). Pre-proparathyroid hormone; amino acid sequence, chemical synthesis, and some biological studies of the precursor region. *Proc Natl Acad Sci U S A* 75: 2616-2620.

Hajnoczky G, Robb-Gaspers LD, Seitz MB, Thomas AP (1995). Decoding of cytosolic calcium oscillations in the mitochondria. *Cell* 82: 415-424.

Harmar AJ (2001). Family-B G-protein-coupled receptors. *Genome Biol* 2(12): REVIEWS3013.

Hayek SM, Zhu X, Bhat MB, Zhao J, Takeshima H, Valdivia HH, Ma J (2000). Characterization of a calcium-regulation domain of the skeletal-muscle ryanodine receptor. *Biochem J* 351: 57-65.

Haynes L, Yau KW (1985). Cyclic GMP-sensitive conductance in outer segment membrane of catfish cones. *Nature* 317: 61-64.

Heimes K, Feistel B, Verspohl EJ (2009). Impact of the 5-HT3 receptor channel system for insulin secretion and interaction of ginger extracts. *Eur J Pharmacol* 624: 58-65.

Henquin JC (2009). Regulation of insulin secretion: a matter of phase control and amplitude modulation. *Diabetologia* 52: 739-751.

Henquin JC, Ravier MA, Nenquin M, Jonas JC, Gilon P (2003). Hierarchy of the β-cell signals controlling insulin secretion. *Eur J Clin Invest* 33: 742-750.

Herrmann-Frank A, Varsanyi M (1993). Enhancement of Ca^{2+} release channel activity by phosphorylation of the skeletal muscle ryanodine receptor. *FEBS Lett* 332: 237-242.

Higaki JN, Fletterick RJ, Craik CS (1992). Engineered metalloregulation in enzymes. *Trends Biochem Sci* 17: 100-104.

Hilge M (2012). Ca^{2+} regulation of ion transport in the Na^{+}/Ca^{2+} exchanger. *J Biol Chem* 287: 31641-31649.

Hoare SR, Rubin DA, Juppner H, Usdin TB (2000). Evaluating the ligand specificity of zebrafish parathyroid hormone (PTH) receptors: comparison of PTH, PTH-related protein, and tuberoinfundibular peptide of 39 residues. *Endocrinology* 141: 3080-3086.

Hoare SR, Usdin TB (2001). Molecular mechanisms of ligand recognition by parathyroid hormone 1 (PTH1) and PTH2 receptors. *Curr Pharm Des* 7: 689-713.

Hofmann F, Bechtel PJ, Krebs EG (1977). Concentrations of cyclic AMP-dependent protein kinase subunits in various tissues. *J Biol Chem* 252: 1441-1447.

Hofmann T, Obukhov AG, Schaefer M, Harteneck C, Gudermann T, Schultz G (1999). Direct activation of human TRPC6 and TRPC3 channels by diacylglycerol. *Nature* 397: 259-263.

Holst JJ, Deacon CF, Vilsboll T, Krarup T, Madsbad S (2008). Glucagon-like peptide-1, glucose homeostasis and diabetes. *Trends Mol Med* 14: 161-168.

Holst JJ, Vilsboll T, Deacon CF (2009). The incretin system and its role in type 2 diabetes mellitus. *Mol Cell Endocrinol* 297: 127-136.

Holz GG (2004). Epac: A new cAMP-binding protein in support of glucagon-like peptide-1 receptor-mediated signal transduction in the pancreatic β-cell. *Diabetes* 53: 5-13.

Holz GG, Leech CA, Heller RS, Castonguay M, Habener JF (1999). cAMP-dependent mobilization of intracellular Ca^{2+} stores by activation of ryanodine receptors in pancreatic β-cells. A Ca^{2+} signaling system stimulated by the insulinotropic hormone glucagon-like peptide-1-(7-37). *J Biol Chem* 274: 14147-14156.

Horne JH, Meyer T (1997). Elementary calcium-release units induced by inositol trisphosphate. *Science* 276: 1690-1693.

Hosono M, Takahira T, Fujita A, Fujihara R, Ishizuka O, Tatee T, Nakamura K (1992). Cardiovascular and adenylate cyclase stimulant properties of NKH477, a novel water-soluble forskolin derivative. *J Cardiovasc Pharmacol* 19(4): 625-634.

Houillier P (2013). Calcium-sensing in the kidney. *Curr Opin Nephrol Hypertens* 22: 566-571.

Howard M, Grimaldi JC, Bazan JF, Lund FE, Santos-Argumedo L, Parkhouse RM, Walseth TF, Lee HC (1993). Formation and hydrolysis of cyclic ADP-ribose catalyzed by lymphocyte antigen CD38. *Science* 262: 1056-1059.

Huang J, Zhou H, Mahavadi S, Sriwai W, Murthy KS (2007). Inhibition of Galphaq-dependent PLC-β1 activity by PKG and PKA is mediated by phosphorylation of RGS4 and GRK2. *Am J Physiol Cell Physiol* 292: C200-208.

Huang LJ, Durick K, Weiner JA, Chun J, Taylor SS (1997). Identification of a novel protein kinase A anchoring protein that binds both type I and type II regulatory subunits. *J Biol Chem* 272: 8057-8064.

Huang XF, Arvan P (1995). Intracellular transport of proinsulin in pancreatic β-cells. Structural maturation probed by disulfide accessibility. *J Biol Chem* 270**:** 20417-20423.

Huang Y, Putney JW, Jr. (1998). Relationship between intracellular calcium stores depletion and calcium release-activated calcium current in a mast cell line. *J Biol Chem* 273: 19554-19559.

Huang Z, Chen Y, Pratt S, Chen TH, Bambino T, Nissenson RA, Shoback DM (1996). The N-terminal region of the third intracellular loop of the parathyroid hormone (PTH)/PTH-related peptide receptor is critical for coupling to cAMP and inositol phosphate/Ca^{2+} signal transduction pathways. *J Biol Chem* 271: 33382-33389.

Hubbard SR, Wei L, Ellis L, Hendrickson WA (1994). Crystal structure of the tyrosine kinase domain of the human insulin receptor. *Nature* 372**:** 746-754.

Hurwitz S (1996). Homeostatic control of plasma calcium concentration. *Crit Rev Biochem Mol Biol* 31: 41-100.

Ichiba T, Hoshi Y, Eto Y, Tajima N, Kuraishi Y (1999). Characterization of GFR, a novel guanine nucleotide exchange factor for Rap1. *FEBS Lett* 457: 85-89.

Iida-Klein A, Guo J, Xie LY, Juppner H, Potts JT, Jr., Kronenberg HM,Bringhurst FR, Abou-Samra AB, Segre GV (1995). Truncation of the carboxyl-terminal region of the rat parathyroid hormone (PTH)/PTH-related peptide receptor enhances PTH stimulation of adenylyl cyclase but not phospholipase C. *J Biol Chem* 270: 8458-8465.

Iida-Klein A, Yee DC, Brandli DW, Mirikitani EJ, Hahn TJ (1992). Effects of calcitonin on 3',5'-cyclic adenosine monophosphate and calcium second messenger generation and osteoblast function in UMR 106-06 osteoblast-like cells. *Endocrinology* 130: 381-388.

Inagaki N, Kuromi H, Gonoi T, Okamoto Y, Ishida H, Seino Y, Kaneko T, Iwanaga T, Seino S (1995). Expression and role of ionotropic glutamate receptors in pancreatic islet cells. *FASEB J* 9: 686-691.

Irannejad R, Tomshine JC, Tomshine JR, Chevalier M, Mahoney JP, Steyaert J, Rasmussen SG, Sunahara RK, El-Samad H, Huang B, von Zastrow M (2013). Conformational biosensors reveal GPCR signalling from endosomes. *Nature* 495: 534-538.

Irvine R (2007). Cell signaling. The art of the soluble. *Science* 316: 845-846.

Islam MS (2010). Calcium signaling in the islets. *Adv Exp Med Biol* 654: 235-259.

Islam MS (2002). The ryanodine receptor calcium channel of β-cells: molecular regulation and physiological significance. *Diabetes* 51: 1299-1309.

Islam MS, Larsson O, Nilsson T, Berggren PO (1995). Effects of caffeine on cytoplasmic free Ca^{2+} concentration in pancreatic β-cells are mediated by interaction with ATP-sensitive K^+ channels and L-type voltage-gated Ca^{2+} channels but not the ryanodine receptor. *Biochem J* 306: 679-686.

Jacobson DA, Philipson LH (2007). Action potentials and insulin secretion: new insights into the role of Kv channels. *Diabetes Obes Metab* 9 Suppl 2: 89-98.

Jacques-Silva MC, Correa-Medina M, Cabrera O, Rodriguez-Diaz R, Makeeva N, Fachado A, Diez J, Berman DM, Kenyon NS, Ricordi C, Pileggi A, Molano RD,Berggren PO, Caicedo A (2010). ATP-gated P2X3 receptors constitute a positive autocrine signal for insulin release in the human pancreatic β cell. *Proc Natl Acad Sci U S A* 107: 6465-6470.

Jahnsen T, Hedin L, Kidd VJ, Beattie WG, Lohmann SM, Walter U, Durica J, SchulzS ZT, Schiltz E, Browner M, Lawrence CB, Goldman D, Ratoosht SL, Richards JS (1986). Molecular cloning, cDNA structure, and regulation of the regulatory subunit of type II cAMP-dependent protein kinase from rat ovarian granulosa cells. *J Biol Chem* 261: 12352-12361.

Jelinek LJ, Lok S, Rosenberg GB, Smith RA, Grant FJ, Biggs S, O'Hara PJ, Foster D, Walker KM, Chen LHJ, McKernan PA, Kindsvogel W (1993). Expression cloning and signaling properties of the rat glucagon receptor. *Science* 259: 1614-1616.

Jeon US (2008). Kidney and Calcium Homeostasis. *Electrolyte Blood Press* 6: 68-76.

Jobert AS, Leroy C, Butlen D, Silve C (1997). Parathyroid hormone-induced calcium release from intracellular stores in a human kidney cell line in the absence of stimulation of cyclic adenosine 3',5'-monophosphate production. *Endocrinology* 138: 5282-5292.

Johnson JD, Kuang S, Misler S, Polonsky KS (2004). Ryanodine receptors in human pancreatic β cells: localization and effects on insulin secretion. *FASEB J* 18: 878-880.

Jouaville LS, Pinton P, Bastianutto C, Rutter GA, Rizzuto R (1999). Regulation of mitochondrial ATP synthesis by calcium: evidence for a long-term metabolic priming. *Proc Natl Acad Sci U S A* 96: 13807-13812.

Juppner H, Abou-Samra AB, Freeman M, Kong XF, Schipani E, Richards J, Kolakowski LF, Janet Hock J, Potts JT, Kronenberg HM, Segre GV (1991). A G protein-linked receptor for parathyroid hormone and parathyroid hormone-related peptide. *Science* 254: 1024-1026.

Juppner H, Schipani E, Bringhurst FR, McClure I, Keutmann HT, Potts JT, Jr. Kronenberg HM, Abou-Samra AB, Segre GV, Gardella TJ (1994). The

extracellular amino-terminal region of the parathyroid hormone (PTH)/PTH-related peptide receptor determines the binding affinity for carboxyl-terminal fragments of PTH-(1-34). *Endocrinology* 134: 879-884.

Kang G, Chepurny OG, Holz GG (2001). cAMP-regulated guanine nucleotide exchange factor II (Epac2) mediates Ca^{2+}-induced Ca^{2+} release in INS-1 pancreatic β-cells. *J Physiol* 536: 375-385.

Kang G, Joeph JW, Cherpurny OG, Monaco M, Wheeler MB, Bos JL, *et al.* (2003). Epac-selective cAMP analog 8-pCPT-2'-*O*-Me-cAMP as a stimulus for Ca^{2+}-induced Ca^{2+} release and exocytosis in pancreatic b-cells. *J Biol Chem* 278**:** 8279-8285.

Kang H, Han K, Jo J, Kim J, Choi MY (2008). Systems of pancreatic β-cells and glucose regulation. *Front Biosci* 13: 6421-6431.

Kaplan AD, Reimer WJ, Feldman RD, Dixon SJ (1995). Extracellular nucleotides potentiate the cytosolic Ca^{2+} but not cyclic adenosine 3',5'-monophosphate response to parathyroid hormone in rat osteoblastic cells. *Endocrinology* 136: 1674-1685.

Kaplan SA (1984). The insulin receptor. *J Pediatr* 104**:** 327-336.

Karashima E, Nishimura J, Iwamoto T, Hirano K, Hirano M, Kita S, *et al.* (2007). Involvement of Na^{+}-Ca^{2+} exchanger in cAMP-mediated relaxation in mice aorta: evaluation using transgenic mice. *Br J Pharmacol* 150**:** 434-444.

Kato I, Yamamoto Y, Fujimura M, Noguchi N, Takasawa S, Okamoto H (1999). CD38 disruption impairs glucose-induced increases in cyclic ADP-ribose, $[Ca^{2+}]_i$, and insulin secretion. *J Biol Chem* 274: 1869-1872.

Kawasaki H, Springett GM, Mochizuki N, Toki S, Nakaya M, Matsuda M, Housman DE, Graybiel AM. (1998). A family of cAMP-binding proteins that directly activate Rap1. *Science* 282: 2275-2279.

Kelley GG, Chepurny OG, Schwede F, Genieser HG, Leech CA, Roe MW, Li X, Dzhura I, Dzhura E, Afshari P, Holz GG (2009). Glucose-dependent potentiation of mouse islet insulin secretion by Epac activator 8-pCPT-2'-O-Me-cAMP-AM. *Islets* 1: 260-265.

Kemper B, Habener JF, Mulligan RC, Potts JT, Jr., Rich A (1974). Pre-proparathyroid hormone: a direct translation product of parathyroid messenger RNA. *Proc Natl Acad Sci U S A* 71: 3731-3735.

Kim BJ, Park KH, Yim CY, Takasawa S, Okamoto H, Im MJ, Kim UH (2008). Generation of nicotinic acid adenine dinucleotide phosphate and cyclic ADP-ribose by glucagon-like peptide-1 evokes Ca^{2+} signal that is essential for insulin secretion in mouse pancreatic islets. *Diabetes* 57: 868-878.

Kirichok Y, Krapivinsky G, Clapham DE (2004). The mitochondrial calcium uniporter is a highly selective ion channel. *Nature* 427: 360-364.

Klin M, Smogorzewski M, Khilnani H, Michnowska M, Massry SG (1994). Mechanisms of PTH-induced rise in cytosolic calcium in adult rat hepatocytes. *Am J Physiol* 267: G754-763.

Knox FG, Lechene C (1975). Distal site of action of parathyroid hormone on phosphate reabsorption. *Am J Physiol* 229: 1556-1560.

Kuhn F, Schulz HJ, Lorenz D, Hahn HJ, Lippert H, Abri O, Wilke T (1985). Morphological investigations in human islets of Langerhans isolated by the Velcro-technic. *Biomed Biochim Acta* 44: 149-153.

Landa LR, Jr., Harbeck M, Kaihara K, Chepurny O, Kitiphongspattana K, Graf O, Nikolaev VO, Lohse MJ, Holz GG, Roe MW (2005). Interplay of Ca^{2+} and cAMP signaling in the insulin-secreting MIN6 b-cell line. *J Biol Chem* 280: 31294-31302.

Lanner JT, Georgiou DK, Joshi AD, Hamilton SL (2010). Ryanodine receptors: structure, expression, molecular details, and function in calcium release. *Cold Spring Harb Perspect Biol* 2: a003996.

Lawler OA, Miggin SM, Kinsella BT (2001). Protein kinase A-mediated phosphorylation of serine 357 of the mouse prostacyclin receptor regulates its coupling to G_s-, to G_i-, and to G_q-coupled effector signaling. *J Biol Chem* 276: 33596-33607.

LeBeau AP, Yule DI, Groblewski GE, Sneyd J (1999). Agonist-dependent phosphorylation of the inositol 1,4,5-trisphosphate receptor: A possible mechanism for agonist-specific calcium oscillations in pancreatic acinar cells. *J Gen Physiol* 113: 851-872.

Lee C, Gardella TJ, Abou-Samra AB, Nussbaum SR, Segre GV, Potts JT, Kronenberg HM, Jüppner H (1994). Role of the extracellular regions of the parathyroid hormone (PTH)/PTH-related peptide receptor in hormone binding. *Endocrinology* 135: 1488-1495.

Lee DC, Carmichael DF, Krebs EG, McKnight GS (1983). Isolation of a cDNA clone for the type I regulatory subunit of bovine cAMP-dependent protein kinase. *Proc Natl Acad Sci U S A* 80: 3608-3612.

Lee HC (1997). Mechanisms of calcium signaling by cyclic ADP-ribose and NAADP. *Physiol Rev* 77: 1133-1164.

Lee HC (2000). Multiple calcium stores: separate but interacting. *Sci STKE* 2000: pe1.

Leech CA, Chepurny OG, Holz GG (2010). Epac2-dependent rap1 activation and the control of islet insulin secretion by glucagon-like peptide-1. *Vitam Horm* 84: 279-302.

Lefkimmiatis K, Srikanthan M, Maiellaro I, Moyer MP, Curci S, Hofer AM (2009). Store-operated cyclic AMP signalling mediated by STIM1. *Nature Cell Biology* 11**:** 433-442.

Lemmens R, Larsson O, Berggren PO, Islam MS (2001). Ca^{2+}-induced Ca^{2+} release from the endoplasmic reticulum amplifies the Ca^{2+} signal mediated by activation of voltage-gated L-type Ca^{2+} channels in pancreatic β-cells. *J Biol Chem* 276: 9971-9977.

Lewis RS (2007). The molecular choreography of a store-operated calcium channel. *Nature* 446: 284-287.

Liman ER (2010). A TRP channel contributes to insulin secretion by pancreatic β-cells. *Islets* 2: 331-333.

Liou J, Kim ML, Heo WD, Jones JT, Myers JW, Ferrell JE, Jr, Meyer T (2005). STIM is a Ca^{2+} sensor essential for Ca^{2+}-store-depletion-triggered Ca^{2+} influx. *Curr Biol* 15: 1235-1241.

Liu C, Hermann TE (1978). Characterization of ionomycin as a calcium ionophore. *J Biol Chem* 253: 5892-5894.

Liu YJ, Gylfe E (1997). Store-operated Ca^{2+} entry in insulin-releasing pancreatic β-cells. *Cell Calcium* 22: 277-286.

Liu YJ, Tengholm A, Grapengiesser E, Hellman B, Gylfe E (1998). Origin of slow and fast oscillations of Ca^{2+} in mouse pancreatic islets. *J Physiol* 508: 471-481.

Lochner A, Moolman JA (2006). The many faces of H89: a review. *Cardiovasc Drug Rev* 24: 261-274.

Lopez-Lopez JR, Shacklock PS, Balke CW, Wier WG (1995). Local calcium transients triggered by single L-type calcium channel currents in cardiac cells. *Science* 268: 1042-1045.

Lordan S, O'Brien NM, Mackrill JJ (2009). The role of calcium in apoptosis induced by 7β-hydroxycholesterol and cholesterol-5β,6β-epoxide. *J Biochem Mol Toxicol* 23: 324-332.

Lou M, Garrett TP, McKern NM, Hoyne PA, Epa VC, Bentley JD, *et al.* (2006). The first three domains of the insulin receptor differ structurally from the insulin-like growth factor 1 receptor in the regions governing ligand specificity. *Proc Natl Acad Sci U S A* 103**:** 12429-12434.

Luik RM, Wu MM, Buchanan J, Lewis RS (2006). The elementary unit of store-operated Ca^{2+} entry: local activation of CRAC channels by STIM1 at ER-plasma membrane junctions. *J Cell Biol* 174: 815-825.

Luzio JP, Pryor PR, Bright NA (2007). Lysosomes: fusion and function. *Nature Reviews: Molecular Cell Biology* 8: 622-632.

MacDonald PE, Joseph JW, Rorsman P (2005). Glucose-sensing mechanisms in pancreatic β-cells. *Philos Trans R Soc Lond B Biol Sci* 360: 2211-2225.

MacMillan D, Chalmers S, Muir TC, McCarron JG (2005). IP_3-mediated Ca^{2+} increases do not involve the ryanodine receptor, but ryanodine receptor antagonists reduce IP_3-mediated Ca^{2+} increases in guinea-pig colonic smooth muscle cells. *J Physiol* 569: 533-544.

Maechler P, Antinozzi PA, Wollheim CB (2000). Modulation of glutamate generation in mitochondria affects hormone secretion in INS-1E β cells. *IUBMB Life* 50: 27-31.

Maechler P, Wollheim CB (2000). Mitochondrial signals in glucose-stimulated insulin secretion in the β cell. *J Physiol* 529: 49-56.

Mahon MJ (2012). The parathyroid hormone receptorsome and the potential for therapeutic intervention. *Cur Drug Targets* 13: 116-128.

Mak RH, DeFronzo RA (1992). Glucose and insulin metabolism in uremia. *Nephron* 61**:** 377-382.

Mannstadt M, Juppner H, Gardella TJ (1999). Receptors for PTH and PTHrP: their biological importance and functional properties. *Am J Physiol* 277: F665-675.

Marchant J, Callamaras N, Parker I (1999). Initiation of IP_3-mediated Ca^{2+} waves in *Xenopus* oocytes. *EMBO.J* 18: 5285-5299.

Marchant JS, Taylor CW (1997). Cooperative activation of IP_3 receptors by sequential binding of IP_3 and Ca^{2+} safeguards against spontaneous activity. *Curr Biol* 7: 510-518.

Marx SO, Ondrias K, Marks AR (1998). Coupled gating between individual skeletal muscle Ca^{2+} release channels (ryanodine receptors). *Science* 281: 818-821.

Marx SO, Reiken S, Hisamatsu Y, Gaburjakova M, Gaburjakova J, Yang YM, Rosemblit N, Marks AR (2001). Phosphorylation-dependent regulation of ryanodine receptors: a novel role for leucine/isoleucine zippers. *J Cell Biol* 153: 699-708.

Matsunaga H, Stanton BA, Gesek FA, Friedman PA (1994). Epithelial Ca^{2+} channels sensitive to dihydropyridines and activated by hyperpolarizing voltages. *Am J Physiol* 267: C157-165.

Meena A, Tovey SC, Taylor CW (2015). Sustained signalling by PTH modulates IP3 accumulation and IP3 receptors through cyclic AMP junctions. *J Cell Sci* 128**:** 408-420.

Mei FC, Qiao J, Tsygankova OM, Meinkoth JL, Quilliam LA, Cheng X (2002). Differential signaling of cyclic AMP: opposing effects of exchange protein directly activated by cyclic AMP and cAMP-dependent protein kinase on protein kinase B activation. *J Biol Chem* 277: 11497-11504.

Meissner G (2004). Molecular recognition of cardiac ryanodine receptor ion channel. *Cell Calcium* 35: 621-628.

Mercado A, Slatopolsky E, Klahr S (1975). On the mechanisms responsible for the phosphaturia of bicarbonate administration. *J Clin Invest* 56: 1386-1395.

Merglen A, Theander S, Rubi B, Chaffard G, Wollheim CB, Maechler P (2004). Glucose sensitivity and metabolism-secretion coupling studied during two-year continuous culture in INS-1E insulinoma cells. *Endocrinology* 145: 667-678.

Michalak M, Corbett EF, Mesaeli N, Nakamura K, Opas M (1999). Calreticulin: one protein, one gene, many functions. *Biochem J* 344 Pt 2: 281-292.

Michelangeli F, East JM (2011). A diversity of SERCA Ca^{2+} pump inhibitors. *Biochem Soc Trans* 39: 789-397.

Mignen O, Thompson JL, Shuttleworth TJ (2007). Both Orai1 and Orai3 are essential components of the arachidonate-regulated Ca^{2+}-selective ARC channels. *J Physiol*.

Miller AT, Sandberg M, Huang YH, Young M, Sutton S, Sauer K, Cooke MP (2007). Production of Ins(1,3,4,5)P_4 mediated by the kinase Itpkb inhibits store-operated calcium channels and regulates B cell selection and activation. *Nat Immunol* 8: 514-521.

Mine T, Kojima I, Ogata E (1989). Calcium rather than cyclic AMP is an intracellular messenger of parathyroid hormone action on glycogen metabolism in isolated rat hepatocytes. *Biochem J* 258: 889-894.

Mitchell KJ, Lai FA, Rutter GA (2003). Ryanodine receptor type 1 and nicotinic acid adenine dinucleotide phosphate receptors mediate Ca^{2+} release from insulin-containing vesicles in living pancreatic b-cells (MIN6). *J Biol Chem* 278: 11057-11064.

Miyawaki A, Llopis J, Heim R, McCaffery JM, Adams JA, Ikura M, Tsien RY (1997). Fluorescent indicators for Ca^{2+} based on green fluorescent proteins and calmodulin. *Nature* 388: 882-887.

Miyazaki S (2007). Intracellular calcium oscillations in mammalian eggs at fertilization. *J Physiol* 584: 713-714.

Mongillo M, Tocchetti CG, Terrin A, Lissandron V, Cheung YF, Dostmann WR, *et al.* (2006). Compartmentalized phosphodiesterase-2 activity blunts b-adrenergic cardiac inotropy via an NO/cGMP-dependent pathway. *Circulation Research* 98**:** 226-234.

Moonga BS, Li S, Iqbal J, Davidson R, Shankar VS, Bevis PJ, Inzerillo A, Abe E, Huang CL, Zaidi M (2002). Ca^{2+} influx through the osteoclastic plasma membrane ryanodine receptor. *Am J Physiol Renal Physiol* 282: F921-932.

Morgan AJ, Murray KJ, Challiss RA (1993). Comparison of the effect of isobutylmethylxanthine and phosphodiesterase-selective inhibitors on cAMP levels in SH-SY5Y neuroblastoma cells. *Biochem Pharmacol* 45: 2373-2380.

Morgan SJ, Deshpande DA, Tiegs BC, Misior AM, Yan H, Hershfeld AV,Rich TC, Panettieri RA, An SS, Penn RB (2014). β-Agonist-mediated relaxation of airway smooth muscle is protein kinase A-dependent. *J Biol Chem* 289**:** 23065-23074.

Munro S, Pelham HR (1987). A C-terminal signal prevents secretion of luminal ER proteins. *Cell* 48**:** 899-907.

Nakade S, Rhee SK, Hamanaka H, Mikoshiba K (1994). Cyclic AMP-dependent phosphorylation of an immunoaffinity-purified homotetrameric inositol 1,4,5-trisphosphate receptor (type I) increases Ca^{2+} flux in reconstituted lipid vesicles. *J Biol Chem* 269(9): 6735-6742.

Nakamura T, Gold GH (1987). A cyclic nucleotide-gated conductance in olfactory receptor cilia. *Nature* 325: 442-444.

Nash MS, Young KW, Challiss RA, Nahorski SR (2001). Intracellular signalling. Receptor-specific messenger oscillations. *Nature* 413: 381-382.

Nelson MT, Cheng H, Rubart M, Santana LF, Bonev AD, Knot HJ, Lederer WJ. (1995). Relaxation of arterial smooth muscle by calcium sparks. *Science* 270: 633-637.

Nemere I, Norman AW (1986). Parathyroid hormone stimulates calcium transport in perfused duodena from normal chicks: comparison with the rapid (transcaltachic) effect of 1,25-dihydroxyvitamin D3. *Endocrinology* 119: 1406-1408.

Newlon MG, Roy M, Hausken ZE, Scott JD, Jennings PA (1997). The A-kinase anchoring domain of type IIalpha cAMP-dependent protein kinase is highly helical. *J Biol Chem* 272: 23637-23644.

Nishi M, Bell GI, Steiner DF (1990). Islet amyloid polypeptide (amylin): no evidence of an abnormal precursor sequence in 25 type 2 (non-insulin-dependent) diabetic patients. *Diabetologia* 33**:** 628-630.

Nussbaum SR, Rosenblatt M, Potts JT, Jr. (1980). Parathyroid hormone renal receptor interactions. Demonstration of two receptor-binding domains. *J Biol Chem* 255: 10183-10187.

O'Rahilly S, Turner RC, Matthews DR (1988). Impaired pulsatile secretion of insulin in relatives of patients with non-insulin-dependent diabetes. *N Engl J Med* 318: 1225-1230.

O'Riordan JL, Barling PM, Hendy GN, Keutmann HT, Jacobs JW, Sauer RT, Niall HD, Tregear G, Potts JT, Aurbach GD. (1973). Isolation of human parathyroid hormone and determination of the amino-acid sequence of the amino-terminal part of the molecule. *Clin Sci* 44: 14P-15P.

Oestreich EA, Wang H, Malik S, Kaproth-Joslin KA, Blaxall BC, Kelley GG, Dirksen RT, Smrcka AV (2007). Epac-mediated activation of phospholipase

C(epsilon) plays a critical role in β-adrenergic receptor-dependent enhancement of Ca^{2+} mobilization in cardiac myocytes. *J Biol Chem* 282: 5488-5495.

Ogunbayo OA, Zhu Y, Rossi D, Sorrentino V, Ma J, Zhu MX, Evans AM (2011). cADPR activates ryanodine receptors while NAADP activates two pore domain channels. *J Biol Chem* 286: 9136-9140.

Ohta Y, Kitanaka A, Mihara K, Imataki O, Ohnishi H, Tanaka T, Taminato T, Kubota Y (2011). Expression of CD38 with intracellular enzymatic activity: a possible explanation for the insulin release induced by intracellular cADPR. *Mol Cell Biochem* 352: 293-299.

Okada T, Inoue R, Yamazaki K, Maeda A, Kurosaki T, Yamakuni T, Tanaka I, Shimizu S, Ikenaka K, Imoto K, Mori Y (1999). Molecular and functional characterization of a novel mouse transient receptor potential protein homologue TRP7. Ca^{2+}-permeable cation channel that is constitutively activated and enhanced by stimulation of G protein-coupled receptor. *J Biol Chem* 274: 27359-27370.

Okamoto H (1999). The CD38-cyclic ADP-ribose signaling system in insulin secretion. *Mol Cell Biochem* 193: 115-118.

Okazaki M, Ferrandon S, Vilardaga JP, Bouxsein ML, Potts JT, Jr., Gardella TJ (2008). Prolonged signaling at the parathyroid hormone receptor by peptide ligands targeted to a specific receptor conformation. *Proc Natl Acad Sci U.S.A.* 105: 16525-16530.

Olson LK, Qian J, Poitout V (1998). Glucose rapidly and reversibly decreases INS-1 cell insulin gene transcription via decrements in STF-1 and C1 activator transcription factor activity. *Mol Endocrinol* 12**:** 207-219.

Olson ML, Chalmers S, McCarron JG (2010). Mitochondrial Ca^{2+} uptake increases Ca^{2+} release from inositol 1,4,5-trisphosphate receptor clusters in smooth muscle cells. *J Biol Chem* 285: 2040-2050.

Ostrowski J, Kjelsberg MA, Caron MG, Lefkowitz RJ (1992). Mutagenesis of the β 2-adrenergic receptor: how structure elucidates function. *Annu Rev Pharmacol Toxicol* 32: 167-183.

Otsu K, Willard HF, Khanna VK, Zorzato F, Green NM, MacLennan DH (1990). Molecular cloning of cDNA encoding the Ca^{2+} release channel (ryanodine receptor) of rabbit cardiac muscle sarcoplasmic reticulum. *J Biol Chem* 265: 13472-13483.

Ozaki N, Shibasaki T, Kashima Y, Miki T, Takahashi K, Ueno H, Sunaga Y, Yano H, Matsuura Y, Iwanaga T, Takai Y, Seino S (2000). cAMP-GEFII is a direct target of cAMP in regulated exocytosis. *Nat Cell Biol* 2: 805-811.

Pantazaka E, Taylor EJA, Bernard W, Taylor CW (2013). Ca^{2+} signals evoked by histamine H_1 receptors are attenuated by activation of prostaglandin EP_2 receptors in human aortic smooth muscle.*B J Pharm* 169: 1624-1634.

Parekh AB, Putney JW, Jr. (2005). Store-operated calcium channels. *Physiol Rev* 85: 757-810.

Park CY, Shcheglovitov A, Dolmetsch R (2010). The CRAC channel activator STIM1 binds and inhibits L-type voltage-gated calcium channels. *Science* 330: 101-105.

Parvez S, Beck A, Peinelt C, Soboloff J, Lis A, Monteilh-Zoller M, Gill DL, Fleig A, Penner R (2008). STIM2 protein mediates distinct store-dependent and store-independent modes of CRAC channel activation. *FASEB J* 22: 752-761.

Patel S, Ramakrishnan L, Rahman T, Hamdoun A, Marchant JS, Taylor CW, Brailoiu E (2011). The endo-lysosomal system as an NAADP-sensitive acidic Ca^{2+} store: Role for the two-pore channels. *Cell Calcium*.

Patterson JE, Geller DM (1977). Bovine microsomal albumin: amino terminal sequence of bovine proalbumin. *Biochem Biophys Res Commun* 74: 1220-1226.

Pellegrini M, Bisello A, Rosenblatt M, Chorev M, Mierke DF (1998). Binding domain of human parathyroid hormone receptor: from conformation to function. *Biochem* 37: 12737-12743.

Perez JF, Sanderson MJ (2005). The frequency of calcium oscillations induced by 5-HT, ACH, and KCl determine the contraction of smooth muscle cells of intrapulmonary bronchioles. *J Gen Physiol* 125: 535-553.

Picotto G, Massheimer V, Boland R (1997). Parathyroid hormone stimulates calcium influx and the cAMP messenger system in rat enterocytes. *Am J Physiol* 273: C1349-1353.

Pines M, Adams AE, Stueckle S, Bessalle R, Rashti-Behar V, Chorev M, Rosenblatt M, Suva LJ (1994). Generation and characterization of human kidney cell lines stably expressing recombinant human PTH/PTHrP receptor: lack of interaction with a C-terminal human PTH peptide. *Endocrinology* 135: 1713-1716.

Pines M, Fukayama S, Costas K, Meurer E, Goldsmith PK, Wu X, Muallem S, Behar V, Chorev M, Rosenblatt M, Tashjian AH Jr, Suva LJ (1996). Inositol 1,4,5-trisphosphate-dependent Ca^{2+} signalling by recombinant human PTH-PTHrP receptor stably expressed in a human cell line. *Bone* 18: 381-389.

Pioszak AA, Parker NR, Gardella TJ, Xu HE (2009). Structural basis for parathyroid hormone-related protein binding to the parathyroid hormone receptor and design of conformation-selective peptides. *J Bio Chem* 284: 28382-28391.

Piserchio A, Bisello A, Rosenblatt M, Chorev M, Mierke DF (2000). Characterization of parathyroid hormone/receptor interactions: structure of the first extracellular loop. *Biochem* 39: 8153-8160.

Pollo A, Lovallo M, Biancardi E, Sher E, Socci C, Carbone E (1993). Sensitivity to dihydropyridines, omega-conotoxin and noradrenaline reveals multiple high-voltage-activated Ca^{2+} channels in rat insulinoma and human pancreatic β-cells. *Pflugers Arch* 423: 462-471.

Poteet-Smith CE, Shabb JB, Francis SH, Corbin JD (1997). Identification of critical determinants for autoinhibition in the pseudosubstrate region of type I alpha cAMP-dependent protein kinase. *J Biol Chem* 272: 379-388.

Potts JT, Jr., Murray TM, Peacock M, Niall HD, Tregear GW, Keutmann HT, Powell D, Deftos LJ (1971). Parathyroid hormone: sequence, synthesis, immunoassay studies. *Am J Med* 50: 639-649.

Qiao J, Mei FC, Popov VL, Vergara LA, Cheng X (2002). Cell cycle-dependent subcellular localization of exchange factor directly activated by cAMP. *J Biol Chem* 277: 26581-26586.

Racke FK, Hammerland LG, Dubyak GR, Nemeth EF (1993). Functional expression of the parathyroid cell calcium receptor in Xenopus oocytes. *FEBS Lett* 333: 132-136.

Rahman T, Taylor CW (2009). Dynamic regulation of IP_3 receptor clustering and activity by IP_3. *Channels* 3: 226-232.

Rahman T, Taylor CW (2010). Nuclear patch-clamp recording from inositol 1,4,5-trisphosphate receptors. In: Whittaker M . *Calcium in living cells*, edn. Amsterdam: Elsevier. p^pp 199-224.

Rampe D, Lacerda AE, Dage RC, Brown AM (1991). Parathyroid hormone: an endogenous modulator of cardiac calcium channels. *Am J Physiol* 261: H1945-1950.

Rehmann H (2013). Epac-inhibitors: facts and artefacts. *Sci Rep* 3: 3032.

Rehmann H, Prakash B, Wolf E, Rueppel A, de Rooij J, Bos JL, Wittinghofer A (2003). Structure and regulation of the cAMP-binding domains of Epac2. *Nat Struct Biol* 10: 26-32.

Rehmann H, Wittinghofer A, Bos JL (2007). Capturing cyclic nucleotides in action: snapshots from crystallographic studies. *Nature Reviews Mol Cell Biol* 8**:** 63-73.

Reiken S, Lacampagne A, Zhou H, Kherani A, Lehnart SE, Ward C, Huang F, Gaburjakova M, Gaburjakova J, Rosemblit N, Warren MS, He KL, Yi GH, Wang J,Burkhoff D, Vassort G, Marks AR (2003). PKA phosphorylation activates the calcium release channel (ryanodine receptor) in skeletal muscle: defective regulation in heart failure. *J Cell Biol* 160: 919-928.

Reimann F, Tucker SJ, Proks P, Ashcroft FM (1999). Involvement of the n-terminus of Kir6.2 in coupling to the sulphonylurea receptor. *J Physiol* 518: 325-336.

Renuka TR, Robinson R, Paulose CS (2006). Increased insulin secretion by muscarinic M1 and M3 receptor function from rat pancreatic islets in vitro. *Neurochem Res* 31: 313-320.

Rizzuto R, Marchi S, Bonora M, Aguiari P, Bononi A, De Stefani D, Giorgi C, Leo S, Rimessi A, Siviero R, Zecchini E, Pinton P (2009). Ca^{2+} transfer from the ER to mitochondria: when, how and why. *Biochim Biophys Acta* 1787: 1342-1351.

Rizzuto R, Pozzan T (2006). Microdomains of intracellular Ca^{2+}: molecular determinants and functional consequences. *Physiol Rev* 86: 369-408.

Robinson DR, Wu YM, Lin SF (2000). The protein tyrosine kinase family of the human genome. *Oncogene* 19**:** 5548-5557.

Rooney TA, Sass EJ, Thomas AP (1990). Agonist-induced cytosolic calcium oscillations originate from a specific locus in single hepatocytes. *J Biol Chem* 265: 10792-10796.

Rosker C, Meur G, Taylor EJ, Taylor CW (2009). Functional ryanodine receptors in the plasma membrane of RINm5F pancreatic β-cells. *J Biol Chem* 284: 5186-5194.

Ross CA, Danoff SK, Schell MJ, Snyder SH, Ullrich A (1992). Three additional inositol 1,4,5-trisphosphate receptors: molecular cloning and differential localization in brain and peripheral tissues. *Proc Natl Acad Sci U S A* 89: 4265-4269.

Rousseau E, Smith JS, Meissner G (1987). Ryanodine modifies conductance and gating behavior of single Ca^{2+} release channel. *Am J Physiol* 253: C364-368.

Rubin DA, Hellman P, Zon LI, Lobb CJ, Bergwitz C, Juppner H (1999). A G protein-coupled receptor from zebrafish is activated by human parathyroid hormone and not by human or teleost parathyroid hormone-related peptide. Implications for the evolutionary conservation of calcium-regulating peptide hormones. *J Biol Chem* 274: 23035-23042.

Rubin DA, Juppner H (1999). Zebrafish express the common parathyroid hormone/parathyroid hormone-related peptide receptor (PTH1R) and a novel receptor (PTH_3R) that is preferentially activated by mammalian and fugufish parathyroid hormone-related peptide. *J Biol Chem* 274: 28185-28190.

Ruiz de Azua I, Gautam D, Guettier JM, Wess J (2011). Novel insights into the function of β-cell M3 muscarinic acetylcholine receptors: therapeutic implications. *Trends Endocrinol Metab* 22: 74-80.

Saleem H, Tovey SC, Rahman T, Riley AM, Potter BVL, Taylor CW (2012). Stimulation of inositol 1,4,5-trisphosphate (IP_3) receptor subtypes by analogues of IP_3. *PLoS One* 8: e54877.

Saleem H, Tovey SC, Riley AM, Potter BVL, Taylor CW (2013). Stimulation of inositol 1,4,5-trisphosphate (IP_3) receptor subtypes by adenophostin A and its analogues. *PLoS One* 8: e58027.

Salomon Y, Londos C, Rodbell M (1974). A highly sensitive adenylate cyclase assay. *Analytical Biochem* 58: 541-548.

Sanger F (1959). Chemistry of insulin; determination of the structure of insulin opens the way to greater understanding of life processes. *Science* 129**:** 1340-1344.

Sanger F (1988). Sequences, sequences, and sequences. *Annu Rev Biochem* 57**:** 1-28.

Sanger F (1950). Some chemical investigations on the structure of insulin. *Cold Spring Harb Symp Quant Biol* 14**:** 153-160.

Schmidt M, Evellin S, Weernink PA, von Dorp F, Rehmann H, Lomasney JW, Jakobs KH (2001). A new phospholipase-C-calcium signalling pathway mediated by cyclic AMP and a Rap GTPase. *Nat Cell Biol* 3: 1020-1024.

Schnurbus R, de Pietri Tonelli D, Grohovaz F, Zacchetti D (2002). Re-evaluation of primary structure, topology, and localization of Scamper, a putative intracellular Ca^{2+} channel activated by sphingosylphosphocholine. *Biochem J* 362: 183-189.

Schulla V, Renstrom E, Feil R, Feil S, Franklin I, Gjinovci A, Jing XJ, Laux D, Lundquist I, Magnuson MA, Obermüller S, Olofsson CS, Salehi A, Wendt A,Klugbauer N, Wollheim CB, Rorsman P, Hofmann F (2003). Impaired insulin secretion and glucose tolerance in β cell-selective $Ca_{(v)}1.2$ Ca^{2+} channel null mice. *EMBO. J* 22: 3844-3854.

Schwindinger WF, Fredericks J, Watkins L, Robinson H, Bathon JM, Pines M, Suva LJ, Levine MA (1998). Coupling of the PTH/PTHrP receptor to multiple G-proteins. Direct demonstration of receptor activation of Gs, Gq/11, and Gi(1) by [alpha-^{32}P]GTP-gamma-azidoanilide photoaffinity labeling. *Endocrine* 8: 201-209.

Scott JD, Glaccum MB, Zoller MJ, Uhler MD, Helfman DM, McKnight GS, Krebs EG. (1987). The molecular cloning of a type II regulatory subunit of the cAMP-dependent protein kinase from rat skeletal muscle and mouse brain. *Proc Natl Acad Sci U S A* 84: 5192-5196.

Seghers V, Nakazaki M, DeMayo F, Aguilar-Bryan L, Bryan J (2000). Sur1 knockout mice. A model for K_{ATP} channel-independent regulation of insulin secretion. *J Biol Chem* 275: 9270-9277.

Seifert R, Lushington GH, Mou TC, Gille A, Sprang SR (2012). Inhibitors of membranous adenylyl cyclases. *Trends Pharmacol Sci* 33: 64-78.

Seino S, Shibasaki T, Minami K (2010). Pancreatic β-cell signaling: toward better understanding of diabetes and its treatment. *Proc Jpn Acad Ser B Phys Biol Sci* 86: 563-577.

Seo M-D, Velamakanni S, Ishiyama N, Stathopulos PB, Rossi AM, Khan SA, Dale P, Li C, Ames JB, Ikura M, Taylor CW (2012). Structural and functional conservation of key domains in $InsP_3$ and ryanodine receptors. *Nature* 483: 108-112.

Sesti G, Federici M, Lauro D, Sbraccia P, Lauro R (2001). Molecular mechanism of insulin resistance in type 2 diabetes mellitus: role of the insulin receptor variant forms. *Diabetes Metab Res Rev* 17**:** 363-373.

Seuwen K, Boddeke HGWM (1995). Heparin-insensitive calcium release from intracellular stores triggered by the recombinant human parathyroid hormone receptor. *Br J Pharm* 114: 1613-1620.

Sharma RK, Kalra J (1994). Characterization of calmodulin-dependent cyclic nucleotide phosphodiesterase isoenzymes. *Biochem J* 299: 97-100.

Sheikh SP, Vilardarga JP, Baranski TJ, Lichtarge O, Iiri T, Meng EC, Nissenson RA, Bourne HR (1999). Similar structures and shared switch mechanisms of the β_2-adrenoceptor and the parathyroid hormone receptor. Zn(II) bridges between helices III and VI block activation. *J Biol Chem* 274: 17033-17041.

Shimizu M, Shimizu N, Tsang JC, Petroni BD, Khatri A, Potts JT, Jr., Gardella TJ (2002). Residue 19 of the parathyroid hormone (PTH) modulates ligand interaction with the juxtamembrane region of the PTH-1 receptor. *Biochem* 41: 13224-13233.

Short AD, Taylor CW (2000). Parathyroid hormone controls the size of the intracellular Ca^{2+} stores available to receptors linked to inositol trisphosphate formation. *J Biol Chem* 275: 1807-1813.

Shoshan-Barmatz V, Ashley RH (1998). The structure, function, and cellular regulation of ryanodine-sensitive Ca^{2+} release channels. *Int Rev Cytol* 183: 185-270.

Showers MO, Maurer RA (1986). A cloned bovine cDNA encodes an alternate form of the catalytic subunit of cAMP-dependent protein kinase. *J Biol Chem* 261: 16288-16291.

Simonds WF (1999). G protein regulation of adenylate cyclase. *Trends Pharmacol Sci* 20: 66-73.

Siso-Nadal F, Fox JJ, Laporte SA, Hebert TE, Swain PS (2009). Cross-talk between signaling pathways can generate robust oscillations in calcium and cAMP. *PLoS One* 4: e7189.

Smith DM, Johnston CC, Jr. (1975). Cyclic 3', 5'-adenosine monophosphate levels in separated bone cells. *Endocrinology* 96: 1261-1269.

Smith IF, Wiltgen SM, Parker I (2009). Localization of puff sites adjacent to the plasma membrane: functional and spatial characterization of Ca^{2+} signaling in SH-SY5Y cells utilizing membrane-permeant caged IP_3. *Cell Calcium* 45: 65-76.

Smith JS, Imagawa T, Ma J, Fill M, Campbell KP, Coronado R (1988). Purified ryanodine receptor from rabbit skeletal muscle is the calcium-release channel of sarcoplasmic reticulum. *J Gen Physiol* 92: 1-26.

Smogorzewski M, Zayed M, Zhang YB, Roe J, Massry SG (1993). Parathyroid hormone increases cytosolic calcium concentration in adult rat cardiac myocytes. *Am J Physiol* 264: H1998-2006.

Sneddon WB, Magyar CE, Willick GE, Syme CA, Galbiati F, Bisello A, Friedman PA (2004). Ligand-selective dissociation of activation and internalization of the parathyroid hormone (PTH) receptor: conditional efficacy of PTH peptide fragments. *Endocrinology* 145: 2815-2823.

Sneyd J, Tsaneva-Atanasova K, Reznikov V, Bai Y, Sanderson MJ, Yule DI (2006). A method for determining the dependence of calcium oscillations on inositol trisphosphate oscillations. *Proc Nat Acad Sci USA* 103: 1675-1680.

Spacek T, Santorova J, Zacharovova K, Berkova Z, Hlavata L, Saudek F, Jezek P (2008). Glucose-stimulated insulin secretion of insulinoma INS-1E cells is associated with elevation of both respiration and mitochondrial membrane potential. *Int J Biochem Cell Biol* 40: 1522-1535.

Sparrow EP, Finger S (2001). Edward Albert Schafer (Sharpey-Schafer) and his contributions to neuroscience: commemorating of the 150th anniversary of his birth. *J Hist Neurosci* 10**:** 41-57.

Squires PE, Hills CE, Rogers GJ, Garland P, Farley SR, Morgan NG (2004). The putative imidazoline receptor agonist, harmane, promotes intracellular calcium mobilisation in pancreatic β-cells. *Eur J Pharmacol* 501: 31-39.

Steiner DF, Oyer PE (1967). The biosynthesis of insulin and a probable precursor of insulin by a human islet cell adenoma. *Proc Natl Acad Sci U S A* 57**:** 473-480.

Straub SG, Cosgrove KE, Ammala C, Shepherd RM, O'Brien RE, Barnes PD, Kuchinski N, Chapman JC, Schaeppi M, Glaser B, Lindley KJ, Sharp GW,Aynsley-Green A, Dunne MJ (2001). Hyperinsulinism of infancy: the regulated release of insulin by K_{ATP} channel-independent pathways. *Diabetes* 50: 329-339.

Straub SV, Giovannucci DR, Bruce JI, Yule DI (2002). A role for phosphorylation of inositol 1,4,5-trisphosphate receptors in defining calcium signals induced by Peptide agonists in pancreatic acinar cells. *J Biol Chem* 277: 31949-31956.

Strehler EE, Treiman M (2004). Calcium pumps of plasma membrane and cell interior. *Curr Mol Med* 4: 323-335.

Sudhof TC, Newton CL, Archer BT, 3rd, Ushkaryov YA, Mignery GA (1991). Structure of a novel $InsP_3$ receptor. *EMBO J* 10: 3199-3206.

Supattapone S, Danoff SK, Theibert A, Joseph SK, Steiner J, Snyder SH (1988). Cyclic AMP-dependent phosphorylation of a brain inositol trisphosphate receptor decreases its release of calcium. *Proc Natl Acad Sci U S A* 85: 8747-8750.

Sutherland EW (1970). On the biological role of cyclic AMP. *JAMA* 214: 1281-1288.

Szaszak M, Christian F, Rosenthal W, Klussmann E (2008). Compartmentalized cAMP signalling in regulated exocytic processes in non-neuronal cells. *Cell Signal* 20: 590-601.

Szollosi A, Nenquin M, Henquin JC (2010). Pharmacological stimulation and inhibition of insulin secretion in mouse islets lacking ATP-sensitive K^+ channels. *Br J Pharmacol* 159: 669-677.

Tada M, Toyofuku T (1998). Molecular regulation of phospholamban function and expression. *Trends Cardiovasc Med* 8**:** 330-340.

Takasawa S, Akiyama T, Nata K, Kuroki M, Tohgo A, Noguchi N, Kobayashi S, Kato I, Katada T, Okamoto H (1998). Cyclic ADP-ribose and inositol 1,4,5-trisphosphate as alternate second messengers for intracellular Ca^{2+} mobilization in normal and diabetic β-cells. *J Biol Chem* 273: 2497-2500.

Takasawa S, Kuroki M, Nata K, Noguchi N, Ikeda T, Yamauchi A, Itaya-Hironaka A, Sakuramoto-Tsuchida S, Takahashi I, Yoshikawa T, Shimosegawa T, Okamoto H (2010). A novel ryanodine receptor expressed in pancreatic islets by alternative splicing from type 2 ryanodine receptor gene. *Biochem Biophys Res Commun* 397: 140-145.

Takasu H, Gardella TJ, Luck MD, Potts JT, Bringhurst FR (1999). Amino-terminal modifications of human parathyoid hormone (PTH) selectively alter phospholipase C signaling via the type 1 PTH receptor: Implications for design of signal-specific PTH ligands. *Biochem* 38: 13453-13460.

Takasu H, Guo J, Bringhurst FR (1999b). Dual signaling and ligand selectivity of the human PTH/PTHrP receptor. *J Bone Miner Res* 14: 11-20.

Takeyama K, Kitanaka S, Sato T, Kobori M, Yanagisawa J, Kato S (1997). 25-Hydroxyvitamin D3 1alpha-hydroxylase and vitamin D synthesis. *Science* 277: 1827-1830.

Tamarina NA, Kuznetsov A, Rhodes CJ, Bindokas VP, Philipson LH (2005). Inositol (1,4,5)-trisphosphate dynamics and intracellular calcium oscillations in pancreatic β-cells. *Diabetes* 54: 3073-3081.

Tang TS, Tu H, Wang Z, Bezprozvanny I (2003). Modulation of type 1 inositol (1,4,5)-trisphosphate receptor function by protein kinase a and protein phosphatase 1alpha. *J Neurosci* 23: 403-415.

Tasken K, Skalhegg BS, Tasken KA, Solberg R, Knutsen HK, Levy FO, Sandberg M, Orstavik S, Larsen T, Johansen AK, Vang T, Schrader HP, Reinton NT,Torgersen KM, Hansson V, Jahnsen T (1997). Structure, function, and regulation of human cAMP-dependent protein kinases. *Adv Sec Mrg Phosphoprotein Res* 31: 191-204.

Taylor CW, Genazzani AA, Morris SA (1999). Expression of inositol trisphosphate receptors. *Cell Calcium* 26: 237-251.

Taylor CW, Laude AJ (2002). IP_3 receptors and their regulation by calmodulin and cytosolic Ca^{2+}. *Cell Calcium* 32: 321-334.

Taylor CW, Tovey SC (2012). From parathyroid hormone to cytosolic Ca^{2+} signals. *Biochem Soc Trans* 40: 147-152.

Taylor CW, Tovey SC (2010). $IP_{(3)}$ receptors: toward understanding their activation. *Cold Spring Harb Perspect Biol* 2: a004010.

Tertyshnikova S, Fein A (1998). Inhibition of inositol 1,4,5-trisphosphate-induced Ca^{2+} release by cAMP-dependent protein kinase in a living cell. *Proc Natl Acad Sci U S A* 95: 1613-1617.

Thrower EC, Mobasheri H, Dargan S, Marius P, Lea EJ, Dawson AP (2000). Interaction of luminal calcium and cytosolic ATP in the control of type 1 inositol (1,4,5)-trisphosphate receptor channels. *J Biol Chem* 275: 36049-36055.

Thurley K, Smith IF, Tovey SC, Taylor CW, Parker I, Falcke M (2011). Timescales of IP_3-evoked Ca^{2+} spikes emerge from Ca^{2+} puffs only at the cellular level. *Biophy. J* 101: 2638-2644.

Thurley K, Tovey SC, Moenke G, Prince VL, Meena A, Thomas AP, Skupin A, Taylor CW, Falcke M (2014). Reliable encoding of stimulus intensities within random sequences of intracellular Ca^{2+} spikes. *Sci Signal* 7: ra59.

Tian J, Smogorzewski M, Kedes L, Massry SG (1993). Parathyroid hormone-parathyroid hormone related protein receptor messenger RNA is present in many tissues besides the kidney. *Am J Nephrol* 13: 210-213.

Togashi K, Hara Y, Tominaga T, Higashi T, Konishi Y, Mori Y, Tominaga M (2006). TRPM2 activation by cyclic ADP-ribose at body temperature is involved in insulin secretion. *EMBO J* 25: 1804-1815.

Tong Y, Zull J, Yu L (1996). Functional expression and signaling properties of cloned human parathyroid receptor in *Xenopus* oocytes. Evidence for a novel signaling pathway. *J Biol Chem* 271: 8183-8191.

Toribio RE, Kohn CW, Chew DJ, Capen CC, Rosol TJ (2002). Cloning and sequence analysis of the complementary DNA for feline preproparathyroid hormone. *Am J Vet Res* 63: 194-197.

Tovey SC, Dedos SG, Rahman T, Taylor EJ, Pantazaka E, Taylor CW (2010). Regulation of inositol 1,4,5-trisphosphate receptors by cAMP independent of cAMP-dependent protein kinase. *J Biol Chem* 285: 12979-12989.

Tovey SC, Dedos SG, Taylor EJ, Church JE, Taylor CW (2008). Selective coupling of type 6 adenylyl cyclase with type 2 IP_3 receptors mediates direct sensitization of IP_3 receptors by cAMP. *J Cell Biol* 183: 297-311.

Tovey SC, Goraya TA, Taylor CW (2003). Parathyroid hormone increases the sensitivity of inositol trisphosphate receptors by a mechanism that is independent of cyclic AMP. *Br J Pharma* 138: 81-90.

Tovey SC, Sun Y, Taylor CW (2006). Rapid functional assays of intracellular Ca^{2+} channels. *Nat Protoc* 1: 259-263.

Tovey SC, Taylor CW (2013). Cyclic AMP directs inositol (1,4,5)-trisphosphate-evoked Ca^{2+} signalling to different intracellular Ca^{2+} stores. *J Cell Sci* 126: 2305-2313.

Toya Y, Schwencke C, Ishikawa Y (1998). Forskolin derivatives with increased selectivity for cardiac adenylyl cyclase. *J Mol Cell Cardiol* 30: 97-108.

Tregear GW, Van Rietschoten J, Greene E, Keutmann HT, Niall HD, Reit B, Parsons JA, Potts JT Jr (1973). Bovine parathyroid hormone: minimum chain length of synthetic peptide required for biological activity. *Endocrinology* 93: 1349-1353.

Tse A, Tse FW, Almers W, Hille B (1993). Rhythmic exocytosis stimulated by GnRH-induced calcium oscillations in rat gonadotropes. *Science* 260: 82-84.

Tsuboi T, da Silva Xavier G, Holz GG, Jouaville LS, Thomas AP, Rutter GA (2003). Glucagon-like peptide-1 mobilizes intracellular Ca^{2+} and stimulates mitochondrial ATP synthesis in pancreatic MIN6 β -cells. *Biochem J* 369: 287-299.

Tsukazaki T, Ohtsuru A, Namba H, Oda J, Motomura K, Osaki M, Kiriyama T, Iwasaki K, Yamashita S (1996). Parathyroid hormone-related protein (PTHrP) action in rat articular chondrocytes: comparison of PTH(1-34), PTHrP(1-34), PTHrP(1-141), PTHrP(100-114) and antisense oligonucleotides against PTHrP. *J Endocrinol* 150: 359-368.

Tu H, Tang TS, Wang Z, Bezprozvanny I (2004). Association of type 1 inositol 1,4,5-trisphosphate receptor with AKAP9 (Yotiao) and protein kinase A. *J Biol Chem* 279: 19375-19382.

Tucker SJ, Gribble FM, Zhao C, Trapp S, Ashcroft FM (1997). Truncation of Kir6.2 produces ATP-sensitive K^+ channels in the absence of the sulphonylurea receptor. *Nature* 387: 179-183.

Uhler MD, Chrivia JC, McKnight GS (1986). Evidence for a second isoform of the catalytic subunit of cAMP-dependent protein kinase. *J Biol Chem* 261: 15360-15363.

Urena P, Kong XF, Abou-Samra AB, Juppner H, Kronenberg HM, Potts JT, Jr., Segre GV (1993). Parathyroid hormone (PTH)/PTH-related peptide receptor messenger ribonucleic acids are widely distributed in rat tissues. *Endocrinology* 133: 617-623.

Usdin TB, Bonner TI, Hoare SR (2002). The parathyroid hormone 2 (PTH2) receptor. *Recep Channels* 8: 211-218.

Usdin TB, Gruber C, Bonner TI (1995). Identification and functional expression of a receptor selectively recognizing parathyroid hormone, the PTH2 receptor. *J Biol Chem* 270: 15455-15458.

Usdin TB, Hoare SR, Wang T, Mezey E, Kowalak JA (1999). TIP39: a new neuropeptide and PTH2-receptor agonist from hypothalamus. *Nat Neurosci* 2: 941-943.

van der Lee MM, Verkaar F, Wat JW, van Offenbeek J, Timmerman M, Voorneveld L, van Lith LH, Zaman GJ (2013). β-Arrestin-biased signaling of PTH analogs of the type 1 parathyroid hormone receptor. *Cell Signal* 25: 527-538.

Vilardaga JP, Krasel C, Chauvin S, Bambino T, Lohse MJ, Nissenson RA (2002). Internalization determinants of the parathyroid hormone receptor differentially regulate b-arrestin/receptor association. *J Biol Chem* 277: 8121-8129.

Vilardaga JP, Lin I, Nissenson RA (2001). Analysis of parathyroid hormone (PTH)/secretin receptor chimeras differentiates the role of functional domains in the pth/ pth-related peptide (PTHrP) receptor on hormone binding and receptor activation. *Mol Endocrinol* 15: 1186-1199.

Volpe P, Alderson-Lang BH (1990). Regulation of inositol 1,4,5-trisphosphate-induced Ca^{2+} release. II. Effect of cAMP-dependent protein kinase. *Am J Physiol* 258: C1086-1091.

Walsh DA, Perkins JP, Krebs EG (1968). An adenosine 3',5'-monophosphate-dependant protein kinase from rabbit skeletal muscle. *J Biol Chem* 243: 3763-3765.

Wang B, Ardura JA, Romero G, Yang Y, Hall RA, Friedman PA (2010). Na/H exchanger regulatory factors control parathyroid hormone receptor signaling by facilitating differential activation of Ga protein subunits. *J Biol Chem* 285(35): 26976-26986.

Wang B, Bisello A, Yang Y, Romero GG, Friedman PA (2007). NHERF1 regulates parathyroid hormone receptor membrane retention without affecting recycling. *J Biol Chem* 282: 36214-36222.

Wang SS, Alousi AA, Thompson SH (1995). The lifetime of inositol 1,4,5-trisphosphate in single cells. *J Gen Physiol* 105: 149-171.

Wang X, Zhang X, Dong XP, Samie M, Li X, Cheng X, Goschka A, Shen D, Zhou Y, Harlow J, Zhu MX, Clapham DE, Ren D, Xu H (2012). TPC proteins are phosphoinositide- activated sodium-selective ion channels in endosomes and lysosomes. *Cell* 151: 372-383.

Wang Y, Deng X, Mancarella S, Hendron E, Eguchi S, Soboloff J, Tang XD, Gill DL (2010). The calcium store sensor, STIM1, reciprocally controls Orai and $Ca_V1.2$ channels. *Science* 330: 105-109.

Wayman GA, Hinds TR, Storm DR (1995). Hormone stimulation of type III adenylyl cyclase induces Ca^{2+} oscillations in HEK-293 cells. *J Biol Chem* 270: 24108-24115.

Wayman GA, Impey S, Wu Z, Kindsvogel W, Prichard L, Storm DR (1994). Synergistic activation of the type I adenylyl cyclase by Ca^{2+} and G_s-coupled receptors in vivo. *J Biol Chem* 269: 25400-25405.

Weber IT, Steitz TA, Bubis J, Taylor SS (1987). Predicted structures of cAMP binding domains of type I and II regulatory subunits of cAMP-dependent protein kinase. *Biochem* 26: 343-351.

Wedel B, Boyles RR, Putney JW, Jr., Bird GS (2007). Role of the store-operated calcium entry proteins Stim1 and Orai1 in muscarinic cholinergic receptor-stimulated calcium oscillations in human embryonic kidney cells. *J Physiol* 579: 679-689.

Wehbi VL, Stevenson HP, Feinstein TN, Calero G, Romero G, Vilardaga JP (2013). Noncanonical GPCR signaling arising from a PTH receptor-arrestin-Gbg complex. *Proc Nat Acad Sci USA* 110: 1530-1535.

Whitaker M, Smith J (2008). Introduction. Calcium signals and developmental patterning. *Philos Trans R Soc Lond B* 363: 1307-1310.

Whitfield JF, Morley P (1995). Small bone-building fragments of parathyroid hormone: new therapeutic agents for osteoporosis. *Trends Pharmacol Sci* 16: 382-386.

Willoughby D, Cooper DM (2006). Ca^{2+} stimulation of adenylyl cyclase generates dynamic oscillations in cyclic AMP. *J Cell Sci* 119: 828-836.

Willoughby D, Cooper DM (2007). Organization and Ca^{2+} regulation of adenylyl cyclases in cAMP microdomains. *Physiol Rev* 87: 965-1010.

Wiltink A, van den Brink AM, Herrmann-Erlee MP, van der Meer JM, van der Plas A, Willems PH, Van Duijn B, Nijweide PJ, Ypey DL (1993). Heterogeneity of intracellular calcium responses to parathyroid hormone and thrombin in primary osteoblast-like cells and UMR106-01 cells: correlations with culture conditions, intracellular calcium concentration and differentiation state. *Cell Calcium* 14: 591-600.

Wojcikiewicz RJ, Luo SG (1998). Phosphorylation of inositol 1,4,5-trisphosphate receptors by cAMP-dependent protein kinase. Type I, II, and III receptors are differentially susceptible to phosphorylation and are phosphorylated in intact cells. *J Biol Chem* 273: 5670-5677.

Wollheim CB, Pozzan T (1984). Correlation between cytosolic free Ca^{2+} and insulin release in an insulin-secreting cell line. *J Biol Chem* 259: 2262-2267.

Woolcott OO, Gustafsson AJ, Dzabic M, Pierro C, Tedeschi P, Sandgren J, Bari MR, Nguyen KH, Bianchi M, Rakonjac M, Rådmark O, Ostenson CG, Islam MS

(2006). Arachidonic acid is a physiological activator of the ryanodine receptor in pancreatic β -cells. *Cell Calcium* 39: 529-537.

Xiao B, Zhong G, Obayashi M, Yang D, Chen K, Walsh MP, Shimoni Y, Cheng H, Ter Keurs H, Chen SR (2006). Ser-2030, but not Ser-2808, is the major phosphorylation site in cardiac ryanodine receptors responding to protein kinase A activation upon β -adrenergic stimulation in normal and failing hearts. *Biochem J* 396: 7-16.

Xiao RP, Avdonin P, Zhou YY, Cheng H, Akhter SA, Eschenhagen T, Lefkowitz RJ, Koch WJ, Lakatta EG (1999). Coupling of β-2-adrenoceptor to Gi proteins and its physiological relevance in murine cardiac myocytes. *Circ Res* 84: 43-52.

Xiao RP, Ji X, Lakatta EG (1995). Functional coupling of the β-2-adrenoceptor to a pertussis toxin-sensitive G protein in cardiac myocytes. *Mol Pharmacol* 47: 322-329.

Yamamoto-Hino M, Sugiyama T, Hikichi K, Mattei MG, Hasegawa K, Sekine S (1994). Cloning and characterization of human type 2 and type 3 inositol 1,4,5-trisphosphate receptors. *Recep Channels* 2: 9-22.

Yamamoto T, Kambe F, Cao X, Lu X, Ishiguro N, Seo H (2007). Parathyroid hormone activates phosphoinositide 3-kinase-Akt-Bad cascade in osteoblast-like cells. *Bone* 40**:** 354-359.

Yang CM, Chiu CT, Wang CC, Tsao HL, Fan LW (1999). Forskolin inhibits 5-hydroxytryptamine-induced phosphoinositide hydrolysis and Ca^{2+} Mobilisation in canine cultured aorta smooth muscle cells. *Cell Signal* 11**:** 697-704.

Yang SN, Berggren PO (2006). The role of voltage-gated calcium channels in pancreatic β -cell physiology and pathophysiology. *Endocr Rev* 27: 621-676.

Yoshimoto Y, Norman AW (1986). Biological activity of vitamin D metabolites and analogs: dose-response study of ^{45}Ca transport in an isolated chick duodenum perfusion system. *J Steroid Biochem* 25: 905-909.

Yu HJ, Ma H, Green RD (1993). Calcium entry via L-type calcium channels acts as a negative regulator of adenylyl cyclase activity and cyclic AMP levels in cardiac myocytes. *Mol Pharmacol* 44: 689-693.

Zaccolo M (2011). Spatial control of cAMP signalling in health and disease. *Curr Opin Pharmacol* 11: 649-655.

Zaccolo M, Di Benedetto G, Lissandron V, Mancuso L, Terrin A, Zamparo I (2006). Restricted diffusion of a freely diffusible second messenger: mechanisms underlying compartmentalized cAMP signalling. *Biochem Soc Trans* 34**:** 495-497.

Zaccolo M, Magalhaes P, Pozzan T (2002). Compartmentalisation of cAMP and Ca^{2+} signals. *Curr Opin Cell Biol* 14: 160-166.

Zeng W, Mak DD, Li Q, Shin DM, Foskett JK, Muallem S (2003). A new mode of Ca^{2+} signaling by G protein-coupled receptors: gating of IP_3 receptor Ca^{2+} release channels by Gbg. *Current Biol* 13: 872-876.

Zhou AT, Bessalle R, Bisello A, Nakamoto C, Rosenblatt M, Suva LJ, Chorev M (1997). Direct mapping of an agonist-binding domain within the parathyroid hormone/parathyroid hormone-related protein receptor by photoaffinity crosslinking. *Proc Natl Acad Sci U S A* 94: 3644-3649.

Zhu L, Luo Y, Chen T, Chen F, Wang T, Hu Q (2008). Ca^{2+} oscillation frequency regulates agonist-stimulated gene expression in vascular endothelial cells. *J Cell Sci* 121: 2511-2518.

Zimanyi I, Buck E, Abramson JJ, Mack MM, Pessah IN (1992). Ryanodine induces persistent inactivation of the Ca^{2+} release channel from skeletal muscle sarcoplasmic reticulum. *Mol Pharma* 42: 1049-1057.

Zuniga-Hertz JP, Rebelato E, Kassan A, Khalifa AM, Ali SS, Patel HH, *et al.* (2015). Distinct pathways of cholesterol biosynthesis impact on insulin secretion. *J Endocrinol* 224**:** 75-84.